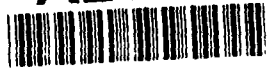


AD-A267 042



Accession For	
NTIS - CRA&I	<input checked="" type="checkbox"/>
DTIC - I/B	<input type="checkbox"/>
Unannounced	<input type="checkbox"/>
Publication	<input type="checkbox"/>
BY	
Date	
Approved by	
DAI	Approved by
A-1	

STRIP - STATED
 Approved for public release
 Distribution Unlimited

**EXPERIMENTAL STUDY OF OXYGEN-
 ASSISTED CRACK GROWTH IN ALLOY 718
 AND ALLOY TI-1100**

**Grant AFOSR - 90-0333
 Final Report February 1993**

E. Andrieu, A. Pineau and H. Ghonem

93-16597



Final Report

**EXPERIMENTAL STUDY OF
OXYGEN-ASSISTED CRACK
GROWTH IN ALLOY 718 AND ALLOY
TI-1100**

by

E. Andrieu and A. Pineau

**Ecole des Mines de Paris
Centre des Materiaux
B.P.87 - 91003 Evry Cedex, FRANCE**

and

H. Ghonem

**University of Rhode Island
Department of Mechanical Engineering
Kingston, RI 02881, USA**

Submitted to

**Department of Air Force
Air Force Office of Scientific Research**

Grant AFOSR - 90-0333

February 1993

REPORT DOCUMENTATION PAGE			Form Approved OMB No. 0704-0188	
<small>Public reporting burden for this collection of information is estimated to average 1 hour per response, including the time for reviewing instructions, searching existing data sources, gathering and maintaining the data needed, and completing and reviewing the collection of information. Send comments regarding this burden estimate or any other aspect of this collection of information, including suggestions for reducing this burden, to Washington Headquarters Services, Directorate for Information Operations and Reports, 1215 Jefferson Davis Highway, Suite 1204, Arlington, VA 22202-4302, and to the Office of Management and Budget, Paperwork Reduction Project (0704-0188), Washington, DC 20503.</small>				
1. AGENCY USE ONLY (Leave blank)	2. REPORT DATE 30.NOV.1991	3. REPORT TYPE AND DATES COVERED Final (30.SEPT.90 - 29 SEPT.1991)		
4. TITLE AND SUBTITLE Expérimental Study of oxygen assisted crack growth in alloy 718 and Alloy Ti - 1100.		5. FUNDING NUMBERS G-AFOSR-90-0333 PR-TA 2301/D1		
6. AUTHOR(S) E. ANDRIEU / A. PINEAU / H. GHONEM				
7. PERFORMING ORGANIZATION NAME(S) AND ADDRESS(ES) Ecole Nationale Supérieure des Mines de Paris Centre des Matériaux P.M. FOURT Locaux SNECMA 91003 EVRY CEDEX FRANCE		8. PERFORMING ORGANIZATION REPORT NUMBER 9/93/EA/AP/HG		
9. SPONSORING/MONITORING AGENCY NAME(S) AND ADDRESS(ES) SPONSORING / Monitoring Agency : European Office of Aerospace Research and Development BOX 14, EPO New York 09510-0200		10. SPONSORING/MONITORING AGENCY REPORT NUMBER TR-93-07		
11. SUPPLEMENTARY NOTES				
12a. DISTRIBUTION / AVAILABILITY STATEMENT Approved for public release Distribution unlimited		12b. DISTRIBUTION CODE		
13. ABSTRACT (Maximum 200 words) <p>The high Temperature fatigue crack growth behavior of alloy 718 is reviewed and investigated.</p> <p>FCGR have then been measured under constant ΔK and various oxygen partial pressures. A transition pressure associated with an important increase of the FCGR is found. At this transition pressure (10^{-2} mbar) the crack propagation path changes from transgranular to intergranular. From this study it is concluded, that intergranular crack growth requires the formation of a Ni based oxide during the early stage of the oxidation as well as high intergranular internal stresses promoted by an inhomogeneous distribution of the deformation.</p> <p>The crack growth behavior of Ti-1100 is investigated for loading frequencies ranging from 30 Hz to 0.005 Hz at temperature levels extending from 23°C to 650°C in both air and vacuum environments. Two types of time-dependent damage mechanisms have been identified; oxidation and creep effects. It is concluded that the effect of oxidation on the crack growth acceleration is rapid and constant in relation to the frequencies tested and is weakly dependent on cycle time. Creep effects, on the other hand, are dominant at low frequencies in both air and vacuum and are loading-rate dependent.</p>				
14. SUBJECT TERMS High temperature fatigue crack growth behavior of Alloy 718 - Ti 1100 in relation with oxidation processes and deformation mechanism.			15. NUMBER OF PAGES 191	
			16. PRICE CODE	
17. SECURITY CLASSIFICATION OF REPORT UNCLASSIFIED	18. SECURITY CLASSIFICATION OF THIS PAGE UNCLASSIFIED	19. SECURITY CLASSIFICATION OF ABSTRACT UNCLASSIFIED	20. LIMITATION OF ABSTRACT	

GENERAL INSTRUCTIONS FOR COMPLETING SF 298

The Report Documentation Page (RDP) is used in announcing and cataloging reports. It is important that this information be consistent with the rest of the report, particularly the cover and title page. Instructions for filling in each block of the form follow. It is important to *stay within the lines* to meet optical scanning requirements.

Block 1. Agency Use Only (Leave blank).

Block 2. Report Date. Full publication date including day, month, and year, if available (e.g. 1 Jan 88). Must cite at least the year.

Block 3. Type of Report and Dates Covered. State whether report is interim, final, etc. If applicable, enter inclusive report dates (e.g. 10 Jun 87 - 30 Jun 88).

Block 4. Title and Subtitle. A title is taken from the part of the report that provides the most meaningful and complete information. When a report is prepared in more than one volume, repeat the primary title, add volume number, and include subtitle for the specific volume. On classified documents enter the title classification in parentheses.

Block 5. Funding Numbers. To include contract and grant numbers; may include program element number(s), project number(s), task number(s), and work unit number(s). Use the following labels:

C - Contract	PR - Project
G - Grant	TA - Task
PE - Program Element	WU - Work Unit Accession No.

Block 6. Author(s). Name(s) of person(s) responsible for writing the report, performing the research, or credited with the content of the report. If editor or compiler, this should follow the name(s).

Block 7. Performing Organization Name(s) and Address(es). Self-explanatory.

Block 8. Performing Organization Report Number. Enter the unique alphanumeric report number(s) assigned by the organization performing the report.

Block 9. Sponsoring/Monitoring Agency Name(s) and Address(es). Self-explanatory.

Block 10. Sponsoring/Monitoring Agency Report Number. (If known)

Block 11. Supplementary Notes. Enter information not included elsewhere such as: Prepared in cooperation with....; Trans. of....; To be published in.... When a report is revised, include a statement whether the new report supersedes or supplements the older report.

Block 12a. Distribution/Availability Statement. Denotes public availability or limitations. Cite any availability to the public. Enter additional limitations or special markings in all capitals (e.g. NOFORN, REL, ITAR).

DOD - See DoDD 5230.24, "Distribution Statements on Technical Documents."
DOE - See authorities.
NASA - See Handbook NHB 2200.2.
NTIS - Leave blank.

Block 12b. Distribution Code.

DOD - Leave blank.
DOE - Enter DOE distribution categories from the Standard Distribution for Unclassified Scientific and Technical Reports.
NASA - Leave blank.
NTIS - Leave blank.

Block 13. Abstract. Include a brief (Maximum 200 words) factual summary of the most significant information contained in the report.

Block 14. Subject Terms. Keywords or phrases identifying major subjects in the report.

Block 15. Number of Pages. Enter the total number of pages.

Block 16. Price Code. Enter appropriate price code (NTIS only).

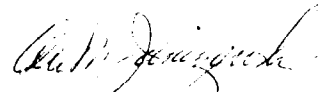
Blocks 17. - 19. Security Classifications. Self-explanatory. Enter U.S. Security Classification in accordance with U.S. Security Regulations (i.e., UNCLASSIFIED). If form contains classified information, stamp classification on the top and bottom of the page.

Block 20. Limitation of Abstract. This block must be completed to assign a limitation to the abstract. Enter either UL (unlimited) or SAR (same as report). An entry in this block is necessary if the abstract is to be limited. If blank, the abstract is assumed to be unlimited.

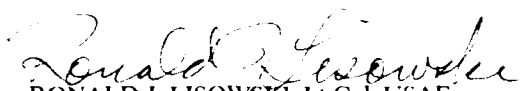
TR-92-07

This report has been reviewed and is releasable to the National Technical Information Service (NTIS).
At NTIS it will be releasable to the general public, including foreign nations.

This technical report has been reviewed and is approved for publication.



ALAN M. JANISZEWSKI, Lt Col, USAF
Chief, Structures/Struc. Material



RONALD J. LISOWSKI, Lt Col, USAF
Chief Scientist

**This report is divided into two separate parts,
the first part deals with research activities
conducted on Alloy 718 while the second part
deals with the work pertaining to Alloy Ti-
1100**

SUMMARY

PART I

EXPERIMENTAL STUDY OF OXYGEN-ASSISTED CRACK GROWTH IN ALLOY 718

INTRODUCTION.....	4
I. MICROSTRUCTURAL AND MECHANICAL EFFECTS.....	4
1.1 Effect of grain size	4
1.2. Effect of mechanical variables.....	5
1.2.1. Frequency.....	5
1.2.2 Hold time effect.....	6
1.2.3. Stress Ratio effect.....	7
II. ENVIRONMENTAL EFFECTS.....	7
III. INFLUENCE OF SLIP CHARACTER.....	9
IV. CONCLUSIONS	10
REFERENCES.....	11
FIGURES	12

PART II.....21

ENVIRONMENTAL INTERACTIONS IN HIGH TEMPERATURE FATIGUE CRACK GROWTH OF Ti-1100

1. INTRODUCTION.....	22
2. EXPERIMENTAL PROCEDURE.....	23
3. EXPERIMENTAL RESULTS.....	23
3.1 Material Behavior and Microstructural Characteristics.....	24
3.2 Crack Growth Tests	24
3.3 Microscopy and Fractography	26
4. ANALYSIS AND DISCUSSION.....	28
4.1 The Nature of Environment Damage.....	28
4.2 The Environment and Crack Closure	29
4.3 The Frequency Effect.....	31
5. CONCLUSIONS	34
REFERENCES.....	35
APPENDIX	51

PART I

EXPERIMENTAL STUDY OF OXYGEN-ASSISTED CRACK GROWTH IN ALLOY 718

ABSTRACT :

The high Temperature fatigue crack growth behavior of alloy 718 is reviewed and investigated. Microstructural and mechanical effects on FCGR are first presented. It is shown that under air environment the necklace microstructure is the less sensitive to the oxidation assisted crack growth. However, under vacuum all the microstructures under investigation behave similarly. It is concluded that minor modifications of the alloy microstructure can induce a significant improvement of the FCGR's behavior of this alloy.

By varying the mechanical loading conditions (frequency, hold time à K_{max} , stress ratio) it is shown that two different domains exist : (i) a Cycle dependent domain and (ii) a time dependent one. The later corresponds to the stronger detrimental interaction between oxidation and deformation processes.

Some important aspects of the oxidation process of this alloy are presented. XSTEM observations and analysis as well as AES study lead to the same conclusions. The oxidation process can be summarized as follows :

When occurring under air environment the early stage of oxidation at 650°C corresponds to the growth of a Ni based oxide followed several minutes later by the formation of a chromia passive subscale. This oxidation sequence takes place either on transgranular or on intergranular surfaces.

When the oxygen partial pressure is smaller than 10^{-2} mbar the oxidation process is modified. The first oxide to appear is chromia oxide.

FCGR have then been measured under constant ΔK and various oxygen partial pressures. A transition pressure associated with an important increase of the FCGR is found. At this transition pressure (10^{-2} mbar) the crack propagation path changes from transgranular to intergranular. From this study it is concluded, that intergranular crack growth requires the formation of a Ni based oxide during the early stage of the oxidation as well as high intergranular internal stresses promoted by an inhomogeneous distribution of the deformation.

INTRODUCTION

Alloy 718 is a precipitation strengthened nickel-base superalloy widely used in aerospace and nuclear applications involving static as well as cyclic loading at both high ($\sim 650^{\circ}\text{C}$) and medium temperature ranges in aggressive air environment. Damage tolerance methodologies needed in some of these applications require accurate predictions of the crack growth rate behavior under typical service conditions. This is the reason why a large research effort has been devoted to this material over the last past decades. In particular it is now well accepted that most of the effects observed at elevated temperature on this material are related to the detrimental influence of oxidation. A number of studies have shown that the fatigue crack propagation rate measured under vacuum is much lower than that determined under air environment but very few studies have been devoted to the micromechanisms of oxidation-induced cracking in Alloy 718, which was the main objective of the first part of the present study devoted to this material. This part of the report is divided into three sections. The first section is devoted to microstructural and mechanical effects while the second part deals with the environmental effects. The third part of the report focuses on the influence of slip character on the deformation and the subsequent oxidation process.

In each of these three sections reference will be made to the publications which were prepared along these lines either directly from the Centre des Materiaux - Ecole des Mines (CM-EMP) or from the cooperative program established between Ecole des Mines and Professor H. Ghonem of the University of Rhode Island. These publications are given in an appendix at the end to the present report.

I. MICROSTRUCTURAL AND MECHANICAL EFFECTS

I.1 Effect of grain size

The effect of grain size on the fatigue crack growth rate (FCGR) behavior was examined by Pedron and Pineau [1] on three widely different microstructures. These are:

- A large grain material with an average grain size equal to $200\text{ }\mu\text{m}$.
- A fine grain material resulting from the recrystallization of rolled plates, with an average grain size of $40\text{ }\mu\text{m}$.
- A necklace microstructure with large grains of $300\text{ }\mu\text{m}$ diameter surrounded by $10\text{ }\mu\text{m}$ diameter fine grains.

A conventional heat treatment was given to each of the above mentioned microstructure consisting of 955°C - 1h - air cooled - 720°C - 8h - cooling rate $50^{\circ}\text{C.h}^{-1}$ down to 620°C - 8h - air cooled.

Fatigue tests were carried out under air or vacuum at 650°C on CT specimens. The results obtained with a (10s - 300s hold time - 10s) cycle are shown in figure I. It is worth noting that under vacuum the fatigue crack growth rate is not influenced by the microstructure. On the other hand under air environment an important effect of the microstructure is observed. The necklace microstructure is less sensitive to environment than the large grain. The fine grain material gives rise to the largest FCGR. These results might be rationalized as follows: The work of Ghonem et al [2] proposed that the crack growth rate increases as the grain boundary area exposed to oxygen penetration increases. Consequently, the grain size effect is attributed to the local oxidation behavior, i.e. oxygen transport along the grain boundaries. Concurrently, one can also put forward that, in spite of having the same fatigue crack growth rate under vacuum the three microstructures do not exhibit the same mechanical behavior at the crack tip. The localization of the deformation at the crack tip might induce for the three microstructures different grain boundary internal stresses. Several attempts have been made to modify the microstructure of Alloy 718 to reduce elevated temperature creep and fatigue crack growth rates. The recent work by Chang and al is worthwhile to be mentioned to this respect [3]. These authors used a modified heat treatment to produce a coarser grain size relative to the standard heat treatment and a serrated grain boundary structure through controlled precipitation of needle like Δ phase at the grain boundaries. A coarse grain size and the presence of serrations are expected to suppress grain boundary sliding and the serrations, like with the necklace microstructure, are also expected to make the crack path more tortuous. It was shown that this modified heat treatment decreases the FCGR's by a factor of about 2 at 525°C and 650°C with no loss in FCGR resistance at room temperature.

1.2. Effect of mechanical variables

1.2.1. Frequency

Among the variables capable of influencing the crack growth rate (FCGR), the loading frequency is an important one. Figure II shows the evolution of FCGR as function of the loading frequency at two temperatures and for several ΔK loading conditions [4]. From this set of curves, several comments can be made:

- for both temperatures the fatigue crack growth rate increases as the loading frequency decreases.
- the crack propagation path triggers from transgranular at high frequency to intergranular at low frequency. A transition frequency between these two propagation modes can be defined.
- the value of the transition frequency increases with ΔK .

This type of curve illustrates the competition between two damaging processes: a time dependent process associated with the interactions between oxidation and deformation and a cycle dependent damaging process related to the interactions between microstructures and deformation process. Under vacuum conditions the frequency effect is expected to be less important in terms of FCGR. Therefore, the transition frequency value can change with temperature, partial pressure of oxygen, and microstructure.

This conclusion would be sufficient if one assumes that no coupling exists between deformation and oxidation process. However, it has been demonstrated in several studies concerned with oxidation process of nickel-chromium [5] or Ni-based superalloys [6] that an important predeformation prior to oxidation promoted the instantaneous formation of a chromium oxide scale. This experimental fact could imply the following idea: A transition frequency under air conditions occurs when the amount of deformation stored ahead of the crack tip is high enough to change the oxidation behavior. Some consistent observations and chemical analysis have been done on transgranular fatigue crack surfaces, showing that they are covered by chromium oxide.

This idea was explored by Zeng and Ghonem [7]. The influence of high frequency loading on the subsequent low frequency crack growth behavior in Alloy 718 is studied. The results, indicate that a prior application of high frequency loading produces a reduction of the crack growth rate during the low frequency block. Consequently, the results obtained by the authors seem to be consistent with the idea of a deformation assisted oxidation process.

1.2.2 Hold time effect

Creep-fatigue effect on the crack growth resistance of Alloy 718 has been investigated by means of loading cycles with a trapezoidal shape. Basically, a hold time at maximum load is superimposed to a triangular fatigue cycle. In figure III, the effect of an hold time equal to 300s on the FCGR's is presented. Two sets of results corresponding to air and vacuum environment are reported.

It is worth noting that under air, the hold time effect is spectacular. The contribution of creep to the crack growth process is much more efficient than the fatigue one. Even in a da/dN versus ΔK plot the trapezoidal cycle remains more detrimental. The situation is quite different under vacuum conditions where the contribution of creep could be considered as "beneficial" for the crack growth process. This set of curves clearly illustrates the time dependency of the crack growth process under air and concurrently the cycle dependency under vacuum when the effect of microstructure and mechanical variables are considered.

1.2.3. Stress Ratio effect

Another way to point out these dependencies is to change the load ratio under constant K_{max} . In figure IV, the effect of load ratio on the FCGR is presented [4,8]. For comparison, a set of results corresponding to a low temperature, pure cycle dependent crack growth process is added. At very low frequency ($5 \cdot 10^{-3}$ Hz) the crack growth process is mainly time dependent. At higher frequency (1 Hz) the curve indicates very clearly that the FCGR is cycle dependent till R reaches 0.8. For the values larger than 0.8, there is an important increase of the FCGR which becomes definitely time dependent.

II. ENVIRONMENTAL EFFECTS

In this part, the results concerning the oxidation behavior of Alloy 718 are presented. Intergranular crack growth rate can reach under certain loading conditions $0.5 \mu\text{m/s}$. This experimental fact implies that the embrittlement process occurs during the early stages of the oxidation. Thus, the type of oxide formed during the onset of the oxidation process has a great importance on the further mechanical behavior of the material.

In figure V, elemental profiles resulting from an Auger electron spectrometry analysis are shown [5]. Mechanically and/or electropolished discs were subjected to oxidation at 650°C , during 8 min - under different oxygen partial pressures. It is observed from elemental profiles that when P_{O_2} is smaller or equal to 10^{-4} Torr, the first oxide to be formed on alloy 718, is chromium oxide. On the other hand, when the oxygen partial pressure exceeds 10^{-2} Torr the first oxide to be formed is a Ni-Fe rich oxide. Thus, it can be concluded from this analysis that selective oxidation of chromium occurs at low pressure. In spite of having a high chromium level, this Ni base superalloy is covered by a Ni iron rich oxide during the early stage of the oxidation process under air environment.

In figure VI, the oxidation sequence on an intergranular fatigue crack surface is presented [2]. The observation and analysis of the oxides ($0.1 \mu\text{m}$ thick) have been carried out by using XSTEM and diffraction techniques. Obviously, this oxide scale results from a long duration oxidation. It is interesting to note that the oxidation sequence is consistent with the one identified on polished transgranular surfaces. The first oxides to be formed are columnar Ni oxide grains and then a microcrystallised chromia subscale giving rise to the well known good static oxidation resistance of this alloy.

From these observations, one can expect strong interactions between deformation and oxygen partial pressure or between deformation and oxide thickness. This is the reason why specific fatigue crack growth tests have been carried out. The first test is concerned with constant ΔK FCGR measurements

under different oxygen partial pressures. A (10s - 300s hold time - 10s) cycle was applied. The results from this test are shown in Fig. VII. A transition pressure is defined below which the fracture mode is transgranular. When the oxygen partial pressure is greater than 10^{-3} mbar the fracture mode changes from transgranular to intergranular.

At first sight this transition pressure does not depend on ΔK . Further studies will be necessary in order to investigate the effect of frequency, and temperature on the value of the transition pressure.

It comes out from these results that there exists a parallel between the transition of oxidation process and the transition of FCGR. A striking correspondence appears between the two oxygen partial pressures required for the two preceding transitions to occur. There are good reasons to think that the Ni-iron rich oxide formation is responsible of the embrittlement of this alloy.

Some attention has been paid to the 2nd step of the oxidation sequence - i.e. - the formation of a subscale composed with chromia. This scale is often called the passive scale. AT 650°C, under air environment, the formation of this protective subscale is expected to be completed after several minutes (10-15min). A specific constant ΔK fatigue test was designed by Diboine and Pineau [9] to find indirectly the time required to passivate Alloy 718. In this test a hold time at minimum load was superimposed to a $5 \cdot 10^{-2}$ Hz triangular cycling. Different hold times (t_h) ranging from 0 to 30 min were used. The results of this test are shown in figure VIII. As t_h increases the crack growth rate increases till t_h reaches a value close to the one mentioned above i.e 20min. Again these results confirm the deleterious role attributed to the Ni oxide growth. Fortunately, they also show the beneficial effect of the chromia scale which stops the damaging process.

A two stage oxidation mechanism was then proposed [10]. An interesting experiment was carried out in the work of Ghonem et al [8] on a fine grain size (20-50 μ m) Alloy 718. They carried out crack growth measurement experiments on compact tension specimens during which the formation process of a continuous oxide scale was disturbed. This was achieved by applying high frequency minor cycle during the hold time at minimum load. The cycle shape is presented in figure IXa. The crack growth rate corresponding to these conditions was higher than that observed when the formation of a continuous chromia layer was not disturbed. This result shown in figure IXb, indicates that, by delaying the formation of Cr_2O_3 , the oxidation process continued, resulting in an increased crack growth rate.

III. INFLUENCE OF SLIP CHARACTER

One objective of this section is to bring experimental observations obtained on smooth or CT specimens of Alloy 718 in order to contribute to the knowledge of the relation between strain rate or loading frequency and slip homogeneity. Slip homogeneity is expected to play an important role in the crack propagation mode. Clavel and Pineau [11] studied the effect of strain rate and temperature on the slip band spacing in Alloy 718. They concluded that when the strain rate increases for a specific strain amplitude, the slip band spacing decreases, giving rise to a better homogenization of the deformation process at the grain scale. In figure X a curve illustrating this phenomenon is shown. When dealing with intergranular internal stresses induced by plasticity, one can expect an effect of the slip homogeneity on the level of these stresses. It is proposed that intergranular cracking is due to the combination of high level intergranular stresses and Ni-oxide growth.

Then, an attempt was done to estimate at least qualitatively the slip character below transgranular and intergranular fatigue crack surfaces. A decoration technique of the slip bands by δ phase precipitation was used [12]. Two CT specimens were heat treated and cut in order to study slip line traces distribution in the plane strain zone. A transgranular fracture surface produced during a high frequency test (30Hz) and an intergranular fracture surface resulting from a (10s - 300s - 10s) cycling were used. Some pictures corresponding to different ΔK levels in both tests conditions are shown in the work of Ghonem et al [8]. These pictures give interesting qualitative results. When the crack path is transgranular i.e. at high loading frequency the plastic zone ahead of the crack tip is generally much smaller than the grain size. Moreover the slip homogeneity increases with ΔK loading conditions, a lower slip line density and a larger plastic zone size. As ΔK increases, the slip line spacing decreases also.

IV. CONCLUSIONS

1) This program has allowed to review the effect of microstructural and mechanical variables on the fatigue crack growth rate behavior of Alloy 718. The emphasis was laid upon two extreme behaviors, one corresponding to a pure cycle-dependent regime, the other one to a pure time-dependent regime. The existence of these regimes is strongly dependent on microstructural variables, in particular grain size and grain boundary microstructure.

2) It is concluded from the work carried out at the Centre des Materiaux-Ecole des Mines that intergranular cracking of Alloy 718 at elevated temperature is due to two effects:

- (i) slip induced intergranular cracking induced by the inhomogeneity in slip character affected by strain rate effect.
- (ii) oxygen induced grain boundary embrittlement.

Detailed investigations have shown that in air environment oxidation of Alloy 718 occurs according to a two-stage mechanism, first the nucleation and growth of a Ni rich oxide scale followed by the growth of a Cr_2O_3 oxide film. Grain boundary embrittlement is associated with the formation of the Ni rich oxide. At lower partial oxygen pressure, chromium oxidation takes place directly. Under these conditions, no detrimental influence of environment is observed.

REFERENCES

- [1] J.P. Pedron and A. Pineau, *Mat. Science and Engineering*, vol. 56, (1982), pp. 143-156.
- [2] E. Andrieu, R. Molins, H. Ghonem and A. Pineau, *Mat. Science and Engineering*, vol. 154, (1992), pp. 21-28.
- [3] M. Chang, P. Au, T. Terada and A. K. Koul, *Superalloys 1992*, Edited by s. Antolovich et al., pp. 447-456.
- [4] S. Venkataraman and T. Nicholas, in *Effects of load and thermal histories*, Edited by P.K. Liaw and T. Nicholas, MTS, Warrendale, Pa, 1987, pp. 81-89.
- [5] C.S. Giggins, F.S. Pettit, *Trans. Met. Soc. AIME*, vol. 245, (Dec. 1969), pp. 2509-2514.
- [6] E. Andrieu, *Influence de l'environnement sur la propagation des fissures dans une superalliage base nickel: l'Inconel 718*. Thesis Ecole des Mines de Paris, (1987).
- [7] D. Zheng and H. Ghonem, *Frequency interactions in high temperature fatigue crackgrowth in superalloys*, *Mets. Trands*. Nov. 1992, pp. 3067-3072.
- [8] H. Ghonem, T. Nicholas and A. Pineau, *Symp. on High Temperature Effects ASME Winter Annual Meeting*, Atlanta, GA, Nov. 1991.
- [9] A. Diboine and A. Pineau, *Fatigue and Fracture of Engineering Materials and Structures*, vol. 10, (1987), pp. 141-151.
- [10] E. Andrieu, R. Cozar and A. Pineau, *Superalloys Metallurgy and Applications*, ed. by E.A. Loria, Pittsburgh, Pa, ASM, (1989), pp. 241-247.
- [11] M. Clavel and A. Pineau, *Mat. Science and Engineering*, vol. 55, (1982), pp. 157-171).
- [12] M. Clavel and A. Pineau, *Metallurgical Transactions*, vol. 9A, (1978), pp. 471-480.

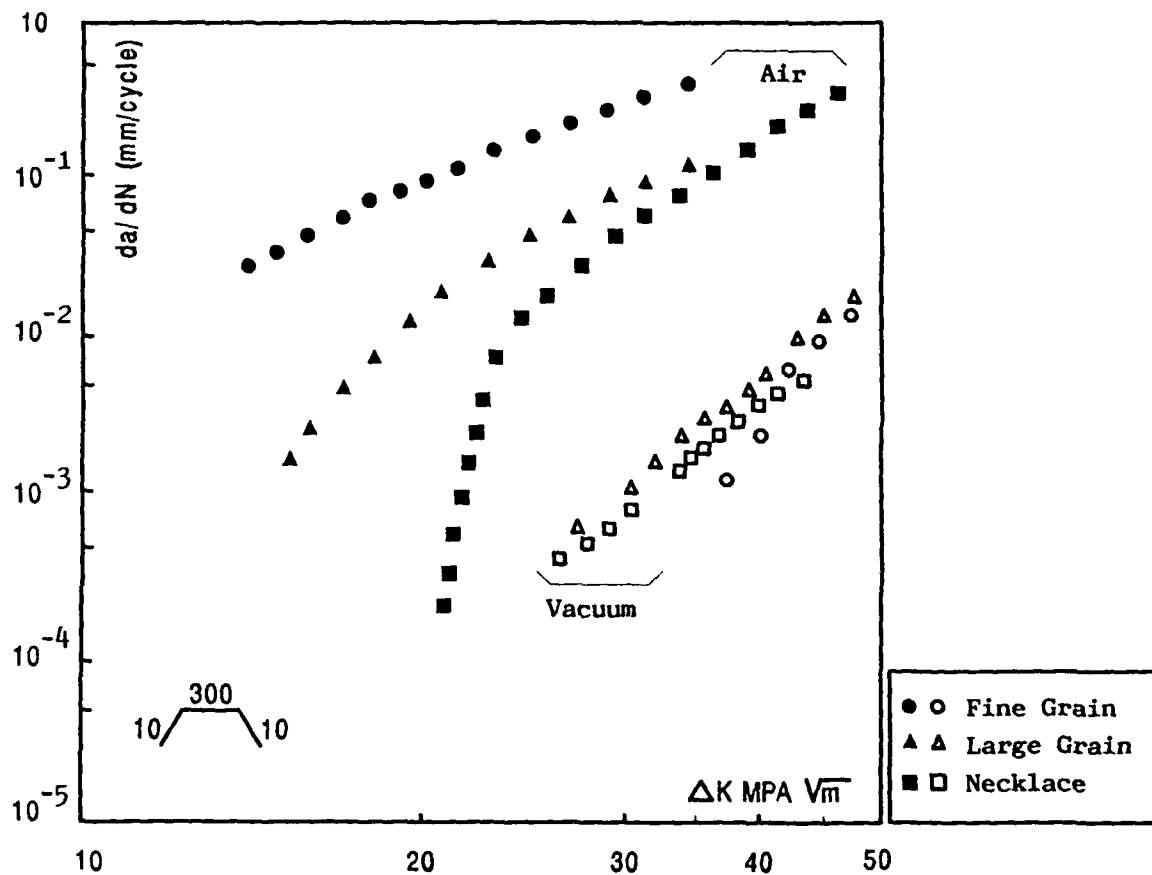


Figure I - Effect of microstructure on the fatigue crack growth rate at 650°C .

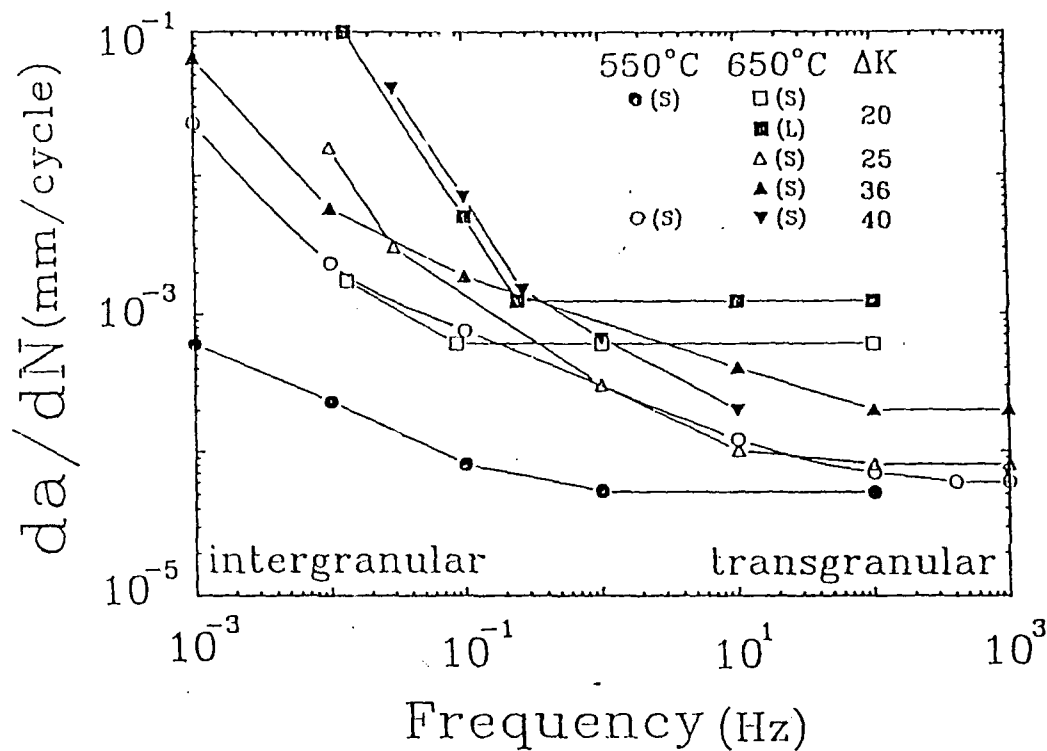


Figure II - Loading frequency effect on F.C.G.R. at 650° and 550°C.

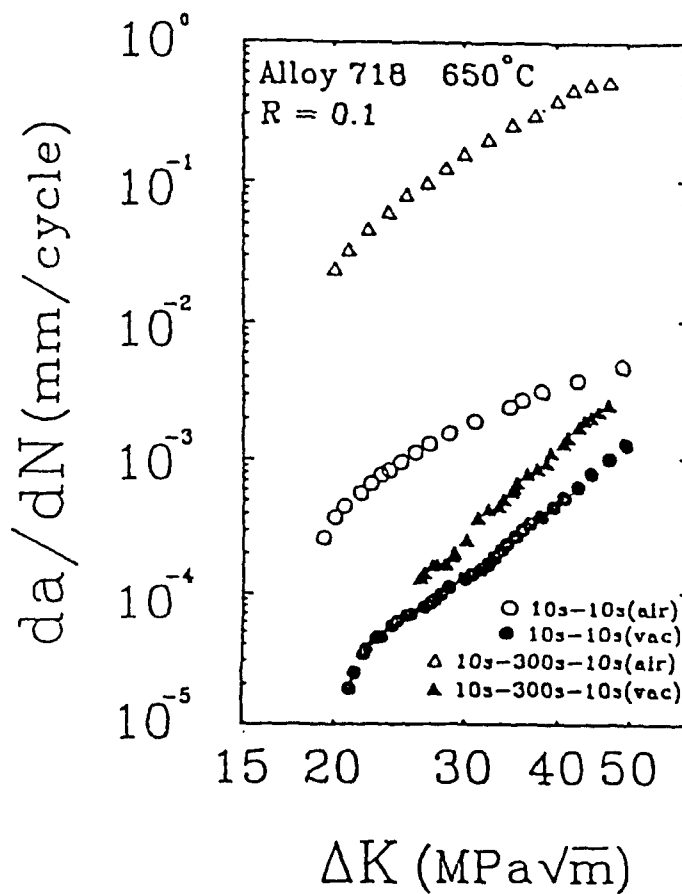


Figure III - Effect of hold time at maximum load on the FCGR at 650°C.

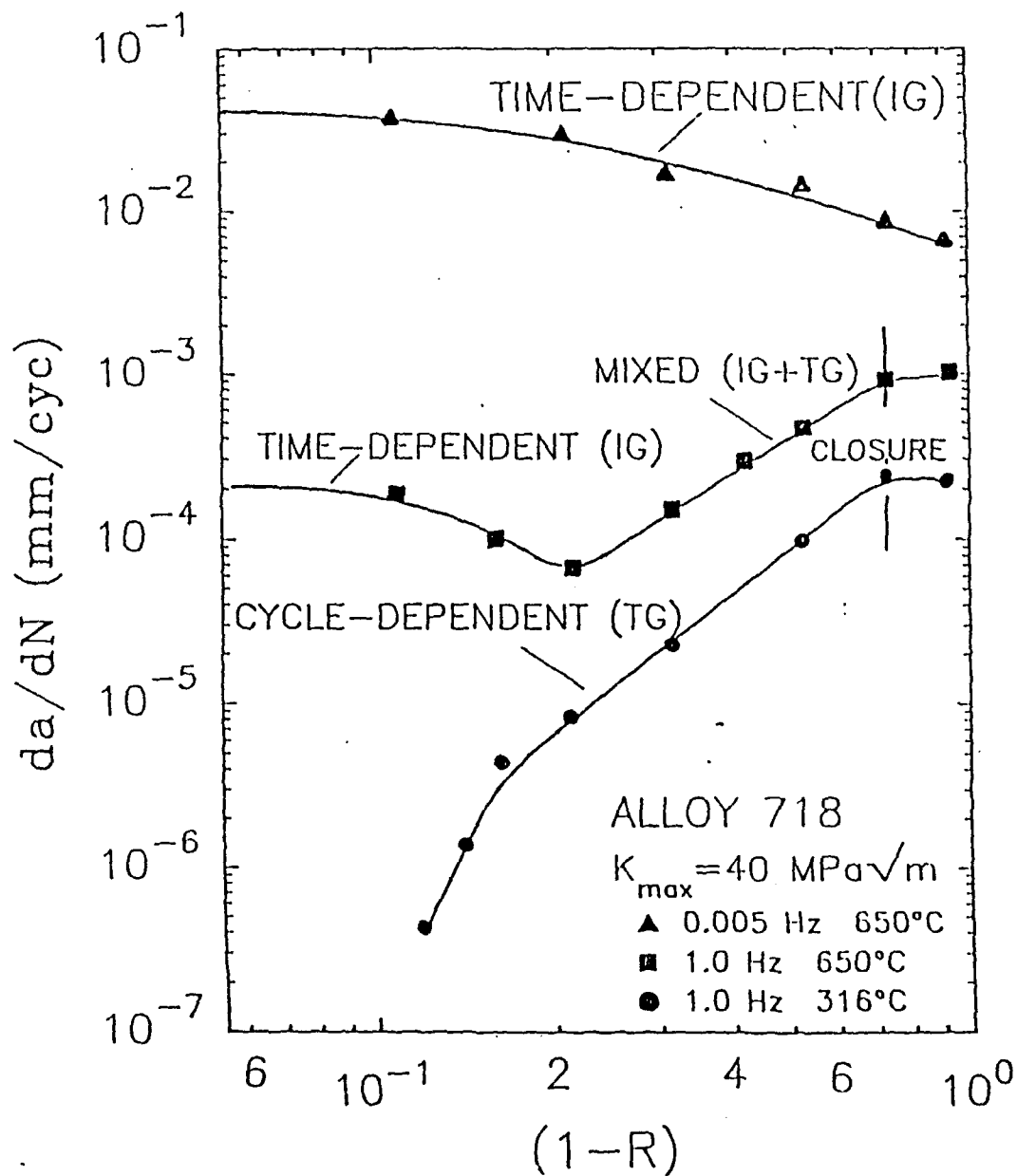


Figure IV - Effect of loading ratio and frequency on the FCGR at 650°C.

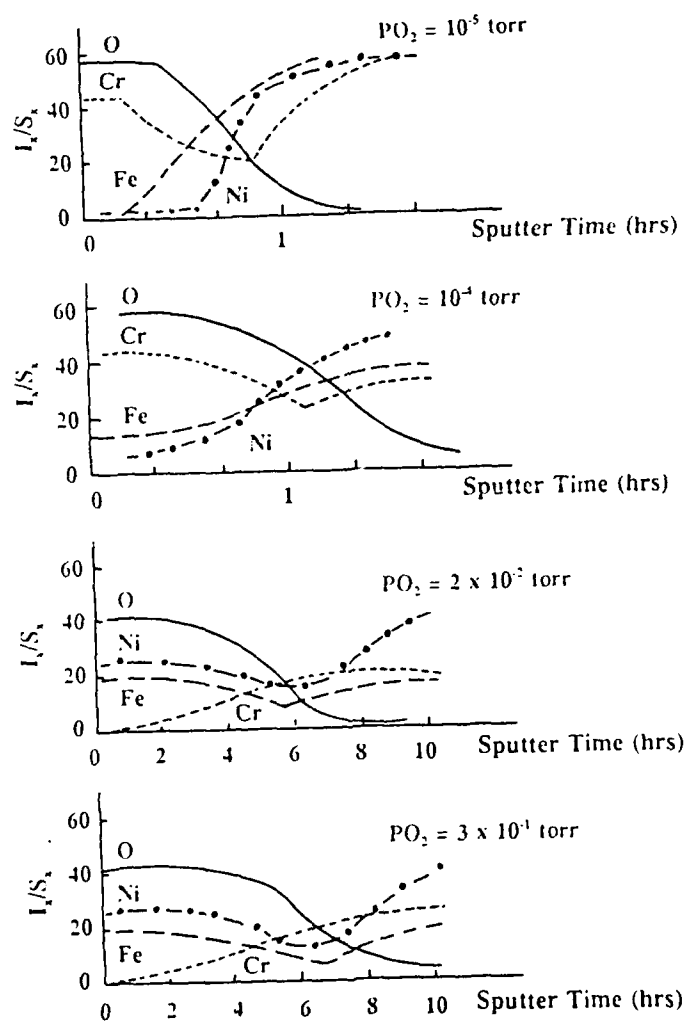
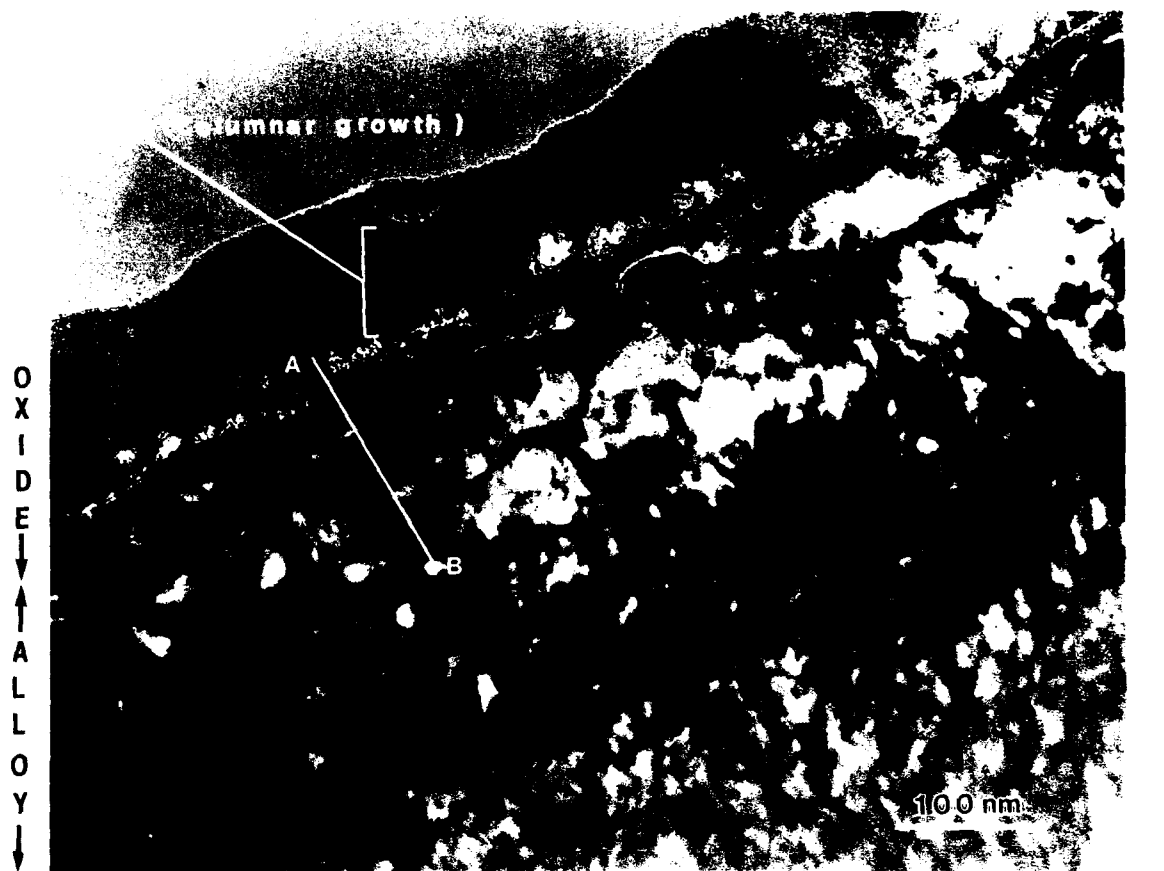


Figure V- Effect of oxygen partial pressure on A.E.S. elemental profiles of oxidized samples, t_{ox} 8 mn - $T = 650^\circ\text{C}$.



Elemental line scan through the interface (200 nm)

A → B

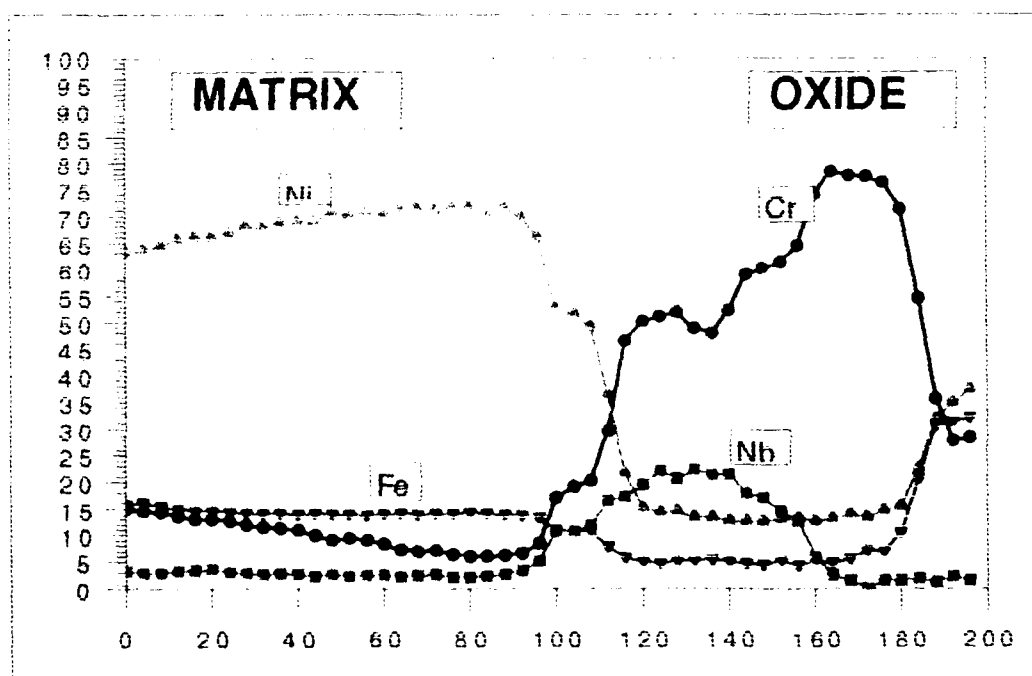


Figure VI - TEM micrograph and microanalysis of oxides developed on a fatigue fracture surface.

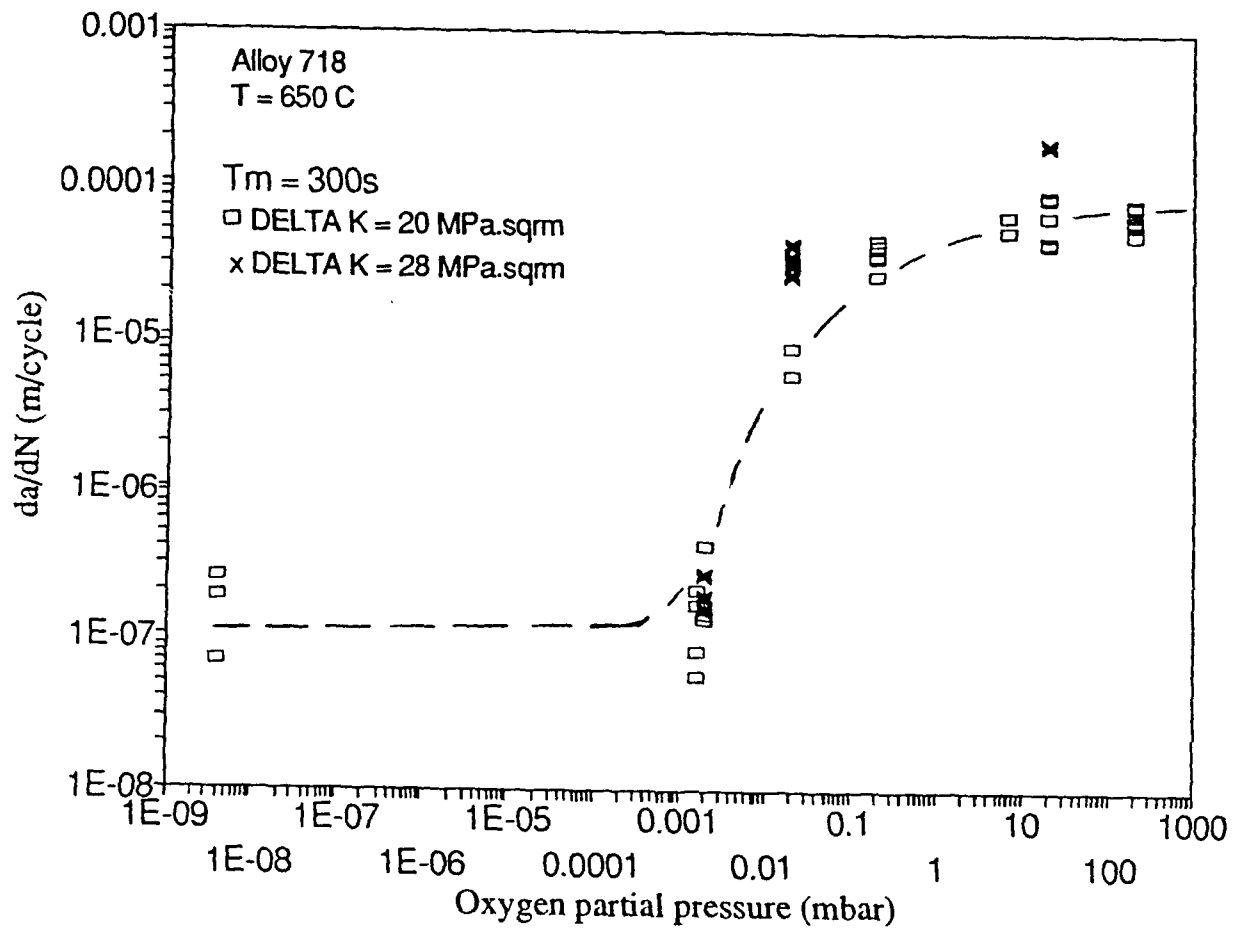


Figure VII - Effect of oxygen partial pressure on the F.C.G.R. of Alloy 718.

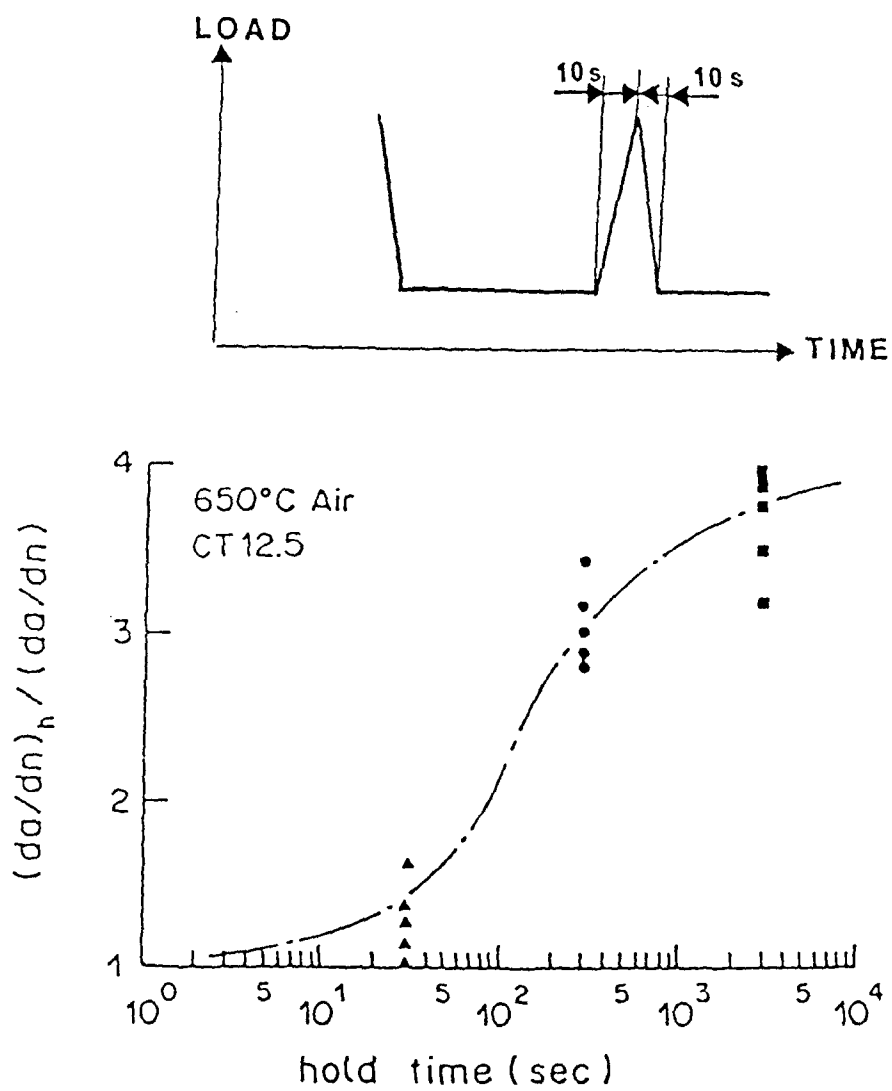
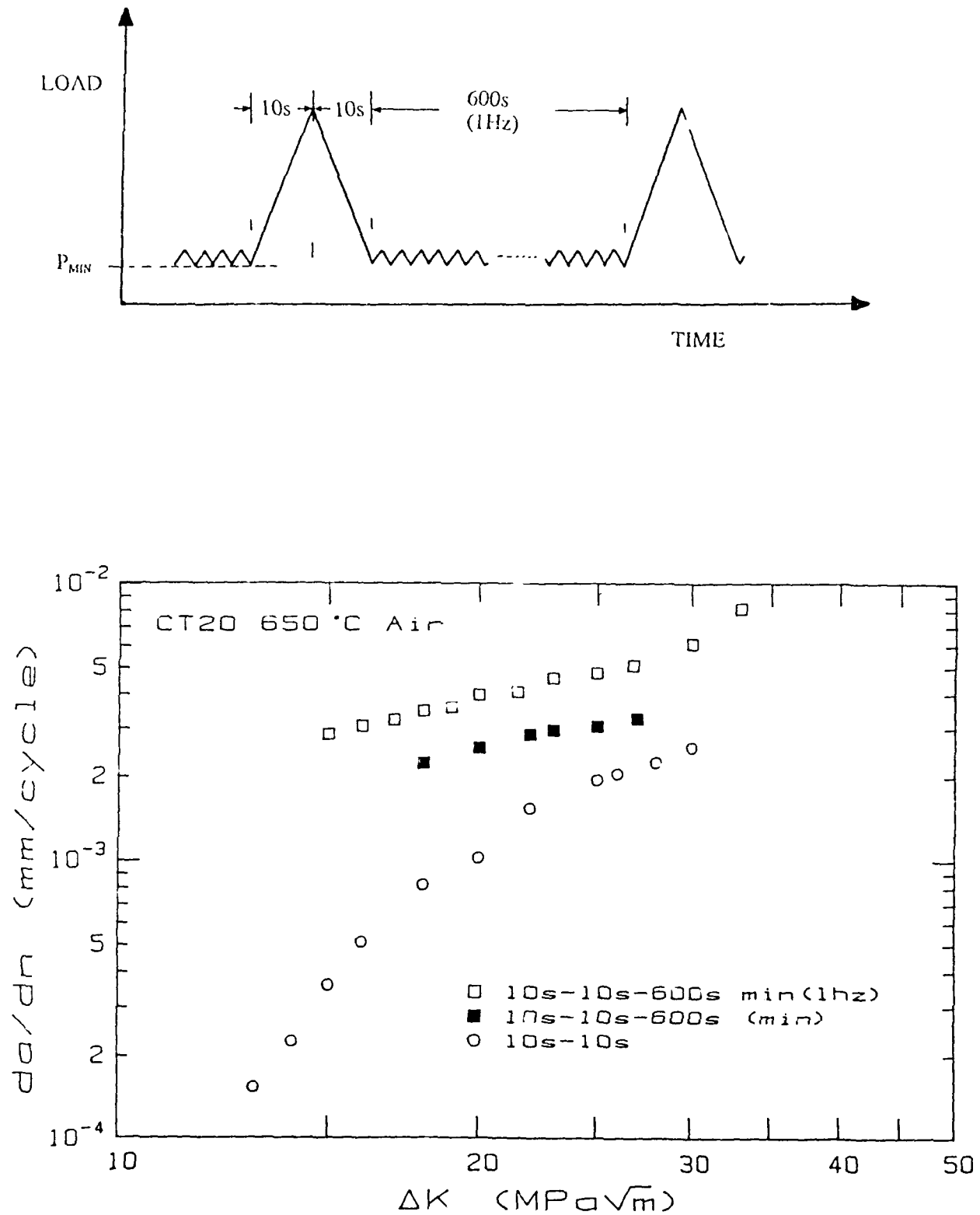


Figure VIII - Effect of hold time at minimum load on the F.C.G.R.



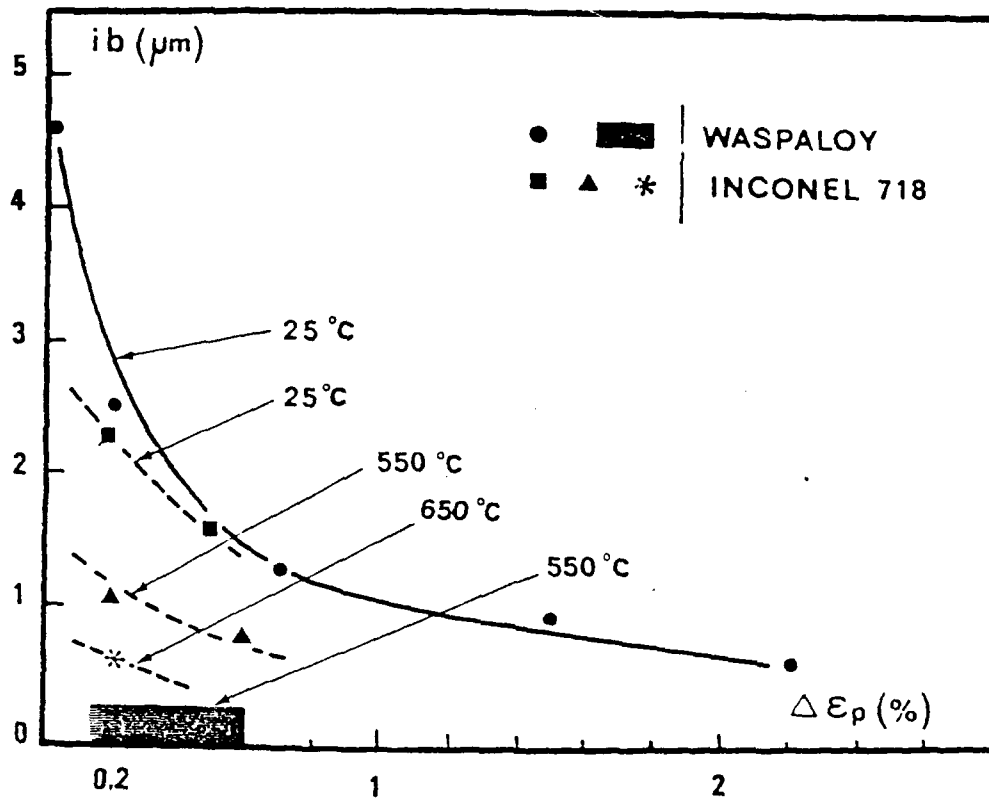


Figure X - Slip band interspacing evolution as function of temperature and strain amplitude.

PART II

ENVIRONMENTAL INTERACTIONS IN HIGH TEMPERATURE FATIGUE CRACK GROWTH OF Ti-1100

ABSTRACT :

The crack growth behavior of Ti-1100 is investigated for loading frequencies ranging from 30 Hz to 0.005 Hz at temperature levels extending from 23°C to 650°C in both air and vacuum environments. Two types of time-dependent damage mechanisms have been identified; oxidation and creep effects. It is concluded that the effect of oxidation on the crack growth acceleration is rapid and constant in relation to the frequencies tested and is weakly dependent on cycle time. Creep effects, on the other hand, are dominant at low frequencies in both air and vacuum and are loading-rate dependent. The degree of contribution of each of these two damage modes during the steady state growth region has been determined by examining the frequency response of the exponent and coefficient parameters of a Paris-type equation. It is found that these parameters are largely determined by the extent of the viscoplastic response of the crack tip region. Furthermore, the physical mechanisms involved in the effect of these damage modes on the crack tip reaction are identified by determining the nature of the crack tip plastic work input as function of loading frequency. The influence of frequency and environment on crack closure and on the appearance of a knee associated with stage-I/stage-II transition is also discussed.

1. INTRODUCTION

Results from air and vacuum crack growth tests carried out on high strength alloys intended for the use in elevated temperature applications often show a significant increase in both fatigue crack propagation resistance and low cycle fatigue strength with removal of air environment [1-5]. This improvement is generally accompanied by a change in fracture mechanism and a modification in fracture surface morphology. Numerous studies have been carried out on these alloys in order to identify the nature of crack tip damage occurring under varied temperature, loading frequency, load geometry, and environmental test conditions, see a review in Ref. [6]. In these studies the detrimental effect of environment was linked to a wide selection of damage processes including crack closure, grain boundary sliding, hydrogen embrittlement and crack tip oxygen diffusion or gas adsorption. The role of each of these mechanisms is further complicated by the fact that, within a single environment, many materials experience ranges of loading frequency in which other time-dependent responses, in particular creep, could exist thus modifying or accelerating environmental damage effects. High temperature titanium alloys, such as Ti-6Al-4V, IMI-829 and Ti-6242

which are susceptible to creep, are affected to a great extent by this type of combined creep-environment-fatigue damage [7]. Recognizing this fact, a new silicon bearing near alpha titanium alloy was developed by TIMET to provide an optimum level of creep and fatigue performance at temperatures up to 593°C. The nominal chemical composition of this alloy which is known as Ti-1100 is: Ti-6Al-2.8Sn-4Zr-0.4Mo-0.45Si-0.07O-<0.03Fe. The work of Bania [8,9] describes in details the microstructure characteristics of this alloy and compares its uniaxial mechanical properties with other β -processed, near-alpha titanium alloys. Ghonem and Foerch [10] have studied the effect of loading frequency on fatigue crack growth behavior of Ti-1100 at 593°C. In their work, the influence of low and high frequency was examined in both air and vacuum environment. While the results has established the role of environment on the crack tip damage, it did not however examine the synergism of time dependent effects due to elevated temperature crack propagation in the pure cyclic and creep-fatigue regimes. This paper will attempt to explore the interrelated effects of these regimes in order to identify the boundary of each corresponding damage mechanism which is an important step towards formulating quantitative damage models pertaining to the Ti-1100 in particular as well as to the near-alpha Ti alloys in general. The first part of this paper describes the experimental procedure and results followed by a detailed analysis of the role of environment, frequency and closure in interpreting these results.

2. EXPERIMENTAL PROCEDURE

Billets of Ti-1100 with the nominal composition described above were rolled above the beta transus to obtain 12 mm plates followed by a solution anneal with air cooling and an 8 hour aging at 593°C. A Widmanstätten microstructure was produced consisting of aligned alpha platelets and regions of basketweave structure contained in large prior- β grains. This microstructure is considered to give good creep performance, while allowing crack growth retardation through bifurcation, deflection, and other crack tip redirection processes.

Fatigue crack growth tests were performed in air and high vacuum (5×10^{-8} Torr, 6.6×10^{-6} Pa) at both room and elevated temperatures (23°C, 593°C and 650°C). All tests utilized compact tension specimens machined with the crack front perpendicular to the rolling direction (L-T). Two specimen geometries were employed, CT-12.5 (W=25, B=6 mm) for tests in vacuum and CT-20 (W=40, B=10 mm) for tests in air. Specimen loading was achieved using closed loop servo-hydraulic test frames equipped with computer data acquisition and control systems. Crack length was measured remotely using the direct current potential drop method, supplemented when possible by optical and compliance crack length measurements. In air, crack closure was measured with the use of a clip gage placed directly in the specimen mouth for all room temperature tests, and with an appropriate extension for elevated temperature tests. Closure was not measured in vacuum with the exception of the 0.5Hz, room temperature test. Other experimental details related to the FCGR tests can be found in Ref. [10].

All the test specimens generated during the experimental portion of this work were examined extensively using SEM and optical techniques. Quantitative measurements of fracture mode were taken by summing like zones of fracture morphology in a modified linear intercept method.

3. EXPERIMENTAL RESULTS

The experimental and analytical philosophy followed in this study was to specifically identify the environmentally related aspects of elevated temperature fatigue crack propagation in Ti-1100. Because the elevated temperature fracture process involves both oxidation and creep damage mechanisms, the test matrix design was based on a series of loading frequencies to be run in air and vacuum environments. In addition, environmental effects were considered only for the localized process of fatigue crack propagation in long cracks - results for crack initiation or small crack behavior are likely to display different characteristics than that seen here under similar test conditions.

3.1 Material Behavior and Microstructural Characteristics

The average prior- β grain size was $\approx 550\text{ }\mu\text{m}$ and the average aligned alpha colony size was $\approx 40\text{ }\mu\text{m}$ as determined by a simple linear intercept method, see Fig. 1(a). The distribution of colony size (intercept length) in terms of cumulative frequency is shown in Fig. 1(b). Transmission Electron Microscopy revealed almost no beta phase layer between the alpha plates or even at colony boundaries. This observation is in keeping with the relatively small amount of beta stabilizing elements in the alloy. In addition although the material was air cooled from the forging temperature and received an 8 hour aging treatment at 593°C , neither precipitates of Ti_3Al nor silicides were apparent in this condition. Prior- β grain boundaries were not contained in the thin regions of the prepared foils so that comment cannot be made regarding precipitation at the grain boundary.

The tensile tests results for various strain rates at 593°C showed almost no strain rate sensitivity for the yield stress. In addition, the stress-strain curves showed broad serrations similar to those observed by Rack [11] and work by Bania [9] shows a plateau in the test temperature vs. yield stress curve indicating that the yield stress has a lack of temperature dependence for temperatures from about $300\text{--}550^\circ\text{C}$. This combination of features is often cited as indicative of dynamic strain aging, a process which has been linked to both silicon and oxygen alloy content in other titanium alloys [12].

3.2 Crack Growth Tests

Experimental data from crack growth tests carried out in air environment are shown in Fig. 2. Results from vacuum tests are shown separately in Fig. 3. Examination of this data supports observations made in Ref. [10] that in this alloy a significant frequency and temperature influence on crack growth rate exists in both air and vacuum environments. Comparison of the air and vacuum results also shows a general improvement in fatigue crack resistance at all loading frequencies in vacuum at both room and elevated temperatures. Note, however, that the improvement in vacuum is most pronounced at lower ΔK , while the effect decreases as ΔK increases.

The data for some high temperature tests, especially in vacuum, show a knee in the FCGR curves at low values of ΔK similar to that frequently observed in other materials at elevated temperature and which is attributed to a change in crack growth mechanism [10,13,14]. At high values of ΔK there is an increase in slope and a convergence of all curves to a single line indicative of the approaching K_{IC} value where environment and creep components are of lesser consequence. Such changes in growth behavior are traditionally labeled as stages I, II, and III, for microstructurally sensitive growth at low ΔK , linear Paris law steady state growth, and nearly unstable fracture regions respectively.

The stage I to II knee is seen to be most pronounced at elevated temperature in the 10 Hz, 0.5Hz, and 0.05 Hz vacuum tests and also in air tests run with frequencies less than 0.05 Hz, while it is relatively absent in air and vacuum at 23°C. Previous explanations for this behavior have varied for different materials under different loading conditions. One should recognize, however, that the change from stage I to stage II needs not be accompanied by a noticeable knee in the curve as shown by Yoder [15] and this is indeed the case in this material under certain conditions as will be discussed in a later section.

It is also observed that, within the stage II steady state behavior, there is a consistent change in slope of the curves, such that the Paris Law exponent decreased with increased cycle time and with increased temperature in both air and vacuum environments. These results are consistent with damage effects produced by combined environmental embrittlement and creep deformation.

In order to explore the link between viscoplastic effects and loading rate, two crack growth tests have been run in air environment at 593°C at a frequency of 0.05Hz but with an asymmetry between the loading and unloading portion of the cycle (1-19sec and 19-1sec) [10]. The basic assumption made here is that environmentally dominated processes are driven by a diffusional mechanism that is dependent on the value of ΔK and the total cycle time, but with little dependence on the waveform symmetry [5]. In contrast, creep deformation will, in general, be dependent on the crack tip loading rate [16,17]. This is due to the fact that the rising portion of the cycle creates an effective tensile load on the crack tip plastic zone thus promoting the spread of viscoplasticity and increasing the maximum crack tip opening displacement. A decreasing loading rate leads to an increase in these effects. Upon unloading, stresses within the reversed plastic zone could become compressive and time dependent deformation could still occur. On the other hand, a fast loading rate would inhibit time dependent deformation and the degree of viscoplastic strain created with a prolonged unloading would, in this case, be limited by the crack faces closing. This argument is supported by the results plotted in Fig. 4 which shows that the 19sec-1sec test has produced faster crack growth than that obtained in the 10sec-10sec and the 1s-19s tests, with the most significant difference occurring at low ΔK . Taking into consideration the assumption that in Ti-1100 the influence of environment is rapid and weakly dependent on the loading frequency, as will be discussed later, these results indicate that viscoplastic effects are significant in explaining the observed increase in crack growth rates with the increase in cycle time.

Temperature effects for the group of tests run at 10Hz are presented in Fig. 5 as crack growth rate versus $(\Delta K/s_{ys}E)$. When ΔK is normalized by yield and modulus changes, there is only a small enhancement of environmental effect when considering a change in temperature from 23°C-650°C. Indeed, the variation in growth rate in air is less than the difference in vacuum, which had a partial pressure of oxygen well below that calculated for even a complete monolayer (10Hz loading) [18].

Crack closure is shown in Fig. 6 as the ratio of the effective ΔK to

nominal ΔK versus nominal ΔK . Fatigue crack growth studies on near- α alloys have identified the importance of crack closure mechanisms [19,20]. In previous work on Ti-1100 under variable loading frequencies it was noted that closure was significant at low ΔK loadings, particularly at room temperature [10]. The effect of closure on a da/dN vs. ΔK plot is to decrease the slope of the FCGR curve, especially in the stage I region. In addition, under decreasing frequencies, where the knee is most evident, the closure levels are found to be much reduced, not significantly altering the shape of the growth curve. The results from the 0.5Hz 23°C vacuum test show a level of closure which is very similar to but slightly less than that of the 10Hz, 23°C air test.

3.3 Microscopy and Fractography

The fracture morphologies seen in Ti-1100 under the test conditions run in the present investigation have been classified as follows:

1) At low ΔK , in air and vacuum, growth takes place in a cyclic cleavage process largely along the basal plane, with furrows connecting the cleaved planes [21-23]. Cleavage is promoted by the Widmanstätten microstructure in which the α phase platelets have the same crystallographic orientation within a colony. The colony diameter is often considered the minimum controlling microstructural parameter [24,25]. In addition, based on the prior BCC structure, different colonies within the same prior- β grain are related by the fact that only 12 variants in α platelet orientation exist in the Widmanstätten microstructure [26]. The colony boundary provides a barrier for dislocations, and accumulated dipole pileups on the basal plane initiate cleavage damage [27], however, due to the Burgers relationship among colonies, slip can extend past this barrier (more easily than a grain boundary, for example) since single, multi-colony facets have been observed [28] in titanium alloys with a similar microstructure. Fracture surfaces from test run in air and vacuum displaying the quasi-cleavage fracture morphology are shown in Figs. 7. It can be seen in Fig. 7(a) that the cleavage process in air is much more glassy in nature than cleavage features in vacuum which has less distinct with a highly textured, ruptured appearance in places. This difference is not unique to titanium, as a very similar morphology can be seen for a stage-I crack in a nickel based superalloy, where the textured surface has been ascribed as the result of increased slip reversibility and increased surface energy in vacuum environment [29].

2) Stage-II growth in air is characterized by striations, Fig. 7(c) which are clearly defined and their spacings accurately represent the crack growth rate. The local crack growth direction indicated by the striations was seen to vary a great deal showing that the local crack growth is often quite different from the macroscopic growth direction. In vacuum, a striation-like morphology was observed as vague ripple patterns which are discontinuous along their length, and often do not have a constant step distance between two lines, Fig. 7(d). The notion of striations existing in vacuum is a controversial subject; while many authors have given reasons to the unexpected appearance

of striations, see for example Refs. [30,31], other authors have observed distinctive striations in vacuum at elevated temperature [5]. In the present results, the observed fracture surface ripples are classified as representing a non-crystallographic, continuum fracture mode and as being analogous to the striated growth seen in air. The surface morphology on which the crack has propagated shows significant similarity to that of the clearly defined air striated regions and is distinctly different from the quasi-cleavage surface seen at lower ΔK in vacuum. In particular, note the appearance of bowed crack fronts, bowled fracture planes, and intersecting cleavage planes perpendicular to the growth plane (Fig. 7b). In addition, the first appearance of the striation-like fracture surface coincides with the position of the knee in the vacuum crack growth curves, further supporting the observation that this morphology represents a mechanism of crack growth which is distinct from the quasi-cleavage mode of growth. In the discussion section, vacuum striation-like morphology will be taken as representative of a homogeneous, symmetric deformation mode, where the crack tip sees a continuum field, even though the growth rate is not directly correlated with the ripple spacings.

3) High ΔK loading at low frequencies and elevated temperature yields intergranular prior- β grain boundary fracture [10]. Air and vacuum intergranular modes display the same rough texture appearance. One of the possible reasons for this rough surface results from the nature of the prior- β grain boundary structure. Upon transformation from the β field, the alpha colony microstructure grows from various nucleation points within the grain towards the existing layer of the primary alpha phase at the grain boundary. The intersection of the primary alpha layer and the transformed alpha colonies has a jagged sawtooth mating surface which could account for the rough intergranular appearance.

Intergranular fracture was seen to begin at a higher frequency in vacuum tests than in air with mixed trans- and intergranular fracture in vacuum at 0.05Hz while in air at the same frequency, fracture is fully transgranular. Fully intergranular fracture in air was not observed until very high ΔK level in the 0.005Hz test, the percentage of intergranular fracture in the 0.05Hz vacuum tests specimen being approximately equal to the 0.005Hz air test. Five minute hold time at maximum load gave fully intergranular fracture in both air and vacuum environments over the entire range of ΔK tested.

All the above modes of fracture represent regions of fracture surfaces in which they dominate the surface, with the remainder being made up of an indistinct rupture morphology. Transition points in fracture mode from cleavage to 50% striations, and from transgranular to 50% intergranular are shown in Fig. 8. In cases where partial intergranular fracture was seen, the striated area has been recorded as a percentage of transgranular surface. It is seen that a homogeneous striation-like growth occurs at a much lower ΔK in vacuum than in air environment, and also intergranular growth takes place in vacuum at lower ΔK and at higher frequencies than those in air.

Examination of etched cross sections of crack tips from intergranular

tests shows cavities located on the prior- β boundary directly ahead of the crack tip. Cavitation was never seen to expand ahead of the crack tip beyond one grain boundary. This observation suggests that intergranular damage in this material is a product of the crack front generated planar slip bands impinging on a microstructural boundary [32]. Materials which accumulate creep damage ahead of the crack due to grain boundary sliding in the ligament elastic field contrast with the present mechanism because that damage process acts in parallel; the crack propagating through already damaged material. The present case is a synergistic problem requiring the description of the spreading of the viscoplasticity in the crack tip zone. The barrier to slip and ease of separation of the unique grain boundary alpha phase layer is also concluded to be much greater than the alpha colony boundary when creep mechanisms are active since "inter-colony" fracture; which might seem to be a viable mode in this type of microstructure, was never clearly identified as a mode of fracture.

Fig. 9 displays surface slip and microcrack traces from four loading frequencies in 593°C vacuum environment at a $\Delta K=25\text{MPa}\sqrt{\text{m}}$. Note that plastic zone sizes are much larger, and less homogeneously deformed as loading frequency is decreased, even within the 0.5Hz loading condition. In addition, the slip traces seen here have a high tendency to crack, forming a large damage zone around the crack tip. Although the present results are obtained in high vacuum, the structure of these cracks are very similar to those identified by Vesier and Antolovich [33] as craze cracks due to surface oxygen embrittlement in Ti-6242 tested in air environment. In the 10s-300s-10s condition, it is also seen that slip lines have been able to pass by alpha colony boundaries relatively uninhibited, and zones of fracture appear to have occurred some distance from, but parallel to the primary crack path.

4. ANALYSIS AND DISCUSSION

4.1 The Nature of Environment Damage

Environmental influence on FCG of metallic materials at elevated temperatures has been seen to manifest itself by one or a combination of the following mechanisms:

(i) Short range stress directed diffusional mechanism where a brittle oxide layer is formed at the crack tip and subsequently fractured by the cyclic process. Time dependent growth due to environment is considered to be proportional to the oxide diffusion depth [5]. (ii) Long range stress directed diffusional mechanisms which may include a multi-layer stable oxide growth or large depth of penetration by oxygen effectively creating a boundary layer of modified alloy in the region of the crack tip. For a stressed crack tip region, this effect will alter the plastic and viscoplastic constitutive response, and therefore the mode of growth. This notion is not easily

quantified and has received limited attention in the literature [1,34]. However, titanium alloys may be subject to this type of influence because of the high solubility of oxygen and high rate of diffusion at elevated temperature [35].

(iii) Adsorption processes requiring the formation of a complete monolayer on the fresh crack surface which lowers the energy required to form new crack surface and which limits the phenomenon of rewelding and reversibility of slip. The absence of this mechanism is often held responsible for the vague appearance of striations in vacuum [2,22].

(iv) Oxide induced crack closure mechanisms which may involve the formation of oxide wedges at the crack tip, or perhaps an indirect mechanism in which the environment alters the nature or extent of roughness induced closure [36].

From the comparison given in Fig. 5, the short range brittle oxide mechanism (i) described above is not evident in our results, since it would be expected that a temperature increase from 23°C to 650°C would promote oxide formation through enhancement of diffusion, but bulk yield and modulus changes were found to be sufficient to consolidate the growth rate curves. It could be argued that 10Hz is too high a frequency to allow environmental effects to influence the crack growth process. This is, however, contrary to the observation that environmental effects are seen when comparing vacuum and air results at 593°C at 10Hz. Likewise, the oxide induced closure mechanism was not found to play a significant role in fatigue crack growth behavior of this alloy. The lack of spalled oxide traces on the fracture surface, lack of enhanced oxide coloration in the low ΔK growth region [2], and closure trends between room and elevated temperatures with closure levels being highest in room temperature, and decreasing with cycle time at elevated temperature [10] support this conclusion. However, significant closure levels in vacuum at room temperature indicate that closure remains an important issue and will be discussed in the next section.

The fact that an environmental effect exists but is weakly temperature-dependent lends credence to a mechanism like (ii) and (iii) above where the environmental effect is through a fast, stress induced, non-Arrhenius type of diffusion, and/or through an adsorption mechanism. Either of these mechanisms or their combined effects appears to "saturate" even at a frequency of 10Hz. This observation will be used later as basis for the notion, which will be developed shortly, that increases in crack growth rate at 593°C in air at frequencies lower than 0.05Hz are due primarily to viscoplastic effects and not environmental effects.

4.2 The Environment and Crack Closure

As mentioned earlier, closure measurements in vacuum have not been obtained except for the case of 0.5Hz at room temperature. However, at elevated temperature, indirect evidence exists that closure may be responsible for the appearance of distinct knees in the vacuum crack growth rate curves.

In air, the existence of knees are found to be the result of a combination of crack closure and some transient effects and not due to a change from stage I to stage II growth mechanisms. This conclusion was reached as a result of constant ΔK tests carried out at low ΔK ($\approx 7 \text{ MPa}\sqrt{\text{m}}$) for which da/dN values fell on the line extended from the stage II region curve. Furthermore, on the basis of fracture surface analysis, the position of the apparent knee in air was found to be at a much lower ΔK value than that at which the transition from quasi-cleavage to striations occurs. The existence of knees as an indicator of transition from stage I to stage II growth is discussed in the work of Yoder [15] in which the sharpness of the knee is directly related to the narrowness of the distribution of aligned alpha colony sizes in the microstructure. The colony size distribution in Ti-1100, as displayed in Fig. 1(b), is more broader than that studied by Yoder in his work on Ti8Al1Mo1V where the knee has all but disappeared. It follows then that the appearance of a knee in vacuum represents an anomaly which could not be attributed to transient effects in part because of the long region of growth ($\approx 2\text{mm}$) that it represents and for the following arguments. One argument considers the possibility that increased viscoplasticity in vacuum environment has the effect of reducing the importance of the smaller alpha colonies so that the colony size distribution is essentially made narrower thus producing a sharper knee. However, this explanation is not supported since the effect is seen even at 10Hz where viscoplasticity should not play an important role. Also, comparing the results of the 10Hz and 0.05Hz tests in vacuum, it can be seen that the knee is least sharp in the 0.05Hz case which is inconsistent with the idea that greater viscoplasticity effectively sharpens the colony size distribution and the knee.

Another argument to explain the existence of knees in vacuum is based on the enhanced crack tip closure in vacuum. Here the sharper knee in the 10Hz vacuum test compared to that of the 0.05Hz in vacuum agrees with the trend towards higher closure levels with increasing frequency as has been observed in air tests [10]. Furthermore, the observation that the onset of formation of striations in vacuum coincides with the appearance of the knee could be caused by a closure mechanism which changes abruptly when the fracture mode changes from quasi-cleavage to a striated-like mode. A final comment in support for high closure levels in vacuum can be seen in Fig. 10. In this case, the precracking was carried out in air by applying a cycle load with mean level of $R=0$ in order to reduce closure caused by possible existence of crack surface asperities. In performing the vacuum testing, closure begins to develop immediately and continues during the crack growth over a considerable length. Current efforts of the authors are directed towards obtaining closure measurements in vacuum testings at elevated temperature conditions

4.3 The Frequency Effect

The FCGR results from 593°C in vacuum indicate clearly a frequency effect which is independent of the environment. The results from air tests, in which environmental effects are expected to play a role, display trends similar to those of vacuum tests, while showing an overall higher crack growth rate for a given condition. This behavior could, in a simple approach, be expressed by employing a Paris-type equation that would incorporate both the frequency effect seen in vacuum and the environmental effect seen in air into the coefficient, C , and exponent, m , of this equation which would then be written as:

By applying this equation to all test conditions at elevated temperature, one obtains relationships between the exponent, m , and coefficient, C , and the test frequency as shown in Figs. 11(a) and 11(b). It is seen that in air and vacuum tests there is a dependence on loading frequency for both parameters; in particular for air environment at frequencies below 0.05 Hz and in vacuum below 0.5 Hz. The nature and magnitude of frequency effect for both conditions below these transitional frequencies is very similar and, assuming that no oxidation effects are present in vacuum, it can be concluded that creep related effects dictate the response of crack growth to frequency.

Environment effects are seen to be most significant at frequencies above 1 Hz, where there is a large difference in both the coefficient and the exponent. This does not mean that the effect of environment decreases with increasing cycle time, but rather that another time-dependent process, such as creep, becomes the controlling factor at lower frequencies. At frequencies lower than the transitional frequencies mentioned above, the Paris exponent decreases rapidly as a logarithm of frequency and is independent of environment. Meanwhile, at these frequencies, the coefficient parameters from the air tests show a constant scaling compared to the vacuum results. This scale value, which can be taken as a direct measure of the environmental effect, results in about a three-fold crack growth rate increase between vacuum and air tests. It is significant that this scale factor is practically independent of cycle time, indicating a mechanism of environmental effect which is fast with respect to the test frequencies while remaining constant in magnitude. The coefficient is seen to have a low order time dependence at frequencies higher than the transitional frequency in air environment, while the vacuum tests are independent of frequency before creep is activated.

In an attempt to understand the physical mechanisms involved in the effect of environment, the variations in Paris Law parameters are considered in the context of several existing theoretical models of crack growth. A fundamental approach in this regard is the relationship between crack growth and plastic work input [37,38]:

where the numerator is the plastic energy input and the denominator is a term representing the intrinsic strength of the material. This equation is a fundamental thermodynamic description of crack driving force versus material strength. The determination of the appropriate work input and strength relations are, however, complex and requires special knowledge of the microstructural response to a given K loading. In the case of a crack tip driven by localized plastic work (striations, and continuous incremental growth), the above can be represented in the general form [38,39]:

where CTOD is the crack tip opening and β is a parameter representing the plastic strain energy consumed in propagating the crack and also the crack tip geometry [40-42]. A similar analysis exists for cases where the crack propagation is governed by accumulated plastic work or displacements ahead of the crack tip, see models described in Refs. [43-45]. The general approach of these models assume a suitable distribution of plastic strain ahead of the crack tip and integrate over a crack length increment, Δa . A failure criterion is then applied to the material at $a+\Delta a$. Although the failure criteria and analysis is somewhat different between these approaches, there is the common notion that discontinuous crack growth may take place, that material within the plastic zone is deteriorating on a cycle basis, and that the fourth power Paris law will result. The plastic work accumulation theory results in an equation of the form:

where C is a proportional constant dependent on loading frequency, s is the appropriate yield stress, μ is the shear modulus, and U is the plastic work required per increment of crack length.

The different Paris exponents and coefficients obtained for the different loadings employed in the present study, shown in Fig. 11(a) and 11(b), implies that a single model chosen from those above cannot be used to express the fatigue crack growth rate for conditions tested here, unless the U terms are themselves functions of the stress intensity factor. Furthermore, these equations are based on assumptions which include; that all the work input has gone into damaging the crack tip material; that the material acts as a continuum; that healing processes such as rewelding are not acting; and that the principals of linear elastic fracture mechanics are applicable. These assumptions indicate that equations (3) and (4) are actually limiting cases describing the crack tip fracture processes when subjected to a variety of damage paths which may vary across the crack front and, may thus require interpolation between these equations.

Of particular interest in our examination of environmental influence is the difference between the results of loading frequencies higher than the transition level, where the Paris exponent assumes the value of 3.45 for vacuum tests while in air tests it decreases from about 2.7 to 2.2. Explanation of these values comes from comparison of the fracture surfaces displayed in

Fig. 7. In this figure it is seen that cleavage and striation-like features display greater ductility and discontinuity in growth rate (striation spacing), as well as increased slip reversibility features when comparing vacuum to air tests. Because slip irreversibility fundamentally originates from two sources: internal (e.g. dislocation entanglements, dislocation-precipitate interaction, etc.) and externally (e.g. oxide formation and corresponding increase in dislocation image forces [2], it can be inferred that irreversibility will be greater in air tests. For the vacuum case where there is a high degree of slip reversibility and a lack of oxide at the crack tip, the fatigue damage would accumulate through a cyclic buildup of dislocations within the plastic zone. Under these conditions, the crack tip radius at peak loading is not preserved, and growth follows a discontinuous process of initiation and propagation steps. This damage process in terms of accumulated work input is best described with the assumptions used in formulating equation (4).

As the crack tip is subjected to conditions enhancing the mechanisms of irreversibility, as the case would be in air tests, the crack growth rate will correlate more closely with equation (3). Indeed, the experimental results support this notion as an important environmental mechanism since the exponent has decreased consistently towards the 2nd power Paris equation with increasing external irreversibility conditions which are linked to the decreased frequency in air. The geometrical and environmental relation included in equation (3) should, therefore, be dependent on the nature of reversibility of the crack tip plasticity.

At conditions below the transition frequency, the mechanisms controlling the crack growth are certainly delocalized from the crack tip, with viscoplastic damage being the dominant factor (figure 7). The equation from above which is most suited to describing delocalized mechanism (i.e. eq 4) must therefore be further adjusted to include viscoplastic effects. A complete representation of equation (1) for these cases would have an exponent of 4 up until the transition frequency is reached. This solution is currently being considered by the Authors.

5. CONCLUSIONS

The effects of the environment on the fatigue crack growth of the titanium alloy, Ti-1100, found in the study can be summarized as follows:

- 1- The primary effect of the air environment is to increase the fatigue crack growth rate. This effect is considered rapid in relation to the frequencies tested and is weakly dependent on cycle time. In addition, at 10Hz in air, growth rate curves from 23°C, 593°C, and 650°C can be consolidated by correcting for changes in Young's modulus and yield stress due to temperature.
- 2- The effect of environment was found to be associated with the increase in the Paris law exponent and the decrease in the Paris law coefficient when going from the vacuum to air environment. Comparing the experimental values of the exponent with those predicted from several existing theoretical models, implies a change in the damage mechanism based on changes in slip reversibility and the nature of damage localization as function of the operating environment. Again these effects appear to be instantaneous and constant within the context of the frequencies tested.
- 3- Viscoplasticity has a dominant effect in controlling fatigue crack growth behavior at 593°C at low frequencies. The effect manifests itself as a shift towards higher ΔK in the transition from quasi-cleavage to striation dominated transgranular growth and as a change from transgranular to intergranular fracture mode. Paris law parameters in stage II growth are largely determined by the extent of viscoplastic response.
- 4- Within the context of viscoplasticity, a significant secondary effect of environment is seen as a reduction of viscoplastic response in air compared to vacuum such that, for example, intergranular growth is evident in vacuum at higher cyclic frequencies than in air.
- 5- An additional effect of environment is an apparent change in crack closure with a greater degree of closure in vacuum. This effect has been measured directly at room temperature but only circumstantial evidence exists for this conclusion at high temperature. Also, because of the increase in viscoplastic response in vacuum, caution should be used in equating increased closure in vacuum with a decrease in the crack growth threshold.

REFERENCES

1. B.I. Verkin and N.M. Grinberg, "The Effect of Vacuum on the Fatigue Behavior of Metals and Alloys," *Materials Science and Engineering*, V 41 (1979) 149-181.
2. J.E. King, and P.J. Cotterill, "Roles of Oxides in Fatigue Crack Propagation," *Materials Science and Technology*, V 6 (1990) 19-31.
3. L.F. Coffin, Jr., "Fatigue at High Temperature," *Fatigue at Elevated Temperatures*, ASTM STP 520, American Society for Testing and Materials, 1973, pp 5-34.
4. M.A. Dubler, H. Grey, L. Wagner, and G. Lutjering, "Fatigue Behavior of High Strength Titanium Alloys at Elevated Temperatures," *Zeitschrift für Metallkunde*, V 78 (1987) 406-411.
5. H. Ghonem and D. Zheng, "The Depth of Intergranular Oxygen Diffusion during Environment-Dependent Fatigue Crack Growth in Alloy 718", *Materials Science and Engineering*, Vol. 150A, 1992 (in press)
6. P. Marshall, "The Influence of Environment on Fatigue and Creep/Fatigue," *Fatigue at High Temperature*, International Spring Meeting, Société Française de Metallurgie, Paris, 1986, pp 109-145.
7. J.A. Ruppen, C.L. Hoffman, V.M. Radhakrishnan, and A.J. McEvily, "The Effect of Environment and Temperature on the Fatigue Behavior of Titanium Alloys," *Fatigue, Environment and Temperature Effects*, 27th Sagamore Army Materials Research Conference, Bolton Landing, NY, ed. J.J. Burke., V. Weiss, Plenum Press, New York, (1983) 265-300.
8. P.J. Bania, "Ti-1100: A New Elevated Temperature Titanium Alloy," in *Sixth World Conference on Titanium, Part II*, Cannes, France, 6-9 June 1988, ed. P. Lacombe, R. Tricot, G. B'eranger, Les editions de physique, Les Ulis Cedex, France (1988), 825-830.
9. P.J. Bania "An Advanced Alloy for Elevated Temperatures," *Journal of Metals*, V 40, Number 3 (1988) 20-22.
10. H. Ghonem, R. Foerch, "Frequency Effects on Fatigue Crack Behavior in a Near- α Titanium Alloy," *Materials Science and Engineering*, V A138, (1991) 69-81.

11. H.J. Rack, "Dynamic Strain Aging of Metastable Titanium Alloys," *Scripta Metallurgica*, V 9, (1975) 829-831.
12. M.R. Winstone, R.D. Rawlings, and D.R.F. West, "Dynamic Strain Aging in Some Titanium-Silicon Alloys," *Journal of Less-Common Metals*, V 31, (1973) 143-150.
13. H.W. Liu, J.J. McGowan, "A Kinetic Analysis of High Temperature Fatigue Crack Growth," AFWAL-TR-81-4036, Air Force Materials Laboratory, Wright-Patterson Air Force Base, OH (1981).
14. A.S. Krausz, K. Krausz *Fracture Kinetics of Crack Growth, Mechanical Behavior of Materials*, V 1, Kluwer Academic Publishers, The Netherlands, 1988.
15. G.R. Yoder, L.A. Cooley and T.W. Crooker, "Quantitative Analysis of Microstructural Effects on Fatigue Crack Growth in WidmanstNO(a,)tten Ti-6Al-4V and Ti-8Al-1Mo-1V," *Engineering Fracture Mechanics*, V 11 (1979) 805-816.
16. H. Riedel, *Fracture at High Temperatures (Materials Research and Engineering)*, Springer-Verlag, Berlin, Heidelberg, New York, (1987).
17. L.F. Coffin, "Overview of Temperature and Environmental Effects on Fatigue of Structural Metals," *Fatigue, Environment and Temperature Effects*, 27th Sagamore Army Materials Research Conference, Bolton Landing, NY, ed. J.J. Burke., V.Weiss, Plenum Press, New York, (1983) 1-40.
18. M. Sugano, S. Kanno, and T. Satake, "Fatigue Behavior of Titanium in Vacuum," *Acta Metallurgica*, V 17 (1989) 1811-1820.
19. N. Walker, C.J. Beevers, "A Fatigue Crack Closure Mechanism in Titanium," *Fat. Engr. Mater. and Struct.*, V 1, (1979) 135-148.
20. M.D. Halliday, C.J. Beevers, "Some Aspects of Fatigue Crack Closure in Two Contrasting Titanium Alloys," *J. Testing and Evaluation*, V 9, (1981) 195-201.
21. J.A. Ruppen and A.J. McEvily, "Influence of Microstructure and Environment of the Fatigue Crack Fracture Topography of Ti-6Al-2Sn-4Zr-2Mo-0.01Si," *Fractography and Materials Science*, ed. Gilbertson and Zipp, ASTM STP 733, American Society for Testing and Matrials, Philidelphia, PA (1981) 32-50.

22. G.R. Yoder, L.A. Cooley, and T.W. Crooker, "Observations on Microstructurally Sensitive Fatigue Crack Growth in a Widmanstatten Ti-6Al-4V Alloy," *Metallurgical Transactions*, V 8A (1977) 1737-1743.
23. C.J. Beevers and C.M. Ward-Close, "DK Thresholds in Titanium Alloys - The Role of Microstructure, Temperature and Environment" *Fatigue, Environment and Temperature Effects*, 27th Sagamore Army Materials Research Conference, Bolton Landing, NY, ed. J.J. Burke., V. Weiss, Plenum Press, New York, (1983) 83-102.
24. K.S. Chan, C.C. Wojcik, and D.A. Koss, "Deformation of an Alloy with a Lamellar Microstructure: Experimental Behavior of Individual Widmanstatten Colonies of an a-b Titanium Alloy," *Metallurgical Transactions*, V 12A (1981) 1899-1907.
25. D. Shechtman and D. Eylon, "On the Unstable Shear in Fatigued b-Annealed Ti-11 and IMI-685 Alloys," *Metallurgical Transactions*, V 9A (1978) 1018-1020.
26. W.G. Burgers, "On the Process of Transformation of the Cubic-Body-Centered Modification into the Hexagonal-Close-yPacked Modification of Zirconium," *Physica*, V 1 (1934) 561-586.
27. J.C. Williams and G. Luetjering, "The Effect of Slip Length and Slip Character on the Properties of Titanium Alloys," in *Titanium '80 Science and Technology*, Proceedings of the Fourth International Conference on Titanium, Kyoto, Japan, ed. Camera and Zuni. TMS-AIME Publications, Warrendale, Pa, (1988) 671-681.
28. D. Eylon, "Faceted Fracture in Beta Annealed Titanium Alloys," *Metallurgical Transactions*, V 10A, (1979) 311-317
29. D.J. Duquette, and M. Gell, "The Effects of Environment on the Mechanism of Stage I Fatigue Fracture," *Metallurgical Transactions*, V 2 (1971) 1325-1331.
30. R.M.N. Pelloux, "Mechanisms of Formation of Ductile Fatigue Striations," *Transactions of the ACM*, V 62 (1969) 281-285.
31. D.A. Meyn, "The Nature of Fatigue crack Propagation in Air and Vacuum for 2024 Aluminum," *Trans. Am. Soc. Met.*, 61 (1968)
32. C.H. Wells, "High-Temperature Fatigue," *ASM Symposium: Fatigue and Microstructure*, St. Louis, Missouri, American Society for Metals, Ohio (1978) 307-333.

33. L.S. Vesier and S.D. Antolovich, "Fatigue Crack Propagation in Ti-6242 as a Function of Temperature and Waveform," *Engineering Fracture Mechanics*, V 37 (1990) 753-775.
34. T. Ericson, "Review of Oxidation Effects on Cyclic Life at Elevated Temperature," *Canadian Metallurgical Quarterly*, V 18 (1979) 177-195.
35. P. Kofstad, *High-Temperature Oxidation of Metals*, The Corrosion Monograph Series, John Wiley, New York, NY (1966).
36. D. Taylor, *Fatigue Threshold*, Butterworth & Co. Ltd, London, England, (1989).
37. S.R. Bodner, D.L. Davidson, and J. Lankford, "A Description of Fatigue Crack Growth in Terms of Plastic Work," *Engineering Fracture Mechanics*, V 17 (1983) 189-191.
38. J. Weertman, "Fatigue Crack Propagation Theories," *ASM Symposium: Fatigue and Microstructure*, St. Louis, Missouri, American Society for Metals, Ohio (1978) 279-306.
39. T. Mura and C.T. Lin, "Theory of Fatigue Crack Growth for Work Hardening Materials," *International Journal of Fracture*, V 10 (1974) 284-287.
40. P. Neumann, "New Experiments Concerning the Slip Processes at Propagating Fatigue Cracks-I," *Acta Metallurgica*, V 22 (1974) 1155-1165.
41. P. Neumann, "The Geometry of Slip Processes at a Propagating Fatigue Crack-II," *Acta Metallurgica*, V 22 (1974) 1167-1178.
42. M. Kikukawa, M. Jono and M. Adachi, "Direct Observation and Mechanism of Fatigue Crack Propagation," in *Fatigue Mechanisms*, Proceedings of and ASTM-NBS-NSF Symposium, Kansas City, Mo, May 1978, Ed. J.T. Fong, ASTM STP 675, American Society for Testing of Materials, Philadelphia, PA (1979) 234-253.
43. J. Weertman, "Theory of Fatigue Crack Growth Based on a BCS Crack Theory with Work Hardening," *International Journal of Fracture*, V 9 (1973) 125-131.
44. S.D. Antolovich, A. Saxena and G.R. Chanani, "A Model for Fatigue Crack Propagation," *Engineering Fracture Mechanics*, V 7 (1975) 649-652.

45. S.B. Chakraborty, "A Model Relating Low Cycle Fatigue Properties and Microstructure to Fatigue Crack Propagation Rates," *Fatigue and Fracture of Engineering Materials and Structures*, V 2 (1979) 331-344.

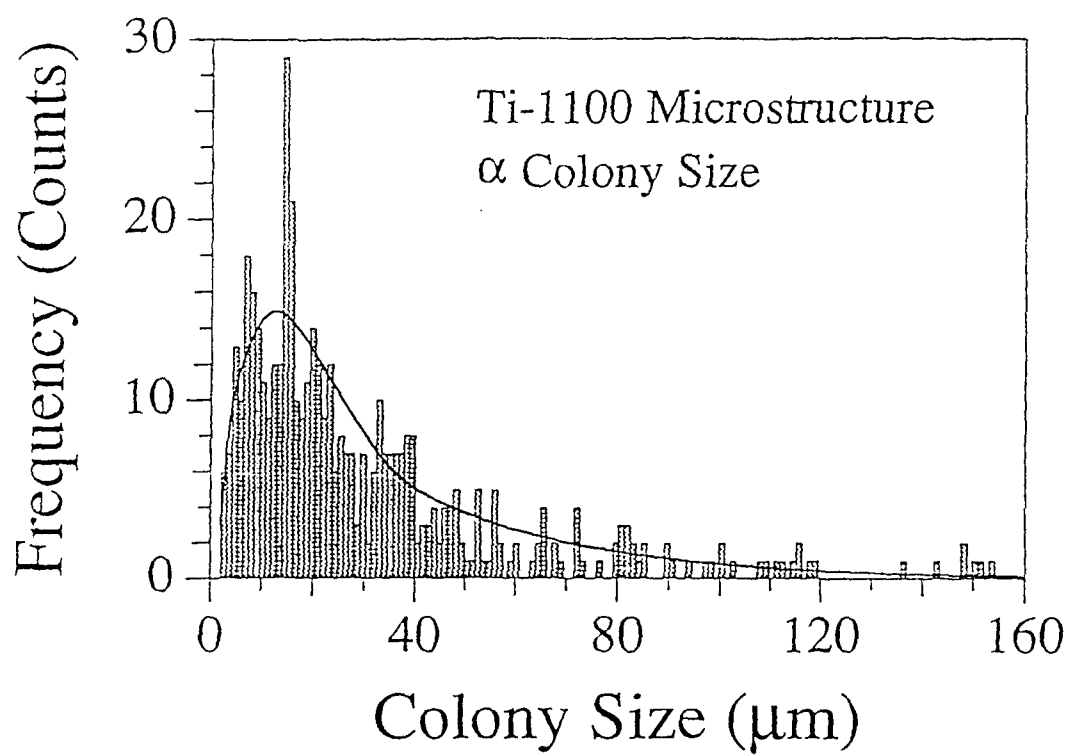


Figure 1(a) : Distribution of Colony Size Using an Intercept Method.

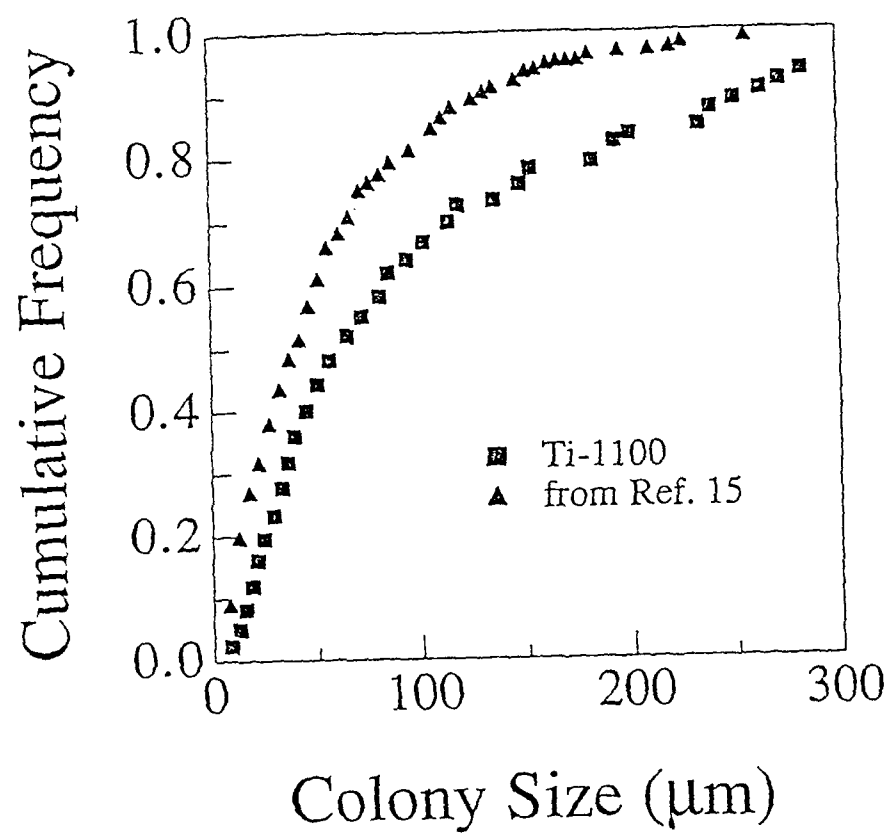


Figure 1(b) : Distribution of Colony Size Using in Terms of Cumulative Frequency..

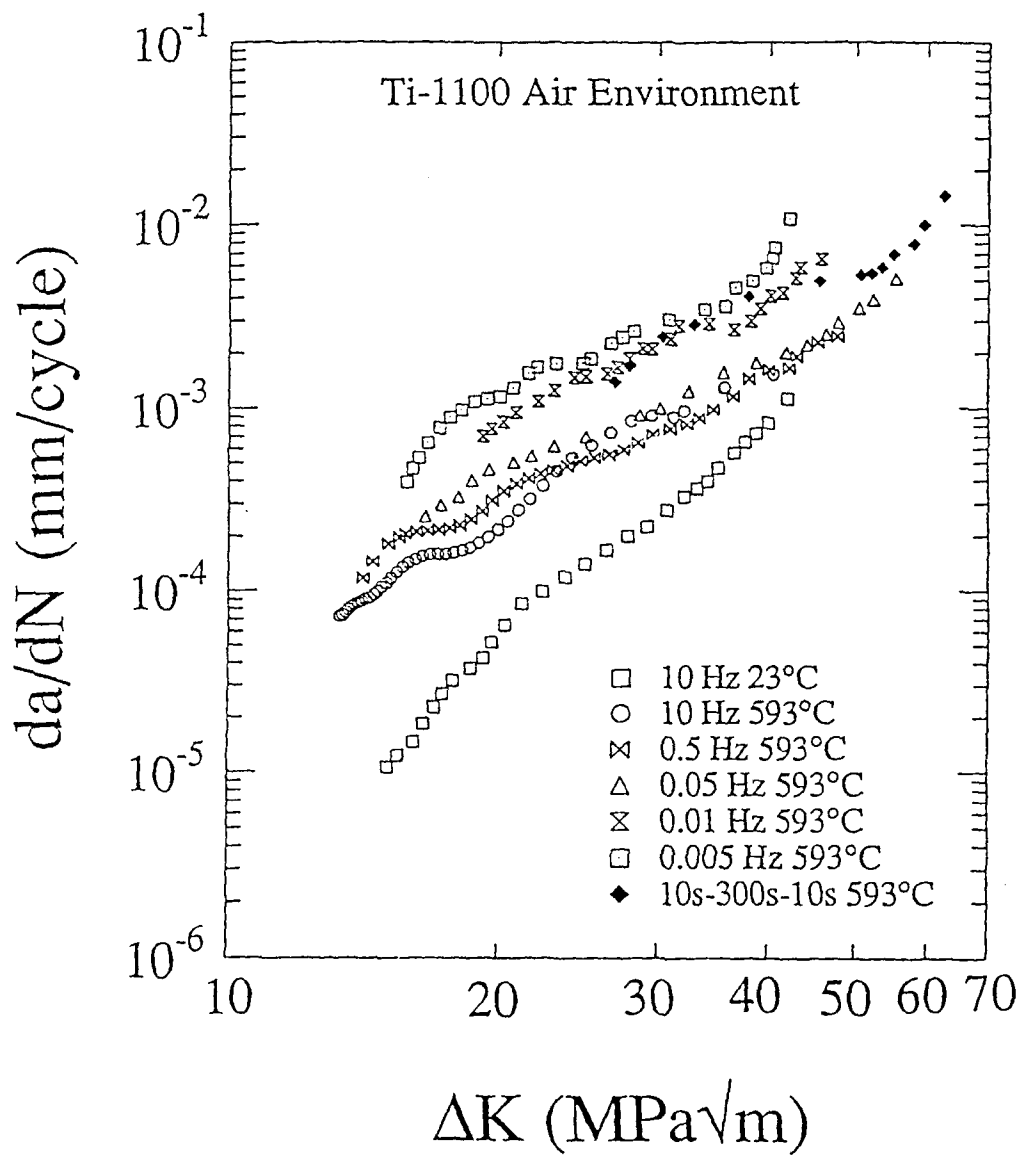


Figure 2 : Crack Growth Rate vs ΔK Air Environment Testing.

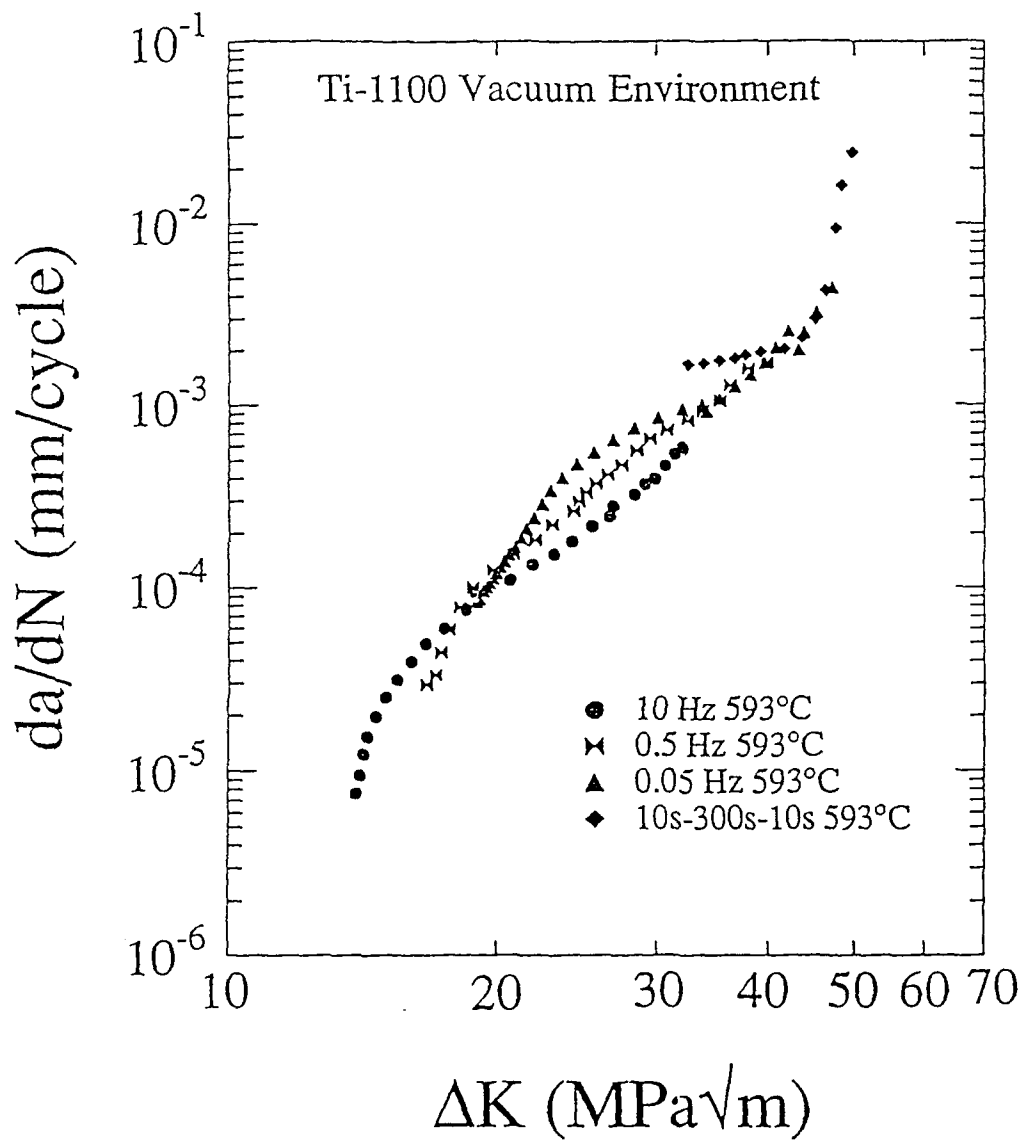


Figure 3 : Crack Growth Rate vs ΔK for Vacuum Environment Testings.

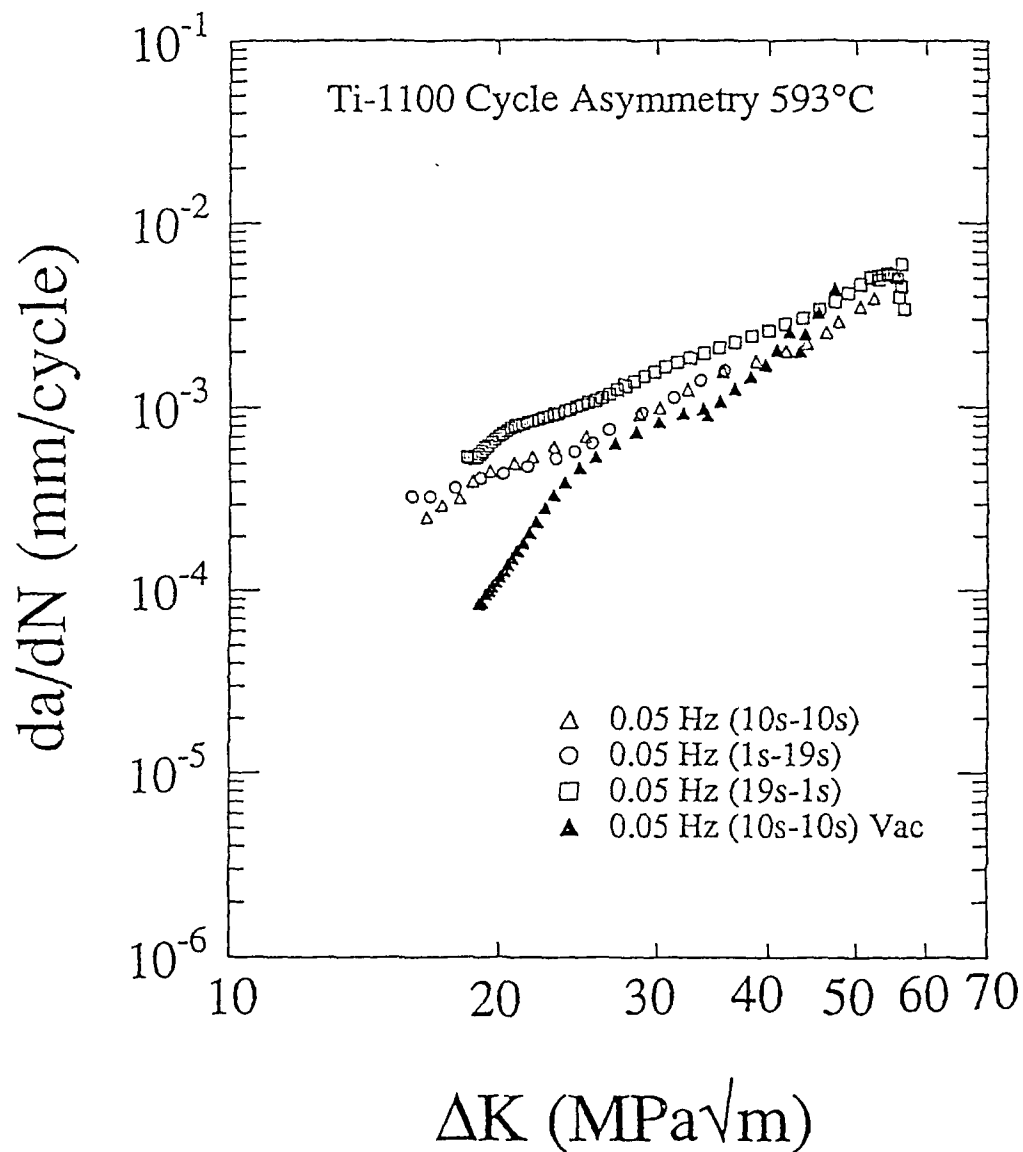


Figure 4 : The Effect of Loading Rate Symmetry on the Crack Growth Rate for 0.05 Hz, 593°C in Air Environment.

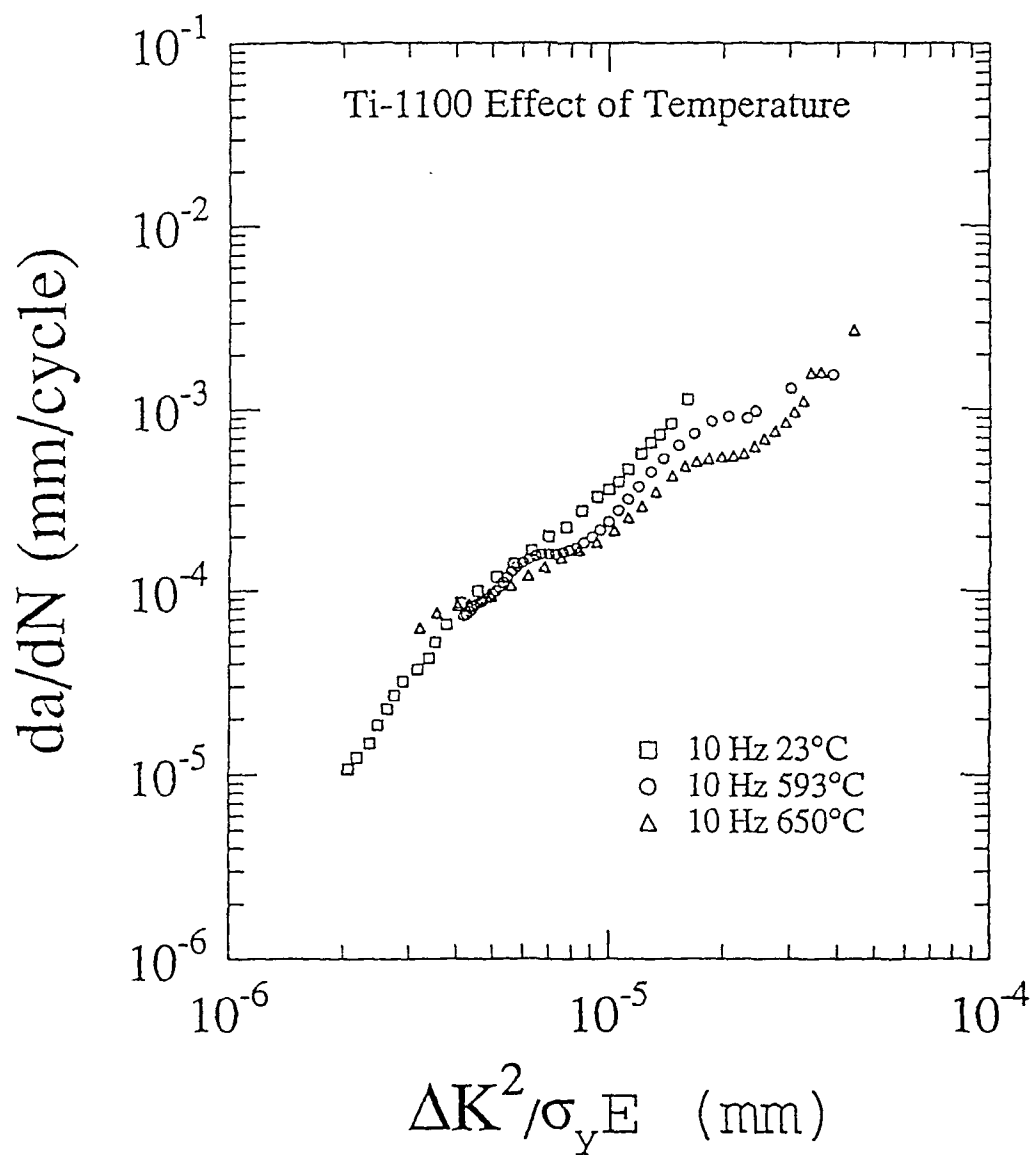


Figure 5 : Effect of Variations of Yield Stress Due to Temperature on the Consolidation of Fatigue Crack Growth of 10Hz, Air Testings.

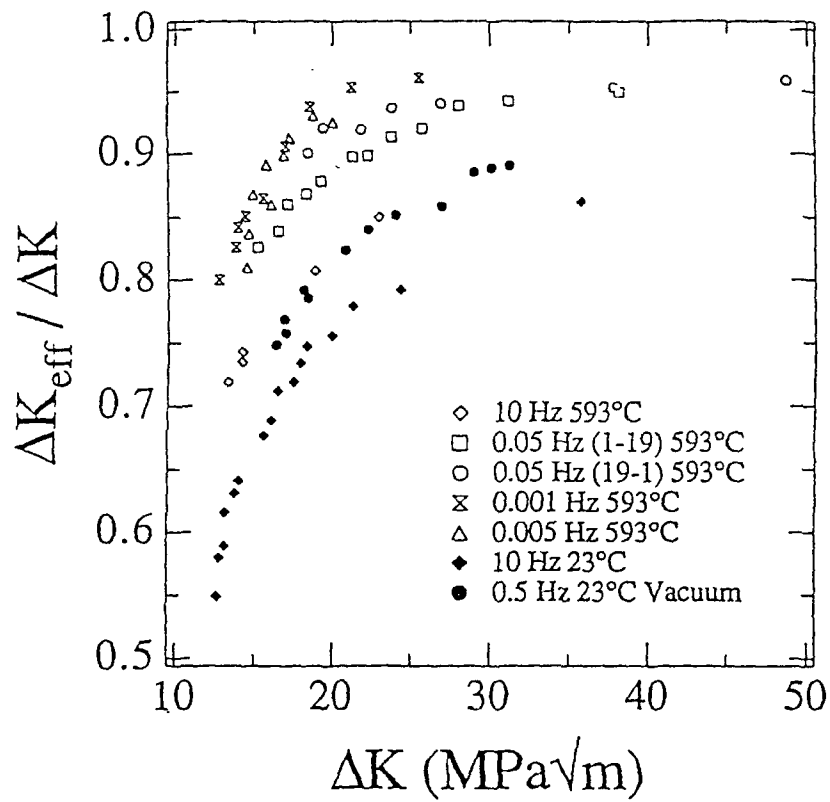


Figure 6 : Crack Closure Data for both Air and Room Temperature Vacuum Testings.

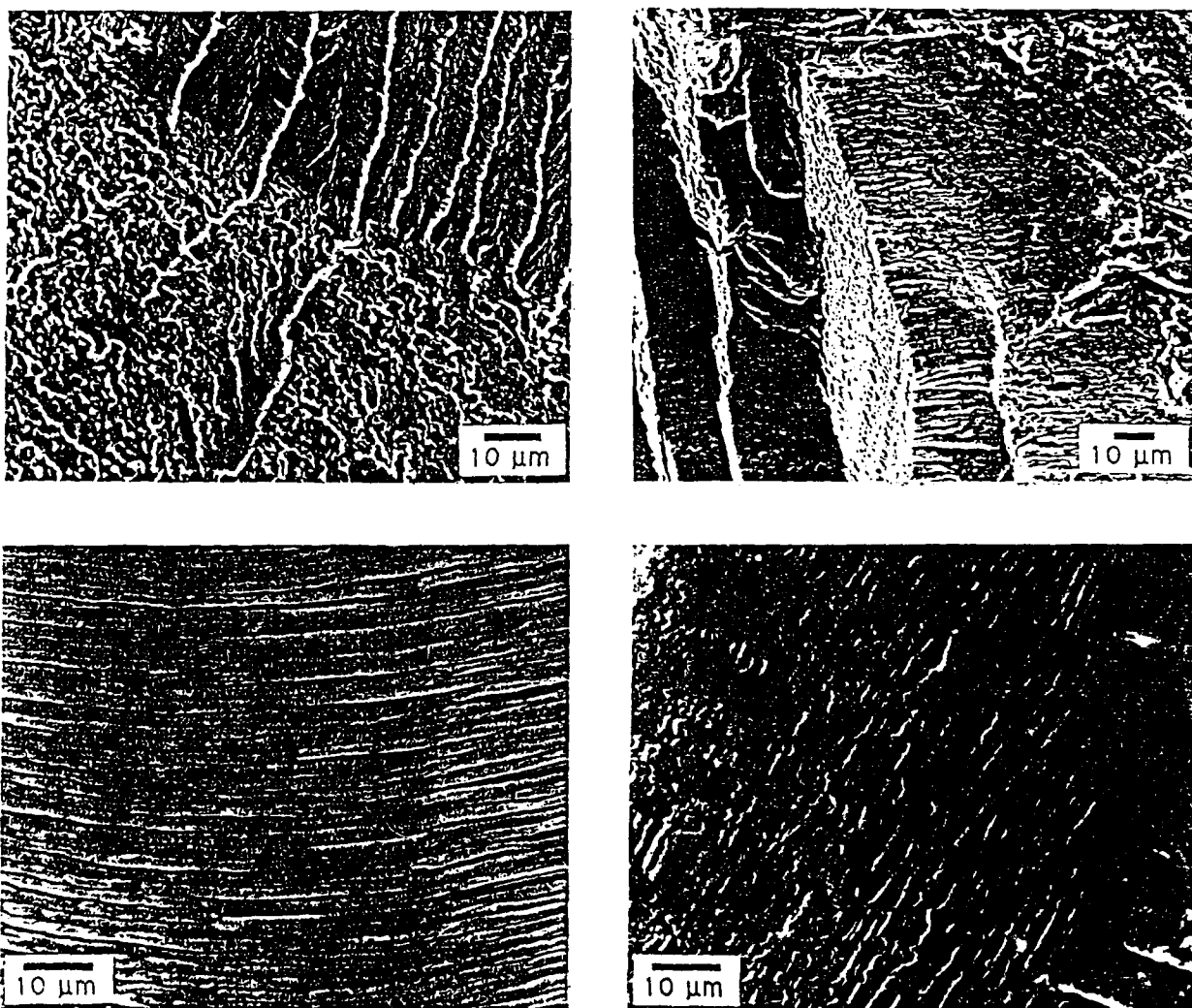


Figure 7 : Fracture Surface Morphologies in both Air and Vacuum a) : difference in cleavage appearance in air (upper right) and vacuum (lower left) (b) : intersecting cleavage planes with crack growth plane in vacuum (c) : appearance of striations in air (d) : appearance of striations in vacuum.

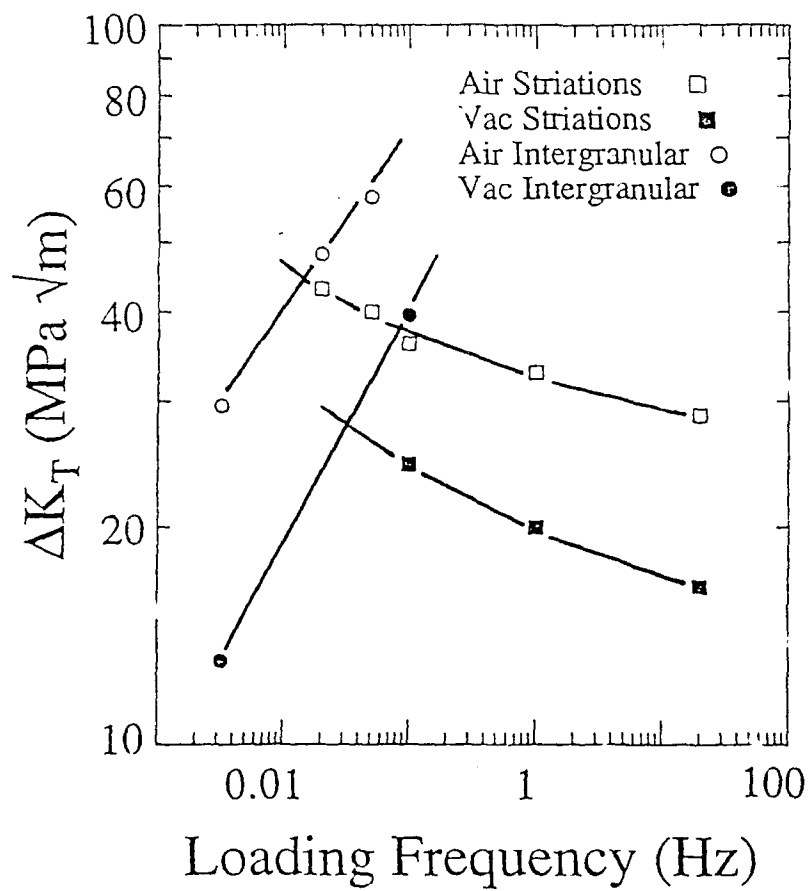


Figure 8 : ΔK Transition (cleavage to striated transgranular and transgranular to intergranular) vs Loading Frequency for both Air and Vacuum Tests.

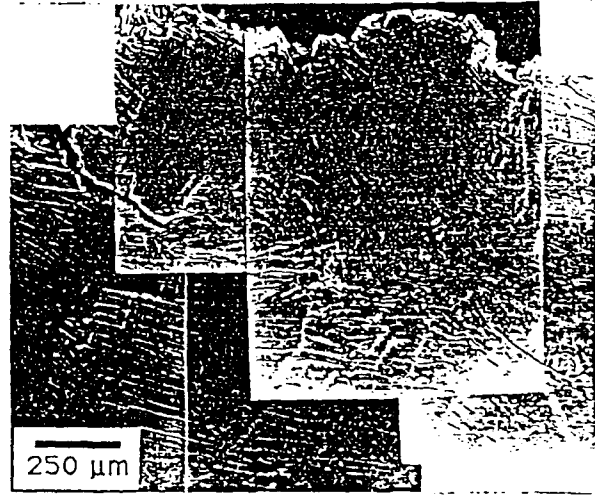
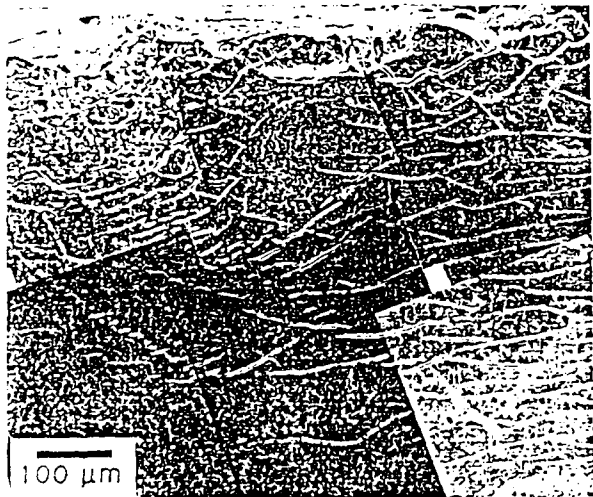
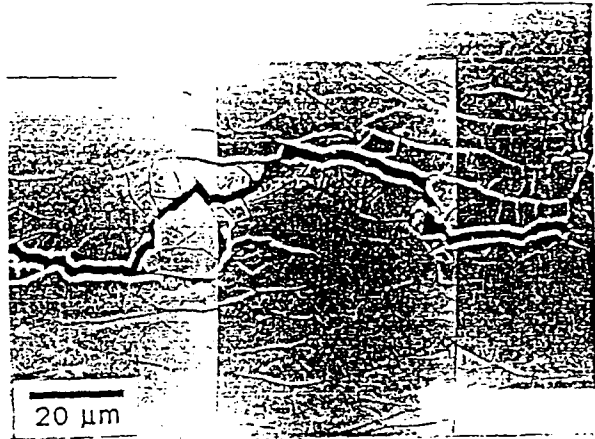
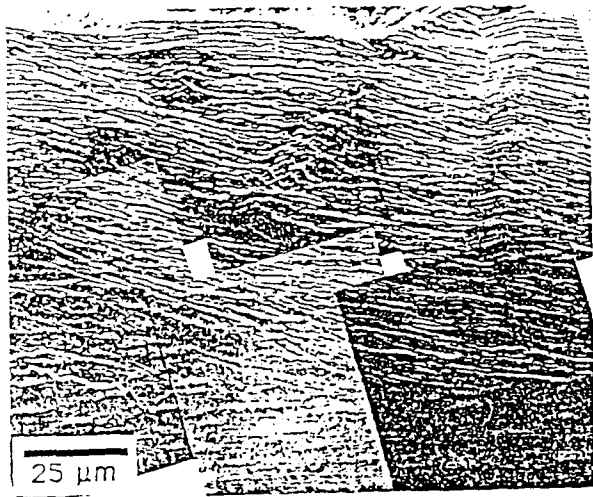


Figure 2 : Surface Slip and Microcrack Traces for Four Loading Frequencies in 593°C, Vacuum at $\Delta K = 25 \text{ MPa } \sqrt{\text{m}}$; (a) 10Hz (b) 0.5Hz (c) 0.05Hz (d) 0.05Hz with 300s hold at maximum load.

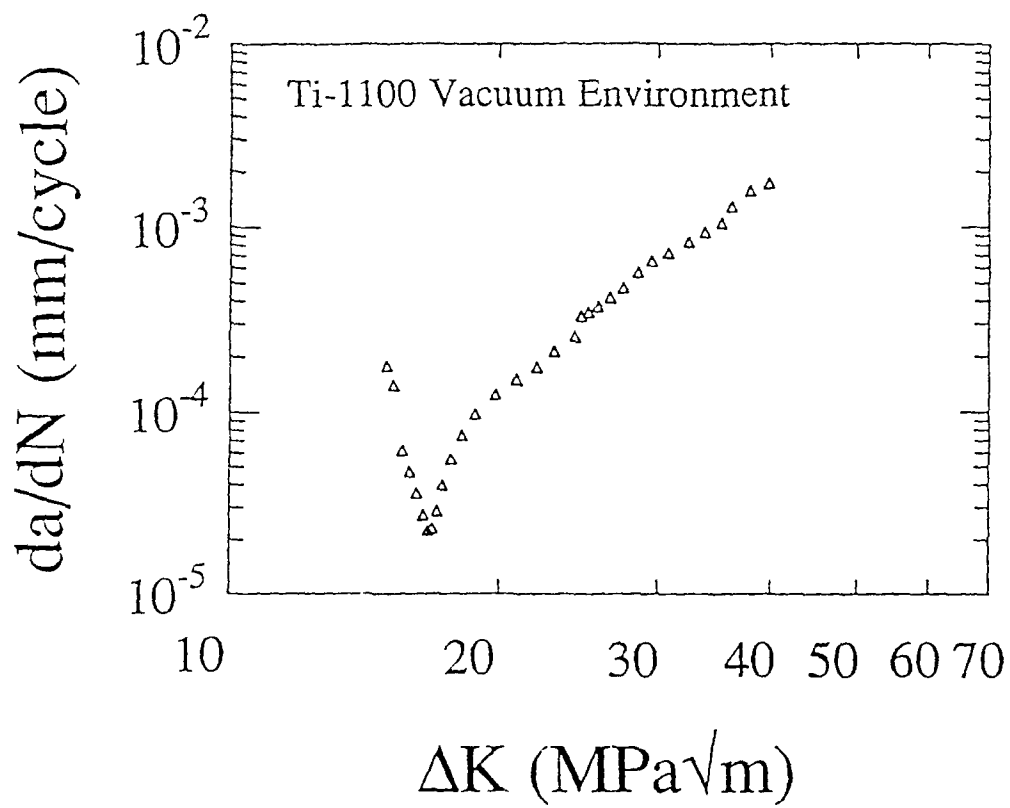


Figure 10 : Effect of Apparent Crack Tip Closure on Growth Behavior in Vacuum.

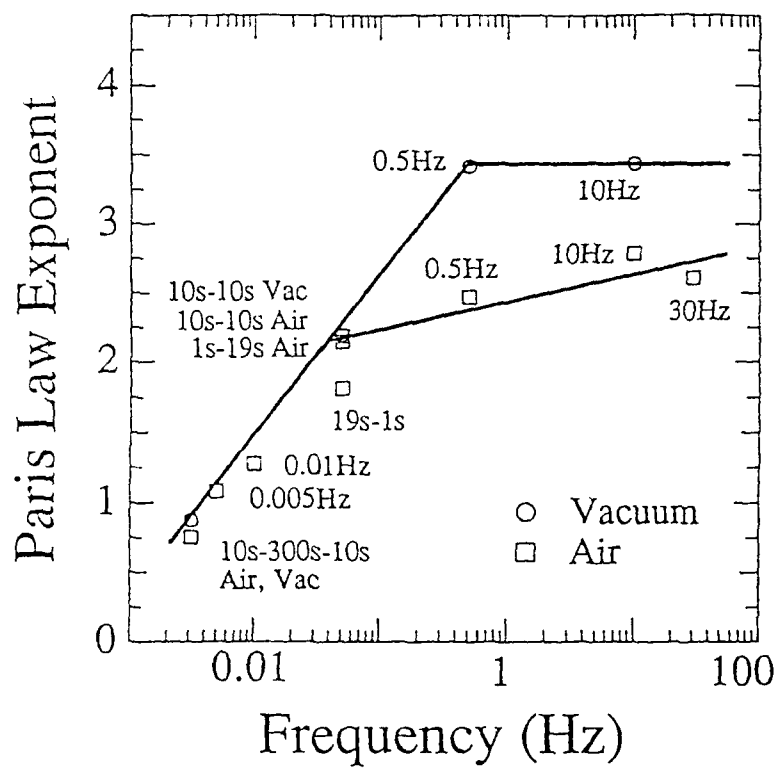


Figure 11(a) : Relationship between Paris Law Exponent and Loading Frequency.

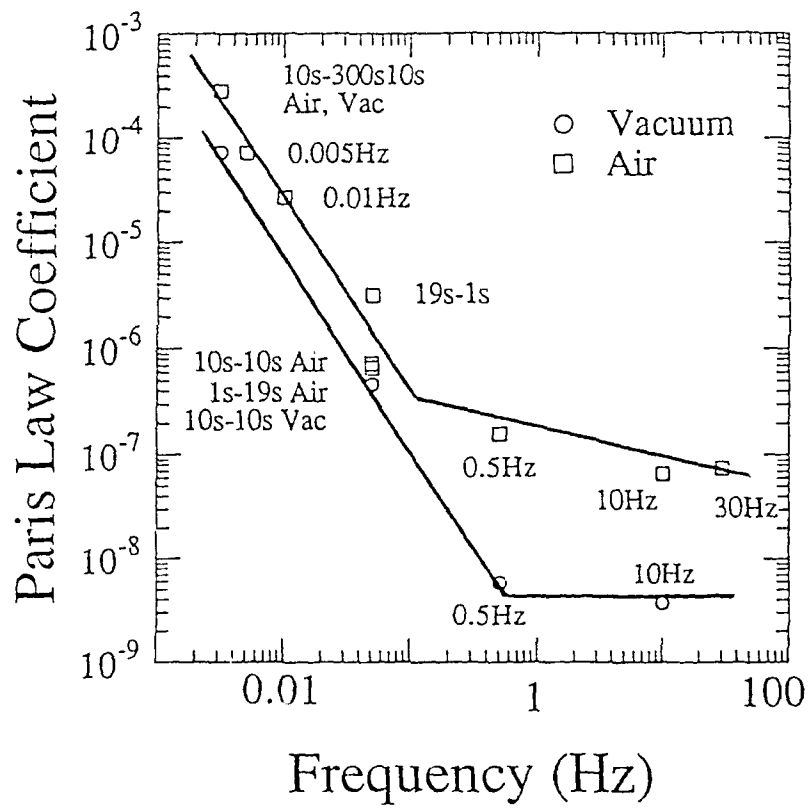


Figure 11(b) : Relationship between Paris Law Coefficient and Loading Frequency.

APPENDIX

- 1 - Depth of intergranular oxygen diffusion during environment - dependent fatigue crack growth in Alloy 718.
H. Ghonem - D. Zheng. Materials Science and Engineering, A150 (1992) 151-160.
- 2 - Intergranular crack tip oxidation mechanism in a Nickel-based superalloy.
E. Andrieu - R. Molins - H. Ghonem - A. Pineau - Materials Science and Engineering. A154 (1992) 21-28.
- 3 - Frequency interactions in high temperature fatigue crack growth in superalloys.
H. Ghonem - D. Zheng - Met. Trans. A, 23A, Nov. 1992, 3067.
- 4 - Oxidation and intergranular cracking behaviour of two high strength Ni-base superalloys.
E. Andrieu - G. Hochstetter - R. Molins - A. Pineau.
Int. Conf. on "Corrosion Deformation interactions", Fontainebleau, France, Oct.5-7, 1992.
- 5 - Influence of prestraining on high temperature, low frequency fatigue crack growth in superalloys.
H. Ghonem - D. Zheng - A. Rosenberger.
(to be published in Materials Science and Engineering).
- 6-7 - Elevated Temperature Fatigue Crack growth in Alloy 718 :
Part I : Effects of mechanical variables.
Part II : Effects of environmental and materials variables.
H. Ghonem - T. Nicolas - A. Pineau.
(to be published in Materials Science and Engineering).

Depth of intergranular oxygen diffusion during environment-dependent fatigue crack growth in alloy 718

H. Ghonem and D. Zheng

Mechanics of Solids Laboratory, Department of Mechanical Engineering and Applied Mechanics, University of Rhode Island, Kingston, RI 02881 (USA)

(Received April 22, 1991; in revised form August 15, 1991)

Abstract

The elevated-temperature fatigue crack growth behavior in alloy 718, when subjected to a loading frequency lower than the transitional frequency of this alloy, is viewed as fully environment dependent. In this process, the crack growth increment per loading cycle is assumed to be equal to the intergranular oxygen diffusion depth at the crack tip during the cycle effective oxidation time. In order to identify the trend of this diffusion depth an experimental program was carried out on compact tension specimens made of alloy 718 at 650 °C in which fatigue crack growth measurements were made for cyclic load conditions with and without hold time periods at minimum load level. This work resulted in establishing a relationship correlating the intergranular oxygen diffusion depth and the value of the stress intensity factor range ΔK . This relationship, when integrated over the cycle effective oxidation time, results in a closed-form solution describing the environment-dependent fatigue crack growth rate. A comparison is made between the results of this solution when applied to different loading frequencies and the corresponding experimental results. This comparison shows good agreement between the two sets of results. Furthermore, by combining the parabolic rate law of diffusion and the equation for the intergranular oxygen diffusion depth, an explicit expression for the oxygen diffusivity of grain boundaries is derived. It is found that this diffusivity is both a ΔK - and a frequency-dependent parameter.

1. Introduction

Time-dependent effects on high-temperature fatigue crack growth behavior in high strength structural alloys are generally ascribed to phenomena involving creep and/or environmental degradation processes. The relative importance of these two processes depends, in general, on the strengthening characteristics of the material, exposure time, load level and temperature. Nickel-base superalloys and in particular alloy 718 are a class of alloys that have been designed as highly creep-resistant materials. Brook and Bridges [1], for example, have shown that alloy 718 is microstructurally stable after 10 000 h exposure at temperatures up to 600 °C. Nicholas and Weerasooriya [2] and Pineau [3] have estimated the Riedel-Rice characteristic time for transition from small-scale yielding to extensive creep in alloy 718 at 650 °C to be in the range from 20 h to 3 years, which is much larger than the possible cyclic periods and hold time durations in practical applications of this material. Furthermore, several studies on alloy 718 have demonstrated that the high-temperature fatigue crack growth rate is decreased several orders of magnitude when results of vacuum tests are compared with those due to low

frequency loading in air test conditions. These observations, supported by the success of linear elastic fracture mechanics (LEFM) in predicting the crack growth rates in nickel-base superalloys at elevated temperatures, give strong support to the conclusion that time-dependent effects in these alloys are principally due to environment degradation. Extensive work was carried out in order to understand the damage mechanisms associated with this type of degradation process. Important results of this work are related to the fact that, in alloy 718, oxygen is the detrimental element in air [4] and that environmental effects are highly localized at the crack tip and are manifested through grain boundary oxidation and subsequent embrittlement.

Attempts to predict fatigue crack growth behavior in alloy 718 have thus relied on assessing both the cyclic and the oxidation damage components, the linear sum of which was assumed to represent the total crack tip damage. The relative contribution of these two components to the total damage has been linked, based on the pioneering work of Coffin [5], to the loading frequency. While a different interpretation could be given for the cause of this linkage, it is, however, established that the damage process ranges from purely cycle dependent at high frequency levels to fully

environment dependent at very low frequency levels. In the environment-dependent crack growth process, the crack increment per cycle is assumed to be directly related to the intergranular depth of oxygen diffusion taking place during the cycle effective oxidation time [6]. The objective of this paper is to examine the limitation of this assumption. The first part of the paper describes the various stages of crack growth processes in relation to the loading frequency. The second part will attempt to determine the cycle effective oxidation time of a loading cycle and provide a quantitative relationship between oxygen diffusion rate and crack tip driving force. This relationship when integrated over the oxidation time yields an explicit crack growth rate expression that will be the focus of analysis and comparison with experimental data.

2. High-temperature fatigue crack growth stages in alloy 718

The relationship between loading frequency and environmental effects on the acceleration of the fatigue crack growth rate in alloy 718 can be explained in terms of the intergranular oxygen diffusion process in the crack tip region. One of the governing factors of this process is the grain boundary diffusivity of oxygen—a subject that has not been extensively studied in the particular case of alloy 718. It is recognized, however, that intergranular oxygen diffusion depends on the stress and strain states along affected grain boundaries [4, 7, 8]. Therefore for a stressed grain boundary the oxygen diffusivity of grain boundaries D_g could be expressed as a function of the inelastic strain energy density $f(W_p)$ of this boundary. This is written as an Arrhenius relationship in the form [6]

$$\begin{aligned} D_g &= D \exp\left(-\frac{Q_g'}{RT}\right) \\ &= D \exp\left[-\frac{Q_g - f(W_p)}{RT}\right] \end{aligned} \quad (1)$$

where Q_g is the activation energy of grain boundary diffusion in the stress-free state, Q_g' is the effective activation energy of grain boundary diffusion for stressed material, D is a diffusion constant, R is the gas constant and T is the temperature in kelvins. Through this definition the influence of loading frequency and the associated deformation mode on the magnitude of D_g , and also consequently $f(W_p)$ on the crack growth response, can be interpreted qualitatively as follows. High frequency loading, which is generally characterized by high slip density and a homogeneous form of deformation, would result in both strain accommoda-

tion as well as stress relief along affected grain boundaries in the crack tip region. Hence variations in $f(W_p)$, and consequently D_g , tend to be minimal. In addition, the increase in slip density generally leads to an increase in the lateral matrix diffusion across the affected grain boundaries. These two combined effects would result in limited or no acceleration of the intergranular oxygen diffusion rate. In this situation, the influence of crack tip oxidation is minimal and crack tip damage becomes generally dominated by cycle-dependent effects, giving rise to transgranular fracture mode. On the other hand, low-frequency loading accompanied by low slip density would promote grain boundary stress concentration resulting in an increase in the magnitude of both $f(W_p)$ and D_g . This is magnified particularly if stress relief by grain boundary sliding is not permitted, as in the case of the highly creep-resistant alloy 718. Furthermore, the decrease in slip density would limit the grain boundary lateral matrix diffusion process. Here the expected increase in the grain boundary diffusivity and associated increase in depth of grain boundary oxidation results in an increase in the crack tip damage due to environment effects, giving rise to the intergranular fracture process.

On the basis of the above argument the crack growth response of alloy 718 with respect to loading frequency f has been divided, following the work of Pineau [9] and Weerasooriya and coworkers [10–12], into three distinctive types as shown in Figs. 1 and 2. The first type is associated with high-frequency loading in which the deformation mode is governed by a high degree of slip homogeneity. Cracking proceeds primarily in the matrix material (in contrast to the grain boundary), resulting in a predominantly transgranular fracture mode. The value of the frequency f required to produce this type of environment-independent behavior decreases as the magnitude of ΔK increases. This type of crack growth behavior is generally predicted by the use of a Paris-type equation.

As the loading rate decreases, the degree of slip line homogeneity in the crack tip zone is lowered, resulting

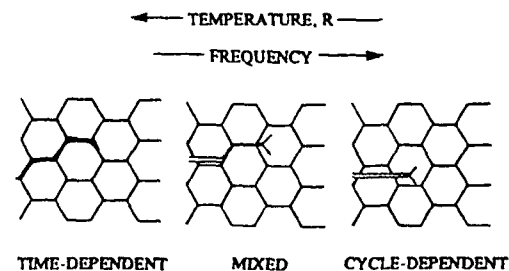


Fig. 1. Schematic of fatigue crack growth mechanisms for time-dependent, mixed and cycle-dependent crack growth regimes in air environment.

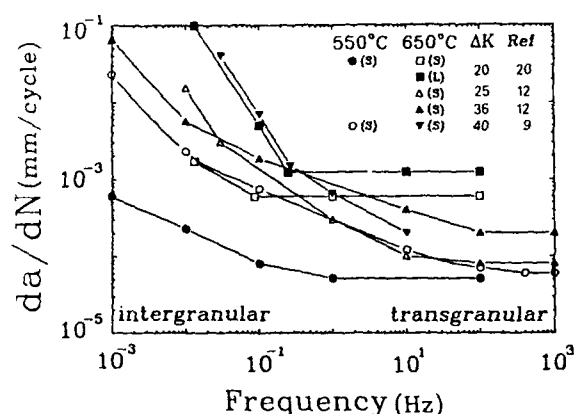


Fig. 2. Effect of frequency on fatigue crack growth rate of alloy 718 at $R = 0.1$ for different temperatures, grain sizes ($S \approx 20$ – $50 \mu\text{m}$, $L \approx 150 \mu\text{m}$) and ΔK levels.

in a relative increase of the intergranular oxygen diffusion. Under this condition, the crack tip damage becomes a combination of oxidation and cycle-dependent components. In this type of response, the total crack tip damage has been described by many authors [12–19] using various models which are generally reduced to a form of the linear summation rule which can be expressed as

$$\left(\frac{da}{dN}\right)_{\text{total}} = \left(\frac{da}{dN}\right)_{\text{cycle}} + \left(\frac{da}{dN}\right)_{\text{time-dependent}} \quad (2)$$

where, in the absence of sustained loading effects (hold times), the time-dependent term represents the contribution of oxidation to crack tip damage and could be written as a time integral in the form

$$\left(\frac{da}{dN}\right)_{\text{time-dependent}} = \int \frac{da}{dt} dt \quad (3)$$

where t_{ox} represents the time period of the cycle during which the oxidation process is an active damaging component. As shown in Figs. 1 and 2, this oxidation-enhanced process is characterized by a mixed transgranular–intergranular fracture mode. The degree of contribution of each of the cycle- and time-dependent terms in the above equation depends on both the frequency and ΔK values. For the same frequency, as ΔK increases, the contribution of the cycle-dependent damage also increases, since increasing ΔK leads to an increase in the degree of slip homogeneity (see refs. 13 and 20). The increase in the cycle-dependent damage is measured by the increase in percentage of the transgranular features along the fracture surface. For the same ΔK value, however, the influence of the time-dependent damage increases as frequency decreases.

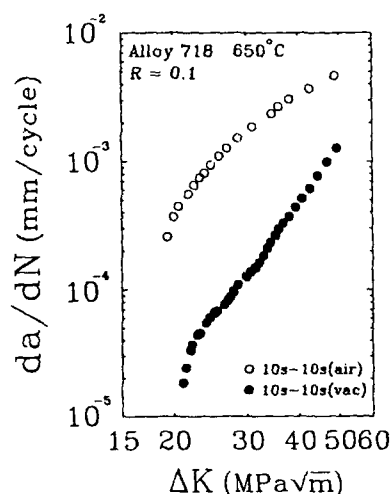


Fig. 3. Comparison of fatigue crack growth rate in alloy 718 in air (○, 10 s–10 s) and vacuum (●, 10 s–10 s) (frequency, 0.05 Hz; temperature, 650°C; $R = 0.1$).

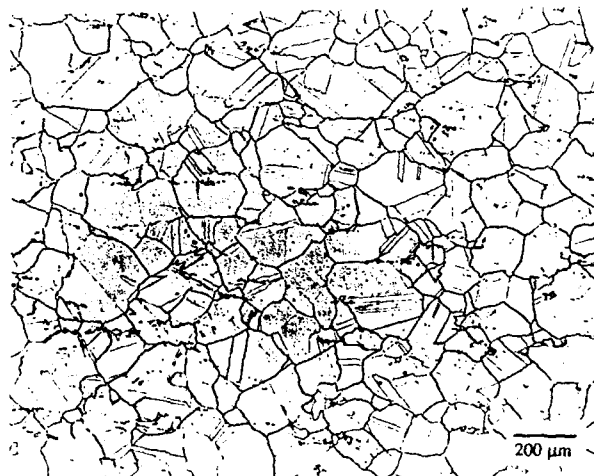


Fig. 4. Microstructure of alloy 718 (average grain size, ASTM number 3).

The third type of response mentioned above occurs for loading frequencies below a transitional level f_c where the crack tip damage becomes mainly an environment-dependent process in which crack growth is largely intergranular. The value of the transitional frequency, for a particular ΔK , in alloy 718 was found to depend on both temperature and microstructure [9, 12, 20]. As shown in Fig. 2, for a grain size around $100 \mu\text{m}$ at 650°C and $\Delta K = 40 \text{ MPa m}^{1/2}$, the value of f_c is on the order of 0.1 Hz. The influence of loading cycle on crack growth behavior, where the test frequency is in the environment-dependent regime ($f < f_c$), is depicted in Fig. 3 by comparing the fatigue crack growth rate of two CT-20 (ASTM E-647, $W = 40 \text{ mm}$, $B = 10 \text{ mm}$) specimens made from a conventionally heat-treated alloy 718 with the microstructure

features shown in Fig. 4. All tests were performed at 650 °C and for a frequency of 0.05 Hz in both air and vacuum (10^{-8} Torr) conditions. The total number of cycles required to propagate the same crack length in both specimens was 5000 cycles and 65 000 cycles in air and vacuum respectively. Furthermore, the fracture surfaces in both cases are shown in Figs. 5(a) and 5(b) where they exhibit fully intergranular fracture in the case of air testing and fully transgranular fracture in the case of vacuum testing.

If one makes the assumption that in the environment-dependent stage the crack growth increment per cycle is equal to the intergranular oxygen diffusion depth X occurring during the cycle effective oxidation time t_{ox} , then the fatigue crack growth rate can be expressed as

$$\begin{aligned} \left(\frac{da}{dN} \right)_{\text{total}} &= \int_{t_{ox}} \frac{da}{dt} dt \\ &= \int_{t_{ox}} \dot{X}(\Delta K, t) dt \end{aligned} \quad (4)$$

where \dot{X} is the instantaneous oxygen intergranular diffusion rate. This implies recognition that oxygen diffusion, in addition to being time dependent, is an energy-activated process and could then be treated as a function of the stress intensity factor range ΔK acting on the crack tip during the cycle effective oxidation time. Testing the validity of this assumption (*i.e.* the ability of the above equation to describe the environment-dependent stage) requires the knowledge of both t_{ox} and the relationship between \dot{X} and ΔK . These two requirements are not readily available in the literature and therefore an attempt will be made here to determine these requirements experimentally.

3. Cycle effective oxidation time

The cycle effective time t_{ox} is defined here as being the period of the cycle during which the oxidation effects take place. Several authors have assigned different measures to t_{ox} . For example, Achter [21], in a study of the effect of oxygen partial pressure on crack growth rate in type 316 stainless steel at elevated temperature, proposed a calculation method which was based on the assumption that the time required for adsorbing a gas atom monolayer at the crack tip is equal to half of the tensile part of the cycle or a quarter of the whole cycle period. Wei and coworkers [22, 23], in their attempt to predict environment-assisted crack growth behavior in AISI 4340 steel, assumed that the value of the maximum load is the controlling factor for crack surface reaction rate. The cycle oxidation time in

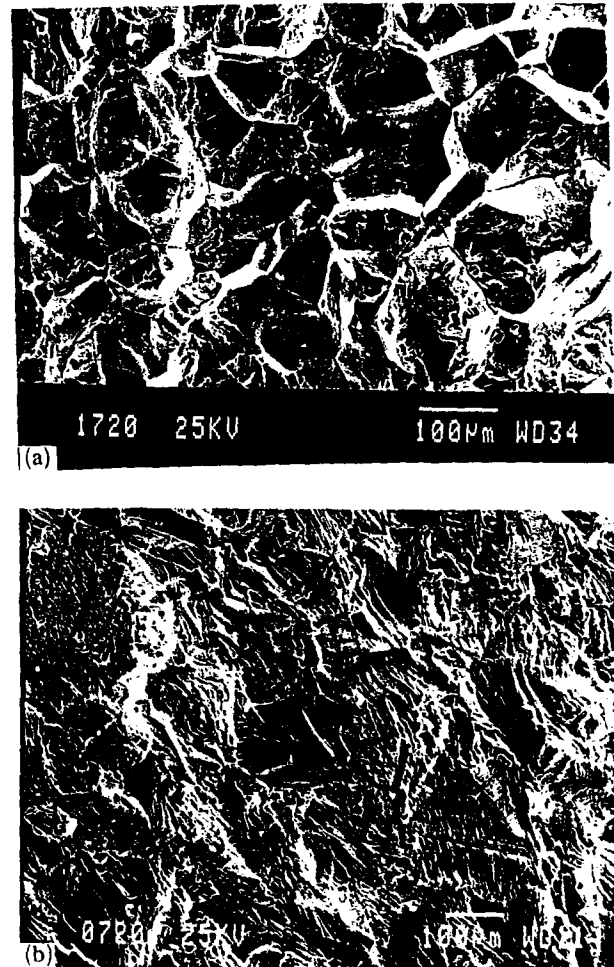


Fig. 5. Scanning electron micrographs of fracture surfaces of alloy 718 tested with 0.05 Hz at 650 °C in (a) air and (b) vacuum.

their work was assumed to be equal to half of the loading period plus half of the unloading period. Nicholas and Weerasooriya [2, 15], in their work on alloy 718, developed a model to predict purely time-dependent fatigue crack growth behavior by integrating the sustained load growth rate. They argued that the loading part of the cycle is the part responsible for the environment-assisted effects. Similar conclusions were made by Floreen [24] in his work on grain boundary diffusion in nickel-base superalloys. Other investigators, especially McGowan and Liu [25], Rechet and Remy [18], Antolovich and Rosa [26], Romanoski *et al.* [27] and Saxena [17], employed, for different materials, different cycle periods to represent t_{ox} . In the face of these different definitions of t_{ox} , an experimental attempt was made here to determine the effective oxidation time for alloy 718 at a temperature level of 650 °C and for loading frequencies less than f_c .

The fatigue crack growth tests were conducted in a constant load range ΔP , and $R=0.1$ where R is the load ratio. These tests involved triangular waveforms with different cycle durations, all satisfying the condi-

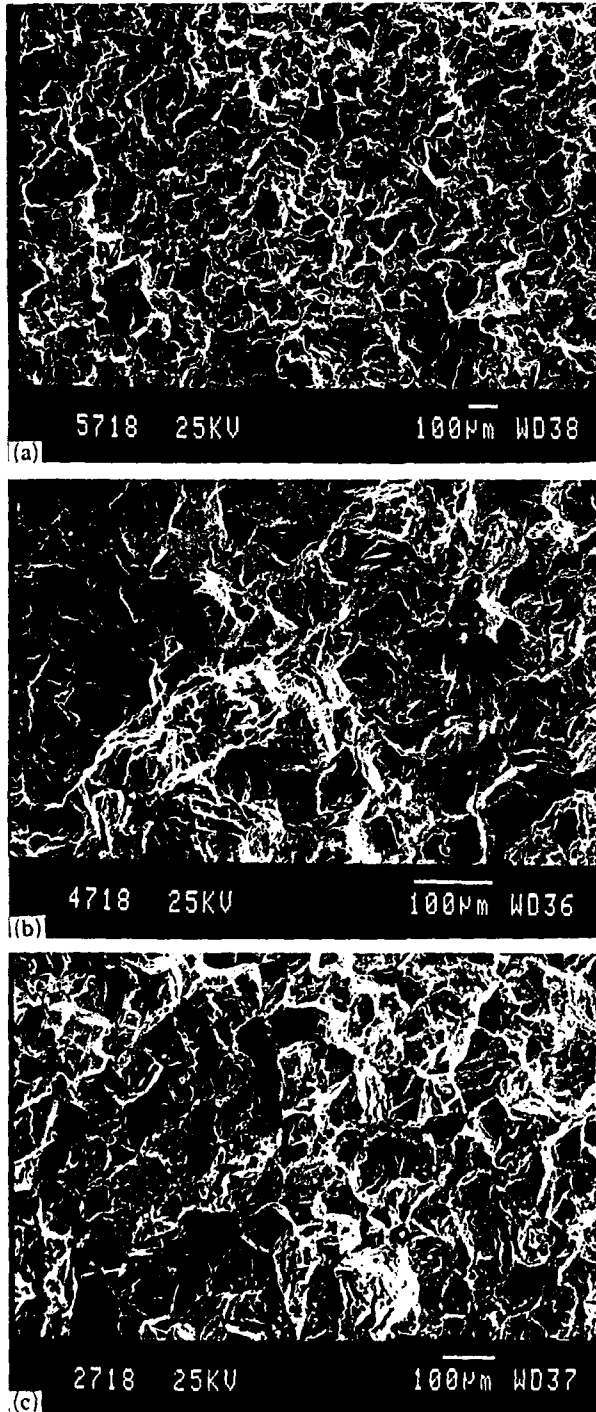


Fig. 6. Scanning electron micrographs of fracture surfaces of alloy 718 tested at 0.05 Hz at 650 °C for (a) 25 s–2.5 s, (b) 25 s–25 s and (c) 90 s–10 s.

tion that $f < f_c$. These durations include 27.5 s (25 s–2.5 s), 50 s (25 s–25 s), 100 s (25 s–75 s) and 100 s (90 s–10 s), labeled here as cases A, B, C and D respectively. Fracture surfaces corresponding to all tests exhibited fully intergranular fracture features (confirming that $f < f_c$), as seen in Fig. 6. Results in the form of a fatigue crack growth rate da/dN vs. ΔK are plotted in Fig. 7. They show the fatigue crack growth rate for case C to be identical to that of case D, indicating that, for the same frequency, varying the ratio of loading and unloading portions of the cycle will not influence the fatigue crack growth behavior. This result is contrary to results obtained, for example, by Coffin [28] in his work on fatigue crack initiation in OFHC copper at 400 °C and on 304 stainless steel at 650 °C. His results showed that, in an asymmetric loading cycle, slow-fast loading is more damaging than fast-slow loading. Similar results have been obtained by other authors for crack growth behavior in various ductile materials [29]. However, their results have been interpreted as time-dependent crack growth caused by grain boundary cavitation. In this cracking mechanism, cavity growth and consequently crack growth are aided by slow rate loading while unloading results in cavity healing with no contribution to the crack growth process. This cavity-growth-related mechanism is not operative in the highly creep-resistant alloy 718. In this alloy, for time-dependent environmental effects which are governed by temperature and load levels, both segments of the loading cycle should exert the same damage effects at the crack tip. Furthermore, cases of A, B and C, which are of different frequencies but identical loading times, did not result in similar crack growth behavior so that an increase in the total cycle duration yields, as expected, an increase in the crack growth rate. The conclusion based on these observations is that, for loading frequencies lower than the

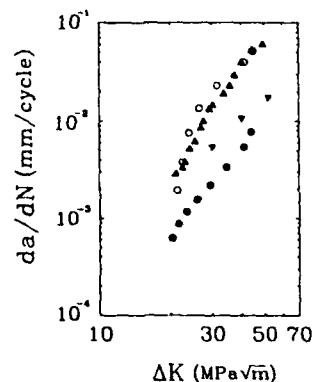


Fig. 7. da/dN vs. ΔK for different frequencies with different loading and unloading ratios (alloy 718 at 650 °C in air; $R=0.1$): ●, 25 s–2.5 s; ▼, 25 s–25 s; ○, 25 s–75 s; ▲, 90 s–10 s.

transitional frequency, the cycle effective oxidation time is equal to the total time of the loading cycle.

4. Relationship between \dot{X} and stress intensity factor range ΔK

4.1. Concept

The work of Nicholas and Weerasooriya [2] has demonstrated that subjecting alloy 718 to elevated-temperature fatigue testing with a loading cycle having a frequency $f > f_c$ and an imposed hold time at the minimum load level for periods up to 1000 s did not result in any measurable acceleration in the crack growth rate when compared with the crack growth rate due to the base cycle without the hold time periods. By lowering the loading frequency to levels below the transitional frequency of the alloy, an accelerated intergranular crack growth was detected when additional hold times at minimum load level were imposed for periods as small as 30 s (see the work of Diboine and Pineau [30]). This observed increase in the crack growth rate is interpreted in the work of Ghonem *et al.* [20] as being a result of further intergranular oxidation taking place at the crack tip during the hold time period, provided that the minimum load level does not contribute to the mechanical driving force of the crack tip. The crack growth rate under this type of loading calculated using a damage summation form similar to that of eqn. (2) can be written as

$$\left(\frac{da}{dN}\right)_{\text{cyc}+h} = \left(\frac{da}{dN}\right)_{\text{cyc}} + \left(\frac{da}{dN}\right)_h \quad (5)$$

where the first term of the right-hand side of the above equation represents the contribution to the crack growth rate due to the reversed part of the cycle and the second term is the contribution due to the hold time period. The above equation can be expressed in terms of da/dt as

$$\left(\frac{da}{dN}\right)_{\text{cyc}+h} = \int_{a_0} \frac{da}{dt} dt + \int_{t_h} \frac{da}{dt} dt \quad (6)$$

The term da/dt is viewed as being equal to the intergranular oxygen diffusion rate \dot{X} which, as mentioned above, is assumed to be a function of the stress intensity factor range ΔK . Therefore eqn. (6) could be rewritten as

$$\left(\frac{da}{dN}\right)_{\text{cyc}+h} = \left(\frac{da}{dN}\right)_{\text{cyc}} + \int \dot{X}(\Delta K, t) dt \quad (7)$$

The intergranular oxygen diffusion depth X could then

be written as

$$X = \left(\frac{da}{dN}\right)_{\text{cyc}+h} - \left(\frac{da}{dN}\right)_{\text{cyc}} \quad (8)$$

The differential form of this equation is expressed as

$$\dot{X} = \lim_{\Delta t \rightarrow 0} \frac{\Delta X}{\Delta t} \approx \frac{(da/dN)_{\text{cyc}+h} - (da/dN)_{\text{cyc}}}{\Delta t} \quad (9)$$

where Δt , in this case, is the hold time duration t_h . Therefore

$$\dot{X} \approx \frac{(da/dN)_{\text{cyc}+h} - (da/dN)_{\text{cyc}}}{t_h} \quad (10)$$

The determination of \dot{X} could thus be achieved through the knowledge of the hold time period t_h and the crack growth rates $(da/dN)_{\text{cyc}+h}$ and $(da/dN)_{\text{cyc}}$ which correspond to the total loading cycle and the reversed part of the cycle respectively. In order to solve this equation an experimental program was carried out to provide these data for different ΔK and t_h values. This experimental program as well as its results and analysis will be described in the following section.

4.2. Experiments, results and analysis

In this program, a set of crack growth experiments were performed on compact tension specimens made of the alloy 718 previously described at a temperature level of 650°C and a stress ratio of 0.1. This set of experiments consisted of constant ΔK tests with and without hold time periods imposed at the minimum load level. Three different values of ΔK were selected: 30, 40 and 50 MPa $m^{1/2}$. For each level of ΔK four different hold time periods were investigated; these are 50, 100, 680 and 3600 s. The load level during the hold time period was determined such that the hold time period would produce, at the longest expected crack length, a stress intensity factor with a value lower than that of the fatigue threshold stress intensity factor for this material which was estimated to be 12 MPa $m^{1/2}$. Under this condition, an observed increase in the crack length would be purely correlated with the oxygen influence at the crack tip. Results of these tests in the form of the ratio $(da/dN)_{\text{cyc}+h}/(da/dN)_{\text{cyc}}$ vs. t_h for different values of ΔK are shown in Fig. 8. They indicate that the influence of the hold time at minimum load level on the crack growth rate is measurable for hold time periods as small as 50 s. This observation confirms similar findings reported by Diboine and Pineau [30]. The influence of the hold time reaches a saturated level at t_h values that increases as ΔK decreases. These results in the form of $(da/dN)_{\text{cyc}+h}/(da/dN)_{\text{cyc}}$ when substituted in eqn. (9) yield values of

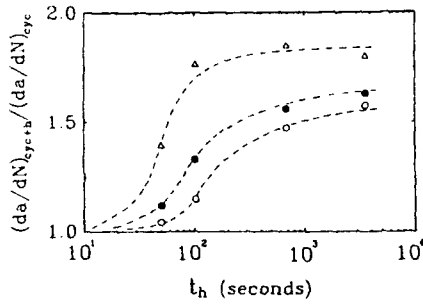


Fig. 8. Effect of hold time at minimum load level on $(da/dN)_{cyc+h}/(da/dN)_{cyc}$ for different K_h levels: \circ , $\Delta K = 30 \text{ MPa m}^{1/2}$; \bullet , $\Delta K = 40 \text{ MPa m}^{1/2}$; Δ , $\Delta K = 50 \text{ MPa m}^{1/2}$.

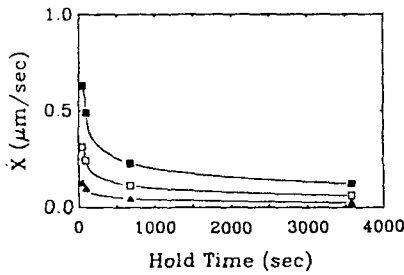


Fig. 9. Oxygen intergranular diffusion rate \dot{X} vs. hold time t_h imposed at minimum load for different ΔK levels (alloy 718 at 650°C in air; $R = 0.1$): \blacktriangle , $\Delta K = 30 \text{ MPa m}^{1/2}$; \square , $\Delta K = 40 \text{ MPa m}^{1/2}$; \blacksquare , $\Delta K = 50 \text{ MPa m}^{1/2}$.

\dot{X} calculated as a function of t_h and ΔK . This type of relationship is illustrated in Fig. 9. It shows that, for all values of ΔK , \dot{X} decreases as t_h increases. This relationship between \dot{X} and t_h could be interpreted on the basis of the two-stage oxidation mechanism [31]. At the onset of the oxidation process, the oxygen diffusion rate reaches its peak since no barrier to diffusion exists. As the oxidation time increases, thus permitting the formation of the dense chromia (Cr_2O_3) layer, the oxygen penetration rate decreases. When the formation of Cr_2O_3 is completed after a certain transition time which is microstructure dependent [32], \dot{X} would approach zero. The relationship between \dot{X} and both t_h and ΔK , as illustrated in Fig. 9, is fitted into the mathematical form

$$\dot{X} = G_1(t) \Delta K^m \quad (11)$$

where $G_1(t)$ assumes the following polynomial form and m is a constant with a value of 3.144:

$$G_1(t) = A t^{-a_1} \exp\left(-\frac{a_2}{t}\right) \left(1 - a_1 + \frac{a_2}{t}\right) \quad (12)$$

A , a_1 and a_2 are coefficients having the values of 1.787×10^{-8} , 0.632 and 28.67 respectively. One should observe that in the above equation, when time t

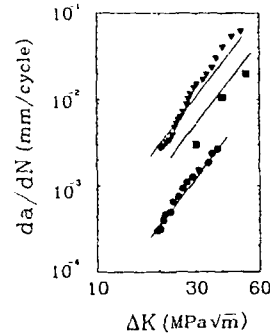


Fig. 10. da/dN vs. ΔK for both experimental and theoretically predicted results (alloy 718 at 650°C in air; $R = 0.1$): \bullet , 0.05 Hz predictions; \blacksquare , 0.02 Hz predictions; \blacktriangledown , 0.01 Hz predictions.

approaches infinity, both $G_1(t)$ and consequently \dot{X} approach zero.

The validity of eqn. (11) cannot be tested through direct measurements of \dot{X} ; it could, however, be verified through the use of \dot{X} to derive a fatigue crack growth rate expression, which can be tested by comparing its predictive results with those experimentally generated. This is achieved as follows. One can write the crack growth rate equation as

$$\frac{da}{dN} = \int_0^{t_{ox}} \dot{X} dt \quad (13)$$

where t_{ox} is the effective oxidation time during a loading cycle. Substituting eqn. (11) into eqn. (13) and considering the oxidation time of a loading cycle to be, as previously discussed, equal to the total cycle time, the fatigue crack growth rate can then be derived as

$$\dot{X} = \frac{da}{dN} = G_2(f) \Delta K^m \quad (14)$$

where

$$G_2(f) = A f^{-a_1} \exp(-a_2 f)$$

f is the loading frequency while A , a_1 and a_2 are constants having the same numerical values as those in eqn. (11). Equation (14) could now be tested by comparing its predictive results with those experimentally obtained for the same loading frequency. The degree of matching between these two sets of results can then determine the validity of eqn. (11). Equation (14) was applied for three different frequencies, 0.01, 0.02 and 0.05 Hz, all of which are below f_c for the alloy 718 used in this study. Results of this application are shown in Fig. 10. It is observed that a reasonable agreement exists in the full range of ΔK between the values and trends of the three experimentally obtained data sets and those theoretically predicted through the use

of eqn. (14). This result is taken in support of the proposition that eqn. (11) is a valid expression for estimating the oxygen diffusion rate in alloy 718 and also as an indirect support for the notion that the growth process governed by eqn. (14) is a fully environment-dependent process.

An important feature of eqn. (11) is in its use to calculate directly the oxygen diffusivity of grain boundaries D_g , a parameter required for the physical understanding and the quantitative modeling of the crack tip oxidation mechanism in alloy 718 [6]. This could be achieved as follows: a parabolic diffusion law when applied to estimate the intergranular depth X of oxygen diffusion during a time interval t could be written as

$$X = \alpha (D_g t)^{1/2} \quad (15)$$

where α is a geometrical constant, and D_g is the oxygen diffusivity of grain boundaries. The intergranular oxygen diffusion depth X during the time interval corresponding to one loading cycle could thus be calculated as

$$X = \alpha \left(\frac{D_g}{f} \right)^{1/2} \quad (16)$$

where f is the loading frequency. Another identification of X is that described in eqn. (14). By equating these two X expressions, i.e. eqns. (14) and (16), an explicit relationship linking the oxygen diffusivity of grain boundaries D_g with both ΔK and frequency f can

be derived. This relationship is obtained here as

$$D_g = G_3(f) \Delta K^{2m} \quad \Delta K > 0 \quad (17)$$

where

$$G_3(f) = \left(\frac{A}{\alpha} \right)^2 f^{-(2a_1+1)} \exp(-2a_2 f)$$

This relationship between D_g , ΔK and f as illustrated in Fig. 11 shows that, for the same ΔK range, the diffusivity D_g is inversely proportional to the loading frequency. This can be explained, as qualitatively discussed in eqn. (1), by considering the influence of frequency on the local stress field near the grain boundary regions. For example, the decrease in the loading frequency is expected to result in an inhomogeneous form of plastic deformation which consequently leads to the increase of stress concentration across the affected grain boundary paths near the crack tip. This would then result in the decrease of the effective diffusional activation energy Q_g' of these affected boundaries. The decrease in Q_g' is expressed in eqn. (1) through the introduction of an inelastic strain energy function $f(W_p)$ which can now be shown, through the comparison between eqns. (1) and (17), to be a ΔK - and f -dependent function. Furthermore, Fig. 11 shows that, for the same loading frequency, the diffusivity D_g increases as ΔK increases. This again can be explained in terms of the direct influence of the crack tip stress field on the diffusional characteristic of the grain boundary path.

Now, if one makes the assumptions that the ratio of matrix diffusivity D_m to grain boundary diffusivity D_g is maintained at 10^4 [33] and, furthermore, D_m is a frequency-independent parameter, one could thus establish profiles of D_m for different ΔK values. These profiles are shown as broken lines in Fig. 11. The point of intersection between two corresponding D_m and D_g lines would then identify the transitional frequency f_c for a particular ΔK level. Below f_c , D_g dominates, giving rise to intergranular crack growth mode; above f_c , D_m dominates, resulting in a transgranular crack growth path. In this case, while f_c decreases as ΔK increases, the variation of f_c is, as described by Weerasooriya and Venkataraman [11, 12], confined in the narrow range between 0.1 and 0.2 Hz.

It should be emphasized here that, while some aspects of the above discussion are speculative in nature due to the lack of literature data related to D_m and D_g , the present work is an attempt to bring a certain view to the understanding of the oxidation role in the intergranular fatigue crack growth process. Further work is required in order to obtain enough experimental data related to the oxygen diffusion at the crack tip.

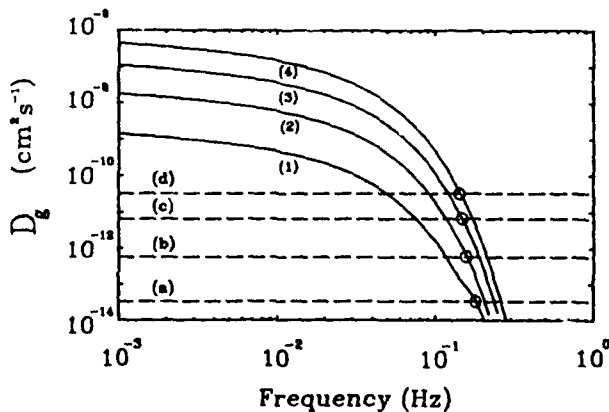


Fig. 11. Variations of the oxygen diffusivity of grain boundaries D_g (—) with loading frequency f and ΔK for alloy 718 with the microstructure shown in Fig. 4: curve 1, $\Delta K = 20 \text{ MPa m}^{1/2}$; curve 2, $\Delta K = 30 \text{ MPa m}^{1/2}$; curve 3, $\Delta K = 40 \text{ MPa m}^{1/2}$; curve 4, $\Delta K = 50 \text{ MPa m}^{1/2}$; lines a, b, c, d, corresponding D_m profiles (see text).

5. Conclusions

For cyclic loading frequencies lower than the transitional frequency of the highly creep-resistant alloy 718, the high-temperature fatigue crack growth behavior is viewed here to be a fully environment-dependent process. Under this condition, the crack extension per cycle is assumed to be equal to the intergranular oxygen diffusion depth taking place at the crack tip region during the cycle effective oxidation time. Two aspects have been particularly investigated—the cycle effective oxidation time and the grain boundary diffusion kinetics. The cycle effective oxidation time t_{ox} has been studied by comparing crack growth rates corresponding to symmetrical as well as asymmetrical waveform loadings with different frequencies. The subject of the diffusion kinetics of the grain boundary network in the crack tip region has been studied indirectly by performing a series of environmentally controlled crack growth experiments. The conclusions of these two studies can be summarized as follows.

(1) The existence of an environment-dependent crack growth stage in alloy 718 at elevated temperatures is supported by comparing results of crack growth tests in both air and vacuum conditions.

(2) For creep-resistant high strength alloy 718, the cycle effective oxidation time t_{ox} should be taken as the whole cycle duration including both the loading and unloading part of the cycle.

(3) The oxygen diffusion rate along affected grain boundaries \dot{X} depends on both the oxidation time and the crack tip stress intensity range ΔK . Furthermore, a closed-form solution correlating the intergranular oxygen diffusion rate in the crack tip region with both t_{ox} and ΔK is obtained. This solution, when integrated over the cycle effective oxidation time, provides a measure of the fatigue crack growth rate. A reasonable agreement is observed when comparing the results from this analytical solution with those experimentally generated.

(4) The oxygen diffusivity of grain boundaries D_g is derived as a function of the stress intensity factor range ΔK and the loading frequency f . Through this relationship, the intergranular-transgranular transitional frequency f_c has been identified as a ΔK -dependent parameter.

Acknowledgment

The authors acknowledge valuable discussions with Dr. T. Nicholas of Materials Directorate, Wright Patterson Air Force Base, and Professor A. Pineau of Ecole des Mines de Paris. Mr. A. Madsen, a graduate student at Mechanics of Solids Laboratory, University of

Rhode Island, has contributed to this work by performing vacuum-related tests. This study was supported jointly by United Technologies, Pratt & Whitney Group and USAFOSR, Bolling Air Force Base, under contract AFOSR-89-0285.

References

- 1 J. W. Brook and P. J. Bridges, Long term stability of Inconel alloy 718 for turbine disc applications. In W. Betz, R. Brunetaud, D. Coutouradis, H. Fischmeister, T. B. Gibbons, I. Kvernes, Y. Lindblom, J. B. Marriott and D. B. Meadowcroft (eds.), *High Temperature Alloys for Gas Turbines and Other Applications 1986*, Part II, Reidel, Dordrecht, 1986, pp. 1431–1440.
- 2 T. Nicholas and T. Weerasooriya, Hold-time effects in elevated temperature fatigue crack propagation. In J. H. Underwood, R. Chait, C. W. Smith, D. P. Wilhelm, W. A. Andrews and J. C. Newman (eds.), *Fracture Mechanics*, Vol. 17, *Am. Soc. Test. Mater., Spec. Tech. Publ.*, 905 (1986) 155–168.
- 3 A. Pineau, Intergranular creep-fatigue crack growth in Ni-base alloys. In R. Raj (ed.), *Flow and Fracture at Elevated Temperatures*, American Society for Metals, Metals Park, OH, 1985, pp. 317–348.
- 4 S. Sadananda and P. Shahinian, Effects of environment on high temperature crack growth behavior of several nickel-base alloys. In R. C. Scarberry (ed.), *Corrosion of Nickel-Base Alloys*, American Society for Metals, Cincinnati, OH, 1985, pp. 101–115.
- 5 L. F. Coffin, Jr., Fatigue at high temperature. In A. E. Carden, A. J. McEvily and C. H. Wells (eds.), *Fatigue at Elevated Temperatures*, *Am. Soc. Test. Mater., Spec. Tech. Publ.*, 520 (1973) 5–34.
- 6 H. Ghonem and D. Zheng, Oxidation-assisted fatigue crack growth behavior in alloy 718—Part I: Quantitative modeling, *Fatigue Fract. Eng. Mater. Struct.*, 14 (1991) 749–760.
- 7 S. J. Balsone, T. Nicholas and M. Khobai, Effects of stress history on the magnitude of the environmental attack in Rene 80. In W. B. Lisagor, T. W. Croofer and B. N. Leis (eds.), *Environmentally Assisted Cracking: Science and Engineering*, *Am. Soc. Test. Mater., Spec. Tech. Publ.*, 1049 (1990) 303–318.
- 8 L. F. Coffin, Jr., Cyclic-strain-induced oxidation of high-temperature alloys, *Trans. Am. Soc. Met.*, 56 (1963) 339–344.
- 9 A. Pineau, High temperature fatigue: creep-fatigue-oxidation interactions in relation to microstructure. In L. H. Larsson (ed.), *Subcritical Crack Growth due to Fatigue, Stress Corrosion and Creep*, Elsevier, London, 1984, pp. 483–530.
- 10 T. Nicholas, T. Weerasooriya and N. E. Ashbaugh, A model for creep/fatigue interaction in alloy 718. In M. F. Kannien and A. T. Hopper (eds.), *Fracture Mechanics: 16th Symp. Am. Soc. Test. Mater., Spec. Tech. Publ.*, 868 (1985) 167–180.
- 11 T. Weerasooriya and S. Venkataraman, Frequency and environment effect on crack growth in Inconel 718. In P. K. Liaw and T. Nicholas (eds.), *Effects of Load and Thermal Histories*, Metallurgical Society of AIME, Warrendale, PA, 1987, pp. 101–108.
- 12 T. Weerasooriya, Effect of frequency on fatigue crack growth rate of Inconel 718 at high temperature. In T. A. Cruse (ed.), *Fracture Mechanics: 19th Symp. Am. Soc. Test. Mater., Spec. Tech. Publ.*, 969 (1988) 907–923.

- 13 M. Clavel, D. Fournier and A. Pineau, Plastic zone sizes in fatigued specimens of INCO 718, *Metall. Trans. A*, 6 (1975) 2305-2307.
- 14 R. P. Wei and J. D. Landes, Correlation between sustained-load and fatigue crack growth in high-strength steels, *Mater. Res. Stand.*, 9 (7) (1969) 25-28, 44, 46.
- 15 T. Nicholas, Fatigue crack growth modeling at elevated temperature using fracture mechanics. In S. Mall and T. Nicholas (eds.), *Elevated Temperature Crack Growth*, American Society of Mechanical Engineers, New York, NY, 1990, pp. 107-112.
- 16 M. R. Winstone, K. M. Nikbin and G. A. Webster, Modes of failure under creep/fatigue loading of a nickel-based superalloy, *J. Mater. Sci.*, 20 (1985) 2471-2476.
- 17 A. Saxena, A model for predicting the environment enhanced fatigue crack growth behavior at high temperature. In E. J. Carl, J. H. Stephen, Jr., and E. M. Michael (eds.), *Thermal and Environmental Effects in Fatigue: Research-Design Interface*, American Society of Mechanical Engineers, New York, NY, 1983, pp. 171-184.
- 18 J. Rechet and L. Remy, Fatigue oxidation interaction in a superalloy—application to life prediction in high temperature low cycle fatigue, *Metall. Trans. A*, 14 (1983) 141-149.
- 19 P. Shahinian and K. Sadananda, Crack growth behavior under creep-fatigue conditions in alloy 718, *Creep Fatigue Interaction*, American Society of Mechanical Engineers, New York, NY, 1976, pp. 365-390.
- 20 H. Ghonem, D. Zheng, E. Andrieu and A. Pineau, Experimental observations and quantitative modelling of oxidation-assisted crack growth behavior in alloy 718 at 650°C, *Annu. Rep. AFOSR-89-0285*, Bolling AFB, Washington, DC, 1990.
- 21 M. R. Achter, The adsorption model for environmental effects in fatigue crack propagation, *Scripta Metall.*, 2 (1968) 525-528.
- 22 R. P. Wei, On understanding environment-enhanced fatigue crack growth—a fundamental approach. In J. T. Fong, *Fatigue Mechanisms*, Am. Soc. Test. Mater., Spec. Tech. Publ., 675 (1979) 816-840.
- 23 T. W. Weir, G. W. Simmons, R. G. Hart and R. P. Wei, A model for surface reaction and transport controlled fatigue crack growth, *Scripta Metall.*, 14 (1980) 357-364.
- 24 S. Floreen, Effects of environment on intermediate temperature crack growth in superalloys. In K. Sadananda, B. B. Rath and D. J. Michel (eds.), *Micro and Macro Mechanics of Crack Growth*, Metallurgical Society of AIME, Warrendale, PA, 1981, pp. 177-184.
- 25 J. J. McGowan and H. W. Liu, A kinetic model for high temperature fatigue crack growth. In J. B. John and W. Volker (eds.), *Fatigue Environment and Temperature Effects*, Plenum, New York, NY, 1983, pp. 377-390.
- 26 S. D. Antolovich and E. Rosa, Low cycle fatigue of Rene 77 at elevated temperatures, *Mater. Sci. Eng.*, 47 (1981) 47-57.
- 27 G. R. Romanoski, S. D. Antolovich and R. M. Pelloux, A model for life predictions of nickel-base superalloy in high temperature low cycle fatigue. In H. D. Solomon, G. R. Halford and B. N. Leis (eds.), *Low Cycle Fatigue*, Am. Soc. Test. Mater., Spec. Tech. Publ., 942 (1988) 456-469.
- 28 L. F. Coffin, Jr., Overview of temperature and environmental effects on fatigue of structural metals. In J. J. Burke and V. Weiss (eds.), *Fatigue: Environment and Temperature Effects*, Plenum, New York, NY, 1980, pp. 1-40.
- 29 H. Ghonem and R. Foerch, Frequency effects on fatigue crack growth behavior in a near- α titanium alloy. In S. Mall and T. Nicholas (eds.), *Elevated Temperature Crack Growth*, American Society of Mechanical Engineers, New York, NY, 1990, pp. 93-105.
- 30 A. Diboine and A. Pineau, Creep crack initiation and growth in Inconel 718 at 650°C, *Fatigue Fract. Eng. Mater. Struct.*, 10 (1987) 141-151.
- 31 E. Andrieu, H. Ghonem and A. Pineau, Two stage crack tip oxidation mechanism in alloy 718. In S. Mall and T. Nicholas (eds.), *Elevated Temperature Crack Growth*, American Society of Mechanical Engineers, New York, NY, 1990, pp. 25-29.
- 32 E. Andrieu, Influence de l'environnement sur la propagation des fissures dans un superalliage base nickel: l'Inconel 718, *Ph.D. Dissertation*, L'Ecole Nationale Supérieure des Mines de Paris, 1987.
- 33 P. G. Shewmon, *Diffusion in Solids*, McGraw-Hill, New York, NY, 1963.

Intergranular crack tip oxidation mechanism in a nickel-based superalloy

E. Andrieu and R. Molins

Centre de Materiaux, URA CNRS 860, Ecole des Mines de Paris, B.P. 87, 91003 Evry Cedex (France)

H. Ghonem

Mechanics of Solids Laboratory, Department of Mechanical Engineering, University of Rhode Island, Kingston, RI 02881 (USA)

A. Pineau

Centre des Materiaux, URA CNRS 860, Ecole des Mines de Paris, B.P. 87, 91003 Evry Cedex (France)

(Received April 29, 1991; in revised form November 19, 1991)

Abstract

This paper is concerned with the intergranular crack tip oxidation mechanism in alloy 718 at elevated temperatures. The basic concept is based on the ability of the oxygen partial pressure to control the preferential formation of oxide layers at the crack tip. The time required to complete the build-up of the protective oxide type at the metal-oxide interface is considered a measure of the limits of the oxidation process. Identification by transmission electron microscopy of oxide scale formed along fracture surfaces during a low frequency fatigue crack process in alloy 718 at 650°C supports the proposed model concepts. An experimental program was carried out to investigate the role of passivation time in controlling the progressive process of crack tip oxidation. This was achieved by testing the influence of oxide build-up during hold time at minimum load, as well as the effect of a minor high frequency cycle imposed on the hold time period. It was established that an increase in fatigue crack growth rate accompanies the increase in passivation time period. These results were interpreted on the basis of the oxidation formation concepts.

1. Introduction

Extensive evidence exists in the literature showing that the time dependence of high temperature crack initiation and propagation is the result of the aggressive effect of the environment. The early work of Smith *et al.* [1] has clearly demonstrated that environmental degradation is a result of oxygen penetration at the crack tip. Efforts have been made in the last decade to detail the crack tip oxidation mechanism and provide correlations between these mechanisms and both material and loading parameters. When not considering simple adsorption of oxygen at the crack tip, oxidation mechanisms could be identified, in general in terms of short- and long-range oxygen diffusion processes. In short-range diffusion, oxygen forms an oxide layer at the crack tip with a depth that depends on many operating and materials parameters. The formation of this layer, under the restricted concave crack tip geometry, results in high stresses that could easily be transmitted to the substrate. The important aspect of this oxidation mechanism, however, is the possible formation of wedge-shaped oxide intrusions along the

crack front. The rupture of these wedges at grain boundary intersections, could result in an accelerated, intergranular crack growth rate, see refs. 2-5. In long-range diffusion, oxygen penetrates the crack tip material along rapid diffusion paths, such as slip planes and grain boundaries. The internal oxidation process taking place along these paths could occur in the form of internal oxide sites, cavity formations, and/or solute segregation. As pointed out by Woodford and Bricknell [6], it is also possible for oxygen to take part in chemical reactions releasing known embrittlement agents onto a grain boundary. Each, or all, of these may be operative in any particular alloy under a given set of conditions. These processes, in particular along grain boundaries, result in inhibition of sliding and migration of these boundaries and thus reduce their ability to relieve local stresses built up during deformation.

While it is recognized that the oxidation mechanisms associated with short- and long-range diffusion are not completely separated, experimental observations indicate that, for alloy 718, at an intermediate temperature range and at a low level of loading frequency, short-range oxygen diffusion contributes primarily to the

occurrence of an intergranular fracture mode. Recognizing that oxygen partial pressure plays an important role in the development of this oxidation process, Andrieu [7] has studied the type and sequence of oxide layer formation at the crack tip. The objective of this paper is to examine experimentally the validity of his results. The first part of the paper reviews the concepts of the oxide formation mechanism and governing parameters while the second part presents experimental work carried out to verify these concepts.

2. Concept

The damage process associated with short-range oxygen diffusion at the crack tip has been studied by several authors, see for example refs. 8–10. Important factors to be considered in this process are those related to temperature, frequency, alloy chemistry and oxygen partial pressure, $P(\text{O}_2)$. The first clear demonstration of the effect of $P(\text{O}_2)$ was exhibited in the work of Smith *et al.* [1]. They observed that reducing the oxygen partial pressure during fatigue crack propagation in 316 stainless steel at both 500 and 800 °C led to a lower crack growth rate. Transition to higher crack growth rates, as $P(\text{O}_2)$ increased, was also observed, for example by Michel and Smith [11] in their work on a cobalt-base alloy at 427 °C, by Stegmann and Shahinian [12] on nickel alloy at 500 °C and by Smith and Shahinian [13] on silver at 20, 150 and 350 °C; ref. 14 gives a review of the subject. This transition was interpreted by Achter *et al.* [15] in terms of the impingement rate of oxygen molecules on successive rows of freshly exposed metal atoms at the crack tip. As discussed by Ericsson [14], the geometry of the impingement concepts has, in general, been described in vague terms facing the difficulty of providing an explanation for the severity of damage that a monolayer of oxide could cause at the crack tip. Furthermore, these concepts cannot support the experimental observations made, for example, by Smith and Shahinian [13]. They reported that the effect of oxygen pressure on the fatigue life of silver at 350 °C is small compared with the effect at 20 and 150 °C. An increase in the initial rate of oxygen adsorption has, however, been observed with increased temperature in the 20–350 °C range.

Another interpretation of the influence of $P(\text{O}_2)$ on crack growth is related to the ability of oxygen at different pressures to control the preferential formation of one given species of oxide that may shield or contribute to crack tip damage through passivation or enhancement of the oxidation process respectively. It is known, for example, that oxidation of chromium as an alloying element produces a protective layer of Cr_2O_3 . If chromium diffusion in the alloy is too low to sustain the

supply of chromium at the scale-metal interface, less noble elements of the alloy, e.g. iron, will be oxidized at the scale-metal interface. This will result in an increased reaction rate [15]. Andrieu [7] has experimentally examined the influence of $P(\text{O}_2)$ on the formation of selective oxides. In his work, small discs with a thickness of 3 mm and diameter of 20 mm were machined from alloy 718 containing about 18% iron and characterized by both an average grain size of 150 μm and β -phase free grain boundaries, see Fig. 1. These electropolished and mechanically polished discs were subjected to different $P(\text{O}_2)$ levels ranging from 3×10^{-1} to 10^{-5} Torr for periods of 480 s at 650 °C using a high-vacuum device equipped with a mass spectrometer. Auger spectrometry analysis was subsequently used to identify the oxide type formed on the free surfaces of these discs as a function of the operating $P(\text{O}_2)$ level. Sputter profiles of the formed oxides are summarized in Fig. 2. It is interesting to observe that an oxygen partial pressure as high as 10^{-4} Torr promotes selective oxidation of chromium and that, under a pressure of 10^{-1} – 10^{-2} Torr, the first oxides to appear are nickel and iron-base oxides. The relationship between time required to form the chromium oxide as a function of oxygen partial pressure is shown schematically in Fig. 3; at atmospheric pressure this passivation time is estimated to be in the range 5–8 min. Throughout this study it was difficult to tell whether the surface being analyzed was a matrix or a grain boundary interface. Transmission electron microscopy was therefore carried out on a foil made of the same alloy 718 in which the grain boundary interface was identified and subjected to a temperature of 650 °C for 240 s in a room environment. Results are

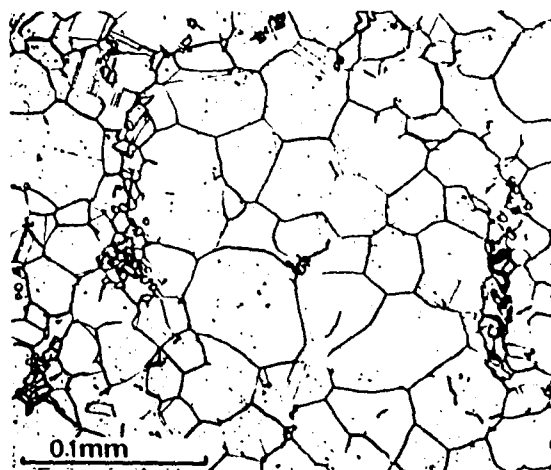


Fig. 1. Microstructure of alloy 718 used in the experimental study.

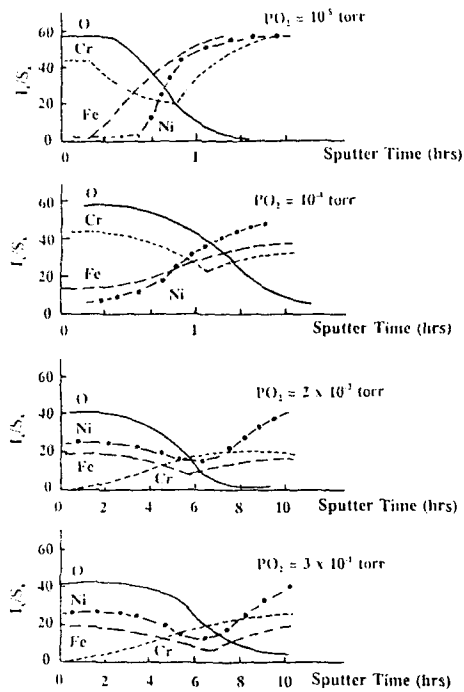


Fig. 2. Sputter-depth profiles of the surface oxides (oxidation time 8 min, temperature 650 °C).

shown in Fig. 4. They indicate that, under atmospheric pressure, microcrystallized oxides of nickel and iron developed rapidly along the grain boundary interface.

In addition, attempts have been made to identify the role of $P(O_2)$ in determining the cracking mode. This was achieved by carrying out a series of slow strain-rate, tensile tests on axisymmetrically precracked fatigue round bars made of the same alloy. These tests were performed at 650 °C in an ultrahigh vacuum apparatus detailed in ref. 7. Using a mapping technique

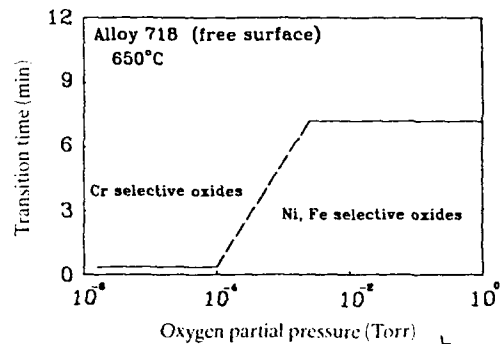


Fig. 3. Types of oxide as a function of transition time t_p and oxygen partial pressure.

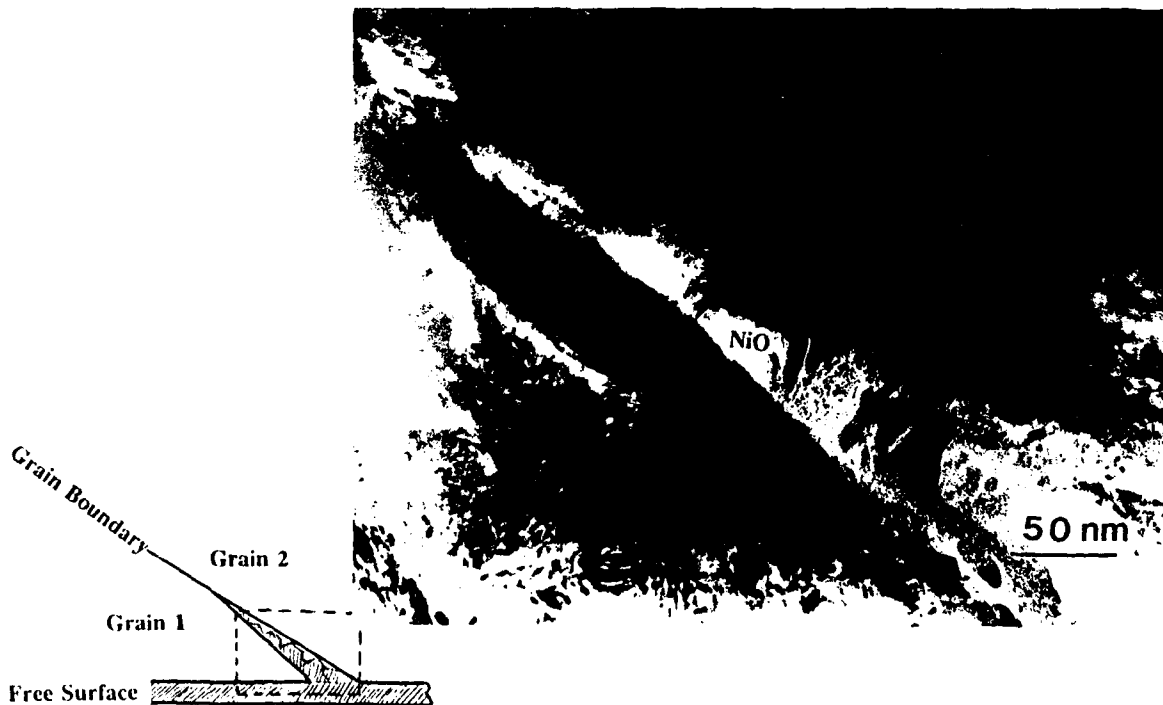


Fig. 4. Static oxidation of a grain boundary (exposure time 4 min, temperature 650 °C)

employed on the resulting fracture surfaces, examples of which are shown in Fig. 5, the percentage of transgranular fracture area, with respect to the total fracture surface area, was measured. These percentages are reported in Fig. 6 in terms of oxygen partial pressure. They indicate that the intergranular fracture ratio increases as $P(O_2)$ increases; under atmospheric pressure, 60% of the fracture surface of the test specimens

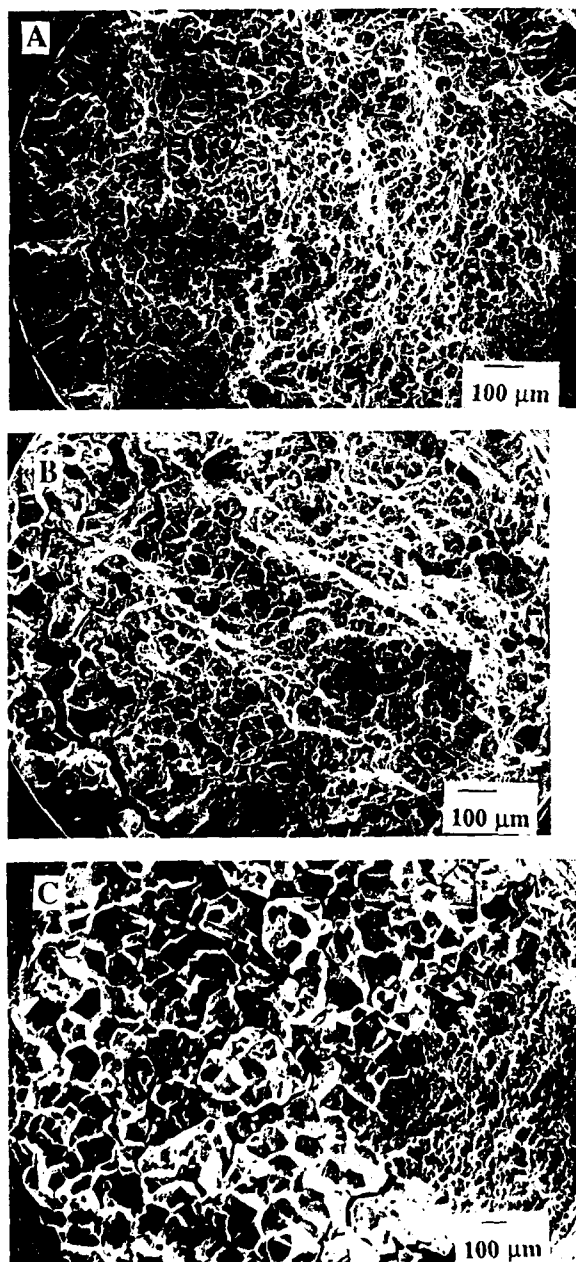


Fig. 5. Fracture surfaces corresponding to different oxygen partial pressures: A, 10^{-4} Torr; B, 1 Torr; C, 4 Torr.

was found to be intergranular. Also, a transition exists between 10^{-2} and 1 Torr, below which the failure mode is fully transgranular. This range of transitional pressure is consistent with observations made on different alloys [11–13]. These results, when linked to those in Fig. 2 showing the influence of $P(O_2)$ in determining the type and sequence of selective oxides, could provide a qualitative view of crack tip oxidation along a preferred grain boundary path. This view suggests that oxidation occurs in two stages, depicted schematically in Fig. 7. The first stage influenced by the atmospheric level of oxygen partial pressure, would result in the formation of FeO and NiO and their spinels. For these oxides which are porous and pervious to oxygen, gas diffusion through the pores plays an important role in determining the reaction rate as a function of time.

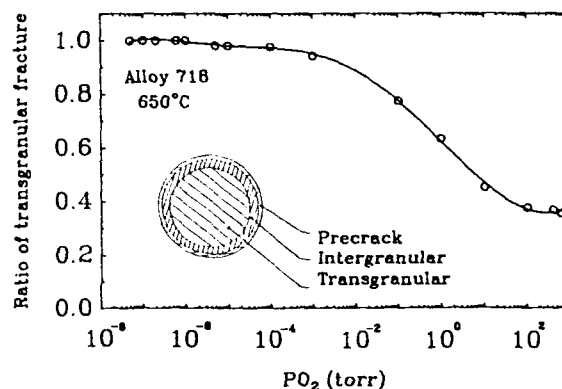


Fig. 6. Ratio of transgranular fracture vs. oxygen partial pressure.

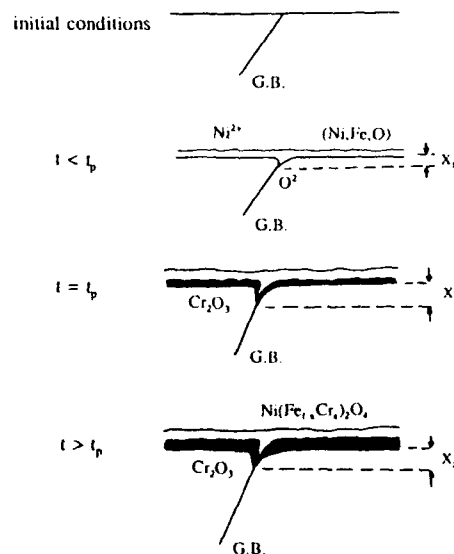


Fig. 7. Suggested mechanism of grain boundary oxidation.

The build-up of these oxide products would result, at the oxide-metal interface, in a lowering of the oxygen partial pressure [16]. This, consistent with the Ellingham-Richardson diagram, would provide the reaction kinetics required for the formation of a denser Cr_2O_3 oxide sublayer. This dense layer is thermodynamically stable at high temperatures and is considered protective in the sense that it limits oxygen diffusion to the grain boundary material, thus limiting the reaction rate [17]. The complete formation of this layer along the crack front is regarded as an attainment of oxide depth saturation. The time required to reach this stage is identified as the transition time t_p , which is a function of temperature, $P(\text{O}_2)$ and localized stress and strain fields. When this time is reached, it is assumed that the condition for oxygen passivation is met and no further oxygen penetration can take place along the affected grain boundary paths. One should observe that the passivation effect is not assumed here to be a discrete process, but a continuous gradual decrease in the oxide depth formation rate as the ratio of the Cr_2O_3 to the total oxide weight increases.

3. Experimental verification

The experimental program described here was carried out using compact tension specimens made of the same alloy 718 previously described. All tests were performed at 650°C for a constant amplitude loading with a frequency of 0.05 Hz and load ratio $R=0.1$. The first part of this program was to insure that the loading frequency of 0.05 Hz would yield fatigue crack growth data that were fully dominated by environment effects. This was achieved by comparing the fatigue cracking mode corresponding to this frequency in both vacuum and air. Vacuum tests were conducted in a chamber inside which elevated temperature was reached by using a 10 kHz induction heating system. The degree of vacuum was monitored with a residual gas analyzer and showed a testing vacuum of better than 5×10^{-8} Torr total pressure, which consisted primarily of nitrogen and oxygen with a partial pressure of less than 10^{-9} Torr. Results of air as well as vacuum tests, which are detailed in ref. 17, are shown in Fig. 8. It is observed that the total number of cycles to propagate the same crack length ($a/w=0.4$ to 0.7) was about 5000 cycles in air while it was 65 000 cycles in vacuum. The fracture surfaces in both air and vacuum tests were examined; typical results are shown in Fig. 9. Air results show complete intergranular fracture mode compared with a fully transgranular mode in vacuum. These results indicate the total domination of the environment on fatigue crack growth behavior at a frequency of 0.05 Hz. Furthermore, the types of oxide

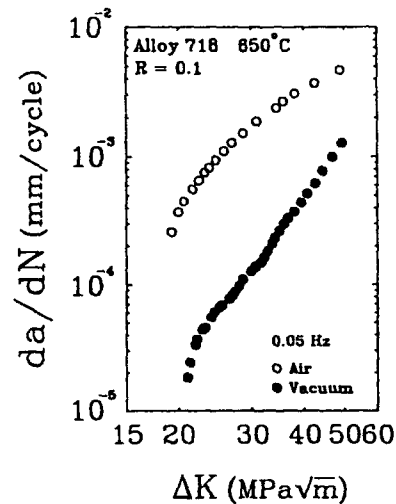


Fig. 8. Fatigue crack growth rate in air and vacuum at 650°C [17].

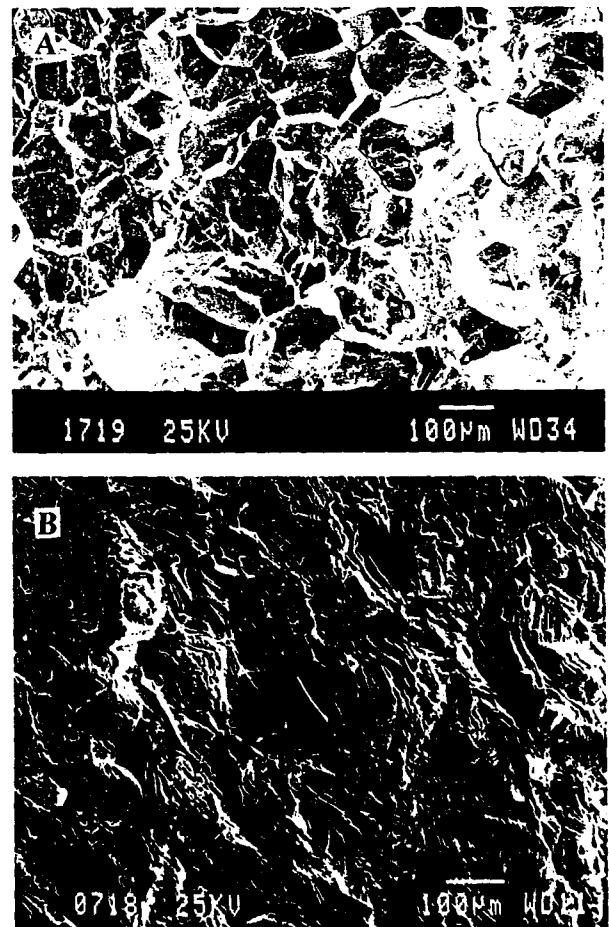


Fig. 9. Typical fracture surfaces in both air (A) and vacuum (B) at 650°C [17].

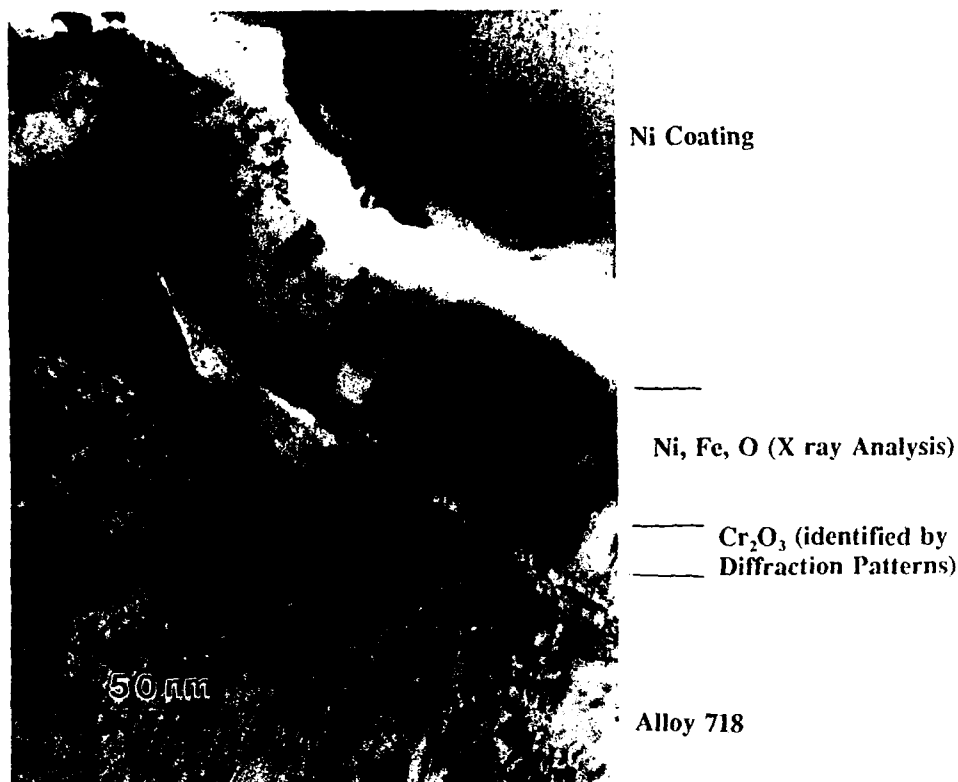


Fig. 10. Transmission electron micrographs and microanalysis of oxide types developed on the fracture surface.

formed on the fracture surface of the air-tested specimen were identified by analytical transmission electron microscopy on a thin foil of a fracture surface edge. Figure 10 indicates the existence of two oxide layers—the inner layer (A) at the metal–oxide interface is identified as Cr_2O_3 while the outer layer has been identified as a spinel oxide $\text{Ni}(\text{FeCr})_2\text{O}_4$ in the same order as suggested in the proposed model.

Attention was then focused on validating the two-stage oxidation concept by investigating the effect of crack tip oxidation during a time duration equal to t_p on the subsequent fatigue crack growth rate. This was accomplished by comparing the crack growth rate of specimens subjected to continuous cycle loading (condition 1) with those subjected to the same type of loading but with an added hold time at the minimum load level (condition 2). The duration of this hold time was selected to be 600 s which is in the order of the oxide saturation time for this alloy [11]. In these tests, carried out at 650 °C, care was taken that the minimum load level during the hold time period would produce, at the longest expected crack length ($a/w = 0.7$), a stress intensity with a value lower than that of the fatigue threshold stress intensity factor for this material which was estimated to be 12 MPa $\text{m}^{1/2}$. This is to insure that

this minimum load does not contribute to the “mechanical” crack growth during the hold time period. Results of these tests are shown in Fig. 11. They show a distinct increase in the crack growth rate as a result of imposing a hold time at minimum load during which crack tip oxidation is assumed to be the only active process. These results could be explained on the basis of the hold time, being approximately equal to t_p , having a chromia layer. Upon applying a loading cycle with a frequency that induces intergranular cracking, the ruptured oxides would represent an additional advance of the crack tip. The results of this work, in fact, confirm the work of Diboine and Pineau [18], who carried out a similar experiment on a similar material but with a hold time of 300 s. Similar results are reported by Shahinian and Sadananda [19].

As mentioned before, the depth of the oxide layers under test condition 2 would correspond to a saturated depth since the hold time is of the same order as the passivation time. If, however, in the experiment described above, the formation of the Cr_2O_3 could be delayed by manipulating the test parameters so that the 600 s hold at minimum load becomes smaller than the required t_p , oxide passivation would not then occur and one should expect a crack growth rate higher than that

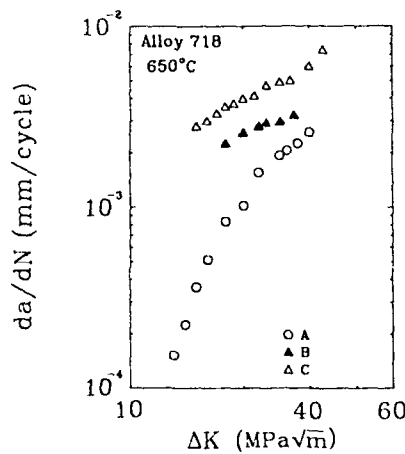


Fig. 11. Effect of hold time at minimum load as well as effect of minor cycle superimposed on hold time at minimum load level on crack growth rate (frequency 0.05 Hz): curve A, 0.05 Hz with a minor 1 Hz cycle imposed at minimum load level for a duration of 600 s; curve B, 0.05 Hz with hold time duration of 600 s at minimum load level; curve C, continuous 0.05 Hz.

obtained in test condition 2. This idea was experimentally examined by repeating test condition 2, described above, with the addition of a minor high frequency cycle having an amplitude of 0.5 kN imposed on the hold time duration. The objective of this minor cycle is to disturb the metal-oxygen reaction processes by continuously rupturing the rapidly forming spinel oxide layers. The effect would then be continuous variation in $P(\text{O}_2)$ and, consequently, in the oxygen flux rate which in turn prolongs the duration of t_p and delays the formation of a saturated Cr_2O_3 layer, thus permitting deeper oxide penetration. Results of this work in the form of da/dN vs. ΔK , are shown in Fig. 10. These results, which clearly indicate an increase in the crack growth rate when compared with results of test conditions 1 and 2, are seen here as indirect support of the two-stage oxidation concept.

It should be mentioned, however, that the present work does not provide a clear conclusion concerning the rate controlling factor in terms of the relative influence of chromium and oxygen diffusion on the rate of formation of the chromia layer. Recent work by Chang [20] has, however, shown that an increase in chromium content of alloy 718 to the level of 24 wt.% would result in a decrease in crack growth rate at 538 °C in air. The subject of oxidation kinetics in alloy 718 is currently under investigation by the authors.

4. Conclusion

A crack tip oxidation mechanism pertaining to short-range oxygen diffusion was examined. The

premise of this mechanism, supported by transmission electron microscopy observations, is that oxidation, controlled by the operating oxygen partial pressure, occurs in two stages: spinel oxide type followed at the metal-oxide interface by a protective chromia layer. The rate of build-up of this layer towards its saturation level governs the time required to reach a crack-tip, oxide-passivation condition. Through a delay of this build-up a definite increase in the crack growth rate was observed. The significance of this model is that the influence of the environment on crack growth behavior could be quantitatively described on the basis of calculating the rate of build-up of the chromia layer by taking into account the oxygen partial pressure as well as the degree of chromium depletion from the matrix surrounding the affected grain boundary paths. This approach is described in a recent work by Ghonem and Zheng [21]. Furthermore, the concepts presented here, in particular that of the parameter t_p , could be used to view the role of the environment as being either an oxidation-assisted or oxidation-dominated phenomenon. This classification would depend on the depth of oxide penetration during a specific loading cycle compared with the corresponding "mechanical" crack growth rate; this concept is currently under study by the authors.

Acknowledgment

The support of this work, as well as the support of one of the authors (H.G.) during his sabbatical stay at Ecole des Mines, is provided by SNECMA Group, Evry, France.

References

- 1 H. H. Smith, P. Shahinian and M. R. Achter, Fatigue crack growth rates in types 316 stainless steel at elevated temperature as a function of oxygen pressure, *Trans. Am. Inst. Min. Eng.*, 245 (1969) 947-953.
- 2 R. H. Bricknell and D. A. Woodford, The embrittlement of nickel following high temperature air exposure, *Metall. Trans. A*, 12 (1981) 425-433.
- 3 C. J. McMahon and L. F. Coffin, Mechanisms of damage and fracture in high-temperature low cycle fatigue of a cast nickel-based superalloy, *Metall. Trans.*, 1 (1970) 3443-3451.
- 4 L. F. Coffin, Fatigue at high temperature, *ASTM STP 520*, 1973 (American Society of Testing Materials, Philadelphia, PA), pp. 5-34.
- 5 C. J. McMahon, Jr., On the mechanism of premature in-service failure of nickel-base superalloy gas turbine blades, *Mater. Sci. Eng.*, 13 (1974) 295-297.
- 6 D. A. Woodford and R. H. Bricknell, Environmental embrittlement of high temperature alloy by oxygen. In *Treatise on Materials Science and Technology*, Vol. 25, Academic Press, New York, 1983, pp. 157-199.

- 7 E. Andrieu, Influence de l'environnement sur la propagation des fissures dans un superalliage base nickel: l'Inconel 718, *Ph.D. Thesis*, Ecole des Mines de Paris, 1987.
- 8 R. P. Skelton and J. Bucklow, Cyclic oxidation and crack growth during high strain fatigue of low alloy steel, *Met. Sci.*, **12** (1978) 64-70.
- 9 H. Teranishi and A. J. McEvily, Effect of oxidation on hold time fatigue behavior of 2.25Cr-1Mo steel, *Metall. Trans. A*, **10** (1979) 1806-1808.
- 10 S. Floreen and R. Raj, Environmental effects in nickel-base alloys. In R. Raj (ed.), *Flow and Fracture at Elevated Temperatures*, American Society for Metals, Metals Park, OH, 1985, pp. 383-402.
- 11 D. J. Michel and H. H. Smith, Fatigue crack propagation in neutron irradiated type 304 and type 308 stainless steel plate and weld materials, *J. Nucl. Mater.*, **71** (1) (1977) 173-177.
- 12 R. L. Stegman and P. Shahinian, Effect of temperature on the fatigue of nickel at varying oxygen pressures, *Fatigue at High Temperature*, ASTM STP-459, 1969 (ASTM, Philadelphia, PA), pp. 42-58.
- 13 H. H. Smith and P. Shahinian, Environmental effects on fatigue crack growth rates in silver, *J. Int. Met.*, **99** (1971) 243-247.
- 14 T. Ericsson, Review of oxidation effects on cyclic life at elevated temperature, *Can. Metall. Q.*, **18** (1979) 177.
- 15 M. R. Achter, G. J. Danek and H. H. Smith, Effect on fatigue of gaseous environments under varying temperature and pressure, *Trans. Am. Inst. Min. Eng.*, **227** (1963) 1296-1301.
- 16 P. Kofstad, *High Temperature Corrosion*, Elsevier Applied Science, London, 1988.
- 17 H. Ghonem and D. Zheng, Depth of intergranular oxygen diffusion during environment-dependent fatigue crack growth in alloy 718, *Mater. Sci. Eng.*, **150** (1992) 151-160.
- 18 A. Diboine and A. Pineau, Creep crack initiation and growth in Inconel 718 at 650 °C, *Fatigue Fract. Eng. Mater. Struct.*, **10** (1978) 141-151.
- 19 P. Shahinian and K. Sadananda, Effects of stress ratio and hold-time on fatigue crack growth in Alloy 718, *J. Eng. Mater. Technol.*, **101** (1979) 224-230.
- 20 K.-M. Chang, in E. A. Loria (ed.), *Metallurgical Control of Fatigue Crack Propagation in Alloy 718, Superalloys 718, 625 and Various Derivatives*, The Minerals, Metals & Materials Society, Warrendale, PA, 1991.
- 21 H. Ghonem and D. Zheng, Oxidation assisted fatigue crack growth behavior in Alloy 718—part I, *Fatigue Fract. Eng. Mater. Struct.*, **14** (1991) 749-760.

Frequency Interactions in High-Temperature Fatigue Crack Growth in Superalloys

H. GHONEM and D. ZHENG

The influence of high frequency loading on the subsequent low frequency crack growth behavior in nickel-based alloy 718 in laboratory air environment at 923 K has been investigated through the use of a sequential high/low frequency load waveform. The parameters that have been examined include the crack growth rate, fracture surface morphology, and slip line density at and below the fracture surface. Results of this study indicate that prior application of high frequency loading results in reduction of the subsequent low frequency crack growth rate. An attempt is made to interpret this type of modification as being a result of the crack tip conditioning through the increase in the slip line density during the high frequency part of the loading cycle. Furthermore, by linking the type of selective oxide formed at the crack tip to the degree of deformation in the crack tip zone, a correlation has been made between the increase in the slip line density in the crack tip zone during the preceding high frequency loading and the increase of the crack resistance to environment degradation effects during the subsequent low frequency loading.

I. INTRODUCTION

ALLOY 718 is a nickel-based superalloy characterized by high creep resistance and good mechanical properties at elevated temperatures up to 923 K.^[1,2,3] It is widely used in different industries, including aerospace applications where alloy 718 represents the main material in manufacturing hot section components of gas turbine engines. In these components, the load interaction effects due to sequential high/low frequency loadings on crack growth behavior, although important in design and failure prediction considerations, have received little attention. VanStone *et al.*^[4] have studied crack growth transients in alloy 718 where one type of cycling using a given waveform is followed by another waveform. In their investigation, fatigue loading with a 0.33 Hz cycle with a superimposed hold time of 300 seconds at K_{max} was followed by a pure 0.33 Hz cycle at a constant K_{max} level higher than the one achieved in the prior cycle. It was observed that upon the change in waveshape, the crack achieved transient growth rates higher than the subsequent steady-state value under constant K_{max} conditions. This effect was observed at both 866 and 923 K and demonstrates the existence of a damage state ahead of the crack tip due to sustained loads which is more degraded than the one obtained under pure fatigue cycling.

The influence of low frequency cycle loading on the subsequent high frequency crack growth behavior has also been investigated by Ghonem *et al.*^[5] for the case of alloy 718 at 923 °K. They have utilized constant load spectra, the basic structure of which is the repetition of a low frequency loading (0.05 Hz) with a superimposed 300 seconds hold time at maximum load level followed by a high frequency loading of 30 Hz. The time durations of both low and high frequency loading blocks were

identical. It was observed that under all load conditions, the crack growth rate corresponding to the high frequency part of the cycle is higher than that corresponding to a pure, continuous cyclic loading with the same frequency. This accelerated crack growth behavior was interpreted as being a result of stress concentration positions produced along the unsmooth intergranular crack front at the end of the low frequency part of the loading spectrum. This conclusion was based on observations made on the fracture surface showing finger-like morphologies at different positions along the crack front within the low/high frequency transition regions. Once these regions attained a smooth front due to the transgranular fracture mode associated with high frequency loading, the crack growth rate became equal to that corresponding to continuous high frequency cycle at the same ΔK value. Furthermore, the validity of the linear summation rule was examined by calculating the crack growth rate of the compound loading cycle on the basis of the growth rate data of the individual components of the cycle. It was shown that the linear summation underestimates the actual growth rate of the compound cycle for the reason mentioned previously. The influence of the high frequency loading on the subsequent low frequency crack growth process, however, was not examined due to the fact that testing under conditions of constant load did not permit isolating the transient effects in the low frequency crack tip zone.^[5] The objective of this article, therefore, is to investigate the high/low frequency effects through the use of constant ΔK waveform. The first part of the article deals with the significance of frequency interaction from a point of view of the influence of the loading frequency on deformation and slip line density in the corresponding crack tip zone. The second part of the article describes experimental procedure and test concept. This is followed by analysis and interpretation of results related to low frequency crack growth performance with emphasis being placed on crack growth rate, fracture mechanisms, and slip line density.

H. GHONEM, Professor, Department of Mechanical Engineering, and D. ZHENG, Research Associate, Mechanics of Solids Laboratory, are with the University of Rhode Island, Kingston, RI 02881.
Manuscript submitted March 10, 1992.

II. SIGNIFICANCE OF FREQUENCY INTERACTION

Experimental studies have been carried out by several authors (for example, References 6 through 10), investigating the effect of loading frequency on fatigue crack growth mechanisms in alloy 718 in both air and vacuum environments at elevated temperatures. Ghonem *et al.*^[11,12] have analyzed these effects by considering the relationship between the loading frequency, being a strain rate related parameter, and the associated slip line density and resulting mode of deformation in the crack tip region. It has been shown that the slip line density increases proportionally to the loading frequency. Furthermore, at frequencies higher than the transitional frequency, the increased slip density was assumed to lead to strain accommodation as well as stress relief along strained grain boundaries in the crack tip region. Cracking in this case proceeds in a predominantly transgranular mode. The loading frequency required to produce this type of cycle-dependent response decreases as the magnitude of applied ΔK increases. As loading frequency decreases, the degree of slip homogeneity in the crack tip zone was found to decrease, thus resulting in grain boundary stress concentration and a relative increase of the intergranular oxygen diffusion. Under this condition, the crack tip damage becomes a combination of oxidation and cycle-dependent components. As discussed in the work of Ghonem *et al.*,^[12] the degree of contribution of each of these components to the total crack tip damage process depends on both the frequency and ΔK values. For loading frequencies below the transitional frequency level of this alloy, the crack tip damage becomes mainly an environment-dependent process in which crack growth largely follows an intergranular fracture path.

The relationship between slip density and fracture mode characteristics has been investigated in Reference 5 using compact tension specimens made of alloy 718 with large grain size tested at 923 K in laboratory air environment. In this work, fatigue fracture mode and slip line density were compared for a loading frequency of 10 Hz vs 0.05 Hz. Slip line traces at and below the fracture surface of the test specimens were obtained using the slip lines decoration technique. Results of this work show that for fully transgranular fracture (10 Hz condition), the degree of homogeneous deformation becomes evident through the observed high slip line density and the confinement of the reversed plastic zone to a narrow band near the fracture surface. This contrasts with the fully intergranular fracture process (0.05 Hz) which displayed a lower slip line density as well as larger plastic zone size.

On the basis of the preceding discussion, one should expect that by subjecting the crack tip to a sequence of loading blocks with different frequencies, transient effects would take place in the crack tip region, thus affecting the crack growth behavior. This effect would come about through changes exerted by the nature of the slip line density and related deformation mode produced by the preceding loading frequency in the crack tip region. These transient effects, in particular those introduced by the high frequency loading on the low frequency crack

growth, will be investigated by carrying out a series of crack growth measurements using a sequential high/low frequency waveform. The characteristic of this waveform will be discussed in Section III.

III. EXPERIMENTAL PROCEDURE AND TEST CONCEPT

The test material used in this study was alloy 718 in the form of rolled ring forging having the chemical composition listed in Table I. Blocks of this material were conventionally heat-treated (1227 K for 1 hour, air-cooled + 991 K for 8 hours + furnace-cooled to 894 K at a rate not to exceed 311 K/h + hold at 894 K for 8 hours and air-cooled to room temperature). The chemical composition and microstructure of this material are the same as those used in Reference 11. The treated blocks were machined in the compact tension geometry CT-30 (thickness $B = 11$ mm, width $W = 63.5$ mm, and the ratio of height to width $H/W = 0.6$). All specimens were precracked at room temperature, and tests were conducted in laboratory air environment at stress ratio $R = 0.1$. A two-zone resistance furnace was used to achieve the required testing temperature level of $923 \text{ K} \pm 4 \text{ K}$. The compliance method was employed to measure the on-line crack length which was used on real time basis as a feedback signal to the test controller of the servo-hydraulic testing system in order to produce the load range required to maintain the ΔK level at the desired constant level. Post-test examination included determination of slip line density at and below the plane strain cross section of selected fractured specimens. Fracture surface analysis was carried out using scanning electron microscopy in order to determine the fracture mode in relation to the applied frequency condition.

As stated previously, the objective of this study is to investigate the influence of high frequency loading on the transient crack growth characteristics when the loading frequency is decreased to a level below that of the transitional frequency of the alloy under study. To achieve this objective, a combination of constant load/constant ΔK spectrum, schematically shown in Figure 1, was utilized. It consists of repetition of two different frequency blocks: a high frequency loading block (15 Hz) followed by a low frequency block (0.0167 Hz). The start and end of each of these blocks were based on the following concept. Within the high frequency block (AB), the cycle load range was maintained at a constant level, thus permitting ΔK to increase with the increase in the crack length. Upon achieving a particular ΔK value, the test was switched to low frequency loading during which the previous ΔK was maintained constant until the crack tip crossed a length equal to the diameter of the plane-strain plastic zone generated by the last cycle of the previous

Table I. The Nominal Composition of Alloy 718 (Weight Percent)

Ni	Cr	Fe	Ti	Mo	Nb + Ta	Al	
52.5	19	18	0.9	3.05	5.15	0.5	
C	S	Si	P	B	Co	Mn	Cu
<0.08	<0.015	<0.35	<0.015	<0.006	<1.0	<0.35	<0.3

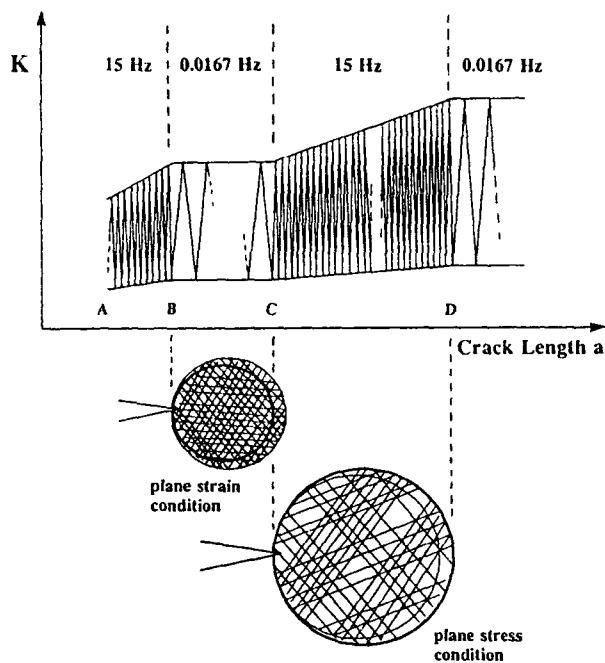


Fig. 1—Schematic of the test concept and the loading spectrum applied in the present study. *BC* is a low frequency loading region in which the crack propagates within the plane strain zone of the previous high frequency loading. *CD* is a high frequency region in which the crack propagates within the plane stress zone of the previous low frequency loading.

high frequency loading block (*AB*). In this way, the crack length increment due to the low frequency loading is assumed to have occurred in a region fully preconditioned by the previous high frequency loading effects. Once this requirement was achieved, the test was again switched to high frequency constant load (block *CD*). This would then continue until the crack achieved an increment larger than the diameter of the plane-stress plastic zone generated by the preceding low frequency loading block. This condition was necessary in order to insure that the crack tip extended far enough from the material that may have been affected by low frequency loading. This sequence of high/low frequency loading was repeated for investigating the low frequency crack growth behavior at ΔK values of 30, 40, 45, and 50 $\text{MPa}\sqrt{\text{m}}$. For the purpose of comparison, the constant ΔK tests were also conducted under the condition of continuous cycling with frequency of 0.0167 Hz for the same ΔK values mentioned earlier.

IV. RESULTS AND DISCUSSION

The fatigue crack growth rate data obtained at four different values of ΔK for the low frequency part of the loading spectrum are shown in Figure 2, curve (*a*). These results are compared in the same figure with curve (*b*) which was obtained from continuous loading with the same frequency (0.0167 Hz) and for the same ΔK values. This comparison indicates that prior crack tip conditioning with high frequency loading results in relative

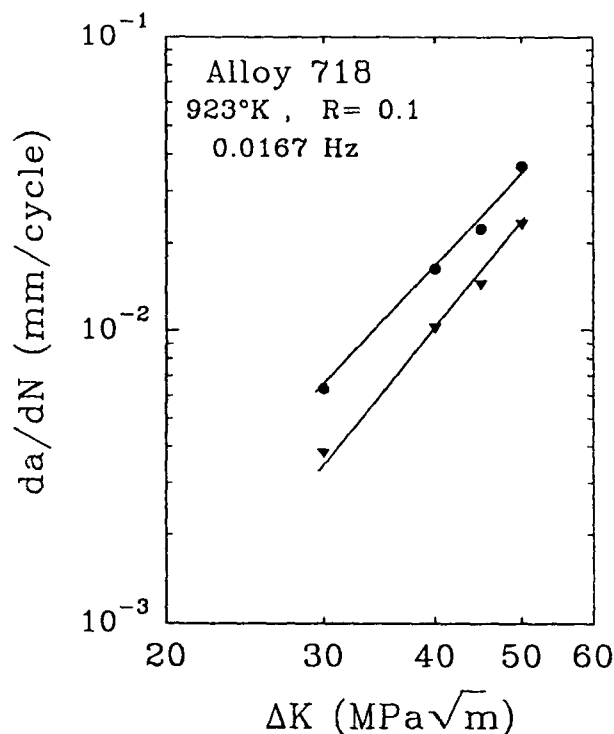
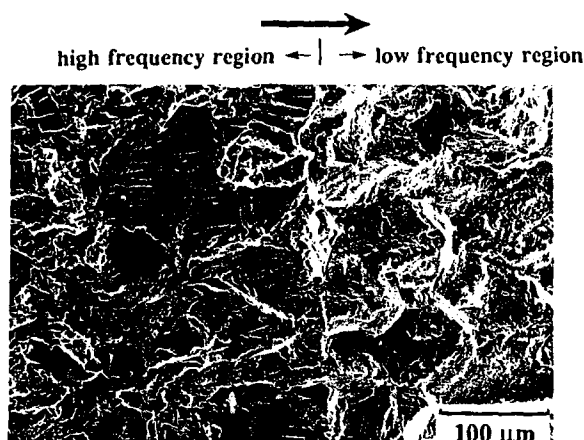


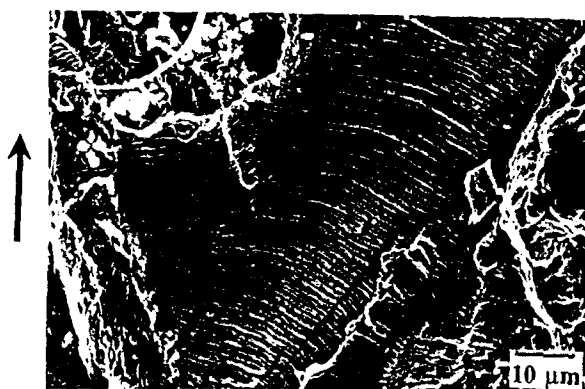
Fig. 2—Influence of preceding high frequency loading on low frequency fatigue crack growth behavior. ∇ —curve (*a*) which corresponds to the low frequency part of the complex loading cycle; \bullet —curve (*b*) which corresponds to continuous low frequency cycle schematically illustrated in Fig. 1.

decrease of the following low frequency crack growth rate. Furthermore, the slope of curve (*a*) is shown to be relatively larger than that of curve (*b*) which represents the continuous low cycle loading. The increased slope in the conditioned loading case indicates increased dependency of the corresponding growth process on the crack tip stresses. Recognizing that the two operating damage mechanisms at frequency of 0.0167 Hz in air are crack tip stress field and oxidation environment,^[12] it can then be concluded, following observations made by the authors^[11] on the nature of the slope of the crack growth curves in both air and vacuum conditions, that the influence of environment on curve (*a*) decreased when compared to that of curve (*b*).

Scanning electron microscopy was carried out on the fracture surface of the high and low frequency loading regions. This examination shows that the fracture mode due to the high frequency cycle is transgranular with striation markings, as seen in Figure 3. Spacings between these striations were found to match closely with the corresponding crack growth rate. The transition from transgranular fracture to intergranular fracture due to low frequency loading was observed to be immediate and took place along a relatively smooth, straight front, as shown in Figure 3. It is interesting to observe that the transgranular/intergranular transition front includes the finger-like morphologies reported in the earlier work of Ghonem *et al.*^[13] (Figure 4). Typical fracture surface corresponding to the low frequency regions is shown in



(a)



(b)

Fig. 3—(a) Fracture surface appearance of the low/high frequency transition region—high frequency region (left) and low frequency region (right). (b) Striation markings appeared on the fracture surface of the high frequency region.

Figure 5. It displays intergranular fracture features which differ in appearance from the brittle intergranular fracture generally associated with the response of this alloy to pure low frequency loading (0.0167 Hz) at 923 K, as shown in Figure 6.

The slip line traces resulting from the different parts of the loading cycle have been identified by exposing plane strain cross sections of selected fractured specimens to 993 K for 20 hours in air environment. This treatment permitted the precipitation of δ phase along the slip lines, making them visible and suitable for microscopic observations (for details concerning this decoration technique, see Reference 13). Slip line densities for both the low and high frequency regions at approximately the same $\Delta K = 30 \text{ MPa}\sqrt{\text{m}}$ are shown in Figures 7 and 8, respectively. It is observed that the slip line density in areas of low frequency cycles, while lower than that in areas of high frequency loading, is qualitatively higher than the slip density corresponding to continuous low frequency loading (Figures 7 and 9). These

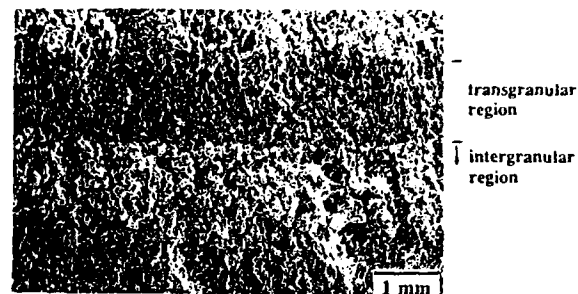


Fig. 4—Fracture surface feature, showing finger-like morphology produced at the end of the low frequency part of the complex cycle.

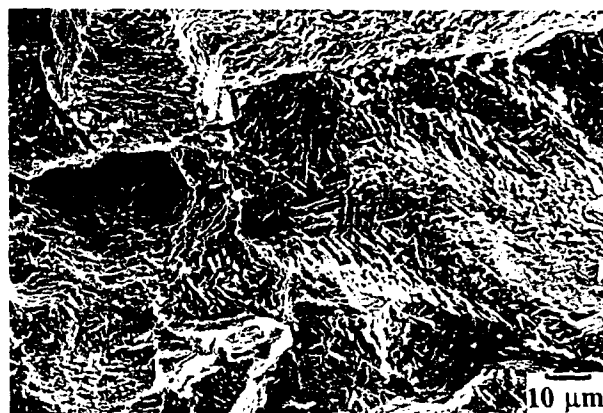


Fig. 5—Intergranular fracture morphology corresponding to the low frequency (0.0167 Hz) part of the compound loading spectrum ($\Delta K = 40 \text{ MPa}\sqrt{\text{m}}$) displaying oxide scale formation.



Fig. 6—Intergranular fracture morphology for continuous cycling at frequency of 0.0167 Hz and $\Delta K = 40 \text{ MPa}\sqrt{\text{m}}$ displaying brittle fracture pattern with a smooth thick layer of surface oxide.

results support the conclusion that prior high frequency loading results in high slip line density in the crack tip zone which tends to modify the low frequency crack growth rate within this zone. A possible reason for this type of modification is the view that slip line/grain boundary intersection represents a stress concentration point with a high content of the chromium element which

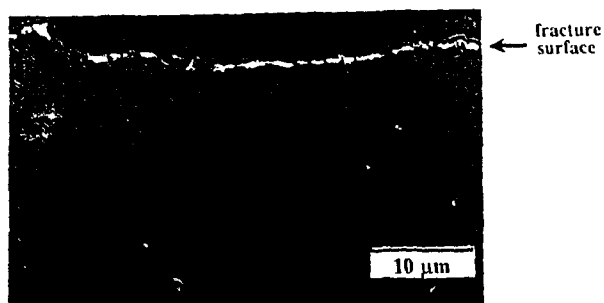


Fig. 7—Plane strain cross section showing slip line traces below the fracture surface due to continuous low frequency loading (0.0167 Hz) at $\Delta K = 30 \text{ MPa}\sqrt{\text{m}}$.

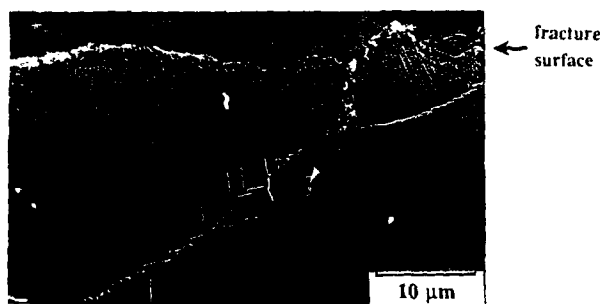


Fig. 8—Plane strain cross section showing slip line traces below the fracture surface due to high frequency loading (15 Hz) at $\Delta K = 30 \text{ MPa}\sqrt{\text{m}}$.

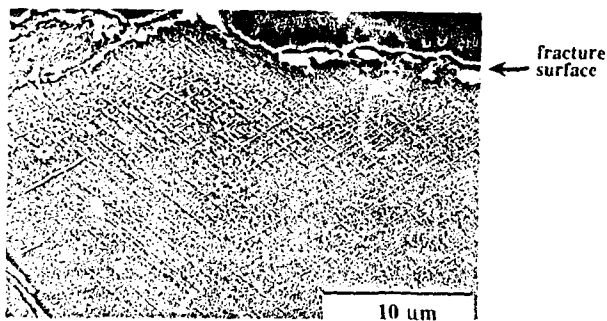


Fig. 9—Plane strain cross section showing slip line traces below the fracture surface due to the low frequency loading part (0.0167 Hz) of the compound loading spectrum at $\Delta K = 30 \text{ MPa}\sqrt{\text{m}}$. Compare this figure with Fig. 7 for the slip line density.

facilitates the formation of the protective Cr_2O_3 oxide faster than grain boundary regions free of such intersection. In this view, the intersection points act as oxidation shielding nodes.^[5] Therefore, the higher the slip line density in the crack tip zone, the higher the grain boundary resistance in this zone to environmental degradation during intergranular cracking and the lower the corresponding crack growth rate. This view could further be explained by identifying the role of slip line density in determining the rate of formation of selective oxides at the intergranular crack tip. As explained in Section II, low frequency loading of alloy 718 particularly at levels

below that of the transitional frequency, results in an environment-dependent crack growth behavior. The influence of environment, which in the case of alloy 718 is mainly due to the oxygen element in the laboratory air,^[7,8,14] occurs as a result of selective oxide formation at the crack tip. At the start of the oxidation process, when atmospheric oxygen partial pressure is available for the crack-tip material, the first oxides to form consist of NiO and FeO as well as their spinels. These porous oxides, which cannot serve as an oxygen diffusion barrier, permit the continuous oxidation reaction at the base grain boundary material. As the thickness of these oxides increases, thus leading to a decrease in the oxygen partial pressure at the oxide/metal interface, the reaction kinetics required for the formation of a denser Cr_2O_3 sublayer are attained.^[15,16] This dense layer is oxide protective due to the fact that it controls the oxygen diffusion toward the grain boundary material, thus resulting in a decrease in the oxidation reaction rate as time elapses. When the buildup of the chromia layer is fully completed along the intergranular crack front, no further oxidation of the base metal takes place until the chromia layer is fractured, thus exposing fresh metal to the repetition of the oxidation cycle.

This crack tip oxidation mechanism suggests that the rate of chromia buildup at the crack tip controls the depth of oxygen penetration along grain boundaries in the crack tip region. This rate depends primarily on the content of chromium existing in the affected grain boundary material which is in part transported from the interior of the matrix along the active slip lines. Indeed, recent results of Chang^[17] showed that the reduction of the intergranular fatigue crack growth rate can be achieved by increasing the chromium content in alloy 718. By assuming that the oxidation sequence and its kinetics requirements, as described earlier, are applicable to the grain boundary/slip line intersection regions, one observes that these regions, which are the ends of the transport process of their corresponding slip lines, are higher in chromium content than that of either the grain boundary material or the basic matrix.^[18] In addition, these regions are highly stressed due to expected dislocation pileup, provided that the condition of plastic homogeneity and associated stress relaxation has not been reached in the neighboring grain. The availability of higher chromium and the increase in the rise in the stress level provide the intersection regions with the kinetics required for the chromia buildup with a rate faster than that in the grain boundary regions which are free of these intersections. If the saturated chromia layer is looked upon as a shield against further oxygen diffusion, then the higher the slip line density along a grain boundary fracture path, the lower the oxidation-assisted fatigue crack growth rate along such a path. This mechanism thus implies that the number of cycles required for the crack tip to advance a certain distance along an affected grain boundary increases as the number of slip line/grain boundary intersections increases. This view is consistent with the results of the present work in that the increased slip line density in the crack tip region through the application of high frequency loading lowered the influence of environment during low frequency crack growth through this modified region.

V. CONCLUSIONS

In this study, the influence of high frequency loading on the subsequent low frequency fatigue crack growth behavior in alloy 718 has been investigated. The two major conclusions of the present work can be summarized as follows.

1. Density of slip lines and associated homogeneity of plastic deformation in the crack tip region are closely related to the frequency level of the cyclic loading. The higher the level of frequency, the higher the slip density and the more homogeneous the plastic deformation.
2. The preceding high frequency loading modifies the following low frequency crack growth behavior. This modification is signified by reduction in low frequency crack growth rate due to relatively high density of slip lines introduced by the previous high frequency loading. This crack growth reduction is interpreted as enhancement of the crack tip resistance to oxidation due to the increase of the buildup rate of the protective Cr_2O_3 sublayer.

ACKNOWLEDGMENTS

Mr. A. Rosenberg of MSL, URI has contributed to this work by obtaining slip line traces. The authors also acknowledge helpful discussions with Dr. T. Nicholas of the Materials Directorate, WPAFB, OH, and Professor A. Pineau and Dr. E. Andrieu of the Centre des Matériaux, Ecole des Mines de Paris, France. This work is supported by the Air Force Office of Scientific Research under Contract No. AFOSR-89-0285; Dr. W. Jones is the program manager.

REFERENCES

1. J.F. Barker: in *Superalloy—Metallurgy and Applications*, A. Loria, ed., TMS, Warrendale, PA, 1989, pp. 269-77.
2. E.A. Loria: *J. Met.*, 1988, July, pp. 36-41.
3. T.H. Sanders, Jr., R.E. Frishmuth, and G.T. Embley: *Metall. Trans. A*, 1981, vol. 12A, pp. 1003-10.
4. R.H. VanStone, O.C. Gooden, and D.D. Krueger: *Advanced Cumulative Damage Modeling*, AFWAL-TK-88-4146, Materials Laboratory, Wright-Patterson AFB, OH, 1988.
5. H. Ghonem, D. Zheng, E. Andrieu, and A. Pineau: *Experimental Observations and Quantitative Modelling of Oxidation-Assisted Crack Growth Behavior in Alloy 718 at 650 °C*, AFOSR-89-0285, Bolling AFB, Washington, DC, 1990.
6. L.A. James: *J. Eng. Mater. Technol.*, 1973, vol. 95, pp. 254-56.
7. M. Clavel and A. Pineau: *Metall. Trans. A*, 1978, vol. 9A, pp. 471-80.
8. S. Floreen and R.H. Kane: *Fatigue Eng. Mater. Struct.*, 1980, vol. 2, pp. 401-12.
9. T. Weerasooriya and S. Venkataraman: in *Effects of Load and Thermal Histories*, P.K. Liaw and T. Nicholas, eds., TMS-AIME, Warrendale, PA, 1987, pp. 101-08.
10. T. Weerasooriya: in *Fracture Mechanics: 19th Symp.*, ASTM STP 969, T.A. Cruse, ed., ASTM, Philadelphia, PA, 1988, pp. 907-23.
11. H. Ghonem and D. Zheng: *Mater. Sci. Eng.*, 1992, vol. 150A, pp. 151-60.
12. H. Ghonem, T. Nicholas, and A. Pineau: *High Temperature Effects*, ASME Winter Annual Meeting, Atlanta, GA, Nov. 1991.
13. M. Clavel, D. Fournier, and A. Pineau: *Metall. Trans. A*, 1975, vol. 6A, pp. 2305-07.
14. K. Sadananda and P. Shahinian: in *Corrosion of Nickel-Based Alloys*, R.C. Scarberry, ed., ASM Publication, Cincinnati, OH, 1985, pp. 101-15.
15. E. Andrieu, H. Ghonem, and A. Pineau: in *Elevated Temperature Crack Growth*, S. Mall and T. Nicholas, eds., ASME, New York, NY, 1990, pp. 25-29.
16. P. Kofstad: *High Temperature Corrosion*, Elsevier Applied Science Publishers Ltd., London, 1988.
17. K.-M. Chang: in *Superalloy 718, 625 and Various Derivatives*, E.A. Loria, ed., TMS, Warrendale, PA, 1991, pp. 447-56.
18. H. Ghonem and D. Zheng: *Mater. Sci. Eng.*, 1992, in press.

OXIDATION AND INTERGRANULAR CRACKING BEHAVIOUR OF TWO HIGH STRENGTH NI-BASE SUPERALLOYS

E. Andrieu, G. Hochstetter, R. Molins and A. Pineau

**Centre des Matériaux - Ecole des Mines
B.P.87 - 91003 EVRY Cedex (France)
URA CNRS 866**

Abstract

The oxidation behaviour of two Ni base superalloys used for the fabrication of turbine discs, Inconel 718 and N18 alloy, was investigated in relation with their cracking resistance under creep and fatigue loading at 650°C. N18 alloy was examined with two different microstructures. Mechanical tests were carried out either in air or under various oxygen partial pressures, including high vacuum (10^{-8} Torr). Dramatic effects of oxidation on the fatigue crack growth rate are observed to take place beyond a transition oxygen partial pressure. TEM observations and X Ray microanalyses show that, in both materials, under high oxygen pressure, oxidation leads to the formation of a two layers oxide film, an outer Ni, (Fe or Co)-rich scale and an inner protective Cr-rich subscale. The conditions prevailing for strong environmental effects are briefly discussed. It is shown that, in these materials, two conditions must be fulfilled : (i) the formation of a Ni-rich oxide scale which is not protective and (ii) inhomogeneities in deformation modes which lead to high intergranular stresses.

1 Introduction

The detrimental effect of oxidation on creep cracking or fatigue crack growth behaviour of Ni-base superalloys is well documented (see eg.[1]). Most of the conclusions dealing with this effect are drawn from the comparison of test results carried out either in air environment or under vacuum. These tests show that, in many high strength Ni base superalloys, in particular those used in the fabrication of turbine discs, such as Alloy 718, a significant part of the increase in fatigue crack growth rate with temperature is closely related to environmental

effects. This acceleration in fatigue crack growth rate which is not usually observed when the tests are performed under high vacuum ($\sim 10^{-6}$ Torr) is associated with a change in fracture mode from transgranular to intergranular. On the other hand, there are very few studies dealing with the identification of the nature of the oxides formed ahead of the crack tip or on the fracture surface, as well as the kinetics of oxide formation.

This study deals with the oxidation behaviour of two high strength Ni-base superalloys, Inconel 718 and N18 alloy in relation with their cracking behaviour under either creep loading or fatigue loading. Inconel 718 is a conventional wrought Ni base superalloy widely used in the fabrication of turbine discs. N18 alloy which is also used in the same type of application is one of the most advanced superalloys prepared from powder metallurgy. The aims of the present study were the following : (i) to determine the nature of the oxides formed in these materials at temperatures close to 650°C, (ii) to investigate the formation of these oxides in relation with the partial pressure of oxygen and (iii) to relate the oxidation behaviour of these materials to their mechanical properties. In addition to this, this study contributes also to the understanding of the effect of microstructural details, in particular the slip homogeneity, on the creep-fatigue-oxidation interactions, since these materials exhibit widely different microstructures and since N18 alloy with two different microstructures was investigated.

2 Materials and Experimental procedures

2-1 Materials

The chemical compositions of both alloys investigated in the present study are given in Table I.

Inconel 718 was received as a wrought bar of 200 mm diameter. A conventional heat treatment was given: 955°C during 1 hour then air-cooled, down to 720°C for 8 hours, then air-cooled 50°C/hour down to 620°C and maintained for 8 hours. The resulting microstructure presented in figure 1a corresponds to a large grain material ($\phi=150\mu\text{m}$) with a small amount of δ phase (Ni_3Nb) precipitated along the grain boundaries. The strengthening of this alloy results from the precipitation of two phases named γ' (Ni_3Nb) and γ'' ($\text{Ni}_3\text{Al,Ti}$) homogeneously distributed, with a volume fraction of about 15%. The tensile properties of this material are reported in Table II.

The N18 alloy is a powder metallurgy Ni base superalloy containing much more strengthening elements as compared to Inconel 718. This material was received as a turbine disc which was given the following heat treatment : Forging at 1150°C followed by a controlled cooling at about 100°C/mn and further aged at 700°C for 24h, air cooled and then aged at 800°C for 24 h, air cooled. The microstructure of the material is dependent on the cooling rate after 1150°C heat-treatment. This is the reason why the specimens were taken from the bulk and from the skin of the disk. The microstructure of these materials is shown in Fig 1b and 1c. In both cases the average grain size is 10µm. Large primary γ particles ($\phi \approx 1.5 \mu\text{m}$) are located along the grain boundaries, while the matrix is strengthened by much smaller secondary particles ($\phi \approx 0.2 \mu\text{m}$, $v_f=45\%$). The microstructure of the bulk specimens is more homogeneous as compared to that of the specimens taken close to the surface of the disc. In particular, in the latter case, the size of the secondary γ particles close to the grain boundaries is so small that at magnification of 5000, a thin zone similar to a precipitate free zone is observed along the grain boundaries. The tensile properties of this material are not dependent on these microstructural variations (Table II).

2-2 Experimental procedures

In the creep and fatigue tests, CT20 specimens ($B=10\text{mm}$, $W=40\text{mm}$) were used. The specimens were first precracked at room temperature at a frequency of 50 Hz up to $a/w=0.35$ and then precracked at high temperature (with a 10s-300s hold time -10s cycle) till $a/w = 0.40$ was reached. The maximum a/w values reached during the experiments was equal to 0.7. The crack length was measured by using the potential drop technique. The fatigue testing frame was equipped with a high vacuum chamber. Pressures were measured from 1 bar to 10 mbar with a manometer, with a Pirani gauge for pressures between 10^{-3} mbar and 5 mbar and a Bayard-Alpert gauge for high vacuum measurements. A technique, similar to that used by other investigators [2] was developed to prepare thin foils located close to the fracture surfaces using cross sections which were cut by spark machining.

TEM investigation was carried out using a 300 kV microscope equipped with an x-ray (EDS) spectrometer. The oxides and microstructural variations have been identified by using electron diffraction techniques and elemental concentration linescans with a few nanometers probe size.

3 Results

3-1 Chemical microanalysis

Inconel 718;

TEM examination of a polished cross sectioned sample oxidized during 15 min at 650°C under air and the associated elemental concentration linescan perpendicular to the oxide/metal interface, show the existence of a two oxides layer : an inner Cr_2O_3 subscale and an outer NiO type oxide, with observable columnar grains containing also Cr and Fe (Fig.2) The chromium rich oxide layer is a passive scale decreasing the global oxide scale growth kinetic and enhibiting the Nickel oxide growth. The build-up of this continuous chromium oxide subscale requires several minutes (~ 5 to 10 minutes).

TEM micrograph and associated concentration linescan taken on a transverse section of an intergranular fracture surface oxidized during 20 hours at 650°C under air allow us to observe the same duplex scale (Fig.3). This figure summarizes the oxidation behaviour of the grain boundaries. No major difference appears between transgranular and intergranular oxides in terms of chemical composition and scale morphology.

N18 alloy :

The cross sections of specimens tested under fatigue cycling with a hold time at maximum load of 300s (10-300-10) were observed. These tests performed at 650°C lasted approximatively 200 hours. The fracture surfaces were fully intergranular. Fig.4 illustrates the oxide scale morphology formed in this complex alloy. The oxide scale is formed by an outer layer of Ni,Co-rich oxide and an inner passive Cr-rich layer which contains also some Ti. It was also observed that γ' phase oxidation can give rise to the local formation of alumina oxide.

The oxidation behaviour of a secondary intergranular crack observed on the fracture surface of a creep crack growth rate specimen tested at 650°C for about 100 hours is illustrated in Fig.5. Fig.5a is a sketch showing also the formation of a two layers oxide scale. The composition of these layers is shown in Fig.5b and 5c from linescans taken perpendicularly to the crack axis, as indicated in Fig.5a. Both types of oxides, the Ni, Co-rich oxide and the Cr-rich oxide, are also observed, which indicates that the oxidation mechanism is operative under all test conditions.

3-2 Creep and Creep-fatigue crack growth tests

The results presented in this section are part of a more extensive study on creep and fatigue crack growth properties of both alloys, see eg [3,4,5]. As far as environmental effects are concerned, the results included in this section are only those in which environment plays an important role. The shape and the frequency of the cycles are chosen so that the coupling between oxidation and the crack tip deformation mode gives rise to a significant embrittlement of the grain boundaries.

In figure 6, the results of creep crack growth rate measurements and fatigue crack growth rate tests (10-300-10) carried out on Inconel 718 at 650°C are shown. Under air environment, the creep crack growth resistance of this "creep resistant" Ni-base alloy is low as observed in Fig. 6a. Fatigue crack growth rate was also measured when superimposing to a triangular $5 \cdot 10^{-2}$ Hz cycle a hold time (300s) at maximum load. This test was performed under air and high vacuum environment. Figure 6b shows that air environment induces a large increase of the crack growth rate in comparison with the one measured under vacuum.

Environmental effects on creep and creep-fatigue crack propagation for N18 alloy are also presented in Fig. 7. Both microstructures (bulk-skin) were tested under creep loading conditions (Fig 7a). The results obtained indicate that the microstructure with the heterogeneous precipitate distribution is less resistant than the homogeneous one (bulk). Fatigue tests (10-300-10) with a load ratio $R = K_{Min}/K_{Max} = 0.30$ have been carried out under vacuum and air environment at 650°C on CT specimens taken in the bulk of the disc. As indicated in Fig. 7b, the crack growth rates under air environment are increased by a factor of ten in comparison with those measured under high vacuum.

Further tests were carried out under constant ΔK and different oxygen partial pressures on both materials. In each test, the variations of the fatigue crack growth rate were measured when varying the total pressure from atmospheric pressure to high vacuum. The results are shown in Fig. 8.

It is worth noting that each material exhibits a transition in the fatigue crack growth rate when the oxygen pressure reaches 10^{-2} mbar. Furthermore the transition pressure appears to be independent of ΔK , at least for the values which were investigated. Scanning electron microscope observations showed that this transition in fatigue crack growth rate was closely related to a transition in fracture mode, from intergranular at high oxygen partial pressure to transgranular at low partial pressure.

4 Discussion

These results clearly show a dramatic oxidation effect on the intergranular cracking behaviour of both materials. Moreover the results of creep crack growth rate measurements obtained on N18 alloy show also a strong microstructural effect which is related to the deformation mode of the materials. Both effects are discussed successively.

4-1 Oxidation mode:

Among all the interesting studies devoted to the oxidation of Nickel and Nickel alloys, the work carried out by Bricknell and Woodford (6) dealing with the embrittlement of Nickel after high temperature exposure is of particular interest in the present study. They clearly demonstrate that at high temperature, Nickel oxide growth is accompanied by oxygen diffusion along the grain boundaries. This phenomenon induces an embrittlement of this particular interface. TEM observation and the results of micro-analyses presented in figure 2 to 5 indicate that, in spite of the high chromium content present in the matrix, the early stage of oxidation leads, for both investigated materials, to the formation of an Ni-base oxide even along the grain boundaries. Fortunately, after several minutes, the high chromium content induces a passivation process that lowers the global oxidation kinetic and stops the grain boundary embrittlement effect. An attempt to measure indirectly the time required to reach the passivation stage of Inconel 718 at 650°C associated with the formation of the protective Cr_2O_3 oxide film was made by Diboine and Pineau [3]. This was accomplished by comparing the fatigue crack growth rate at constant ΔK under continuous cycling with those obtained when superimposing an increasing holdtime at minimum load till the saturation in the crack growth rate was reached. The corresponding hold time was found to be in good agreement with those measured by using elemental profiles in AES [7,8]. The passivation time (t_p) is influenced by the oxygen partial pressure, the temperature, the alloy chemical composition and the mechanical deformation. A decrease of the passivation time, t_p is of particular interest in the problem of grain boundaries embrittlement. For Inconel 718 the effect of a predeformation has also been investigated so that the asymptotic behaviour is known. The oxidation of a shot-peened surface leads to the selective oxidation of chromium and simultaneously to the instantaneous passivation of this alloy [8]. Similar results were obtained by Giggins and Pettit on Ni-Cr alloys (9). This simple experiment suggests that there exists a coupling between oxidation mode and the amount

of deformation stored in the material. The effect of oxygen partial pressure on the oxidation mode was also investigated [10]. It was shown that the selective oxidation of chromium occurred when the oxygen partial pressure was less than 10^{-3} torr. The agreement between this transition pressure and that measured during the creep fatigue tests of N18 alloy and Inconel 718 (Fig 8) is a striking phenomenon. In particular this indicates that Ni-rich oxide formation during the early stage of oxidation is a prerequisite for a nickel base alloy to be sensitive to the effect of environment. Nevertheless this requirement is necessary but not sufficient, since microstructural effects play also an important role.

4-2 Deformation mode

Deformation localization is also an essential parameter in this problem. Measurements of the plastic zone sizes were made on the same Inconel 718 alloy in the plane strain zone of CT specimens [11]. This work was accomplished by using a decoration technique of the intense slip bands, described in [12]. It was found that below a transgranular fracture surface (high frequency test) slip traces are homogeneously distributed and confined in a narrow band close to the fracture surface, smaller than the alloy grain size. On the other hand, when intergranular fracture takes place, at lower frequency, slip traces are heterogeneously distributed even for high ΔK values. In this case too the plastic zone size remains smaller than the grain size. These observations might be an illustration of the coupling between oxidation and crack tip strain rate. In particular they suggest that high strain rates promote the selective oxidation of the chromium. These observations might also be interpreted as an effect of strain rate on the slip heterogeneity which can be summarized as follows : as the strain rate decreases, the slip heterogeneity increases giving rise to greater intergranular internal stresses resulting from inelastic strain incompatibilities. As shown in Figure 7a, the N18 alloy microstructure presented in Figure 1c seems to be more sensitive to environment than the one taken from the bulk of the disc. This behaviour could be due to the localization of the deformation in a narrow band close to the grain boundaries corresponding to the observable microstructural gradient. It is therefore concluded that not only the formation of a Ni-rich oxide film is a prerequisite for strong environmental effect but also high intergranular stresses resulting from strain incompatibilities due to either slip character or microstructural inhomogeneities, or both.

5 Conclusions

The oxidation mechanism of two different Ni-base superalloys has been studied. In spite of the high Chromium content present in the matrix, both alloys are Ni-rich oxide formers during the early stage of oxidation. Several minutes later this stage is followed by a passivation stage due to the formation of a Cr rich oxide. Intergranular fracture surfaces as well as transgranular mechanically polished surfaces, exhibit the same oxidation behaviour.

By varying the oxygen partial pressure in constant delta K fatigue loading conditions, a transient in the FCGR is found for both alloys in the range of 10^{-2} mbar. This transition corresponds to the selective oxidation of Chromium at low oxygen partial pressure. It is shown that Ni-rich oxide formation is a necessary but not a sufficient requirement to observe dramatic environmental effect on intergranular cracking at high temperature. The effect of the deformation localization promoting high intergranular stresses is also shown by testing two different microstructures of N18 alloy. It is concluded that microstructural gradients as well as slip heterogeneities can increase intergranular stresses and enhance the deleterious effect of oxidation.

Table I - Chemical composition (wt%)

a) Alloy 718

C	Cr	Mo	Ti	Al	Nb+Ta	Fe	Si	Co	Mn	P	S	B
0.035	18.25	3.06	1.02	0.54	5.27	19.00	0.09	0.25	0.13	0.009	0.0015	0.006

b) N18 Alloy

C	Co	Ni	Cr	Mo	Al	Ti	B	Hf	Zr	O	N
0.015	15.7	balance	11.5	6.5	4.35	4.35	0.015	0.45	0.03	0.010	0.005

Table II: Tensile properties.

a) Alloy 718

Temperature (°C)	R _{0,2} (MPa)	R _m (MPa)	A (%)
25	1145	1290	24
650	885	960	17

b) N18 Alloy

Temperature (°C)	R _{0,2} (MPa)	R _m (MPa)	A (%)
20	1048	1575	31
650	1020	1323	30

ACKNOWLEDGEMENTS

The authors would like to acknowledge the SNECMA Company and DRET (Direction des Recherches Etudes et Techniques) who showed a constant interest in this study. Financial support of the project by SNECMA and DRET is gratefully acknowledged.

RÉFÉRENCES

1. A. Pineau, Elevated temperature creep-fatigue cracking in relation to oxidation effects. "Environment induced cracking of metals". Ed. R.P. GANGLOFF and M.B. IVES. NACE 10, Oct.2-7, (1988), pp.111-122.
2. S.B. Newcomb, C.B. Boothroyd and W.M. Stobbs, J. Microscopy, 140, (1985), p.195.
3. A. Diboine and A. Pineau, Fatigue Fract. Eng. Mater. Struct., vol.10, (1987), pp.141-151
4. J.P. Pédrón and A. Pineau, Mat. Sci. Eng., vol.56, 1982, pp.143-156.
5. J.P. Pédrón and A. Pineau, in Advances in Fracture Research, vol.5, (1981), pp.2385-2392..
6. R.H. Bricknell and D.A. Woodford, Metal. Trans. A, (1981), pp.425-433.
7. E. Andrieu, R. Cozar and A. Pineau, 718 Superalloys, Metallurgy and Applications, ed. by E.A. Loria, Pittsburgh, Pa, ASM, (1989), pp.241-247.
8. E. Andrieu, Influence de l'environnement sur la propagation des fissures dans un superalliage base Nickel : l'Inconel 718, PhD.thésis, Ecole des Mines de Paris, 1987.
9. C.S. Giggins, F.S. Pettit, Trans. Met. Soc. AIME, vol.245, (1969), pp.2509-2514.
10. E. Andrieu, R. Molins, H. Ghonem and A. Pineau, Mat. Sci. Eng., A154 (1992), pp.21-28.

11. H. Ghonem, T. Nicholas and A. Pineau, Symp. on high temp. effects. ASME, Winter Annual Meeting, Atlanta, Ga, Nov. 1991.
12. M. Clavel, D. Fournier and A. Pineau, Met. Trans. vol.6A, (1975), pp.2305-2307.

FIGURES CAPTIONS

- Fig.1 - Microstructure of the materials, a) Inconel 718; b) and c) N18 alloy from the bulk of the disc; d) N18 alloy from the skin of the disc.
- Fig.2 - Inconel 718, a) TEM observation showing the formation of a two layers oxide on a polished surface oxidized at 650°C for 15 minutes; b) Elemental linescan across the alloy/oxide interface.
- Fig.3 - Inconel 718. Oxidation of an intergranular fracture surface, a) TEM observation; b) Elemental linescan across the alloy/oxide interface..
- Fig.4 - N18 alloy. Oxidation of an intergranular fracture surface, a) TEM observation; b) Elemental linescan across the alloy/oxide interface.
- Fig. 5 - N18 alloy. Oxidation of a secondary intergranular crack, a) Sketch showing the formation of two oxide along the grain boundary; b and c) Elemental profiles along the lines indicated in a), as line (1) and (2), respectively.
- Fig.6 - Inconel 718, a) Creep crack growth rates measured at 650°C; b) Fatigue crack growth rates (cycle : 10s-300s-10s) measured at 650°C in air and under vacuum.
- Fig. 7 - N18 alloy, a) Creep crack growth rates determined at 650°C, with two different microstructures,; b) Fatigue crack growth rates (cycle : 1s-300s-10s) at 650°C in air and under vacuum.
- Fig.8 - Influence of oxygen partial pressure on the fatigue crack growth rate at 650°C, a) Inconel 718; b) N18 alloy.

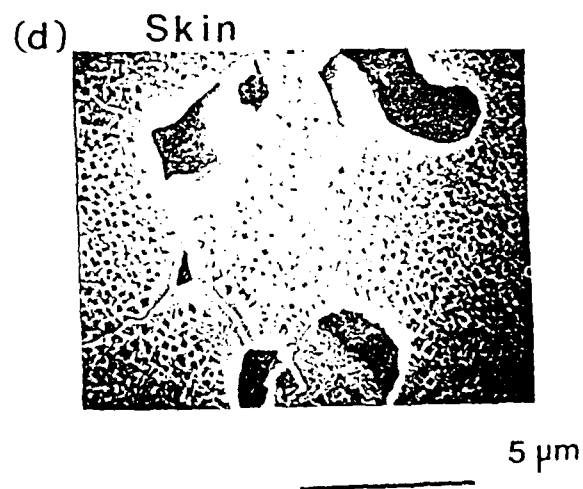
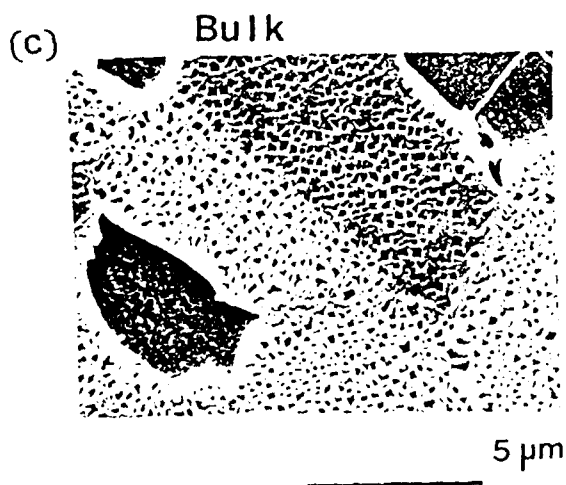
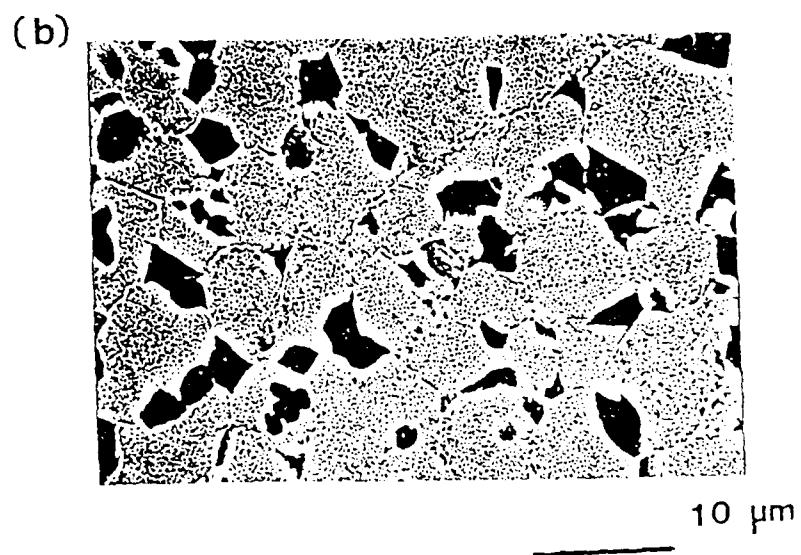


Fig.1 - Microstructure of the materials, a) Inconel 718; b) and c) N18 alloy from the bulk of the disc; d) N18 alloy from the skin of the disc.

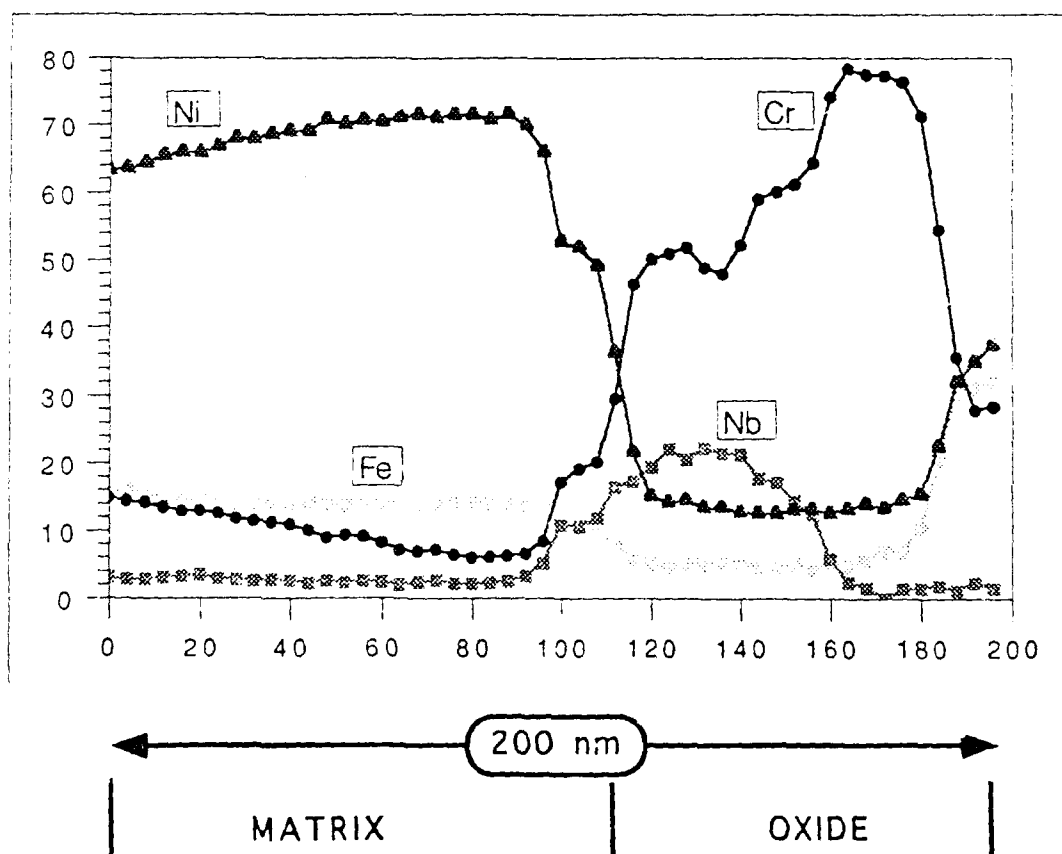
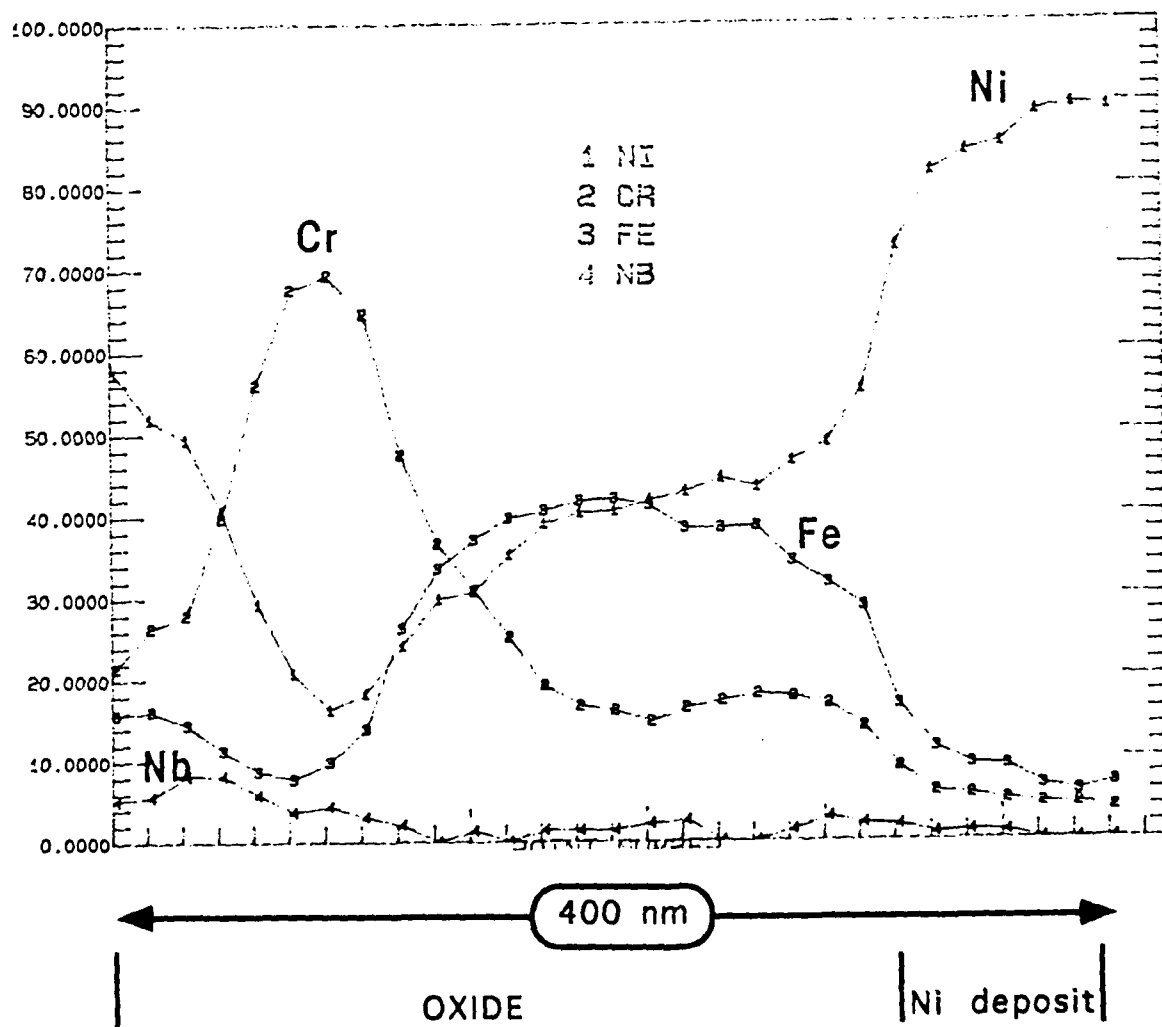
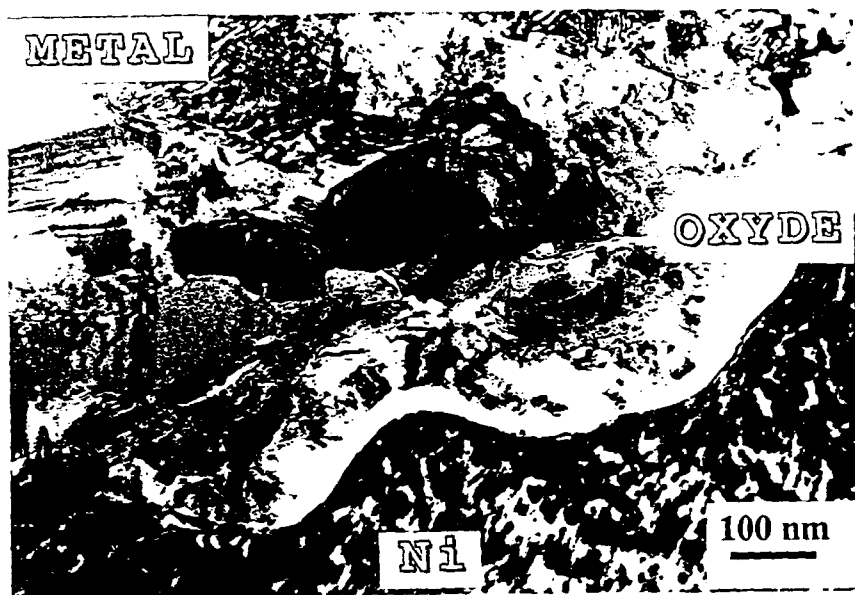
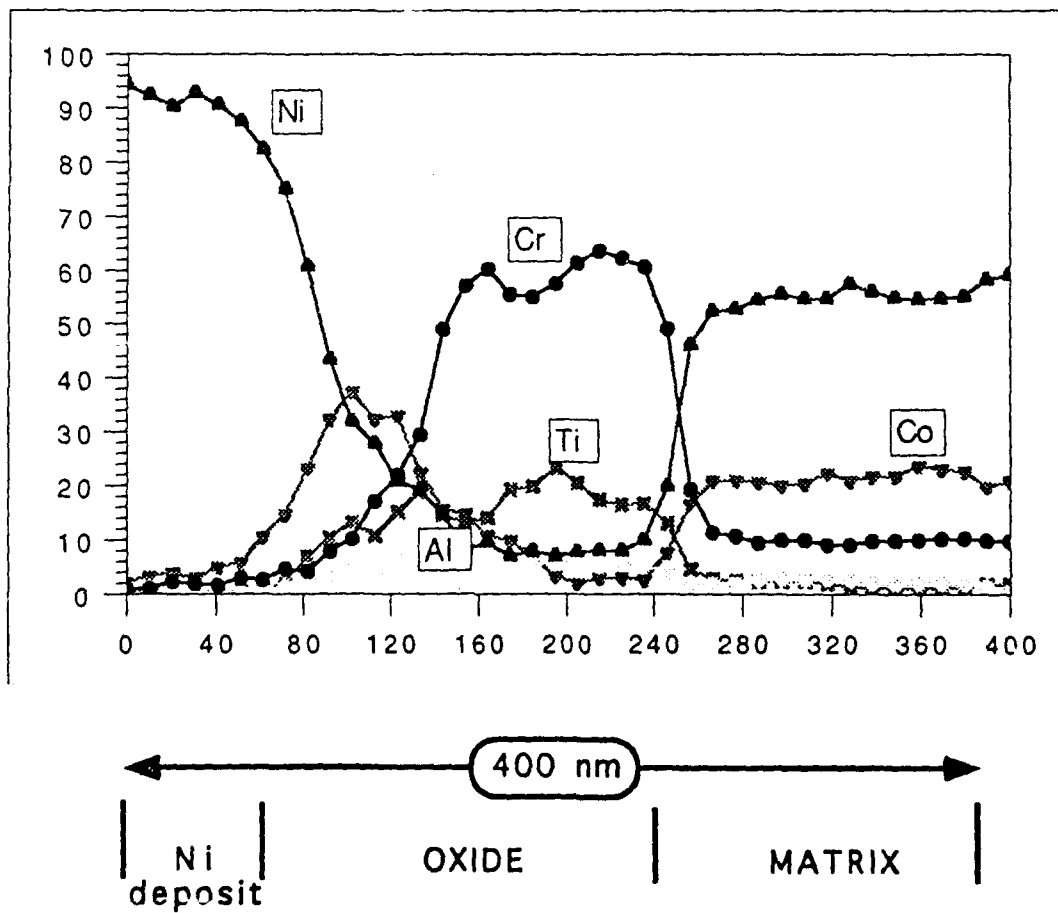
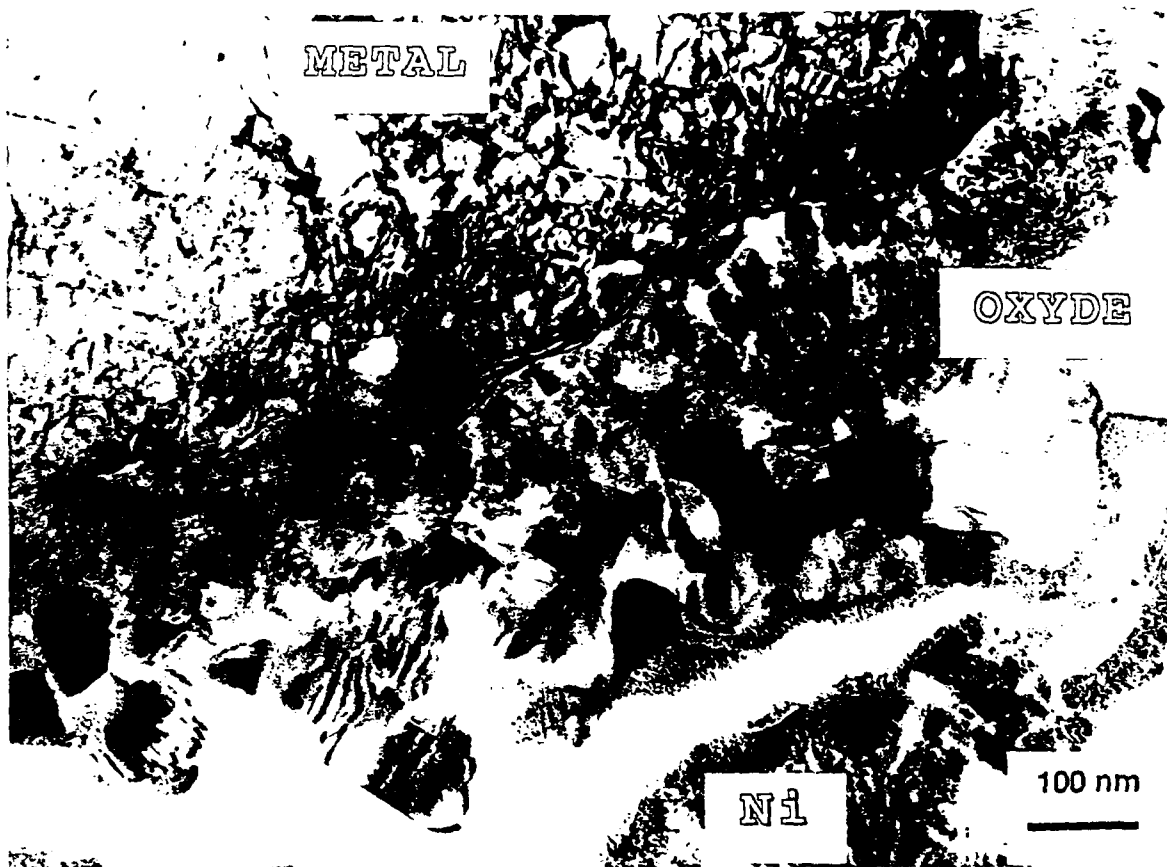
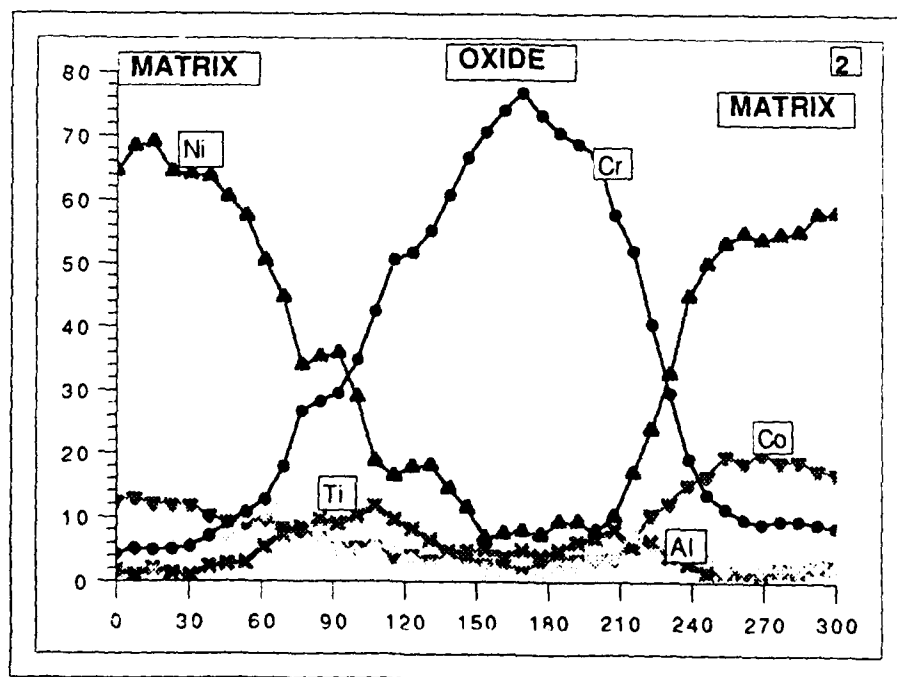
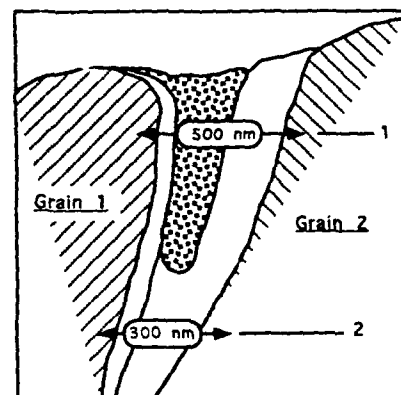
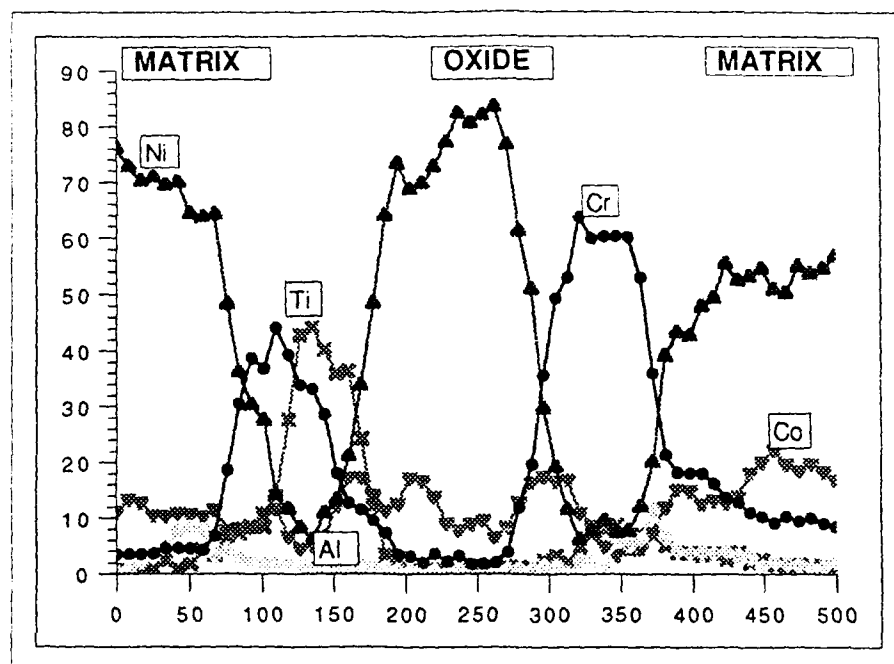


Fig.2 - Inconel 718, a) TEM observation showing the formation of a two layers oxide on a polished surface oxidized at 650°C for 15 minutes; b) Elemental linescan across the oxide/metal interface.





Elemental linescan through 500 nm



Elemental linescan through 300 nm

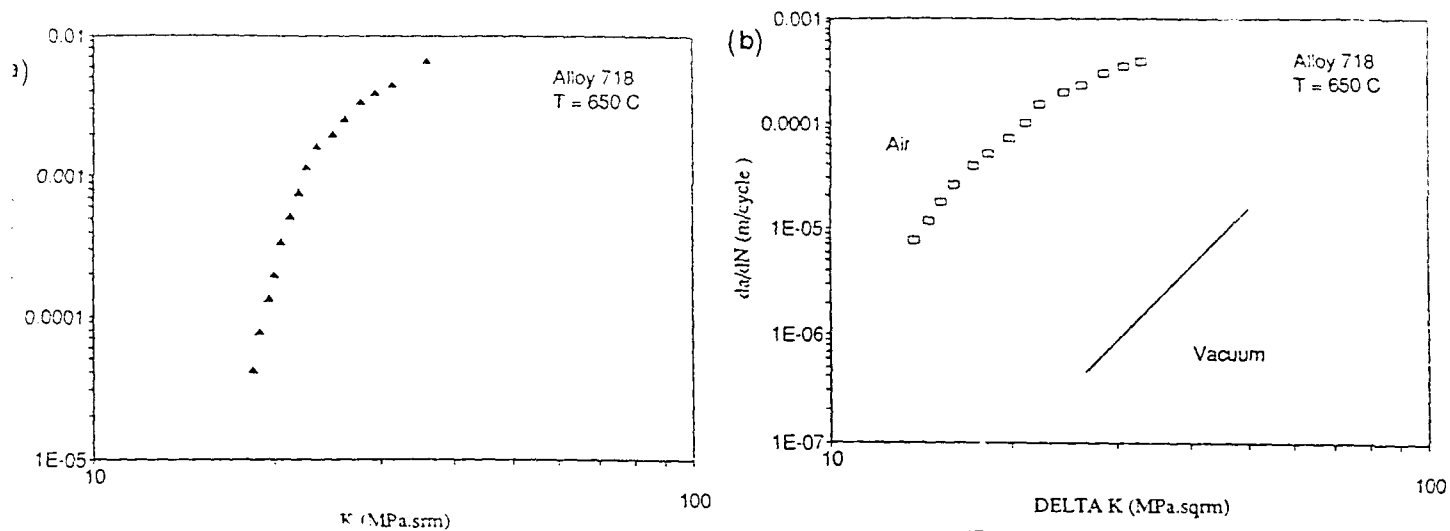


Fig.6 - Inconel 718, a) Creep crack growth rates measured at 650°C; b) Fatigue crack growth rates (cycle : 10s-300s-10s) measured at 650°C in air and under vacuum.

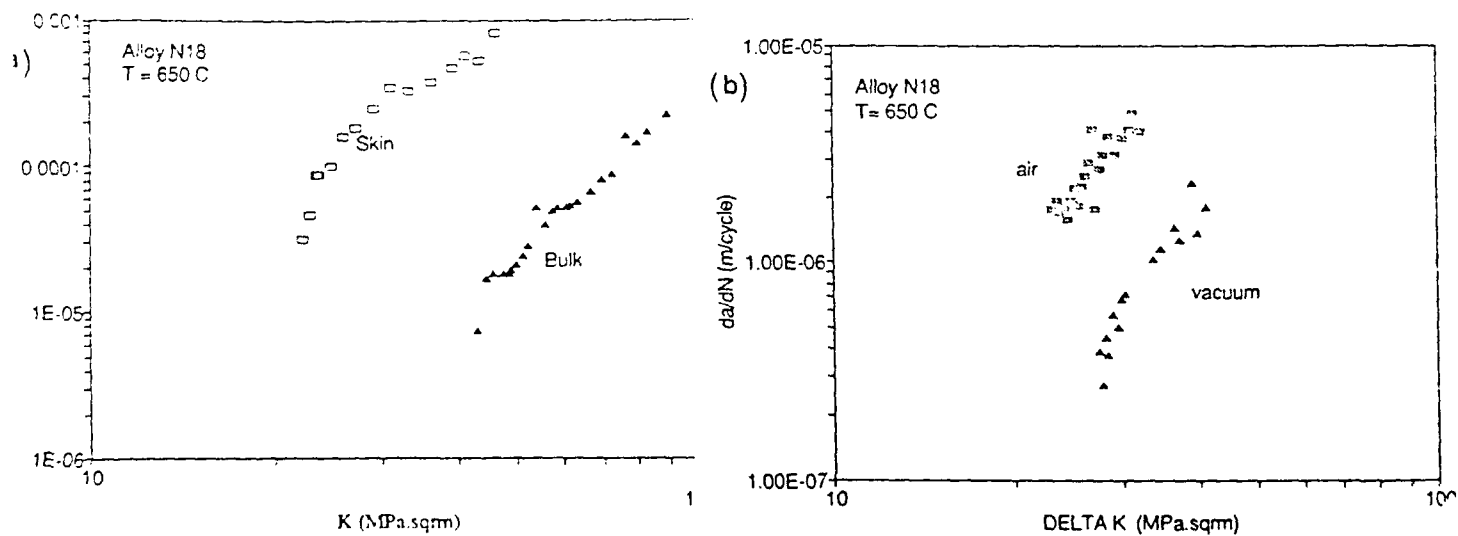


Fig. 7 - N18 alloy, a) Creep crack growth rates determined at 650°C, with two different microstructures; b) Fatigue crack growth rates (cycle : 1s-300s-10s) at 650°C in air and under vacuum.

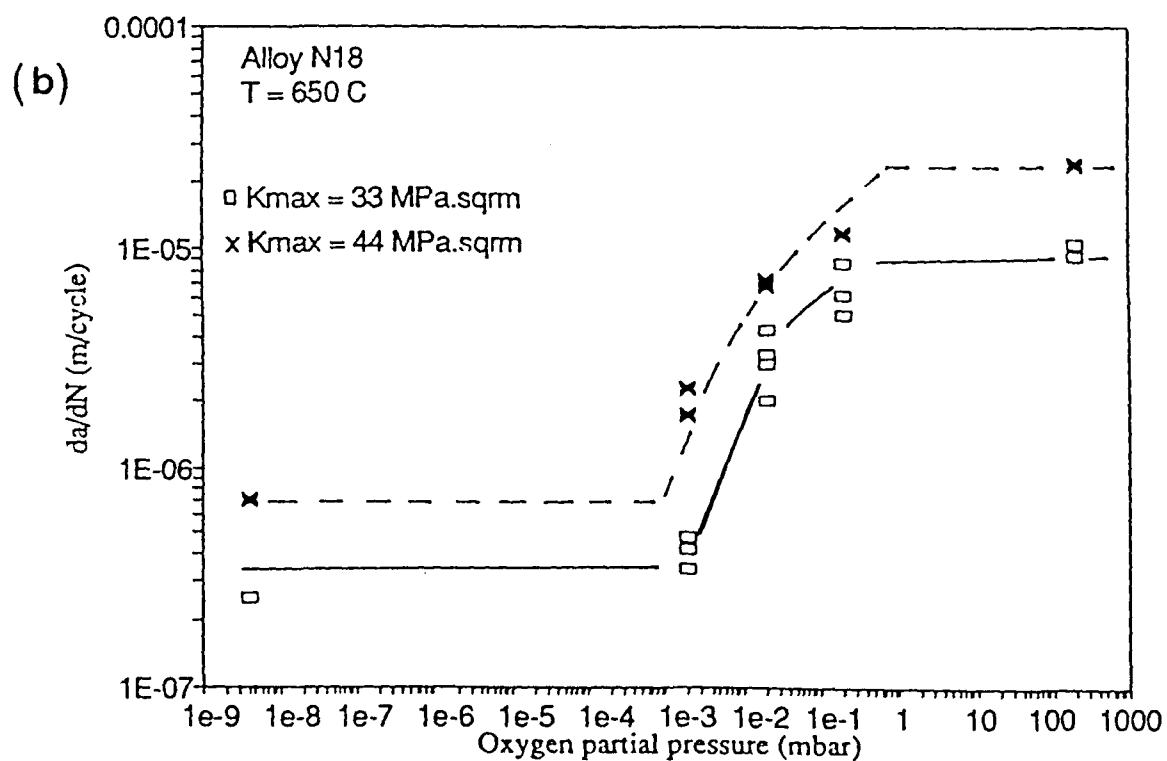
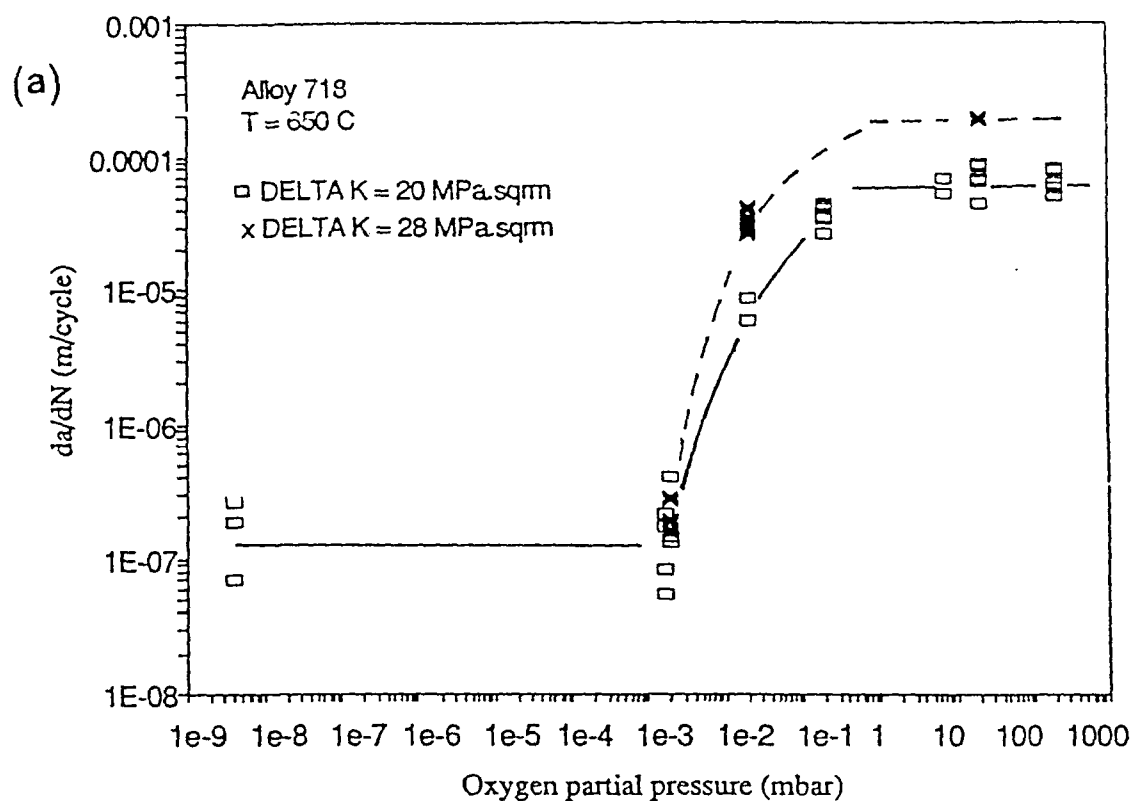


Fig.8 - Influence of oxygen partial pressure on the fatigue crack growth rate at 650°C,
a) Inconel 718; b) N18 alloy.

Influence of prestraining on high temperature, low frequency fatigue crack growth in superalloys

H. Ghonem, D. Zheng and A. Rosenberger

Mechanics of Solids Laboratory, Department of Mechanical Engineering and Applied Mechanics, University of Rhode Island, Kingston, RI 02881 (USA)

Abstract: The objective of this paper is to investigate the influence of prestraining on the low frequency crack growth behavior of wrought Alloy 718 at 650°C. A series of crack growth experiments were carried out on specimens with two levels of prestraining, 1% and 2%, in addition to specimens with no prior deformation. Work in these experiments included continuous measurements of crack length and near field crack tip displacements, fractographic analysis of fracture surface facets, qualitative determination of the slip density in the crack tip region and Auger Spectroscopy analysis for the objective of determining the thickness of surface oxide layers formed during the fracture process. It is concluded from this work that prestraining leads to a reduction in the crack growth rate. This conclusion has been examined on the basis of the notion that the deformation-associated slip line density is the rate controlling element of the chromium oxide build up taking place at the slip line/grain boundary intersection nodes within the crack tip region.

1. Introduction

Many authors have shown that the fatigue crack tip damage in high strength structural alloys ranges from purely cyclic-dependent at high frequency levels to a fully time-dependent at very low frequency loadings [1-4]. In Alloy 718 which is a precipitate hardened

material with high creep resistant characteristics, the time dependent damage at frequencies lower than the transitional frequency of this alloy, is measured in terms of the intergranular crack tip oxygen diffusion during the effective oxidation time of the loading cycle [5]. Attempts have been made in the work of Ghonem et al [5,6] to explain the link between the crack tip damage mode and loading frequency. Their analysis has suggested that this link is controlled by the frequency-associated slip line density and the related degree of homogeneity of plastic deformation generated in the plastic zone region. On the basis of this view, detailed in Ref. [6], the high slip line density produced in the crack tip region due to high frequency loadings is assumed to result in homogeneous plastic deformation. This type of deformation would limit the stress build up along affected grain boundaries due to high percentage of slip line matching across these boundaries [7]. In this case the grain boundary oxygen diffusivity, being a stress-dependent parameter, is assumed not to increase and the influence of the crack tip oxidation is kept to a minimum thus permitting the dominance of the cyclic damage effects. On the other hand, low frequency loadings are observed to produce a lower slip line density thus leading to an inhomogeneous crack tip plastic deformation. This localized deformation process would promote stress concentration along grain boundaries in the crack tip region. The expected increase of the oxygen diffusivity of these boundaries and the subsequent increase in the oxygen intergranular depth of diffusion could then give rise to the crack tip environmental damage contribution. This view while supported indirectly by qualitative measurements of the slip line density on planes located immediately below the fracture surface in cases of pure low frequency as well as pure high frequency loadings [6], has also been examined by the authors [8] in a series of high/low frequency crack growth tests carried out on a conventionally heat treated Alloy 718

at 650°C using a complex loading spectrum. Their work included crack growth rate measurements, fractographic analysis of fracture surface facets and qualitative determination of the slip density in regions subjected to low as well as high frequency loadings. Results of their study showed that prior increase of slip line density in the crack tip region through high frequency load application leads to a modification in the proceeding low frequency crack growth rate. Furthermore, the role of loading parameters in determining the slip line spacing in Alloy 718 has been identified by the authors using a simplified mathematical model based on concepts developed by Venkataraman et al [9,10] and Mura et al [11]. This simplified model, summarized in Appendix A, shows that the slip line spacing is inversely proportional to both loading frequency and total accumulated bulk plastic strain. This mathematical treatment thus provides the grounds for the notion that increasing bulk deformation leads to a higher slip line density which in turn promotes higher degree of homogeneous plastic deformation thus leading to a lower crack growth rate. This notion of the ability to control the high temperature crack growth behavior in Alloy 718 through global effects, opposite to the concept of control through crack tip localized deformation effects [8], is the objective of the work to be described in this paper. The following section the experimental procedure employed in prestraining as well as crack growth measurements will be discussed. This will be followed by a discussion focusing on the the details of the experimental results and their significance in relation to the influence of prestraining on crack growth behavior.

2. Experimental Procedure

The objective of this experimental work, as been mentioned above, is to investigate the low frequency crack growth response to the prior increase in the slip line density that has been achieved through an imposed bulk plastic deformation. The material used here was a conventionally heat treated Alloy 718 with an average grain size of $80\text{ }\mu\text{m}$ (ASTM 3); for details of the material microstructure and alloying elements see Ref. [5,8]. Blocks of this material were machined in threaded end longitudinal specimens with a rectangular flat gage section. Some of these specimens were subjected to different monotonic loads at room temperature to achieve different levels of monotonic plastic strains; 1% and 2% which corresponds to the load levels of 1128 MPa and 1311 MPa, respectively. These loads were reached using a strain rate of $4 \times 10^{-6} \text{ s}^{-1}$. These low levels of prestraining were used here in order to avoid detrimental effects produced by excessive ductility reduction that may accompany higher levels of prestraining [6]. The prestrained specimens, in addition to specimens without prior deformation, have then been machined in the single edge notched specimen geometry shown in Fig. 1. This was followed by precracking procedure carried out at room temperature. Crack growth measurement testings were performed on all the specimens at 650°C in laboratory air environment using a 10 KHz induction heating unit. Test temperature was achieved with variations along the gage length of less than $\pm 5^\circ\text{C}$. All tests were carried out under load range control with a load ratio maintained at 0.1 and loading frequency of 0.05 Hz. This frequency which is lower than the transitional frequency of the test material was selected in order to insure that the fracture process is environmentally controlled and the cracking mechanism is fully intergranular [5,12]. During each of these tests, the crack length was measured continuously using the direct current potential drop technique while the near field crack opening displacement was measured

using a laser interferometric displacement gage system (IDG) similar to that developed by Sharpe [13]. The resolution of this system is about 10 nm. In order to account for the bending nature of the SEN specimen geometry on the correlating ΔK parameter, the K solution for fixed end SEN specimen [14] has been applied here.

Post test examinations included fractographic analysis of fracture surface in order to identify related fracture mechanisms. These surfaces were also subjected to an Auger Spectroscopy with energetic beam sputtering technique for the objective of determining the thickness of surface oxide layers formed during the fracture process. Furthermore, the slip line density at and below the fracture surface along plane strain crosssections in specimens with different levels of prestraining have been qualitatively estimated. In this latter analysis the slip line traces were made visible by decorating them with the δ phase using a particular heat treatment procedure that cause the precipitation of stable delta phase nucleating from sheared γ'' precipitates and growing along active slip planes, see Ref. [15].

3. Results and Discussion

The fatigue crack growth rates corresponding to the 1% and 2% prestrained specimens have been plotted in Fig. 2 as function of the stress intensity range ΔK . These rates are compared in the same figure to those of the specimens without prestraining. This figure shows that the effect of 1% prestraining is negligible while the 2% level has produced an increase in the ΔK threshold and a decrease in the crack growth rate in both low and high ΔK regimes. This decrease occurs with a factor of 8 at the threshold level while maintaining a decreasing level of factor of 3 up to $\Delta K=4\text{MPa}/\text{m}$. These results could be

compared with those obtained by Kindell et al [16] from their work on the nickel-base alloy N901 at 600°C. They studied the crack growth rate in as-received and 5.5% prestrained single edge notched specimens subjected to loading frequency of 50 Hz and a stress ratio of 0.1. Their results are shown in Fig. 3. They concluded that prestraining leads to a lower ΔK threshold value and higher corresponding crack growth rate. The trend of their data, however, show that prestraining reduced crack growth rates at ΔK values above 10 MPa \sqrt{m} . While results of N901 material were difficult to interpret in terms of monotonic tensile parameter and fatigue crack closure, the authors believed that the nature of the dislocation substructure introduced by prestraining might be one of a significant factors. They, however, did not examine the role of the fatigue crack closure in relation to effects of prestraining. This role was investigated here by determining the relationship between the near field crack opening displacement and the applied cyclic load through the use of a laser interferometric technique. From this relationship the load corresponding to the onset of crack opening was obtained as function of crack length and was then used to calculate the effective ΔK values [17,18]. Results of this analysis in the form of ΔK_{eff} versus da/dN for all test conditions are shown in Fig. 4. They show that while a shift to a higher crack growth rate has occurred in the entire ΔK range of all crack growth curves, the difference between the crack growth rates of the as-received condition and that of the 2% prestrained condition have persisted. This difference is greater than a factor of 3 at around the threshold region and decreasing to a factor of 2.4 up to $\Delta K=27\text{MPa}\sqrt{m}$. The correction for closure has also distinguished the 1% prestraining crack growth curve from that of the as-received condition. This difference is, however, smaller than a factor of 2 and vanishes for ΔK values above 18 MPa \sqrt{m} . On the basis of these results one could assume that crack closure could not be

used to explain the influence of prestraining on the low frequency crack growth behavior.

In order to identify the fracture mechanisms associated with each of the test conditions, the related fracture surfaces were examined using Scanning Electron Microscopy. Fig. 5 shows the fracture surfaces for each test condition. In all cases intergranular fracture mode was found to dominate these surfaces. This time-dependent* environmentally controlled fracture mode is in fact a typical response of Alloy 718 when tested using loading frequencies below its transitional frequency level [5,19].

The slip line densities generated in the crack tip zone on plane strain cross sections at and below the fracture surface were also determined by making the slip line traces visible using a δ phase decoration technique [15]. This analysis was applied to the 2% deformed specimen as well as to the as-received condition using fracture surface regions that have been subjected to the same ΔK levels of 12 and 27 MPa \sqrt{m} . Selecting regions of the same ΔK value was found necessary so that comparison between the different test conditions would not include the influence of the stress intensity range on the slip line density [6]. Results of this analysis are shown in Fig. 6. They indicate that at each of the two ΔK levels the slip line density in the prestrained condition is qualitatively higher than that in as-received condition. This is consistent with the results of Merlin et al [20] who observed an increase in dislocation density with increase in the prestraining level in the oxide dispersion strengthened nickel base alloy MA754 tested at 760°C. Similar results could also be deduced from the work of Jin [21] where deformed copper crystals exhibited increase in the surface persistent slip bands with the increase in the applied plastic strain amplitude.

From these above results, it could be argued that the reduction in the low frequency crack growth rate due to prestraining while associated with the increase in the slip line

density, could not be assessed in terms of the crack tip closure or the changes in the cracking mechanism. This conclusion could then provide grounds for examining the role of the slip density in modifying the crack growth behavior in Alloy 718 on the basis of the oxidation shielding concept suggested by Ghonem et al [6]. This concept assumes that the slip line density is the rate controlling element of the chromium oxide build up taking place at the slip line/ grain boundary intersection nodes within the crack tip region. The decrease of the slip line spacing along a grain boundary path in this region signifies the occurrence of two effects: (a) the decrease of the stress concentration due to the increased possibility of slip line matching and consequently the decrease of dislocation pile up along this path and (b) the increase of the chromium concentration along this path due to the increased transport of this element from the matrix via slip bands. These effects are assumed to result in the formation of the protective Cr_2O_3 oxide with a rate higher than that along grain boundary regions free of such intersection. If one views the intersection points to act as oxidation shielding nodes, see Ref. [6], therefore, the higher the slip line density in the crack tip zone, the higher the grain boundary resistance in this zone to environment degradation during intergranular cracking and the lower is the corresponding crack growth rate.

If this shielding mechanism is operative one should then expect to observe two outcomes: (i) the thickness of the oxide layer formed at the crack tip in the case of the prestrained material should be smaller than that formed in the case of as-received material, and (ii) the chromium content in the crack tip region of the prestrained material would be higher than that corresponding to the as-received material. These two expected observations have been explored here by determining the composition of fracture surface layers of the two test conditions; as-received and 2% prestraining, along regions having the

same ΔK using Auger spectroscopy with energetic ion beam sputtering technique. This analysis has also been performed on a virgin surface of the test material in order to use its results as a base data line. One should mention here that this Auger analysis was carried out with the assumption that the rate of the material removal from the sputtered region on the fracture surfaces of the test specimens is equal to that obtained using a standard calibration T_{1205} thin film specimen. During this analysis carbon intensities were continuously monitored in order to insure that ion sputtering is occurring in the area of interest and no shadowing due to surface roughness exists. Furthermore, the sputtered area was chosen as large as $90 \mu\text{m} \times 70 \mu\text{m}$ in order for the sputtering results to be representative of the fracture surface material and to minimize surface roughness effects.

Results of this analysis in the form of element concentration versus ion sputtered depth are shown in Fig. 7. It is shown, particularly in comparing Figs. 7(b) and 7(c), that the decrease in oxygen content in the 2% prestrained material is faster than in the as-received material; at a depth of $0.5\mu\text{m}$, oxygen concentration in the latter condition is approximately six times higher than that of the prestrained surface at the same depth. This comparison indicates that the thickness of oxide layer, and consequently the depth of oxygen penetration, is higher in the case of the as-received fracture process.

This result could also qualitatively be supported by observing that the intergranular facets in the case of prestrained specimens, Fig. 5(b), are covered with smooth undisturbed oxide layer. This is in contrast to the peeled cracked features associated with the surface layer in the case of the as-received condition, Fig. 5(c). The difference in these two surfaces features could be explained in terms of the difference in the oxide layer thickness in the two test conditions; as the thickness increases, the compatibility between the base material and

the oxide layer decreases resulting in microcracks of this layer and the curling of its edges [22]. Concerning the degree of the chromium content of the grain boundary network in the crack tip zone, one could observe that the concentration of chromium in the top $0.2\ \mu\text{m}$, as seen in Fig. 7(b), is distinctively higher in the prestrained surface than that of the as-received one as illustrated in Fig. 7(c). This observation supports the assumption that the grain boundary chromium content is generally enhanced by the increase in the slip line density.

The importance of the present work lies in the possibility that high-temperature intergranular oxidation properties of high-strength alloys can be modified through cold work at room temperature or forging at relatively low temperature to enhance the slip homogeneity at the crack tip region and thus produce a built-in intrinsic mechanical resistance to high temperature fatigue crack growth.

4. Conclusions

In this paper the influence of prestraining on the high temperature, low frequency crack growth behavior of Alloy 718 has been investigated. Major conclusions of this work could be summarized as:

1. Density of slip lines and associated homogeneity of plastic deformation in the crack tip region are closely related to the degree of prestraining imposed on the virgin material prior to the cracking process. The higher the degree of prestraining, the higher the slip line density.

2. The increase in slip line density due to prestraining results in a decrease in the low frequency crack growth rate. This decrease, while not due to the effect of fatigue crack closure, can be interpreted in terms of the influence of the slip line density on modifying both the stress field and the chromium content in the crack tip region. These modifications lead to enhancement of the low frequency crack tip resistance to oxidation due to the increase of the build-up rate of the protective Cr_2O_3 sublayer.

Acknowledgement: Concepts of this work were developed during the sabbatical stay of H. Ghonem at Ecole des Mines de Paris in 1989 (see Ref.[6] of this paper). Ideas and discussions with both Professor A. Pineau and Dr. E. Andrieu of Ecole des Mines were key elements in development of this study. This research program is supported by the Air Force Office of Scientific Research under contract AFOSR-89-0285. Dr. W. Jones is the program manager.

5. Appendix A

The relationship between slip line spacing and loading parameters

Venkataraman et al [9] have proposed a quantitative model to estimate slip line spacing in crystal materials on the basis of the minimum energy configuration. In this model, a set of m mutually interacting slip lines was considered, and the formation of the slip lines was given by the ratcheting mechanism, that is, in the loading part of the very first cycle, a set of m parallel slip planes are activated simultaneously. Each plane is a pile-up of positive edge dislocations and are designated as positive plane. They assumed that the dislocations are only partially reversible so that when the applied stress reverses sign, a neighboring set of m negative planes undergo slip in the reverse part of the cycle. In their model, each positive plane together with its neighboring negative plane constitutes a slip line. The spacing between these lines, w , was then written as

$$w \approx \frac{h}{v_{sb}} \quad (1)$$

where h is the slip line width, v_{sb} is the volume fraction of slip lines in a grain. With the region in between the slip lines constituting the matrix, the average plastic strain amplitude within the grain, γ_p , can be written in terms of the law of mixture of a two-phase material, and since the plastic strain in the slip lines is much greater than that in the matrix, so v_{sb} can be expressed as

where $\gamma_{p,sl}$ represent the average shear plastic strain amplitude within a slip line, and it was

$$\nu_{sb} \approx \frac{\gamma_p}{\gamma_{p, sb}} \quad (2)$$

formulated by Venkataraman et al [9] as below:

$$\gamma_{p, sb} = \frac{25d(1-\nu)(\Delta\tau - 2k)}{18wG} \quad (3)$$

where d is the dislocation pile-up length, ν is the Poisson ratio, $\Delta\tau$ is the shear stress range on slip plane, k is the friction stress, G is the shear modulus.

If grains have an orientation with respect to the loading axis that is characterized by an orientation factor M , so the macroscopic quantities can be related to the microscopic quantities by

$$\Delta\sigma = M\Delta\tau, \quad \epsilon_p = \frac{\gamma_p}{M}, \quad \sigma_f = Mk \quad (4)$$

where $\Delta\sigma$ is the applied stress range, ϵ_p is the remote plastic strain amplitude, and σ_f is the friction stress measurable from hysteresis loop. Thus, from eqs.(4), (5), (3) and (1), the slip line spacing, w , can be expressed as

$$w = \frac{5}{3M} \sqrt{\frac{d(1-\nu)(\Delta\sigma - 2\sigma_f)}{2G\epsilon_p}} \quad (5)$$

Eq. (5) gives the explicit relation between the plastic deformation and the slip line spacing (or slip line density), i.e. the slip line spacing has an inverse square root relationship with the plastic strain which is consistent with many experimental observations, e.g. Refs. [20,21]. This model, however, did not show the influence of strain rate on the slip

exhibited lower crack growth rate.

The importance of these results lies in the possibility that high-temperature intergranular oxidation properties of high-strength alloys can be modified through cold working at room temperature or forging at relatively low temperature to enhance the slip homogeneity at the crack tip region and thus produce a built-in intrinsic mechanical resistance for high temperature fatigue crack growth.

MATERIAL VARIABLES

In this section, the role of material variables in influencing the crack tip oxidation and consequently the related time-dependent damage process will be discussed. The variables to be analyzed include chemical composition, precipitate size and morphology, grain size and grain boundary morphology.

ROLE OF CHEMICAL COMPOSITION

The FCGR of Ni base superalloys under creep-fatigue conditions is strongly dependent on the composition of the material [33]. Very minor compositional changes can significantly modify the elevated temperature grain boundary resistance. Floreen and Davidson [334, for example, observed that the creep crack growth resistance in Alloy 718 was noticeably reduced when the material contained small amounts of boron

6. References

- [1] S. Floreen and R. H. Kane. "An Investigation of the Creep-Fatigue-Environment Interaction in a Ni-Base Superalloys", *Fatigue of Engineering Materials and Structures*, Vol. 2, 1980, pp.401-412

- [2] T. Weerasooriya and S. Venkataraman. "Frequency and Environment Effect on Crack Growth in Inconel 718", in *Effects of Load and Thermal Histories*, eds. by P. K. Liaw and T. Nicholas, The Metallurgical Society of AIME, Warrendale, PA, 1987, pp.101-108

- [3] A. Pineau. "Intergranular Creep-Fatigue Crack Growth in Ni-Base Alloys", in *Flow and Fracture at Elevated Temperature*, ed. by R. Raj, American Society for Metals, 1985, pp.317-348

- [4] T. Weerasooriya. "Effect of Frequency on Fatigue Crack Growth Rate of Inconel 718 at High Temperature", in *Fracture Mechanics: Nineteenth Symposium*, ASTM STP 969, ed. by T. A. Cruse, American Society for Testing and Materials, Philadelphia, PA, 1988, pp.907-923

- [5] H. Ghonem and D. Zheng. "Depth of Intergranular Oxygen Diffusion during

Environment-Dependent Fatigue Crack Growth in Alloy 718", *Materials Science and Engineering*, Vol. 150, 1992, pp.151-160

- [6] H. Ghonem, D. Zheng, E. Andrieu and A. Pineau, "Experimental Observations and Quantitative Modelling of Oxidation-Assisted Crack Growth Behavior in Alloy 718 at 650°C", *Annual Report, AFOSR-89-0285*, 1990
- [7] H. H. Smith and D. J. Michel. "Fatigue Crack Propagation and Deformation Mode in Alloy 718 at Elevated Temperatures", in *Ductility and Toughness Considerations in Elevated Temperature Service, MPC-8*, ed. by G. V. Smith, American Society of Mechanical Engineering, New York, 1978, pp.225-246
- [8] D. Zheng and H. Ghonem. "Effects of Frequency Interactions on High Temperature Fatigue Crack Growth Superalloys", submitted to *Metallurgical Transactions*, 1992
- [9] G. Venkataraman, Y.-W. Chung and T. Mura. "Application of Minimum Energy Formation in A Multiple Slip Band Model For Fatigue I. Calculation of Slip Band Spacings", *Acta Metallurgica et Materialia*, Vol. 39, 1991, pp.2621-2629
- [10] G. Venkataraman, Y.-W. Chung, Y. Nakasone and T. Mura. "Free Energy Formulation of Fatigue Crack Initiation Along Persistent Slip Bands: Calculation of S-N Curves and Crack Depths". *Acta Metallurgical et Materialia*, Vol. 38, 1990, pp.31-40

- [11] T. Mura. "A Theory of Fatigue Crack Initiation in Solids". *Journal of Applied Mechanics*, Vol. 57, 1990, pp.1-6
- [12] H. H. Smith and D. J. Michel. "Effect of Environment on Fatigue Crack Propagation Behavior of Alloy 718 at Elevated Temperatures", *Metallurgical Transactions*, Vol. 17A, 1986, pp.370-374
- [13] W.N. Sharpe, Jr.. "Interferometric Surface Strain Measurement", *International Journal of Nondestructive Testing*, Vol.3, 1971, pp.59-76
- [14] N. J. Marchand. "Thermal-Mechanical Fatigue Behavior of Nickel-Base Superalloys", Ph. D. Dissertation, Massachusetts Institute of Technology, 1986
- [15] M. Clavel, D. Fournier and A. Pineau. "Plastic Zone Sizes in Fatigued Specimens of Inco 718", *Metallurgical Transactions*, Vol. 6A, 1975, pp.2305-2307
- [16] J. M. Kendall, M. A. Nicks and J. E. King. "The Effect of Prestraining on Fatigue Crack Growth in Nickel-Base Alloys", *Fatigue '87*, Vol. 1, eds. R. O. Ritchie and E. A. Starke, Jr., Engineering Materials Advisory Service Ltd., West Midlands, U.K., 1987, pp.959-968
- [17] D. -H. Chen and H. Nisitani. "Analytical and Experimental Study of Crack Closure Behavior Based on An S-Shaped Unloading Curve", *Mechanics of Fatigue Crack*

Closure, ASTM STP 982, eds. J. C. Newman, Jr. and W. Elber, ASTM 1988, pp.475-488

- [18] Y. Tanaka and I. Soya. "Fracture Mechanics Model of Fatigue Crack Closure in Steel", *Fracture Mechanics: Perspectives and Directions (Twentieth Symposium)*, ASTM STP 1020, eds. R. P. Wei and R. P. Gangloff, American Society for Testing and Materials, Philadelphia, 1989, pp.514-529

- [19] J. P. Pedron and A. Pineau. "The Effect of Microstructure and Environment on the Crack Growth Behavior of Inconel 718 Alloy at 650°C under Fatigue, Creep and Combined Loading", *Materials Science and Engineering*, Vol. 56, 1982, pp.143-156

- [20] R. T. Marlin, F. Cosandey and J. K. Tien. "The effect of Prestraining on the Creep and Stress Rupture of an Oxide Dispersion Strengthened Mechanical Alloy", *Metallurgical Transactions*, Vol. 11A, 1980, pp.1771-1775

- [21] N. Y. Jin. "Formation of Dislocation Structures during Cyclic Deformation of F.C.C. Crystals I. Formation of PSBs in Crystals Oriented for Single-Slip", *Acta Metallurgica*, Vol. 37, 1989, pp.2055-2066

- [22] P. Kofstad, *High Temperature Corrosion*, Elsevier Applied Science Publisher LTD, 1988.

- [23] Unpublished data, Pratt & Whitney, July, 1988
- [24] M. Khobaib and N. Ashbaugh. "Mechanical Behavior of β 21S". Technique Report, University of Dayton Research Institute, Dayton, Ohio, 1991
- [25] T. Ingham and E. Morland. "Influence of Time-Dependent Plasticity on Elastic-Plastic Fracture Toughness". In Elastic-Plastic Fracture: Second Symposium, Volume I Inelastic Crack Analysis, ASTM STP 803, Eds. C. F. Shih and J. P. Gudas, American Society for Testing and Materials, 1983, pp.I-721 I-746
- [27] H. Mughrabi, K. Herz and X. Stark. "The Effect of Strain-Rate on the Cyclic Deformation Properties of α -Iron Single Crystals". Acta Metallurgica, Vol. 24, 1976, pp.659-668
- [28] D. K.-Wilsdorf and C. Laird. "Dislocation Behavior in Fatigue II. Friction Stress and Back Stress as Inferred from an Analysis of Hysteresis Loops". Materials Science and Engineering, Vol. 37, 1979, pp.111-120
- [29] J. I. Dikson, J. Boutin and L. Handfield. "A Comparison of Two Simple Methods for Measuring Cyclic Internal and Effective Stresses". Materials Science and Engineering, Vol. 64, 1984, L7-L11

Figure Illustrations

- Fig. 1 Single-edge-notched specimen used in the present study (dimensions are in mm).
- Fig. 2 Effect of prestraining on fatigue crack growth rate. The ΔK values are not corrected for the crack tip closure effects.
- Fig. 3 Effect of prestraining on fatigue crack growth rate for Alloy N901 [16].
- Fig. 4 Effect of prestraining on fatigue crack growth rate taking into account the crack tip closure on the value of ΔK .
- Fig. 5 Micrographs of fracture morphologies for Alloy 718: (a) as-received; (b) 1% prestrained; (c) 2% prestrained.
- Fig. 6 Traces of slip lines below the fracture surfaces: (a) as-received, $\Delta K = 12$ MPa \sqrt{m} ; (b) 2% prestrained, $\Delta K = 12$ MPa \sqrt{m} ; (c) as-received, $\Delta K = 27$ MPa \sqrt{m} ; (d) 2% prestrained, $\Delta K = 27$ MPa \sqrt{m} .
- Fig. 7 Depth profiles versus element concentration for three surface conditions: (a) free surface of non-tested Alloy 718 specimen; (b) fracture surface of as-received specimen; (c) fracture surface of 2% prestrained specimen.

Fig 1 Zhang X Gao

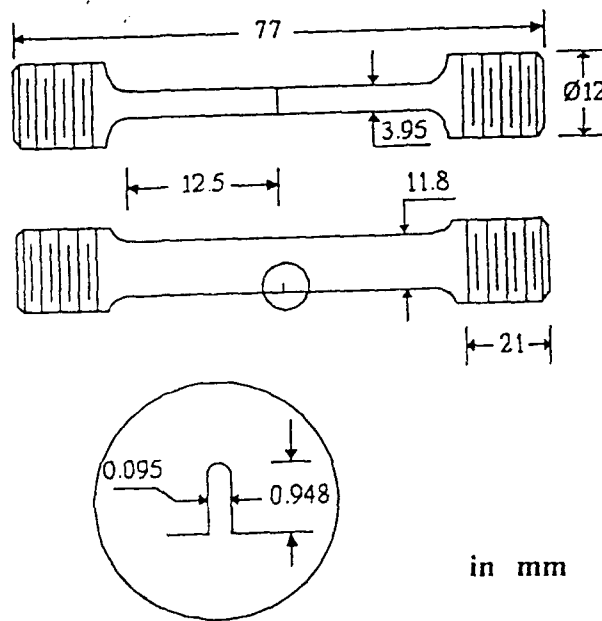


Fig. 1

Fig. 3 Zhong & Gilman

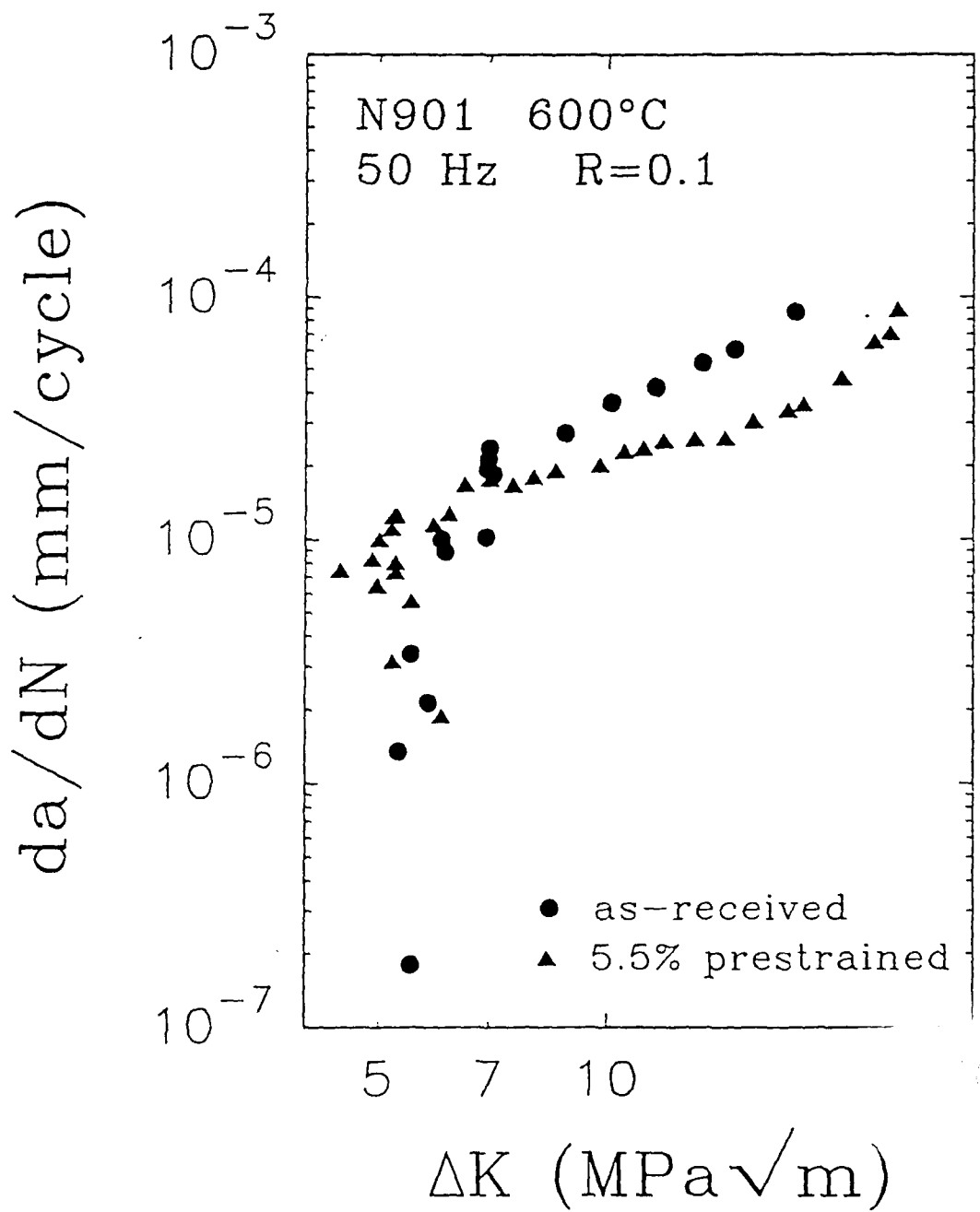
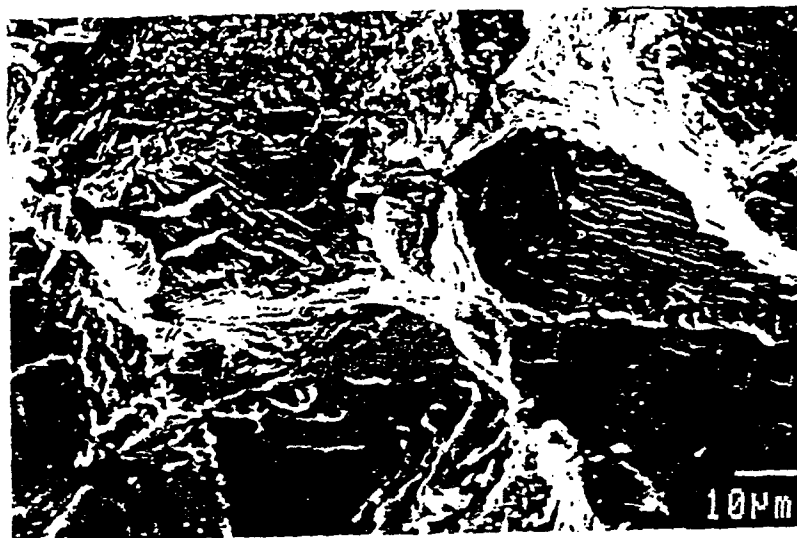


Fig. 3

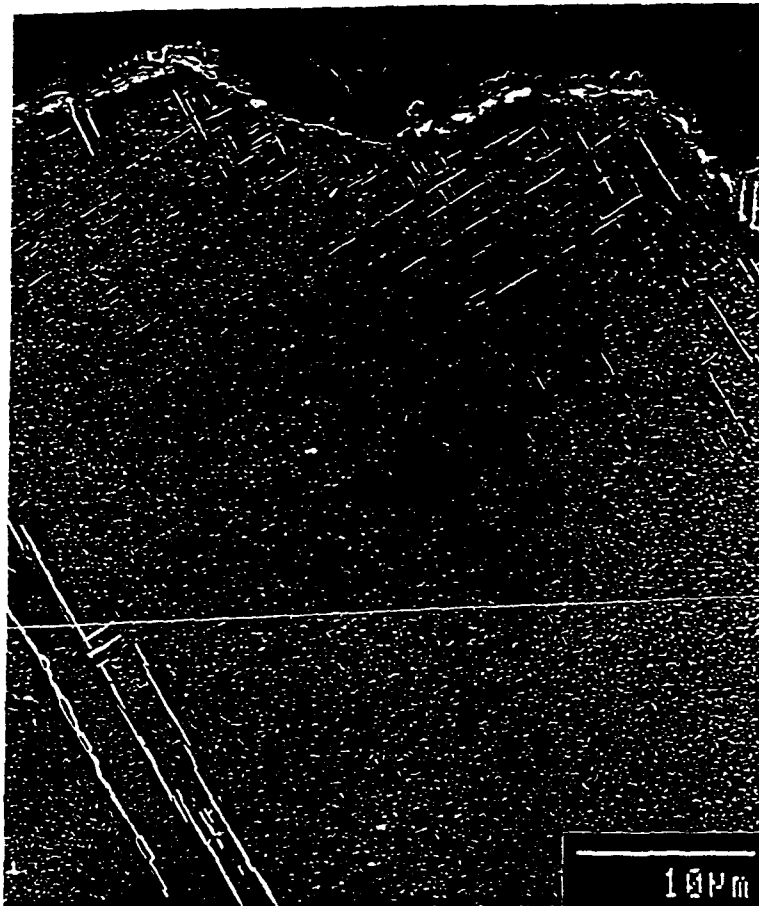


(a)



(b)

Fig. 5



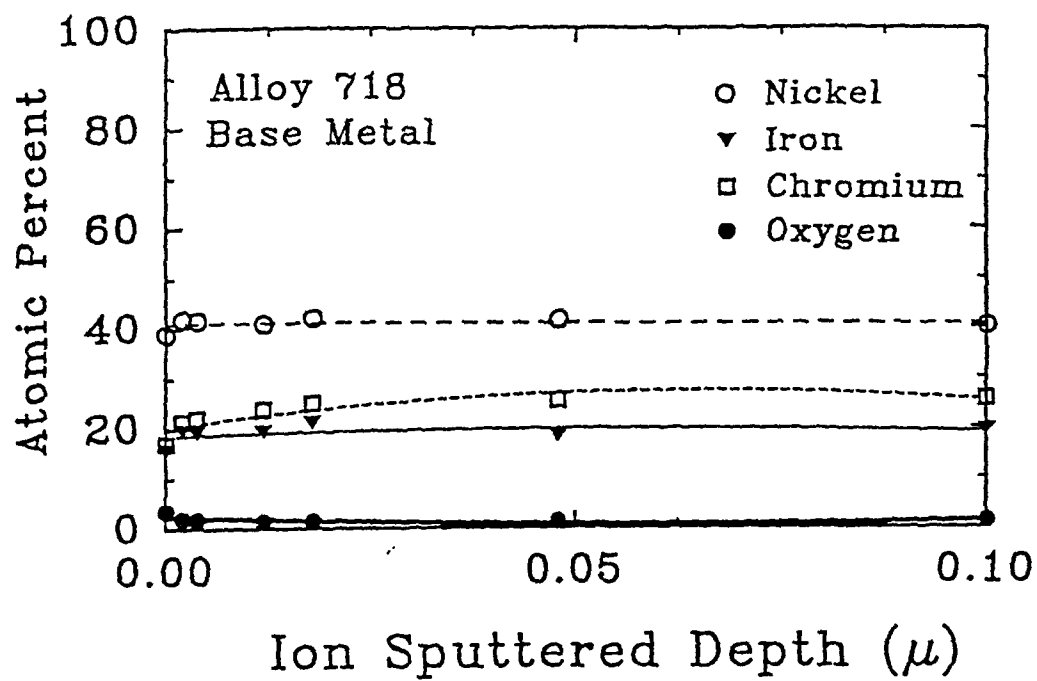
(a)

Fig. 6

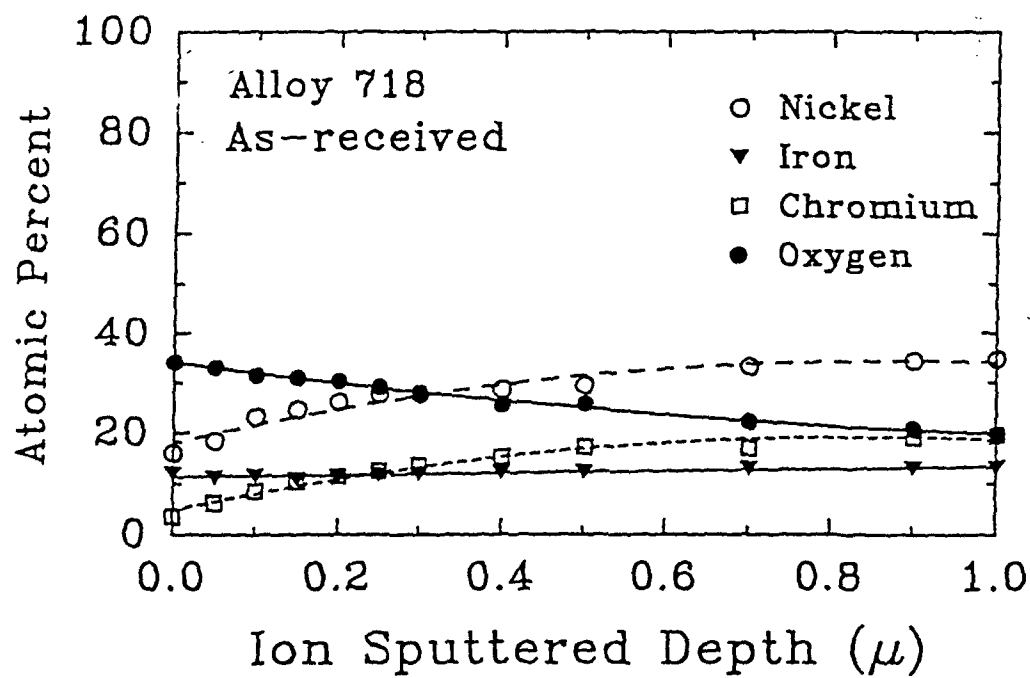


(c)

Fig. 6



(a)



(b)

Fig. 7

ELEVATED TEMPERATURE FATIGUE CRACK GROWTH IN ALLOY 718 - PART I: EFFECTS OF MECHANICAL VARIABLES

H. Ghonem⁺, T. Nicholas⁺⁺ and A. Pineau⁺⁺⁺

⁺ Mechanics of Solids Laboratory, Department of Mechanical Engineering and
Applied Mechanics, University of Rhode Island, Kingston, RI 02881, U.S.A.

⁺⁺ Wright Laboratory, Materials Directorate, Wright-Patterson Air Force Base, Ohio 45433, U.S.A.

⁺⁺⁺ Centre des Materiaux, Ecole des Mines de Paris, 91000 Evry, France

Abstract: In this paper observations concerning effects of mechanical variables on the crack growth process in Alloy 718 are reviewed and analyzed on the basis of the related deformation characteristics in the crack tip region. These variables included temperature, frequency, wave shape, hold time, load ratio, and load interaction. These analysis have suggested that the role of each of these parameters in the crack tip damage acceleration is governed mainly by its relative influence on the nature of the corresponding plastic deformation and associated slip line density. On the basis of this view which assumes that the crack growth damage mechanism in Alloy 718 ranges from cyclic-dependent to fully time-dependent processes, the interactive effects of loading parameters in defining the corresponding fracture mode are discussed and conflicting experimental observations under different operating conditions are examined.

INTRODUCTION

Alloy 718 is a precipitation strengthened nickel-base superalloy with a stable microstructure and high resistance to both creep and stress rupture up to 650°C when not subjected to very long term applications. Because of these characteristics and its excellent mechanical properties it has been widely used in aerospace and nuclear applications involving static as well as cyclic loading at both high and medium temperature ranges in aggressive air environment. Damage tolerance methodologies needed in some of these applications require accurate predictions of the crack growth behaviour under typical service conditions. For this reason, and as a part of material characterization, a large number of studies have been carried out in the last three decades in order to investigate the influence of various operating parameters on the crack growth mechanisms under different environmental conditions. Analysis of these studies appear to conclude that, in general, effects of air at high temperature are primarily due to oxygen and that the combined effects of load, environment and material variables are to alter the crack propagation mode through interaction with the crack tip slip process. The attraction of this view is that it presents the deformation characteristics in the crack tip region as being the unifying mechanism for which an applied operating parameter could be designed to produce a particular crack growth performance. The objective of this work is to present this view by summarizing the influence of different mechanical, environmental and material parameters. The first

part of the work deals with observations of the effects of temperature, frequency, waveshape, hold time and load interactions.

MECHANICAL VARIABLES

In each of the following sections, the influence of a particular loading parameter on the fatigue crack growth performance of Alloy 718 is described on the basis of the governing mechanisms acting at the corresponding test conditions. The parameters under study here include temperature, frequency, wave shape, hold time, load ratio, and load interaction. No attempt is made to present a complete bibliography relating to these aspects of behaviour of Alloy 718, rather, an attempt is made to cover the complete span of observations reported regarding these aspects of behaviour.

Effects of Temperature

A comprehensive evaluation of the effect of temperature on the crack growth in Alloy 718 is that of Weerasooriya [1]. Constant ΔK tests at $R=0.1$ were conducted at $K_{max} = 27.8$ and $40.0 \text{ MPa}\sqrt{\text{m}}$ for frequencies ranging from 0.001 to 1.0 Hz. Results of the tests at $K_{max} = 40 \text{ MPa}\sqrt{\text{m}}$ in the form of FCGR vs reciprocal absolute temperature are shown in Fig. 1. The frequency effects are discussed in the next subsection. For temperatures between room temperature and 650°C , the growth rate increases with increase in temperature. The rate of increase in the lower temperature regime (c) is

limited and is attributed to a combination of the change in modulus and plastic deformation characteristics of the material with temperature. The fracture mode is transgranular and the behaviour is characterized as cycle dependent. At some transition temperature, depending upon frequency, the growth rate increases significantly with further increase in temperature. In this region (b) the fracture is a combination of transgranular and intergranular and the behaviour is characterized as mixed mode. As can be observed in Fig. 1, the temperature at which this transition occurs is higher for higher frequencies. At the highest temperatures, the behaviour of this material becomes purely intergranular, the mode is characterized as time dependent, and the rate of change of growth rate with temperature is maximum. This region is denoted by (a) in Fig. 1. The transition temperature from mixed mode to time dependent, denoted in this figure as T_{tm} , again depends on test frequency and has a higher value for higher frequencies. Similar observations of FCGR behaviour as a function of frequency where the mode of fracture and the rate of crack growth can be correlated are presented in the next subsection.

The effects of temperature on FCGR can also be observed when Alloy 718 is tested in vacuum environment. However, the fatigue crack growth rate only increases slightly with increase in temperature compared to the changes observed in air [2].

Effects of Frequency

The effects of cyclic frequency on the fatigue crack growth behaviour of Alloy 718

has been the subject of many researches [3,4,5-8]. James [3] studied the frequency effects for Alloy 718 at 538°C over the range of 1.39×10^{-3} Hz to 6.67 Hz, the results are shown in Fig. 2. It can be seen from this figure that the fatigue crack growth rates increase as cyclic frequencies decrease, although the rate of change with frequency is fairly small. In this case reducing the frequency by a factor of almost 5000 results in an increase in growth rate of approximately 5. This trend was also noted by Clavel and Pineau [4] in their work at 550°C over the range of 5×10^{-3} Hz to 20 Hz. Crack growth rates in laboratory air at a higher temperature of 650°C are found however, to depend much more strongly on frequency. Increasing the frequency can result in a significant decrease in crack growth rate per cycle. For example, Weerasooriya [6,7] has shown that at two constant ΔK conditions the behaviour ranges from purely time dependent at frequencies below 0.01 Hz to purely cycle dependent at frequencies in excess of 10 Hz. Under purely time-dependent conditions, the crack growth rate changes with reciprocal frequency, that is, halving the frequency results in double the growth rate. On the other hand, cycle-dependent behaviour produces growth rates which are independent of frequency. Weerasooriya's work also shows that different mechanisms of crack growth are activated in each regime: striation formation is generally observed in the cycle-dependent regime, intergranular crack growth is dominant in the time-dependent regime, and a mixed transgranular-intergranular mode of crack extension is observed in the mixed regime. Similar observations of the frequency dependence have been documented by Floreen and Kane [5] and Pedron and Pineau

[9]. Although the magnitude of the change in growth rate with decrease in frequency varies depending on the alloy microstructure, temperature, and frequency, the pattern of behaviour is widely noted in all nickel-base superalloys and is generally attributed to decreasing environmental resistance with increasing exposure time as cyclic frequency decreases.

While most frequency studies have been conducted in air environment, Floreen and Kane [5] studied the fatigue crack growth behaviour of Alloy 718 at 650°C over the range of 0.01 Hz to 1 Hz in air and helium (99.995% purity) as well. In helium environment, as the frequency decreased, the fatigue crack growth rate only increased slightly, while in air environment, the fatigue crack growth rate increased substantially as frequency decreased.

Similar to other high strength superalloys, the frequency effects for Alloy 718 are only observed at elevated temperatures and not at room temperature [8]. Further, the cycle-dependent (high frequency) growth rate at high temperature corresponds closely with the rate observed at room temperature as well as those observed in vacuum, indicating a lack of environmental contributions to the growth rate process when the transgranular fatigue mode dominates [7].

Effects of Wave Shape

Although the behaviour as a function of frequency is widely noted and accepted, the behaviour when more complex wave shapes are involved is not as well understood

nor are the results consistent among the various investigators. There are a number of observations involving other wave shapes which illustrate the variable nature of the elevated temperature crack growth behaviour. James [10] found that growth rate at 538°C in Inconel 718 is significantly faster for a square wave waveform than for a sawtooth waveform of the same cyclic duration when the loading frequency was much lower than the unloading frequency. In these experiments, the hold time contribution in the square wave appears to dominate the cyclic contribution, even for a low loading frequency in the sawtooth wave. Somewhat conflicting results were obtained by Clavel and Pineau [4] who examined the wave-shape effects on FCGR using square and triangular wave shapes at 550°C. Three cyclic wave shapes were chosen (shown in Fig. 3) for differentiating the effect of loading and unloading rate as well as the effect of hold time at maximum and minimum load. Wave-shape 3 corresponds to a frequency of 2 Hz, whereas wave-shape 2 leads to a frequency of 0.05 Hz. Wave-shape 1 has the same loading and unloading rate as wave-shape 3 but superposes a 10 s hold time at the maximum load level and at the minimum load level, and its cyclic duration is the same as that of wave-shape 2. Their results showed that the FCGR of wave shape 2 is higher than those of the other two wave shapes, and the FCGR of wave-shape 1 is only slightly higher than that of wave-shape 3. They inferred that, contrary to the observations of James [10], a hold-time of 10 s both at the maximum and at the minimum load has no significant effect on FCGR, and that the main parameter is not the frequency *per se* but the loading and the unloading rate. As already pointed out by Bathias and Pelloux [11]

the slip character strongly affects the aspect of the fracture surfaces. In fact, their fractographic examination showed that, at 550°C, the cracks propagate by a transgranular mode when the frequency is higher than 0.5 Hz, while at lower frequency (0.05 Hz) the crack growth occurs by a mixture of transgranular and intergranular fracture. The well known fact for this material is that homogeneity in plastic deformation promotes transgranular fracture mode while inhomogeneity in plastic deformation favors intergranular fracture mode [12,13-17]. This subject will be discussed in more detail in the next section. It is postulated, therefore, that for wave-shape 1 the loading and unloading rates promoted the homogeneity in plastic deformation which generally has less time-dependent sensitivity, thus the hold times after the loading and unloading portions are not expected to produce a large influence on FCGR which is why the FCGR of wave-shape 1 is only slightly higher than that of wave-shape 3. For wave-shape 2, the loading and unloading rates produced the inhomogeneity in plastic deformation near the crack tip which, in turn, favors the occurrence of intergranular fracture, and certainly the FCGR is much higher than that of wave-shape 1.

The apparent inconsistency between these results from different wave shapes and those of James [10] can now be explained in terms of the proposed mechanisms as well as careful examination of the conditions present in the experiments in [10]. Noting that the frequencies are quoted in units of cpm, the rising and falling portions of the "square wave" in [10] are 24s each, corresponding to a cyclic frequency of 0.02 Hz. The cyclic

portion of the "square wave is clearly at frequencies which is sufficiently low to produce inhomogeneity in plastic deformation which , in turn, favors the occurrence of intergranular fracture. The addition of a hold time to such a cycle, therefore, is expected to have a large influence on FCGR, as is observed.

Ashbaugh [18] conducted a series of tests at 649°C using triangular waveshapes on C(T) specimens and $R=0.1$. In addition to symmetric waveshapes with frequencies covering the range from 0.01 Hz to 10 Hz, asymmetric waveshapes were used in which the rise and fall times had different values corresponding to the baseline frequencies of the symmetric waveform tests. For various combinations of rising and falling frequencies from 1 Hz to 0.01 Hz, growth rates per cycle were essentially equivalent to those obtained using symmetric waveshapes where the frequency was that of the rising portion of the asymmetric wave. This observation implies that the fatigue damage occurs almost exclusively during the rising load portion of the fatigue cycle. At the temperature and frequencies at which these experiments were conducted, the fracture mode is a mixed mode combination of intergranular and transgranular [7].

The concept of damage accumulation only during the rising load portion of a cycle has been subsequently demonstrated in an investigation of thermomechanical fatigue (TMF) by Nicholas et al. [19]. In that study, crack growth rates were measured under combined thermal and mechanical cycling at $R=0.1$ and a temperature range between 427 and 649°C. For a series of experiments which involved the use of a number of phase angles between load and temperature, and where the growth rates

$$\Delta K \text{ (MPa}\sqrt{\text{m}})$$

Fig. 3

varied for a given K over two orders of magnitude, a linear summation model involving cycle dependent and time dependent contributions integrated over the cycle while K and temperature are both varying provided excellent correlation with the experimental data. Most significant, however, was that the integration of the time dependent contribution was carried out only while the time-dependent contribution, da/dt , was increasing during the cycle. This further illustrates the effect observed in the waveshape experiments, namely that the damage in a fatigue cycle occurs only when the driving force is an increasing function. Under isothermal conditions, this amounts to the rising load portion of the cycle whereas under TMF, it is when da/dt (a function of both load and temperature) is increasing.

The effects of wave shape upon FCGR have also been investigated for Alloy 718 at 650°C by Ghonem and Zheng [20]. Their results appear to be in conflict with those obtained by Ashbaugh [18]. In their work, the cyclic durations of the triangular waves included 27.5 s (25s-2.5s), 50 s (25s-25s), 100 s (25s-75s) and 100 s (90s-10s) which are denoted as case A, B, C and D, respectively and the numbers in parentheses denote the times of the rising and falling portion of the wave. The results of FCGR vs ΔK are shown in Fig. 4. It can be seen from this figure that the FCGR for case C is identical to that of case D indicating that for the same frequency, varying the ratio of the loading and unloading portions of the cycle does not influence the fatigue crack growth behaviour. Furthermore, cases A, B and C, which have different frequencies but identical loading times, did not result in similar crack growth behaviour so that an

increase in the total cycle duration yields an increase in the FCGR. In comparing these results with those of Ashbaugh [18], it should be noted that the variation in loading frequency between case D and the other three is less than a factor of 4 whereas Ashbaugh investigated the effect using frequencies which differed by either one or two orders of magnitude. Further, the growth rates differ by much less than an order of magnitude at low ΔK values in the results of Ghonem and Zheng, whereas Ashbaugh reported that the growth rates were "comparable." Although the loading frequency in the asymmetric wave produced growth rates in Ashbaugh's study which were nearly identical to those from symmetric wave forms of the same frequency at high values of ΔK in excess of 30 MPa \sqrt{m} , differences appeared at lower ΔK . In particular, the slow-fast (50s-5s) wave had a lower FCGR than the symmetric 0.01 Hz (50s-50s) while the fast-slow (5s-50s) had a considerably higher FCGR than the (5s-5s) symmetric wave. This demonstrates that total cycle time as well as loading frequency can influence growth rate, depending on the particular conditions. In general, crack growth rates in nickel-base superalloys due to combinations of hold times and cyclic loading involve a complex interaction which can be attributed to a variety of mechanisms including fatigue, creep or stress relaxation, environmental degradation, and crack tip blunting or crack branching. Further, the ΔK value can influence the results because of the differing contributions of cycle dependent and time dependent mechanisms.

Effects of Hold Time

It is widely reported that the addition of a hold time at maximum load to a fatigue cycle tends to increase the crack growth rate per cycle in Alloy 718 as well as in a number of other nickel-base superalloys [4,21-29]. Fig. 5 shows, for example, results from three separate investigations involving Inconel 718 at 650°C where hold times are added to baseline fatigue cycles. This results in an increase in growth rate per cycle. In all three cases it can be seen that the behaviour at long hold times is essentially purely time dependent, that is, growth rate increases linearly with increase in hold time. There are, however, a number of observations which do not show this same trend. Shahanian and Sadananda [22] show that at 760°C, the addition of hold times of 0.1, 1, or 10 min. does not increase the crack growth rate in Inconel 718. The results of this investigation also showed that growth rates obtained under constant load range (increasing ΔK) conditions depend on load amplitude, thereby demonstrating the inadequacy of ΔK as a correlating parameter at this temperature. At 593°C, VanStone et al. [29] showed that Inconel 718 still exhibits an increase in growth rate with increase in hold time, but the effect is not as pronounced as at 650°C.

There are several instances where hold times retard crack growth instead of accelerating it and even contribute to total crack arrest. This has been observed when hold times occur at other than maximum load [24]. In these cases, either significant creep occurs at the test temperature, thereby blunting the crack tip, or the stress intensity during hold is generally less than the creep crack growth threshold.

Several observations have been made in Inconel 718 at 649°C of the effect of a

hold time at minimum load on the crack growth rate. In these studies, the minimum load has been below the threshold for crack growth under sustained load, thereby producing no contribution in a linear summation model prediction. Nicholas and Weerasooriya [25] found no effect of hold times between 50 and 500 s under constant K conditions. Shahinian and Sadananda [24] and Sadananda and Shahinian [28], on the other hand, observed a definite increase in growth rate due to the addition of a hold time at minimum load. They attributed this acceleration of growth rate to the additional time available for oxidation. Similar observations have been made by Diboine and Pineau [27] where hold times at minimum load between 3 and 3000 s showed an increase in growth rate compared to that obtained under continuous cycling. In comparing these apparently contradictory results, Ghonem et al. [17] have noted that the frequency of the cyclic loading was different in the three cases cited. In the work of Nicholas and Weerasooriya [25], the cyclic frequency was 1 Hz which produces transgranular crack growth. In [24] and [27], the frequencies were 0.1 and 0.05 Hz, respectively, both of which produce intergranular crack growth. Thus, the frequency of the cycle affects the deformation mechanisms which, in turn, affect the subsequent behaviour due to hold time loading. These results will be analyzed again in the next section. Recall that a hold time at minimum load produced no change in growth rate when the cycle frequency was 1 Hz, but the growth rate accelerated due to the hold at minimum load when the cyclic frequency was either 0.1 or 0.05 Hz. The effect of frequency is important in this situation because of the differences in mechanisms

resulting from different rates of diffusion of oxygen into the grain boundaries. As discussed above, the strain rate corresponding to the 1 Hz cycle must promote homogeneity in plastic deformation near the crack tip, and this kind of deformation mode has less time-dependent sensitivity, thus the hold-time effect does not appear. However, strain rates for 0.17 Hz and 0.05 Hz certainly favor the inhomogeneity in plastic deformation near the crack tip, which will enhance time-dependent behaviour and thus will show strong hold-time effects.

In a similar manner, crack growth transients observed when changing from cyclic plus hold time loading to pure cyclic loading as described by Van Stone et al [29], can be explained by the inhomogeneity in plastic deformation ahead of the crack tip due to the hold time loading. Subsequent cyclic loading, even though applied at a higher value of K , tends to produce more homogeneous plastic deformation and higher slip density which lead to less environmental sensitivity. Thus, the transient crack growth rate is higher than after the crack has advanced under cyclic loading because the initial environmental sensitivity is enhanced.

Saturation effects of the hold time at minimum load level on FCGR have been noted by both Sadananda and Shahinian [28] and Diboine and Pineau [27]. The former observed the saturation effect appears for hold times about 1 minute, the latter reported that a saturation effect seems to occur for hold times longer than about 1000 s.

If the test temperature is not sufficiently high, the hold-time effect may disappear. For example, Sadananda and Shahinian [21] showed that at 425°C the 1-min. hold time

period has a negligible effect on the crack growth process. Furthermore, they found that, at 425°C, hold-times up to 10 minutes still produced purely cycle-dependent behaviour. Clearly, the effects of temperature and hold time are synergistic.

Very few studies [2,9,23,29-31] have dealt with the effects of hold time on FCGR in an environment other than in air. Ghonem and Zheng [31] have examined the effects of hold time in vacuum by conducting tests of continuous cycling at a frequency of 0.05 Hz and cycling with a hold time of 300 s at maximum load level. They found that FCGR for a hold time test is higher than that for a continuous cycling test. Similar results have been reported by Smith and Michel [23], Sadananda and Shahinian [30] and VanStone et al. [29]. In all cases, however, the changes are smaller than those observed in air under the same loading conditions.

Effects of Load Ratio

A detailed analysis was performed on mission cycles for advanced engines [29] to establish the loading conditions most prevalent for design. The analysis shows that most of the cyclic loading occurs at stress ratios above 0.5, that there is a large percentage of loading at very high R values between 0.9 and 1.0 (sustained load), and that the primary temperature range encountered is between 400 and 550°C. Because cyclic loading conditions in service generally cover a range of nonzero load ratios, many studies for Alloy 718 have been related to the effects of load ratio, R, on FCGR [1,24,32-36]. The general trend noted in all of these studies is, on a basis of ΔK , FCGR

at a given temperature increases with increasing R value. If FCGR is compared on a K_{max} basis, however, this trend may not always be true. Experimental results of Venkataaraman and Nicholas [32], for example, indicate the following observations at 650°C and $K_{max} = 30 \text{ MPa}\sqrt{\text{m}}$ (shown in Fig. 6): at low frequencies below 1 Hz where time dependent crack growth dominates, the FCGR increases with increase in R , while at high frequencies where a cycle dependent or mixed mode mechanism operates, the stress ratio R has a reverse influence for low values of R indicating a decrease in FCGR with increase in R . This can be attributed to the superimposed influence of the cyclic amplitude on the time dependent behaviour. Further, the trend can have a reversal at high R levels due to a combined effect of mode change and the influence of crack closure. There has been little work on effects of closure on crack growth rate at high temperature in this alloy to date.

Weerasooriya [1] has also studied the effect of load ratio on FCGR under constant K_{max} conditions and interpreted the results in terms of the governing micromechanisms as well as crack closure. Results from his work are presented in Fig. 7 where growth rate is plotted against $(1-R)$ for the three conditions shown. At 650°C and 0.005 Hz, the behaviour is purely time dependent as evidenced by the intergranular failure mode and growth rate is dominated by the mean stress. Thus, as R decreases ($(1-R)$ increases) the mean stress decreases and the growth rate decreases accordingly. At a higher frequency of 1.0 Hz at the same temperature, both mean stress and stress amplitude contribute to the growth process. For high R (low values of $(1-R)$) the cycles

are below the cyclic threshold, the mechanism is intergranular, and only mean stress contributes as in the 0.005 Hz case. As $(1-R)$ further increases, the growth rate starts to increase due to the addition of a cyclic contribution and the behaviour is mixed intergranular and transgranular. When $(1-R)$ exceeds 0.7, that is R is below 0.3, crack closure comes into effect so that the effective cyclic driving force remains unchanged. Here the growth rate remains relatively constant. Finally, at a low temperature of 316°C and $R=0.1$, the behaviour is purely cycle dependent, the mode is transgranular, and the growth rate increases continuously with $(1-R)$ because the cyclic amplitude is increasing. Again, at $(1-R) = 0.7$, crack closure comes into effect and the growth rate levels off. These three cases are examples of the effects of load ratio on crack growth behaviour where mode of failure as well as crack closure must be used to interpret the observed growth rates.

Further insight into effects of R and interaction of fracture modes can be obtained from examination of the results of Nicholas and Ashbaugh [35] who evaluated FCGR at high R values at 649°C . Crack growth rates obtained under conditions of constant $K_{\max} = 30 \text{ MPa}\sqrt{\text{m}}$ are presented in the form of da/dt against R at 10 and 100 Hz in Fig. 8. The data point at $R=1$ represents the sustained load growth rate. In this type of plot, purely time dependent behaviour would show growth rates at both frequencies being the same while purely cycle dependent behaviour would separate the data by a factor of 10 in da/dt . Fig. 8 shows that at low R , the behaviour is essentially cycle dependent. The solid lines in the figure are analytical predictions based upon

purely cycle-dependent behaviour. As R increases, the experimental data from the two frequencies become closer and diverge from the cycle-dependent prediction. Clearly, the time dependent effect is more important at high mean stresses. The curves undergo a minimum in the range of $R=0.8-0.9$ where the superposition of cycles upon a high mean load reduces the growth rate compared to what is obtained under mean load without the cycling. Linear summation modeling which takes into account both time-dependent as well as time-independent effects predicts most of the data quite well except for the high R region. Here, a combination of an intergranular mode from the mean load and a transgranular mode from the cycling produces a retarded growth rate when the mechanisms compete. A similar observation has been made by Venkataraman et al. [37] where low amplitude vibratory stresses (minor cycles) are superimposed on a low frequency, high amplitude cycle with a hold time at maximum load (major cycle). A minimum in growth rate is observed between $R = 0.8$ and 0.9 at a major cycle K_{\max} of $40 \text{ MPa}\sqrt{\text{m}}$ and in a similar range of R for $K_{\max} = 30$ and $20 \text{ MPa}\sqrt{\text{m}}$. The apparent retardation effect is attributed by the authors to an interaction between the fatigue and creep contributions to the crack growth process.

Effects of Load Interactions

Overload and retardation effects, although important in design considerations, have received relatively little attention for Alloy 718, particularly when time-dependent behaviour is present at elevated temperature under sustained loads. Weerasooriya and

Nicholas [38] evaluated the effects of a single fatigue cycle on the sustained load crack growth rate at 649°C. Using 1 Hz cycles, various hold times were added to the cycle at K levels which were either the same or 10, 20, or 50 percent lower than the peak of the fatigue cycle. Denoting the ratio of sustained load K to maximum K in the fatigue cycle by R_{in} , the results showed that the linear summation of fatigue and hold time contributions matched the experimental data for $R_{in} = 1$ and was fairly accurate for $R_{in} = 0.9$. For lower R_{in} values, the linear summation model grossly overpredicted the experimental data, indicating a strong retardation effect of the overload fatigue cycle. In these cases, it appears that the only contribution to crack growth is from the fatigue cycle and that the effect of the sustained load portion is completely retarded for hold times up to 200 s. A simple empirical retardation model was developed in [38] to account for the retardation effect of fatigue overloads on sustained load crack growth. A more extensive series of sustained load retardation experiments is reported in [39] along with details of procedures developed for modeling the retardation phenomenon. VanStone et al. [29] have also evaluated the effects of a fatigue overload on sustained load crack growth behaviour. At 649°C they observe a slight retardation effect when the fatigue overload ratio (ratio of peak fatigue K to sustained load K) is 1.1 and a significant retardation at a ratio of 1.2, similar to the observations in [38]. In addition, they noted that the retardation effect depended on the K value, the amount of retardation increasing with increase in sustained load K . A similar observation was made by Nicholas et al. [39].

Another form of interaction effect, in addition to the retardation effects described above, was reported by VanStone et al. [29]. This involved crack growth transients where one type of cycling using a given waveform is followed by another waveform. In their investigation, cycling under 0.33 Hz fatigue with a superimposed hold time of 300 s at maximum load was followed by pure 0.33 Hz cycling at maximum K higher than in the prior cycle. Upon the change in waveshape, the crack achieved transient growth rates much higher than the subsequent steady state value under constant K_{max} conditions. This effect was observed at both 593 and 649°C and demonstrates the existence of a damage state ahead of the crack tip due to sustained loads which is more degraded than one obtained under pure fatigue cycling.

CONCLUSION

The role of different mechanical parameters on the crack growth performance and related mechanisms in Alloy 718 has been critically reviewed. In this, observations related to the sensitivity of this alloy to variations in temperature, wave shape and loading frequency have been analyzed. Results of these analyses have demonstrated that the crack growth rate is governed by the nature of the crack tip fracture mode which ranges from cycle-dependent, transgranular process resulting in low crack growth rate to time-dependent, intergranular process leading to an accelerated crack growth. The cycle dependent regime is independent of loading frequency and generally

corresponds to low temperatures and low load ratios. The temperature at which the transition to time-dependent damage occurs is function of the test frequency and has a high value for higher frequencies. In this intergranular damage regime, the crack growth rate changes with reciprocal frequency and is sensitive to hold time durations imposed at maximum or minimum load levels. For hold time conditions, the crack tip damage mode is found to depend on the frequency of the loading part of the test cycle. Furthermore, waveshape damage effects, while complex, is sensitive to the combined frequency of the loading and unloading cycle segments in relation to the material transitional frequency.

Acknowledgement: This paper summarizes studies performed by the authors and their colleagues over number of years during which the work of H. Ghonem and T. Nicholas has been supported, independently, by the US Air Force Office of Scientific Research while the work of A. Pineau was supported by SNECMA. Support of the work of H. Ghonem was also provided by United Technologies.

REFERENCES

- [1] T. Weerasooriya et al., "Research on Mechanical Properties for Engine Life Prediction," AFWAL-TR-88-4062, Wright-Patterson AFB, OH, May, 1988
- [2] P. Shahinian and K. Sadananda, "Creep-Fatigue-Environment Interaction on Crack Propagation in Alloy 718", in Engineering Aspects of Creep, Institute of Mechanical Engineers, London, Vol. 2, 1980, Paper C239/80
- [3] L. A. James, "The Effect of Temperature upon the Fatigue-Crack Growth Behavior of Two Nickel-Base Alloy", Journal of Engineering Materials and Technology, Vol. 95, 1973, pp.254-256
- [4] M. Clavel and A. Pineau, " Frequency and Wave-Form Effects on the Fatigue Crack Growth Behavior of Alloy 718 at 298 K and 823 K", Metallurgical Transactions, Vol. 9A, 1978, pp.471-480
- [5] S. Floreen and R. H. Kane, "An Investigation of the Creep-Fatigue-Environment Interaction in a Ni-Base Superalloys", Fatigue of Engineering Materials and Structures, Vol. 2, 1980, pp.401-412
- [6] T. Weerasooriya and S. Venkataraman S., "Frequency and Environment Effect on Crack Growth in Inconel 718," Effects of Load and Thermal Histories, ed. by P. K. Liaw and T. Nicholas, The Metallurgical Society of AIME, Warrendale, PA, 1987, pp.101-108
- [7] T. Weerasooriya, "Effect of Frequency on Fatigue Crack Growth Rate of Inconel 718 at High Temperature," Fracture Mechanics: Nineteenth Symposium, ASTM STP 969, ed. by T. A. Cruse, American Society for Testing and Materials, Philadelphia, PA, 1988, pp.907-923
- [8] L. A. James, "Fatigue Crack Propagation in Alloy 718: A review", in Superalloy 718: Metallurgy and Applications, ed. by E. A. Loria, The Metallurgical Society of AIME, Warrendale, PA, 1989, pp.499-515
- [9] J. P. Pedron and A. Pineau, "The Effect of Microstructure and Environment on the Crack Growth Behavior of Inconel 718 Alloy at 650°C under Fatigue, Creep and Combined Loading", Materials Science and Engineering, Vol. 56, 1982, pp.143-156
- [10] L. A. James, "The Effect of Grain Size upon the Fatigue-Crack Propagation Behavior of Alloy 718 under Hold-Time Cycling at Elevated Temperature",

Engineering Fracture Mechanics, Vol. 25, 1986, pp.305-314

- [11] C. Bathias and R. M. Pelloux, "Fatigue Crack Propagation in Martensitic and Austenitic Steels", Metallurgical Transactions, Vol. 4, 1973, pp.1265-1273
- [12] H. H. Smith and D. J. Michel, "Fatigue Crack Propagation and Deformation Mode in Alloy 718 at Elevated Temperatures", In Ductility and Toughness Considerations in Elevated Temperature Service, MPC-8, ed. by G. V. Smith, American Society of Mechanical Engineers, New York, 1978, pp.225-246
- [13] M. Clavel and A. Pineau, "Intergranular Fracture Associated with Heterogeneous Deformation Modes during Low Cycle Fatigue in a Ni-Base Superalloy", Scripta Metallurgica, Vol. 16, 1982, pp.361-364
- [14] M. Clavel and A. Pineau, "Fatigue Behavior of Two Nickel-Base Alloys, Part I: Experimental Results on Low Cycle Fatigue, Fatigue Crack Propagation and Substructures", Materials Science and Engineering, Vol. 55, 1982, pp.157-171
- [15] D. Fournier and A. Pineau, "Low Cycle Fatigue Behavior of Inconel 718 at 298K and 823K", Metallurgical Transactions, Vol. 8A, 1977, pp.1095-1105
- [16] D. J. Wilson, "Relationship of Mechanical Characteristics and Microstructural Features to the Time-Dependent Edge-Notch Sensitivity of Inconel 718 Sheet", Journal of Engineering Materials and Technology, Vol. 113, 1973, pp.112-123
- [17] H. Ghonem, D. Zheng, E. Andrieu and A. Pineau, "Experimental Observations and Quantitative Modelling of Oxidation-Assisted Crack Growth Behavior in Alloy 718 at 650°C", Annual report, AFOSR-89-0285, 1990
- [18] N. E. Ashbaugh, "Waveshape Effects Upon Crack Growth in Inconel 718," presented at 15th National Symposium on Fracture Mechanics, University of Maryland, College Park, MD, July 8, 1982
- [19] T. Nicholas, M. L. Heil and G. K. Haritos, "Predicting Crack Growth under Thermo-Mechanical Cycling", International Journal of Fracture, Vol. 41, 1989, pp. 157-176.
- [20] H. Ghonem and D. Zheng, "The Depth of Intergranular Oxygen Diffusion during Environment-Dependent Fatigue Crack Growth in Alloy 718", Materials Science and Engineering, A150, 1992, pp.151-160.
- [21] P. Shahinian and K. Sadananda, "Crack Growth under Creep and Fatigue

behaviour. Furthermore, cases A, B and C, which have different frequencies but identical loading times, did not result in similar crack growth behaviour so that an

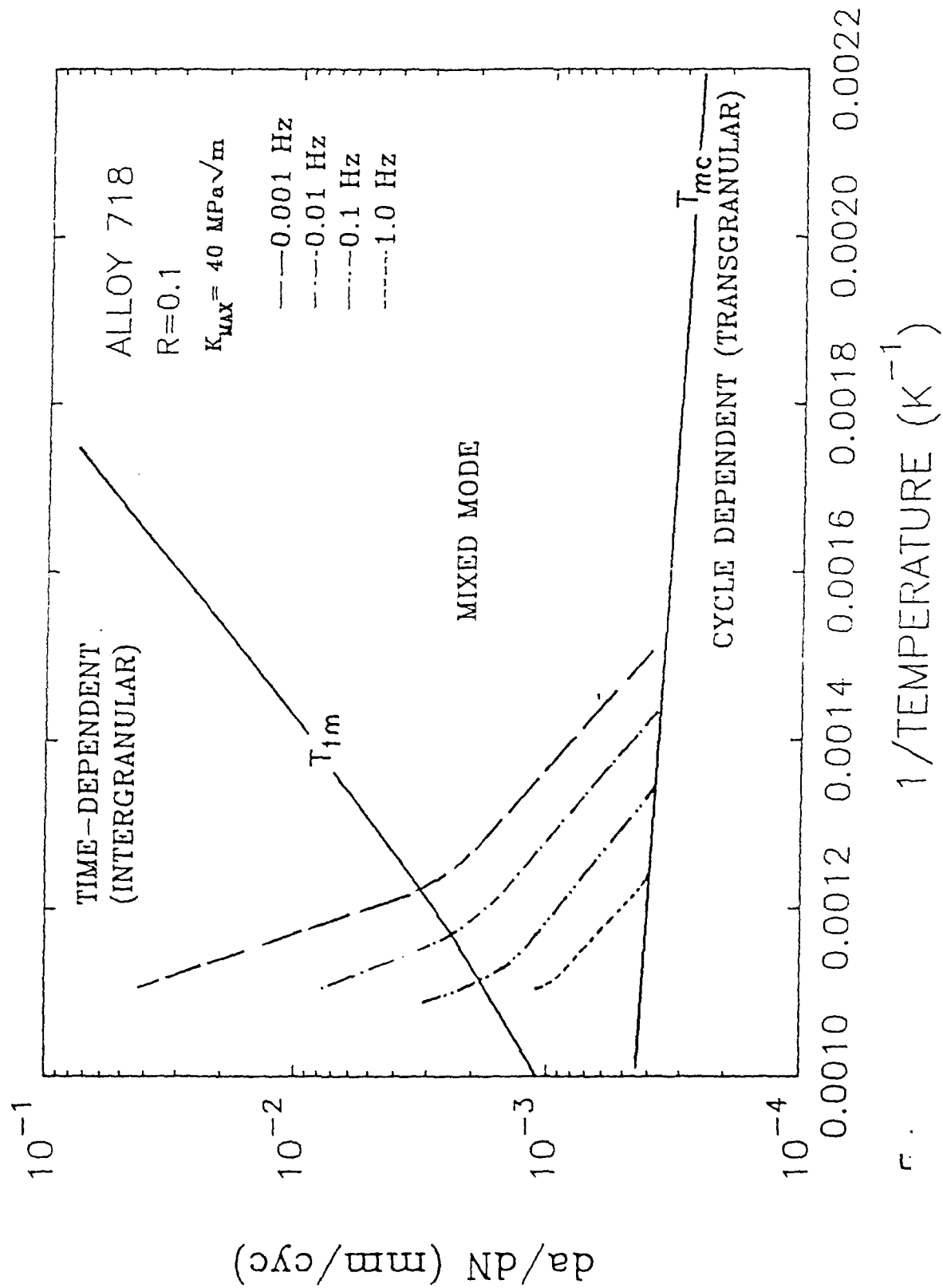
- Conditions", in Creep-Fatigue-Environment Interactions, ed. by R. M. Pelloux and N. S. Stoloff, The Metallurgical Society of AIME, Warrendale, PA, 1981, pp.86-111
- [22] P. Shahinian and K. Sadananda K, "Crack Growth Behavior under Creep-Fatigue Conditions in Alloy 718," In Creep Fatigue Interaction, MPC3, ASME, New York, NY, 1976, pp.365-390
 - [23] H. H. Smith and D. J. Michel, "Effect of Environment on Fatigue Crack Propagation Behavior of Alloy 718 at Elevated Temperatures", Metallurgical Transactions, Vol. 17A, 1986, pp.370-374
 - [24] P. Shahinian and K. Sadananda, "Effects of Stress Ratio and Hold-Time on Fatigue Crack Growth in Alloy 718", Journal of Engineering Materials and Technology, Vol. 101, 1979, pp.224-230
 - [25] T. Nicholas and T. Weerasooriya, "Hold-Time Effects in Elevated Temperature Fatigue Crack Propagation," In Fracture Mechanics, Seventeenth Symposium, ASTM STP 905. Ed. by J. H. Underwood, R. Chait, C. W. Smith, D. P. Wilhem, W. A. Andrews and J. C. Newman, American Society for Testing and Materials, Philadelphia, PA, 1986, pp.155-168
 - [26] J. P. Pedron and A. Pineau, "Effect of Hold Times on the Elevated Temperature Fatigue Crack Growth Behavior of Inconel 718 Alloy," in Advances in Fracture Research, Vol. 5, 1981, pp.2385-2392
 - [27] A. Diboine and A. Pineau, "Creep Crack Initiation and Growth in Inconel 718 at 650°C," Fatigue and Fracture of Engineering Materials and Structure, Vol. 10, 1987, pp.141-151
 - [28] K. Sadananda and P. Shahinian, "Effects of Environment on High Temperature Crack Growth Behavior of Several Nickel-Base Alloys", In Corrosion of Nickel-Base Alloys, ed. by R. C. Scarberry, ASM Publication, Cincinnati, Ohio, 1985, pp.101-115
 - [29] R. H. VanStone, O. C. Gooden and D. D. Krueger, "Advanced Cumulative Damage Modeling", AFWAL-TR-88-4146, Wright-Patterson AFB, OH, 1988.
 - [30] K. Sadananda and P. Shahinian, "Crack Growth Behavior in Alloy 718 at 425°C", Journal of Engineering Materials and Technology, Vol. 100, 1978, pp.381-387
 - [31] H. Ghonem and D. Zheng, "Characterization of Environment-Dependent Fatigue

Crack Growth in Alloy 718 at 650°C", in Superalloy 718, 625 and Various Derivations, ed. by E. A. Loria, The Minerals, Metals & Materials Society, Warrendale, PA, 1991, pp.477-490

- [32] S. Venkataraman and T. Nicholas, "Mechanisms of Elevated Temperature Fatigue Crack Growth in Inconel 718 as a Function of Stress Ratio," In Effects of Load and Thermal Histories, ed. by P. K. Liaw and T. Nicholas, The Metallurgical Society, Inc., 1987, pp.81-99
- [33] A. Coles, R. E. Johnson and H. G. Popp, "Utility of Surface-Flawed Tensile Bars in Cyclic Life Studies", Journal of Engineering Materials and Technology, **Vol. 98**, 1976, pp.305-315
- [34] K. Sadananda and P. Shahinian, "Elastic-Plastic Fracture Mechanics for High Temperature Fatigue Crack Growth", in Fracture Mechanics: Twelfth Conference, ASTM STP 700, American Society for Testing and Materials, Philadelphia, PA, 1980, pp.152-163
- [35] T. Nicholas and N. E. Ashbaugh, Fracture Mechanics: Nineteen Symposium, ASTM STP 969, ed. by T. A. Cruse, American Society for Testing and Materials, Philadelphia, PA, 1987, pp.800-817
- [36] P. Shahinian and K. Sadananda, "Effects of Stress Ratio and Hold-Time on Fatigue Crack Growth in Alloy 718", Journal of Engineering Materials & Technology, **Vol. 101**, 1979, pp.224-230
- [37] S. Venkataraman, T. Nicholas and N.E. Ashbaugh, "Micromechanisms of Major/Minor Cycle Fatigue Crack Growth in Inconel 718", in Fractography of Modern Engineering Materials: Composites and Metals, ASTM STP 948, ed. by J. E. Masters and J. J. Au, American Society for Testing and Materials, Philadelphia, PA, 1987, pp. 383-399.
- [38] T. Weerasooriya and T. Nicholas, "Overload Effects in Sustained Load Crack Growth In Inconel 718", in Fracture Mechanics: Eighteenth Symposium, ASTM STP 945, ed. by D. T. Read and R. P. Reed, American Society for Testing and Materials, Philadelphia, PA, 1987, pp.181-191.
- [39] T. Nicholas, G.K. Haritos, R.L. Hastie, Jr. and K. Harms, "The Effects of Overloads on Sustained-Load Crack Growth in a Nickel-Base Superalloy: Part I-Experiments, Part II-Analysis" Theoretical and Applied Fracture Mechanics, **Vol. 16**, 1991, pp.35-49.

FIGURE CAPTIONS

- Fig. 1 da/dN vs $1/T$ plot at $K_{Max} = 40 \text{ MPa}\sqrt{\text{m}}$ showing the change in micromechanism of crack growth with changes in frequency and temperature [1].
- Fig. 2 The effect of cyclic frequency on Alloy 718 tested under continuous cycling conditions in air at 538°C [3].
- Fig. 3 Cyclic wave shapes used in Ref [4].
- Fig. 4 da/dN vs ΔK for different frequencies with different loading and unloading rate [20].
- Fig. 5 Relationship between cycle time and da/dN for different K_{Max} values at 650°C .
- Fig. 6 Fatigue crack growth rate vs frequency under $K_{Max} = 30 \text{ MPa}\sqrt{\text{m}}$ and load ratios between 0.1 and 0.9. Sustained load crack growth data are also shown in solid line ($R = 1.0$) [32].
- Fig. 7 Three modes of fatigue crack growth behavior presented as a function of $(1-R)$ [1].
- Fig. 8 Comparison of analytical prediction and experimental data of da/dt versus R for different loading frequencies [35].



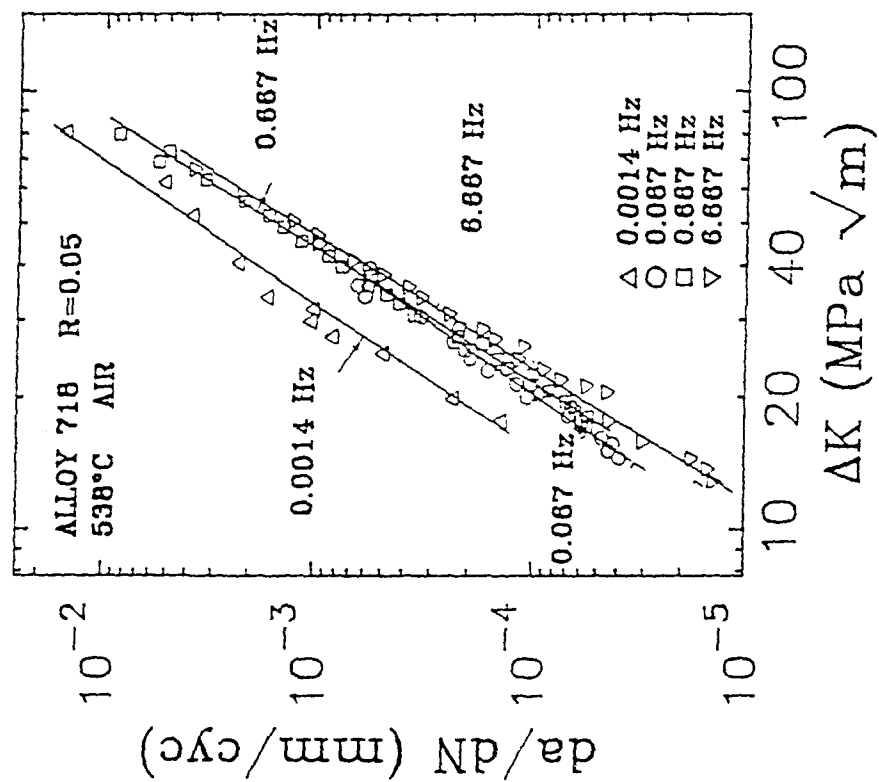


Fig 2

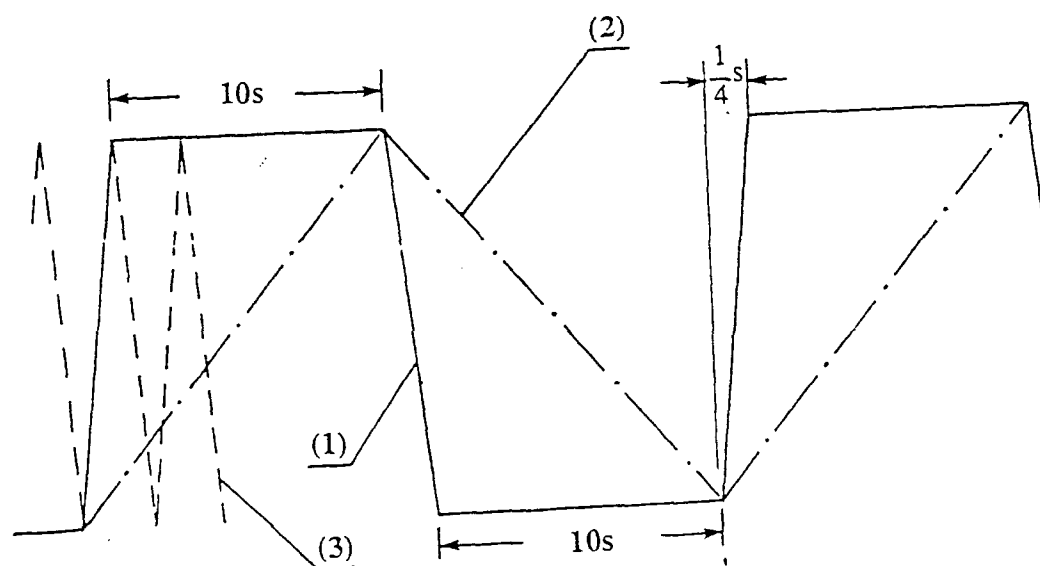
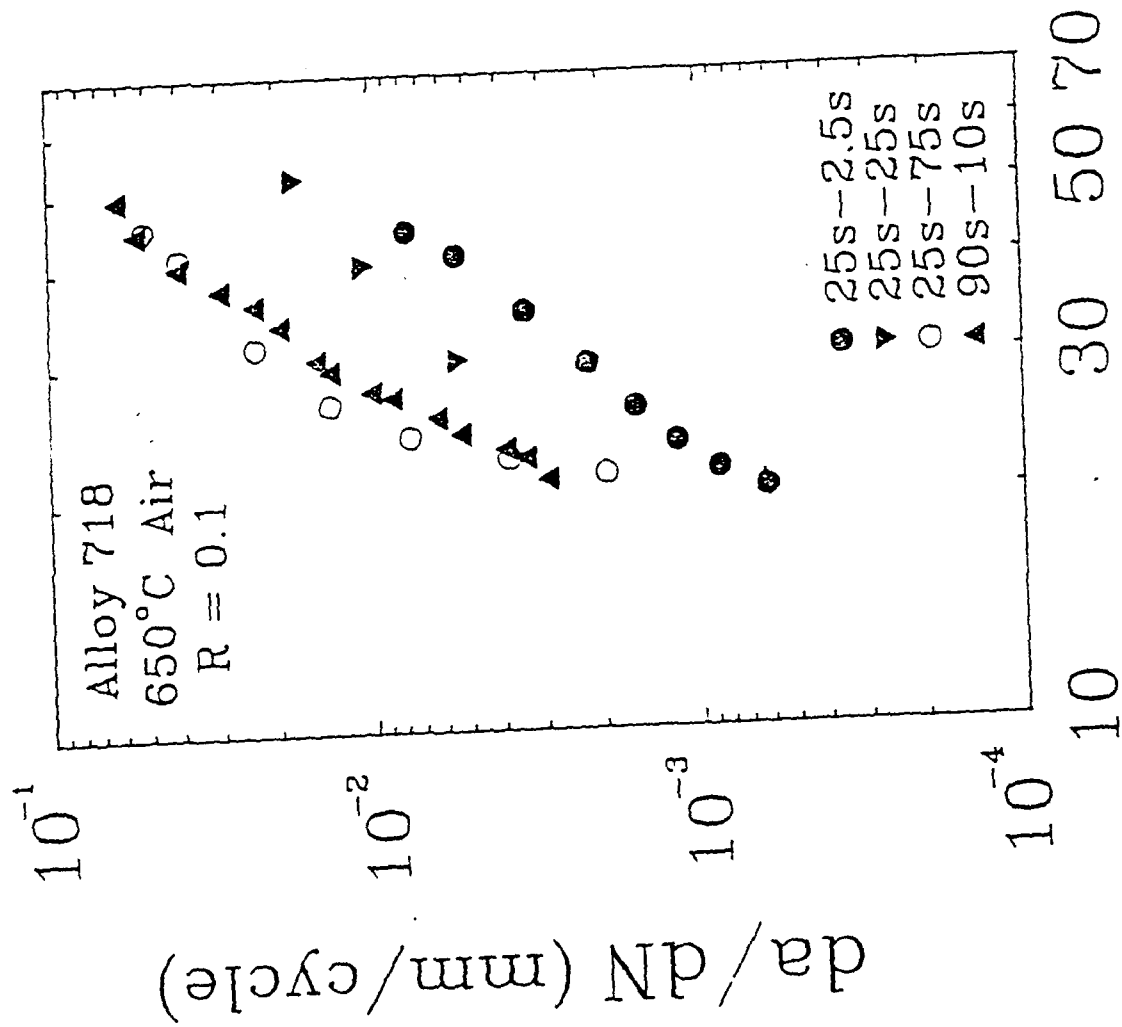


Fig 3



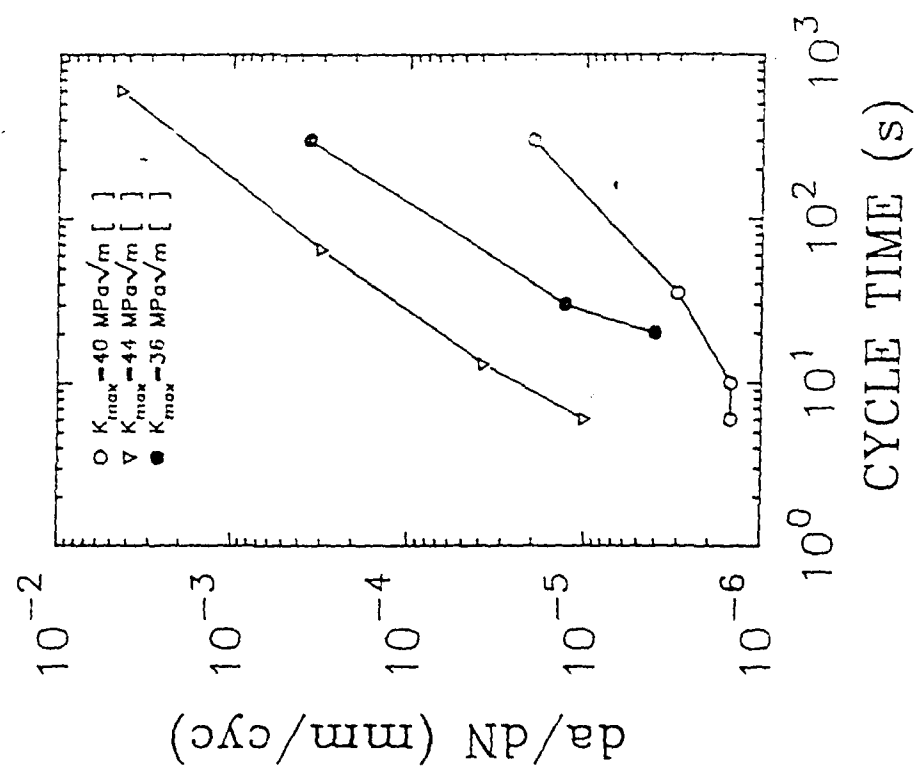


Fig 5

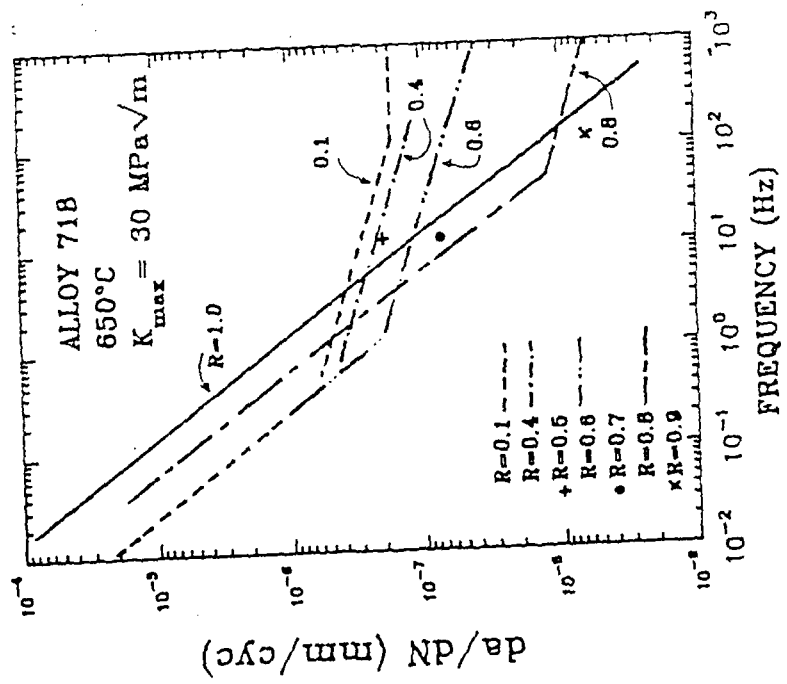
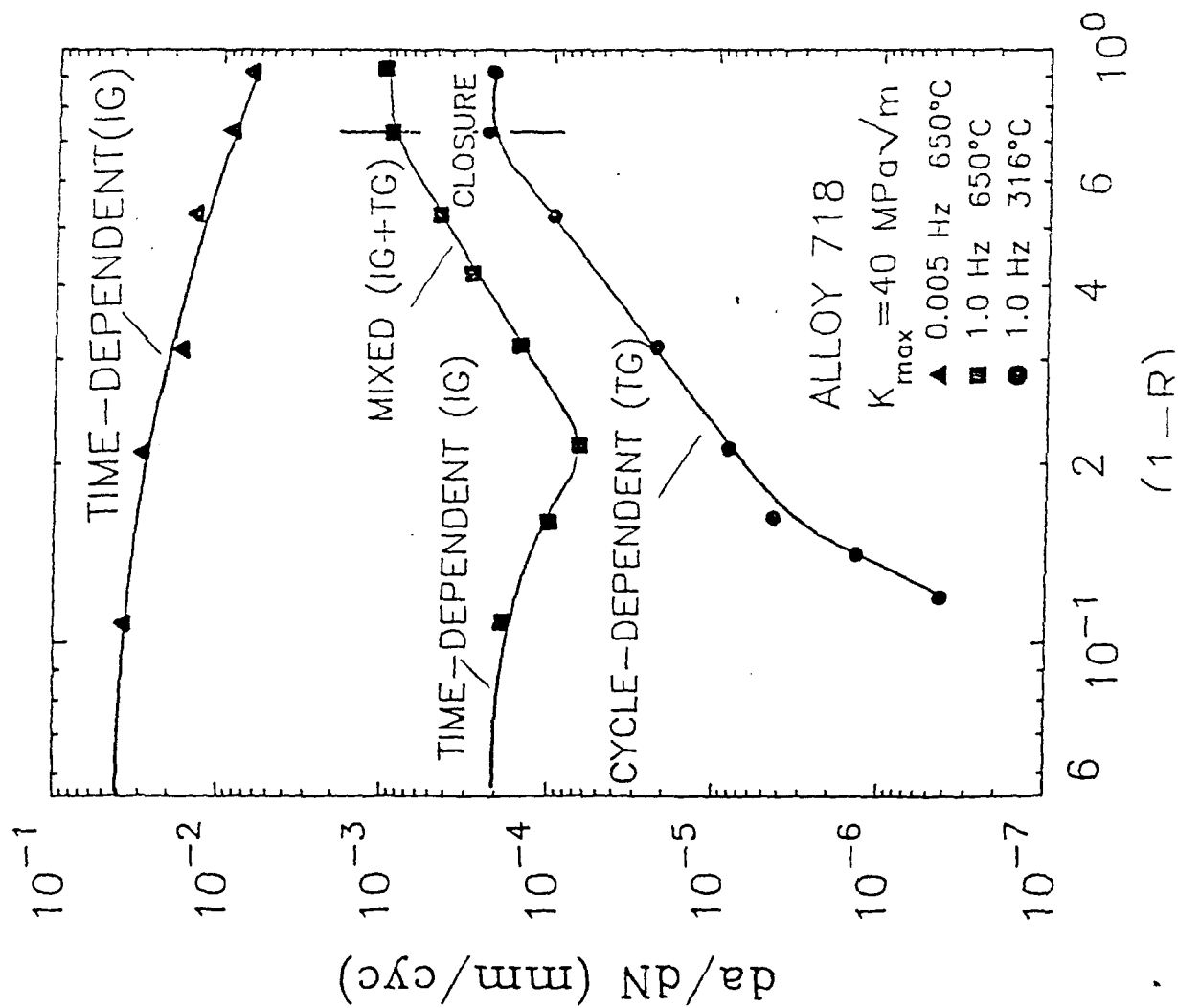


Fig 6



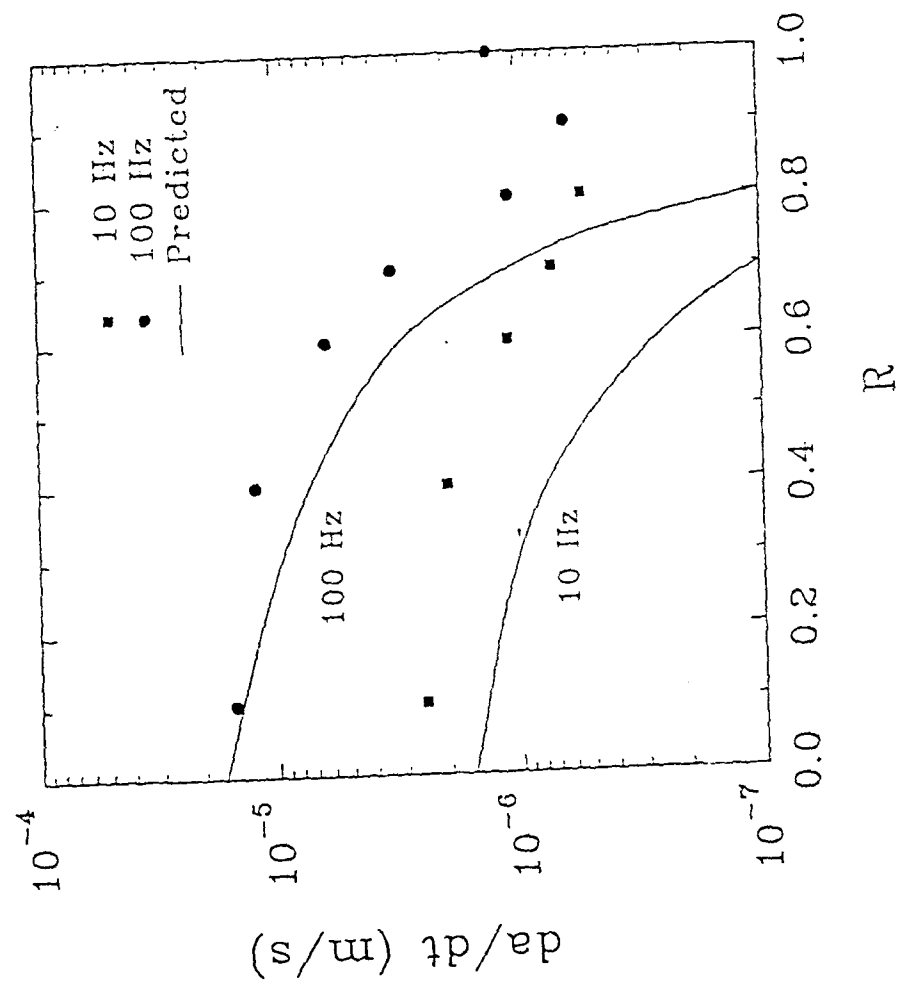


Fig 8

ELEVATED TEMPERATURE FATIGUE CRACK GROWTH IN ALLOY 718 - PART II: EFFECTS OF ENVIRONMENTAL AND MATERIAL VARIABLES

H. Ghonem⁺, T. Nicholas⁺⁺ and A. Pineau⁺⁺⁺

**+ Mechanics of Solids Laboratory, Department of Mechanical Engineering and
Applied Mechanics, University of Rhode Island, Kingston, RI 02881, U.S.A.**

++ Wright Laboratory, Materials Directorate, Wright-Patterson Air Force Base, Ohio 45433, U.S.A.

+++ Centre des Materiaux, Ecole des Mines de Paris, 91000 Evry, France

Abstract: Observations concerning effects of environmental, and material variables on the crack growth process in Alloy 718 are reviewed and analyzed on the basis of the related deformation characteristics in the crack tip region. The environmental aspects have been discussed in relation to frequency, hold time and crack tip oxidation and oxidation shielding mechanisms. the review of the role of material variables has focused on the effects of chemical composition and microstructure parameters including precipitate size and morphology as well as grain size and morphology. These analyses have suggested that the governing mechanism of the crack tip response is the degree of homogeneity of plastic deformation and associated slip density. For conditions promoting homogeneous plastic deformation with a high degree of slip density the environmental damage contribution is shown to be limited, thus permitting the dominance of the cyclic damage effects which is characterized by a transgranular crack growth mode and lower crack growth rate. Under conditions leading to inhomogeneous

plastic deformation and lower slip density the crack tip damage is described in terms of grain boundary oxidation and related intergranular fracture mode. On the basis of the view that the crack growth damage mechanism in Alloy 718 ranges from fully cycle-dependent to fully environment -dependent solely depending on the slip character in the crack tip region, conflicting experimental observations under different operating conditions are examined and a sensitizing approach to increase the alloy resistance to environmental effect is suggested.

INTRODUCTION

Effects of different loading parameters on the fatigue crack growth behaviour of Alloy 718 have been analyzed by the authors in terms of the corresponding crack tip damage mechanisms [1]. These mechanisms were classified as ranging from purely cyclic-dependent to purely time-dependent depending on the nature of plastic deformation and associated slip line density taking place in the crack tip zone. This paper focuses on the latter damage process where an attempt will be made to show that the governing parameters of this damage process are solely dependent on environmental degradation due to oxidation effects. In the first part of the paper a link will be established between the role of environment, loading frequency and slip density. This will be followed by detailing a crack tip oxidation mechanism on the basis of a selective oxide formation process. Results of tests conducted in vacuum or inert environment or under controlled

partial pressure of oxygen are used to confirm the interpretation of the underlying mechanisms. This suggested oxidation mechanism will then be used in order to propose a concept aiming at providing a crack tip oxidation shielding based on manipulating the density of the grain boundary/slip line intersections in the crack tip deformed zone. The second part of the paper deals with the relationship between several material variables and crack tip time dependent damage effects. These variables include chemical composition, precipitate size and morphology, grain size and grain boundary morphology.

TIME-DEPENDENT MECHANISMS

Time dependent effects on high temperature fatigue crack growth behaviour in high strength structural alloys are generally described in terms of creep and/or environmental degradation processes. The individual contribution of these two competing processes depends primarily on the strengthening characteristics of the alloy, load profile and temperature level. The effects due to mechanical loading variables have been summarized in the previous section. Several studies on Alloy 718 [2-7] have demonstrated that high temperature fatigue crack growth rates are decreased several order of magnitude when results of vacuum tests are compared with those due to low frequency loading in air test conditions, see Fig. 1, for example, where crack growth rates in vacuum are considerably lower than those observed in air under identical

loading conditions. Further, as noted in ref. [1], differences in growth rate due to changes in temperature, the lack of an effect of frequency at low temperature, and differences in growth rate due to frequency and hold time are all observed when comparing results in air with those in vacuum or inert environment. These observations, supported by the fact that the stress intensity range ΔK is used successfully to predict the elevated temperature crack growth rates in Alloy 718, give strong support to the conclusion that time-dependent damage in this alloy is due principally to environment related effects. Damage mechanisms associated with an environment degradation process in Alloy 718 are found to depend on the presence of oxygen at the crack tip [7-10]. Attempts to predict fatigue crack growth behaviour in this alloy have thus focused on assessing both the cyclic and the oxidation damage components. The relative importance of these two components to the total damage has been linked by several authors [2,3,7,11] to the loading frequency. In these, it is observed that the damage process ranges from cycle-dependent at high frequency levels to environment assisted at low frequency levels. At frequencies below that of the transitional frequency level the crack growth process is viewed to be fully environment dependent [3,12] or time dependent as noted in the previous section. In this latter process crack increment per cycle is assumed to be a direct measure of the intergranular depth of oxygen diffusion. One of the governing factors of this intergranular oxygen diffusion process, through the parabolic diffusion law, is the grain boundary diffusivity parameter, D_g , which depends on the stress and strain states along affected grain boundary paths [3,13]. Through this

parameter the influence of loading frequency and the associated deformation mode on the crack growth response can be interpreted qualitatively as follows. High frequency loading, which is generally characterized by high slip density and a homogeneous form of deformation, would result in both strain accommodation as well as stress relief along affected grain boundaries in the crack tip region. Hence variations of D_g tend to be minimal. In addition, the increase in slip density, generally, leads to an increase in the lateral volume diffusion across affected grain boundaries. These two combined effects would result in limited or no acceleration of intergranular oxygen diffusion rate. In this situation, the influence of crack tip oxidation is minimal and crack tip damage becomes generally dominated by cycle-dependent effects. On the other hand, low frequency loading accompanied by low slip density would promote grain boundary stress concentration resulting in an increase in the magnitude of D_g . This is magnified, particularly, if stress relief by grain boundary sliding is not permitted, as in the case of the highly creep resistant Alloy 718. Furthermore, the decrease in slip density would limit the grain boundary lateral volume diffusion process. Here, the expected increase in the grain boundary diffusivity and associated increase in depth of grain boundary oxidation would result in an increase in the crack tip damage due to environment effects.

The relationship between slip density and fracture mode characteristics, as described above, has been investigated using compact tension specimens made of Alloy 718 with large grain size (50-120 μm) tested at 650°C in air. In this work, fatigue

fracture mode as well as slip line density were compared for loading frequency of 30 Hz versus that of 0.05 Hz which includes 300 seconds hold time at maximum load level. Slip line traces at and below the fracture surface of the test specimens were obtained using the slip lines decoration technique described in [14]. These traces for different ΔK levels in both test conditions are shown in Figs. 2. In Fig. 2(A), which corresponds to a fully transgranular fracture mode, the degree of homogeneous deformation is evident by the high slip line density and the confinement of the reversed plastic zone to a narrow band near the fracture surface. This could be compared with Fig. 2(B)-b which corresponds to a fully intergranular fracture and displays a lower slip line density as well as larger plastic zone size. One should also observe that in the three intergranular locations in Fig. 2(B), the degree of slip homogeneity, measured as the inverse of the slip line interspacing, increases as ΔK increases.

On the basis of this argument the crack growth response of Alloy 718 with respect to loading frequency, f , is divided into three distinctive types, see Fig. 3. The first type is associated with high frequency loading in which the deformation mode is governed by a high degree of slip homogeneity and cracking proceeds primarily in a predominantly transgranular fracture mode. The value of the frequency, f , required to produce this type of cyclic-dependent response, decreases as the magnitude of ΔK increases. As loading rate decreases, the degree of slip homogeneity in the crack tip zone is lowered, resulting in a relative increase of the intergranular oxygen diffusion. Under this condition, the crack tip damage becomes a combination of oxidation and

cycle-dependent components. The degree of contribution of each of these components depends on both the frequency and ΔK values. For the same frequency, as ΔK increases the contribution of the cycle-dependent damage also increases, since increasing ΔK leads to an increase in the degree of slip homogeneity, see Fig. 2(A). The increase in the cycle-dependent damage is measured by the increase in percentage of the transgranular features along the fracture surface. For the same ΔK value, however, the influence of the time-dependent damage increases as frequency decreases. The third type of response mentioned above occurs for loading frequencies below a transitional level, f_c , where the crack tip damage becomes mainly an environment-dependent process in which crack growth is largely intergranular. The existence of this latter type has been the focus of studies carried out in [3,14,15]. In this work, attempts were made to measure the crack growth in compact tension specimens of Alloy 718 (grain size $120\mu\text{m}$) during a hold time period imposed at the ΔK_{\min} level of a loading cycle in which the loading frequency of the cyclic part is below f_c . Care was taken in these experiments so that ΔK_{\min} does not exceed the threshold level of this material during the entire duration of the growth process. Therefore, the crack growth increment during each of the hold time periods was viewed as being solely due to the crack tip oxidation effects.

Results of these studies in the form of the rate of oxygen depth of penetration X as function of both ΔK and t_h is shown in Fig. 4. This relationship between X and ΔK when integrated over the oxidation time of the loading cycle would yield an environment dependent crack growth rate equation which could then be tested by tested by

comparing its predictive results with those experimentally obtained for three different frequencies; 0.01, 0.02 and 0.05 Hz all of which are below f_c for the Alloy 718 used in this study. Results of this application are shown in Fig. 5. It is observed that a reasonable agreement exists in the full range of ΔK between the values and trends of the three experimentally obtained data sets and those theoretically predicted. This result is taken in support of the notion that the growth process corresponding to frequencies below f_c is fully environment-dependent process.

The notion that the extent of the time-dependent process can be related to the degree of inhomogeneity of plastic deformation and decrease in slip density at the crack tip can be used to explain some of the observations of crack growth behaviour described in the previous section. In particular, the effects of loading frequency as well as the wave shape studied where a longer cycle period produces a higher growth rate can be explained by production of inhomogeneity in plastic deformation under low rate loading cycles. Once this inhomogeneity is produced during a slow loading cycle, it will effect the growth rate upon subsequent cycles whether these are unloading cycles or hold times at minimum or maximum load. In fact, the apparently conflicting results of hold time effects at minimum load described in the previous section can be interpreted in terms of the deformation mechanism.

CRACK TIP OXIDATION MECHANISMS

Extensive efforts have been made in the last two decades to understand the crack tip oxidation mechanisms in Alloy 718 in order to provide correlations between these mechanisms and both material and loading parameters. When not considering simple adsorption of oxygen at the crack tip, oxidation mechanisms could be identified, in general, in terms of oxygen short and long range diffusion processes. In the short range diffusion, oxygen forms an oxide layer at the crack tip with a depth that depends on many operating and materials parameters. The formation of this layer, under the restricted concave crack tip geometry, results in high stresses that could easily be transmitted to the substrate. The important aspect of this oxidation mechanism, however, is the possible formation of wedge-shaped oxide intrusions along the crack front. The rupture of these wedges at grain boundary intersections, could result in an accelerated, intergranular crack-growth rate, see Bricknell and Woodford [16], McMahon and Coffin [17], Woodford and Coffin [18] and McMahon [19]. In the long range diffusion oxygen penetrates the crack-tip material along rapid diffusion paths, such as, slip planes and grain boundaries. The internal oxidation process taking place along these path could occur in the form of internal oxide sites, cavity formations, and/or solute segregation. As pointed out by Woodford and Bricknell [20], it is also possible for oxygen to take part in chemical reactions releasing known embrittlement agents onto a grain boundary. Each, or all, of these may be operative in any particular alloy under a given set of conditions. These processes, in particular, along grain boundaries result in the inhibition of the sliding and migration of these boundaries and

thus reduce their ability to relieve local stresses built up during deformation.

While it is recognized that the oxidation mechanisms associated with the short and long range diffusion are not completely separated, experimental observations indicate that, for Alloy 718, at an intermediate temperature range and at a low level of loading frequency, short-range oxygen diffusion contributes primarily to the occurrence of an intergranular fracture mode. The influence of the oxygen partial pressure on this oxidation mechanism and its role in crack tip oxide formation will be discussed in the following two subsections. *a- Oxygen Partial Pressure*

The damage process associated with short-range oxygen diffusion at the crack tip has been studied by several authors, see for example [21-23]. One of the important factors to be considered in this process is oxygen partial pressure, PO_2 , at the crack tip material. The first clear demonstration of the effect of PO_2 was exhibited in the work of Smith et al [24] on 316 stainless steel in which transition to higher crack growth rates accompanied the increase in PO_2 . Similar observations were made by, among others, Michel and Smith [25], Stegmann and Shahinian [26] and Smith and Shahinian [27]. This transition was interpreted by Achter et al [28] in terms of the impingement rate of oxygen molecules on successive rows of freshly exposed metal atoms at the crack tip. The impingement concepts, see Ericsson [29], face the difficulty of providing an explanation for the severity of damage that a monolayer of oxide could cause at the crack tip. These concepts furthermore, cannot support the experimental observations made, for example, by Smith and Shahinian [27] who reported that the effect of oxygen

partial pressure on fatigue life of silver at 350°C is small compared to the effect at 20 and 150°C. An increase in the initial rate of oxygen adsorption has, however, been observed with the increase of temperature in the 20-350°C range. Another interpretation of the influence of PO_2 on crack growth is related to the ability of oxygen at different pressures to control the preferential formation of one given species of oxides that may either shield or contribute to the crack tip damage process through the passivation or the enhancement of the oxidation process, respectively. It is known, for example, that oxidation of chromium as an alloying element produces a protective layer of Cr_2O_3 . If chromium diffusion in the alloy is too low to sustain the supply of chromium at the scale/metal interface, less noble elements of the alloy, e.g. iron, will be oxidized at the scale/metal interface. This will result in an increased reaction rate [28]. Andrieu [30] has used Auger Spectrometer analysis to examine the influence of PO_2 on the formation of selective oxides which were formed on deformed and non-deformed free surfaces of specimens of Alloy 718 that have large grain size (100-200 μ m) as a function of the oxygen partial pressure. By making an analogy between the steps of the oxidation process on a deformed free surface and those along a grain boundary oxidation path, a qualitative view of the grain boundary oxidation mechanism has been proposed. A schematic of a two-stage crack tip oxidation mechanism is presented in Fig. 6. At the start of the oxidation process, when atmospheric oxygen partial pressure is available for the crack-tip material, the first oxides to form will consist of selective oxides of FeO and NiO and their spinels. These porous oxides, which cannot serve as

an oxygen diffusion barrier, would permit the continuous oxidation reaction at the base grain boundary material. This process, during a time period equal to or less than the oxide passivation time, t_p , leads to a decrease in the oxygen partial-pressure at the oxide/metal interface, thus providing the reaction kinetics required for the formation of a denser sub-layer of Cr_2O_3 oxide. This dense layer, which is thermodynamically stable at high temperature, is considered protective in the sense that it limits oxygen diffusion to the grain boundary material, thus resulting in a decrease in the oxidation reaction rate as time elapses. When the build-up of the Cr_2O_3 layer is fully completed no further oxidation of the base material would take place and a condition of oxidation passivation is said to occur. This two-stage crack-tip oxidation mechanism was validated experimentally in the work Ghonem et al [31] on fine grain size ($20\text{-}50\mu\text{m}$) material of Alloy 718. They carried out crack growth measurement experiments on compact tension specimens during which the formation process of a continuous oxide layer was disturbed. This was achieved by the application of a loading spectrum including a minor cycle with high frequency imposed on hold time at minimum load. The crack growth rate corresponding to these conditions was higher than that observed when the continuous formation of the oxide layer was not disturbed. This result, detailed in Ref [31] and shown in Fig. 7, indicates that, by delaying the formation of Cr_2O_3 , the oxidation process continued, resulting in a high crack growth rate.

b- Crack Tip Oxidation Shielding

An important result of the two-stage oxidation mechanism is the conclusion that the rate of chromia (Cr_2O_3) build-up at the crack tip controls the depth of oxygen penetration along grain boundaries in the crack tip region. This build-up rate depends primarily on the chromium existing in the affected grain boundary material which is in part transported from the interior of the matrix via a mobile dislocation network. The grain boundary/slip line intersections can thus be considered nodes at which chromia build-up would be more rapid than in regions free of such intersections. If the saturated chromia layer is looked upon as a shield against further oxygen diffusion, then the higher the slip line density along a grain boundary fracture path, the lower the oxidation-assisted fatigue crack growth rate along such a path. The slip line density could be controlled by several methods, one of which is subjecting the test specimen to prior deformation; the higher the deformation is, the higher and more homogeneous the slip line density is. Therefore, on the basis of the above assumption, when subjecting two specimens having two different levels of pre-deformation conditioning to a loading frequency which promotes intergranular oxidation-assisted cracking, the specimen with the higher degree of pre-deformation should provide a crack growth rate lower than that in the specimen with the lower degree of pre-deformation. This oxidation notion was examined by comparing the crack growth rate in two specimens of alloy 718 at 650°C ; one with a prior 10% longitudinal deformation (thus higher slip line density) while the second is without predeformation. Results of this comparison which is detailed in Ref.[32] and shown in Fig. 8 indicate that the specimen with prior deformation has

exhibited lower crack growth rate.

The importance of these results lies in the possibility that high-temperature intergranular oxidation properties of high-strength alloys can be modified through cold working at room temperature or forging at relatively low temperature to enhance the slip homogeneity at the crack tip region and thus produce a built-in intrinsic mechanical resistance for high temperature fatigue crack growth.

MATERIAL VARIABLES

In this section, the role of material variables in influencing the crack tip oxidation and consequently the related time-dependent damage process will be discussed. The variables to be analyzed include chemical composition, precipitate size and morphology, grain size and grain boundary morphology.

ROLE OF CHEMICAL COMPOSITION

The FCGR of Ni base superalloys under creep-fatigue conditions is strongly dependent on the composition of the material [33]. Very minor compositional changes can significantly modify the elevated temperature grain boundary resistance. Floreen and Davidson [334, for example, observed that the creep crack growth resistance in Alloy 718 was noticeably reduced when the material contained small amounts of boron

(10ppm) and zirconium (60 ppm). This beneficial effect was observed in air and not in vacuum thus indicating, as mentioned before, the important role of environment. It was also recently shown [35] that in Alloy 718 the substitution of chromium for iron tends to decrease the FCGR at 538°C when the material is subjected to fatigue cycling with a superimposed hold time. While no interpretation was given to this behaviour, one could speculate that the result is due to the fact that increasing chromium concentration tends to promote the formation of the protective Cr_2O_3 oxide film which was shown, in the last section, to help retarded time-dependent crack growth. It is also worth mentioning the work of Xie [36] which showed that Mg addition raises noticeably high temperature tensile and stress rupture ductilities and increases smooth and notch stress rupture life. These modifications in mechanical properties were associated with changes in the fracture mode; Mg addition tends to improve the resistance to intergranular fracture. The basic role of Mg which is believed to be segregated along the grain boundaries is not yet fully understood. It is however, suggested that the addition of this element produces a more globular and discrete shape of the δ phase precipitated along the grain boundaries. This change is believed to be beneficial in terms of improving the resistance to oxidation and, hence, to time-dependent crack growth. It can also be assumed that magnesium segregation along the grain boundaries plays a more fundamental role in modifying the mechanisms of intergranular oxidation, i.e. in changing the nature of the oxide film and thus in controlling the oxygen penetration rate along the grain boundaries in the crack tip zone. This assumption which is speculative,

at this time, deserves further investigation.

MICROSTRUCTURE EFFECTS

The details of the Alloy 718 microstructure can have a significant effect on influencing the oxidation assisted or time-dependent crack growth behaviour. To illustrate this aspect, two metallurgical factors are examined here; the precipitate size and morphology, and the grain size and grain boundary morphology.

a- Effect of precipitate size and precipitate morphology

The precipitate hardening heat treatment, see Table 1, can significantly influence the elevated temperature grain boundary cracking resistance. Wilson [37], almost 25 years ago, showed that the creep cracking resistance of Alloy 718 was significantly improved by a modification in the conventional heat treatment which produced larger precipitates. Sadananda and Shahinian [38] observed that the prolonged aging process increases the tensile ductility of the alloy by nearly fifty percent. This increased ductility was taken as a cause for the crack tip blunting which indirectly resulted in the decrease of the material sensitivity to environmental effects [39]. Floreen and Kane [40] have also observed that an overaging treatment (732°C/48h) reduces the crack growth rates at low frequencies when the material is tested in air environment, see Fig. 9. This observation has been confirmed recently in the work of Zheng and Ghonem [41]. The primary

influence of overaging is to homogenize slip distribution within the grains which is favorable for the grain boundary resistance, as discussed in the previous section. Smith and Michel [42] suggested that the improvement in crack growth resistance produced by the modified heat treatment (higher solutioning temperature and longer aging time) is likely to be a result of the alteration of dislocation interactions with γ'' particles and grain boundaries. Comparison of the slip line appearance for the conventional and modified heat treatments at 427°C in vacuum revealed that the modified heat treatment produced a microstructural condition conducive to homogeneous deformation which has been found by Fournier and Pineau [43] to result in significant decrease in crack growth rate. Another method which can be used to control the slip homogeneity in Alloy 718 is based on slight modification in the chemical composition (Ti, Al, and Nb) and in heat treatment. It was shown that these modifications give rise to associated growth of γ' and γ'' precipitates, and, in particular, to the shaped γ' particles covered by γ'' platelet on their six faces [44]. This particular morphology has proved to be extremely stable after long exposure at elevated temperature.

The fact that overaging reduces the FCGR can be considered a beneficial aspect in material subjected to long exposure. Alloy 718 is relatively stable at 650°C as indicated in the work of Brooks and Bridges [45]. Long time exposure, however, generates number of transgranular and intergranular microstructural modifications [46]. Recent study by Radavich [47] showed that the γ'' coarsening rate obeys the classical Lifshitz-Slovozov-Wagner law, where the diameter of the disc-shaped particles increase

as $(\text{time})^{1/3}$, see Fig. 10. This figure shows that an overaging treatment applied at 750°C leads to significant increase in γ'' size.

b- Effect of grain size and grain boundary morphology

In air environment, microstructural parameters particularly grain size and grain boundary morphology can be changed to produce orders of magnitude changes in high temperature crack growth behaviour. Thamburaj et al [48] observed that high temperature fatigue crack growth rate was much faster in fine-grained structure than in coarse-grained structure for Alloy 718 at 650°C. Thus they deduced that more severe grain boundary oxidation can occur in relatively fine grained material due to the greater grain boundary area available along which rapid, stress assisted diffusion of oxygen can occur. The works of James [49], Smith and Michel [50], and Pedron and Pineau [51] also show that the coarse-grained structure improves crack growth resistance, and the necklace microstructure renders the highest fatigue crack growth resistance. Again, they attribute this grain size effect on crack growth rate to the larger grain boundary area exposed to oxygen penetration in the fine-grained structure compared with that in the coarse-grained structure.

Grain boundary morphology is another important microstructural factor that controls the high temperature crack growth behaviour. Thamburaj et al [48] have pointed out that an irregular grain boundary morphology developed by grain boundary α phase precipitates will enhance creep ductility and resistance to high temperature fatigue crack growth rate. Andrieu et al [52] observed that the presence of δ

precipitates along the grain boundaries leads to an improvement in creep crack growth resistance. Apart from the factor of irregular grain boundary morphology created by δ phase particles, he suggested that this beneficial influence of δ phase might be related to grain boundary oxidation behaviour either because of the intrinsic oxidation resistance of Ni_3Nb phase or because of the existence of oxygen traps formed along grain boundaries.

While the effects of grain size and grain boundary morphology are important, there have been a number of investigations [53-57] in which indirect evidence of an inverse relationship between matrix γ' and γ'' particle size and the sensitivity to environmental embrittlement has been demonstrated. When the matrix precipitate is very fine, dislocations cut the precipitate particles instead of bypassing them and are confined to move in coplanar arrays, causing planar pile-ups and consequently, intense stress concentrations at grain boundaries and other obstacles to their motion. If at the same time, the grain boundary cohesive strength has been weakened as a result of an oxidation effect, intergranular cracking would be promoted. Besides, it is also thought that in materials exhibiting predominantly planar slip character, oxygen diffusion into the material can occur quite rapidly along planes of intense deformation at elevated temperatures and be swept to the grain boundaries as a result of a solute-dislocation interaction [58]. In the presence of more homogeneous slip, the number of dislocations arriving at a grain boundary would be reduced and consequently, the stress concentrations and oxygen transport to the grain boundaries occurring due to a

dislocation "sweep-in" mechanism will be reduced as well. Examining thin foils prepared from regions immediately below fracture surfaces by means of TEM, Thamburaj et al [48] observed that planar deformation was predominant in the case of existing the finest γ'' particle size distributions, and the poor resistance of fatigue crack growth in this case is consistent with the mechanism discussed above.

CONCLUSION

The role of different environmental and material parameters on the crack growth performance and related mechanisms in Alloy 718 has been critically reviewed. In this, observations related to the sensitivity of this alloy to variations in grain size and morphology, precipitate size and oxygen partial pressure have been analyzed. Results of these analyses have demonstrated that the interactive influence of each of these operating parameters is governed by the degree of homogeneity of plastic deformation and associated slip density in the crack tip zone. Under combined loading and material conditions promoting homogeneous plastic deformation with a high degree of slip density the contribution of the time dependent damage is limited giving rise to the dominance of the cyclic damage effects. The corresponding crack growth mode is essentially transgranular with a lower crack growth rate. On the other hand, under conditions leading to inhomogeneous plastic deformation and lower slip density the

contribution of time-dependent damage to the intergranular crack growth acceleration is provided through the increased role of grain boundary oxidation and subsequent fracture. The oxidation mechanism of the affected grain boundary path has been described in terms of a two stage oxidation process which depends on the oxygen partial pressure at the crack tip and the grain boundary chromium content. On the basis of the view that the crack growth damage mechanism in Alloy 718 ranges from fully cyclic-dependent to fully environment-dependent depending solely on the slip character in the crack tip region, a sensitizing approach to increase the alloy resistance to environmental effect could be achieved by increasing the deformation homogeneity in the crack tip region through cold working or lower temperature forging.

Acknowledgement: This paper summarizes studies performed by the authors and their colleagues over number of years during which the work of H. Ghonem and T. Nicholas has been supported, independently, by the US Air Force Office of Scientific Research while the work of A. Pineau was supported by SNECMA. Support of the work of H. Ghonem was also provided by United Technologies.

REFERENCES

- [1] H. Ghonem, T. Nicholas and A. Pineau, "Elevated temperature fatigue crack growth in alloy 718 - Part II: Effects of environmental and material variables, this issue
- [2] T. Weerasooriya and S. Venkataraman S., "Frequency and Environment Effect on Crack Growth in Inconel 718," Effects of Load and Thermal Histories, ed. by P. K. Liaw and T. Nicholas, The Metallurgical Society of AIME, Warrendale, PA, 1987, pp.101-108
- [3] H. Ghonem and D. Zheng, "The Depth of Intergranular Oxygen Diffusion during Environment-Dependent Fatigue Crack Growth in Alloy 718", Materials Science and Engineering, A150, 1992, pp.151-160.
- [4] H. H. Smith and D. J. Michel, "Effect of Environment on Fatigue Crack Propagation Behavior of Alloy 718 at Elevated Temperatures", Metallurgical Transactions, Vol. 17A, 1986, pp.370-374
- [5] J. P. Pedron and A. Pineau, "Effect of Hold Times on the Elevated Temperature Fatigue Crack Growth Behavior of Inconel 718 Alloy," in Advances in Fracture Research, Vol. 5, 1981, pp.2385-2392
- [6] K. Sadananda and P. Shahinian, "Effects of Environment on High Temperature Crack Growth Behavior of Several Nickel-Base Alloys", In Corrosion of Nickel-Base Alloys, ed. by R. C. Scarberry, ASM Publication, Cincinnati, Ohio, 1985, pp.101-115
- [7] H. Ghonem and D. Zheng, "Characterization of Environment-Dependent Fatigue Crack Growth in Alloy 718 at 650°C", in Superalloy 718, 625 and Various Derivations, ed. by E. A. Loria, The Minerals, Metals & Materials Society, Warrendale, PA, 1991, pp.477-490
- [8] A. Saxena, "A Model for Predicting the Environment Enhanced Fatigue Crack Growth Behavior at High Temperature," in Thermal and Environmental Effects in Fatigue: Research-Design Interface, ed. by E. J. Carl, J. H. Stephen, Jr. and E. M. Michael, American Society of Mechanical Engineers, New York, NY, 1983, pp.171-184
- [9] G. R. Romanoski, S.D. Antolovich and R. M. Pelloux, "A Model for Life Predictions of Nickel-Base Superalloy in High Temperature Low Cycle Fatigue", in Low Cycle Fatigue, ASTM STP 942, ed. by H. D. Solomon, G. R. Halford and B. N. Leis, American Society for Testing and Materials, Philadelphia, PA, 1988, pp.456-469
- [10] E. Andrieu, R. Molins, H. Ghonem and A. Pineau, "Intergranular Crack Tip Oxidation Mechanism in a Nickel-Based Superalloy", Materials Science and

Engineering, 1991 (in press)

- [11] M. Clavel and A. Pineau, "Intergranular Fracture Associated with Heterogeneous Deformation Modes during Low Cycle Fatigue in a Ni-Base Superalloy", *Scripta Metallurgica*, **Vol. 16**, 1982, pp.361-364
- [12] A. Pineau, "High Temperature Fatigue: Creep-Fatigue-Oxidation Interactions in Relation to Microstructure", in *Subcritical Crack Growth due to Fatigue, Stress Corrosion and Creep*, ed. by L. H. Larsson, Elsevier Applied Science Publishers, London, U.K., 1984, pp.483-530
- [13] H. Ghonem and D. Zheng, "Oxidation-Assisted Fatigue Crack Growth Behavior in Alloy 718 Part I: Quantitative Modelling," *Fatigue and Fracture of Engineering Materials and Structure*, **Vol. 14**, 1991, pp.749-760
- [14] M. Clavel, D. Fournier and A. Pineau, "Plastic Zone Sizes in Fatigued Specimens of INCO 718", *Metallurgical Transactions*, **Vol. 6A**, 1975, pp.2305-2307
- [15] D. Zheng and H. Ghonem, "Effects of frequency interactions on crack growth behavior of Alloy 718", *Metallurgical Transactions*, 1992, *in press*.
- [16] R. H. Bricknell and D. A. Woodford, The embrittlement of nickel following high temperature air exposure, *Metall.Trans. 12A*, 1981a, pp. 425-433.
- [17] C. J. McMahon and L. F. Coffin, Mechanisms of damage and fracture in high-temperature low cycle fatigue of a cast nickel-based superalloy, *Metall. Trans. 1*, 1970, pp. 3443-3451.
- [18] L. F. Coffin, Fatigue at high temperature, ASTM STP 520, American Society of Testing Materials, Philadelphia, Pa., 1973, pp.5-34.
- [19] C. J. McMahon, Jr., On the mechanism of premature in-service failure of nickel-base superalloy gas turbine blades, *Mat. Sci. Eng. 13*, 1974, pp. 295-297.
- [20] D. A. Woodford and R. H. Bricknell, Environmental Embrittlement of High Temperature Alloy by Oxygen, in *Treatise on Materials Science and Technology*, Vol. 25, Editor ???, Academic Press, Inc. 1983, pp. 157-199.
- [21] R. P. Skelton and J. Bucklow, "Cyclic Oxidation and Crack Growth during High Strain Fatigue of Low Alloy Steel", *Metal Science*, **Vol. 12**, 1978, pp.64-70
- [22] H. Teranishi and A. J. McEvily, "Effect of Oxidation on Hold Time Fatigue Behavior of 2.25 Cr-1 Mo Steel", *Metallurgical Transactions*, **Vol. 10A**, 1979, pp.1806-1808

- [23] S. Floreen and R. Raj, "Environmental Effects in Nickel-Basc Alloys", in Flow and Fracture at Elevated Temperatures, ed. by R. Raj, American Society for Metals, Metals Park, Ohio, 1985, pp. 383-402
- [24] H. H. Smith, P. Shahinian and M. R. Achter, "Fatigue Crack Growth Rates in Types 316 Stainless Steel at Elevated Temperature as a Function of Oxygen Pressure, 2, Vol. 245, 1969, pp.947-953.
- [25] D. J. Michel and H. H. Smith, "Fatigue Crack Propagation in Neutron Irradiated Type 304 and Type 308 Stainless Steel Plate and Weld Materials", Journal of Nuclear Materials, Vol. 71, 1977, pp.173-177
- [26] R. L. Stegman, and P. Shahinian, "Effect of Temperature on the Fatigue of Nickel at Varying Oxygen Pressures", in Fatigue at High Temperature, ASTM STP 459, American Society for Testing and Materials, Philadelphia, PA, 1969, pp.42-58
- [27] H. H. Smith and P. Shahinian, "Environmental Effects on Fatigue Crack Growth Rates in Silver", Institute of Metals, Vol. 99, 1971, pp.243-247
- [28] M. R. Achter, G. J. Danek and H. H. Smith, "Effect on Fatigue of Gaseous Environments under Varying Temperature and Pressure", Transactions of American Institute Mine Engineers, Vol. 227, 1963, pp.1296-1301
- [29] T. Ericsson, "Review of Oxidation Effects on Cyclic Life at Elevated Temperature", Canadian Metallurgical Quarterly, Vol. 18, 1979, pp. 177-195
- [30] E. Andrieu, "Influence de L'environmnt sur la Propagation des Fissures dans und Superalliage Base Nickel: L'Inconel 718", Ph.D. Thesis, Ecole des Mines de Paris, 1987
- [31] H. Ghonem, D. Zheng, E. Andrieu and A. Pineau, "Experimental Observations and Quantitative Modelling of Oxidation-Assisted Crack Growth Behavior in Alloy 718 at 650°C", Annual report, AFOSR-89-0285, 1990
- [32] D. Zheng and H. Ghonem, "Influence of prestraining on low frequency crack growth rate in superalloys at elvated temperature", Material Science and Engineering, 1992, in press.
- [33] A. Pineau, "Intergranular Creep-Fatigue Crack Growth in Ni-Base Alloys", in Flow and Fracture at Elevated Temperature, ed. by R. Raj, ASM, 1985, pp.317-348
- [34] S. Floreen and J. M. Davidson, "Effects of B and Zr on the Creep and Fatigue Growth Behavior of a Ni-Base Superalloy", Metallurgical Transactions, Vol. 14A, 1983, pp.895-901

- [35] K. M. Chang, "Metallurgical Control of Fatigue Crack Propagation in Alloy 718", in Superalloys 718, 625 and Various Derivations, ed. by E. A. Loria, The Minerals, Metals & Materials Society, Warrendale, PA, 1991, pp.447-456
- [36] X. Xie, Z. Xu, B. Qu, G. Chen and J. F. Radavich, "The role of Mg on Structure and Mechanical Properties of Alloy 718", in Superalloys 1988, ed. by S. Reichman et al, The Metallurgical Society of AIME, Warrendale, PA, 1988, pp.635-642
- [37] D. J. Wilson, "Relationship of Mechanical Characteristics and Microstructural Features to the Time-Dependent Edge-Notch Sensitivity of Inconel 718 Sheet", Journal of Engineering Materials and Technology, Vol. 113, 1973, pp.112-123
- [38] K. Sadananda and P. Shahinian, "High Temperature Time-Dependent Crack Growth", Micro and Macro Mechanics of Crack Growth, ed. by K. Sadananda, B. B. Rath and D. J. Michel, The Metallurgical Society of AIME, Warrendale, PA, 1981, pp.119-130
- [39] K. Sadananda and P. Shahinian, "Creep Crack Growth Behavior and Theoretical Modelling", Metal Science, Vol. 15, 1981, pp.425-432
- [40] S. Floreen and R. H. Kane, "An Investigation of the Creep-Fatigue-Environment Interaction in a Ni-Base Superalloys", Fatigue of Engineering Materials and Structures, Vol. 2, 1980, pp.401-412
- [41] D. Zheng and H. Ghonem, "Influence of Prolonged Thermal Exposure at 650°C on Intergranular Fatigue Crack Growth Behavior in Alloy 718", Metallurgical Transactions, 1992, in press
- [42] H. H. Smith and D. J. Michel, "Fatigue Crack Propagation and Deformation Mode in Alloy 718 at Elevated Temperatures", In Ductility and Toughness Considerations in Elevated Temperature Service, MPC-8, ed. by G. V. Smith, American Society of Mechanical Engineers, New York, 1978, pp.225-246
- [43] D. Fournier and A. Pineau, "Low Cycle Fatigue Behavior of Inconel 718 at 298K and 823K", Metallurgical Transactions, Vol. 8A, 1977, pp.1095-1105
- [44] R. Cozar and A. Pineau, "Morphology of γ' and γ Precipitates and Thermal Stability of Inconel 718 Type Alloys", Metallurgical Transactions, Vol. 4, 1973, pp.47-59
- [45] J. W. Brooks and P. J. Bridges, "Long Term Stability of Inconel Alloy 718 for Turbine Disc Applications", in High Temperature Alloys for Gas Turbines and Other Applications 1986, ed. by W. Betz, R. Brunetaud, D. Coutsouradis, H. Fischmeister, T. B. Gibbons, I. Kvernes, Y. Lindblom, J. B. Marriott and D. B. Meadowcroft, Reidel Publishing Company, Dordrecht, 1986, pp.1431-1440

- [46] R. Moline, E. Andrieu and A. Pineau, "Overaging, Deformation and Rupture Micromechanisms of Alloy 718", in Superalloys 718, 625 and Various Derivations, ed. by E. A. Loria, The Minerals, Metals & Materials Society, Warrendale, PA, 1991, pp.583-602
- [47] J. F. Radavich, "Long Time Stability of a Wrought Alloy 718 Disk", in Superalloy 718: Metallurgy and Applications, ed. by E. A. Loria, The Minerals, Metals & Materials Society, Warrendale, PA, 1989, pp.257-268
- [48] R. Thamburaj, T. Terada, A. K. Koul, W. Wallace and M. C. de Malherbe, "The Influence of Microstructure and Environment upon Elevated Temperature Crack Growth Rates in Inconel 718", in Proceedings of the International Conference on Creep, Tokyo, Japan, 1986, pp.275-282
- [49] L. A. James, "The Effect of Grain Size upon the Fatigue-Crack Propagation Behavior of Alloy 718 under Hold-Time Cycling at Elevated Temperature", Engineering Fracture Mechanics, Vol. 25, 1986, pp.305-314
- [50] H. H. Smith and D. J. Michel, "Effects of Thermal and Thermomechanical Treatments on the Mechanical Properties of Centrifugally Cast Alloy 718", Materials Science and Engineering, Vol. 102A, 1988, pp.161-168
- [51] J. P. Pedron and A. Pineau, "The Effect of Microstructure and Environment on the Crack Growth Behavior of Inconel 718 Alloy at 650°C under Fatigue, Creep and Combined Loading", Materials Science and Engineering, Vol. 56, 1982, pp.143-156
- [52] E. Andrieu, R. Cozar and A. Pineau, "Effect of Environment and Microstructure on the High Temperature Behavior of Alloy 718", Superalloys 718: Metallurgy & Applications, ed. by E. A. Loria, The Minerals, Metals & Materials Society, Warrendale, PA, 1989, pp.241-247
- [53] S. Floreen, "High Temperature Crack Growth Structure-Property Relationships in Nickel Base Superalloys", in Creep-Fatigue-Environment Interactions, ed. by R. M. Pelloux and N. S. Stoloff, The Metallurgical Society of AIME, Warrendale, PA, 1982, pp.112-128
- [54] R. Thamburaj, W. Wallace, T. L. Prakash and Y. N. Chari, "Influence of Processing Variables on Prior Particle Boundary Precipitation and Mechanical Behavior in PM Superalloy APK1", Powder Metallurgy, Vol. 27, No.3, 1984, pp.169-180
- [55] M. Clavel, C. Levaillant and A. Pineau, "Influence of Micromechanisms of Cyclic Deformation at Elevated Temperature on Fatigue Behavior", in Creep-Fatigue-Environment Interactions, ed. by R. M. Pelloux and N. S. Stoloff, The Metallurgical Society of AIME, Warrendale, PA, 1980, pp.24-45

- [56] S. D. Antolovich and N. Jayaraman, "Metallurgical Instabilities During the High Temperature Low Cycle Fatigue of Nickel-Base Superalloys", *Materials Science and Engineering*, Vol. 57, 1982, pp.L9-L12
- [57] R. B. Scarlin, "Some Effects of Microstructure and Environment on Fatigue Crack Propagation", in *Fatigue Mechanisms*, ASTM STP 675, ed. by J. T. Fong, American Society for Testing and Materials, Philadelphia, PA, 1979, pp.396-419
- [58] J. M. Davidson and J. K. Tien, "Environmental Effects on the Creep Behavior of a Nickel-Base Superalloy", *Metallurgical Transactions*, Vol. 12A, 1981, pp.865-876

Conventional Heat Treatment (CHT)	
Solutioning: (Annealing)	954°C for 1 hr then air cool or faster.
Precipitation Aging: to (Duplex Aging)	718.3°C for 8 hrs, furnace cool to 621.1°C at a rate not exceed 37.8°C/hr, hold at 621°C for 8 hrs and air cool to room temperature.
Modified Heat Treatment (MHT)	
Solutioning:	1093°C for 1 hr, furnace step cooled at 38°C/hr to below 538°C, He cooled to room temperature.
Precipitation Aging:	718.3°C for 4 hr step cooled at 37.8°C/hr to 621°C for 16 hr, then He cooled to room temperature.

Table 1 Heat Treatments of Alloy 718

FIGURES CAPTIONS

- Fig. 1 Comparison of fatigue crack growth rates in air and vacuum (frequency 0.05 Hz, temperature 650°C).
- Fig. 2(A) Slip line traces corresponding to high frequency loading at $\Delta K = 27 \text{ MPa}\sqrt{\text{m}}$.
- Fig. 2(B) Slip line traces corresponding to low frequency loading at different ΔK values a) $21 \text{ MPa}\sqrt{\text{m}}$, b) $27 \text{ MPa}\sqrt{\text{m}}$, c) $38 \text{ MPa}\sqrt{\text{m}}$.
- Fig. 3 Effect of frequency on fatigue crack growth rate of Alloy 718 at $R = 0.1$ for different temperatures, grain sizes ($S \approx 20\text{-}50 \mu\text{m}$, $L \approx 150 \mu\text{m}$) and ΔK levels.
- Fig. 4 Intergranular diffusion rate of oxygen, X , vs hold time, t_h , imposed at minimum load for different ΔK levels.
- Fig. 5 da/dN vs ΔK for both experimentally and theoretically predicted results.
- Fig. 6 Suggested mechanism of two stages grain boundary oxidation mechanism (30).
- Fig. 7 Effect of hold time at minimum load as well as effect of minor cycle superimposed on hold time at minimum load.
- Fig. 8 Effect of predeformation on crack growth rate in alloy 718 at 650°C.
- Fig. 9 Comparison of fatigue crack growth rates with and without prolonged thermal exposure.
- Fig. 10 Variation of the length of isolated γ'' precipitates during overaging.

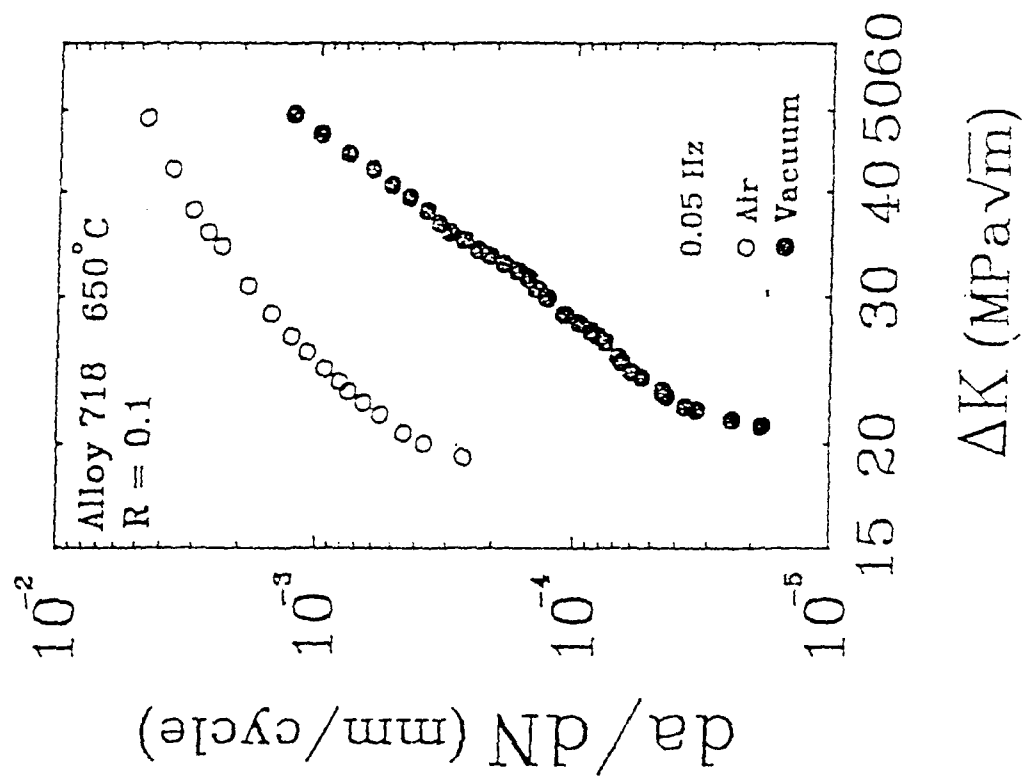


Fig 9

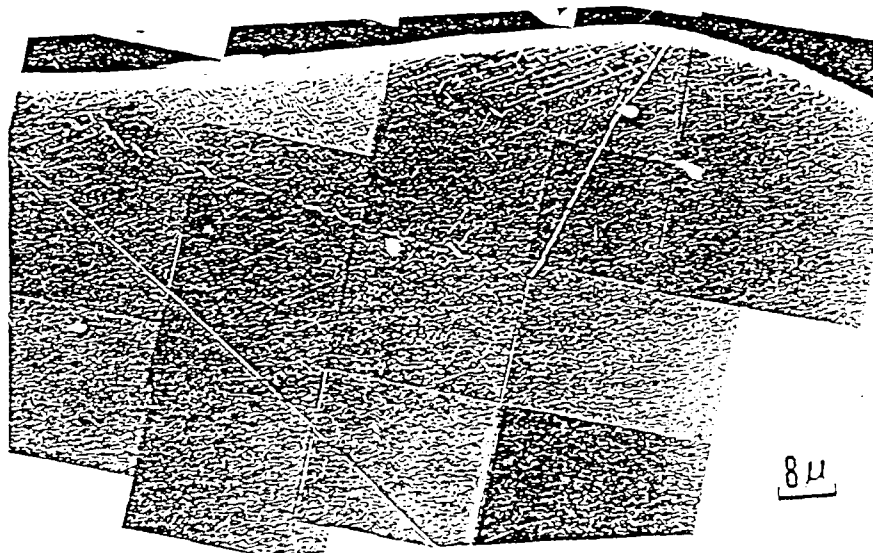
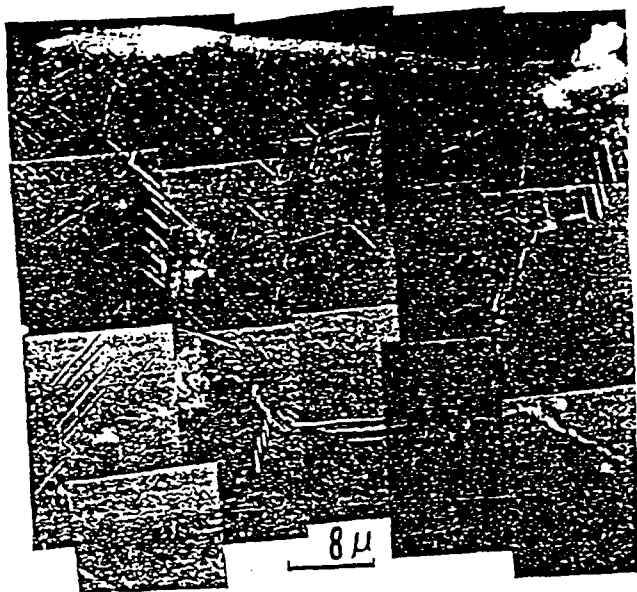
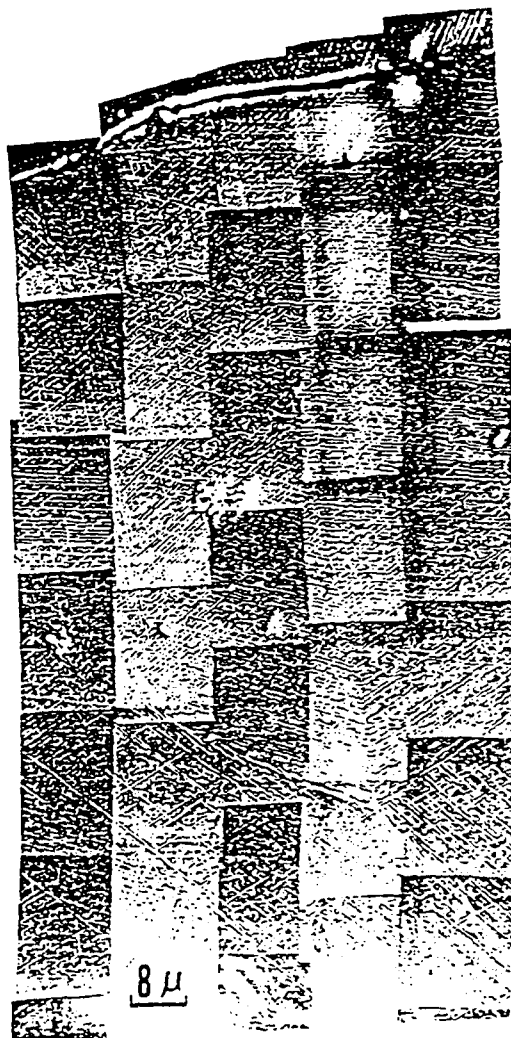


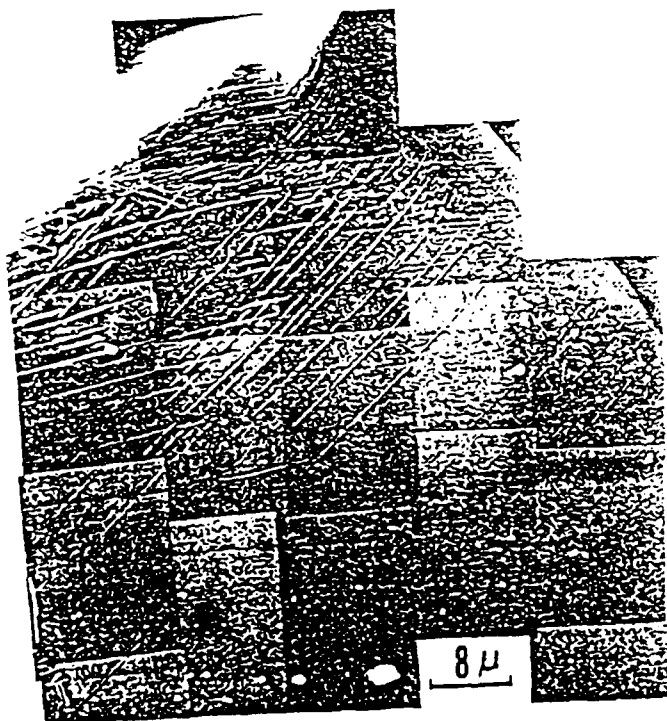
Fig 2(A)



A)



C)



B)

Fig 2(8)

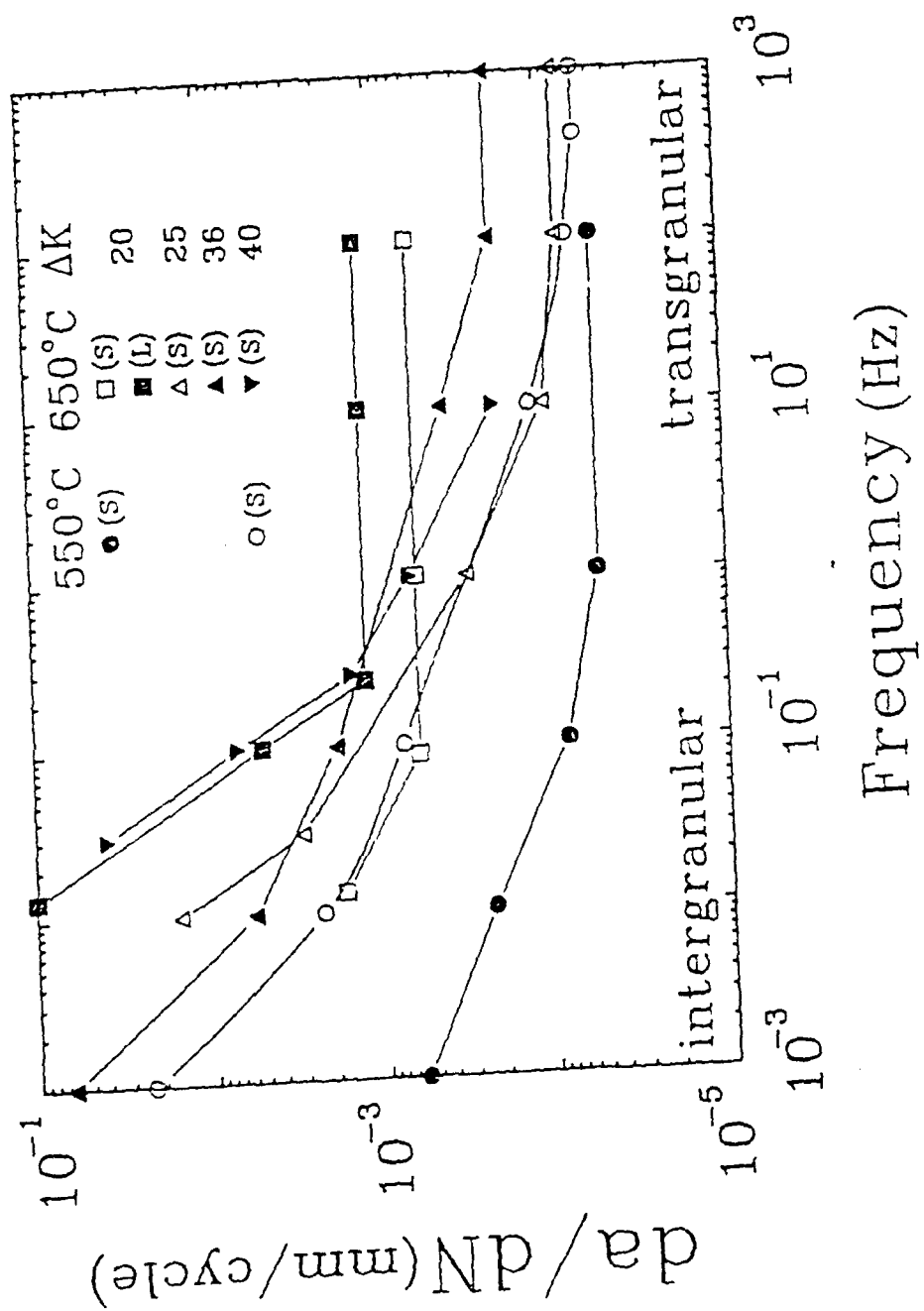


Fig. 2

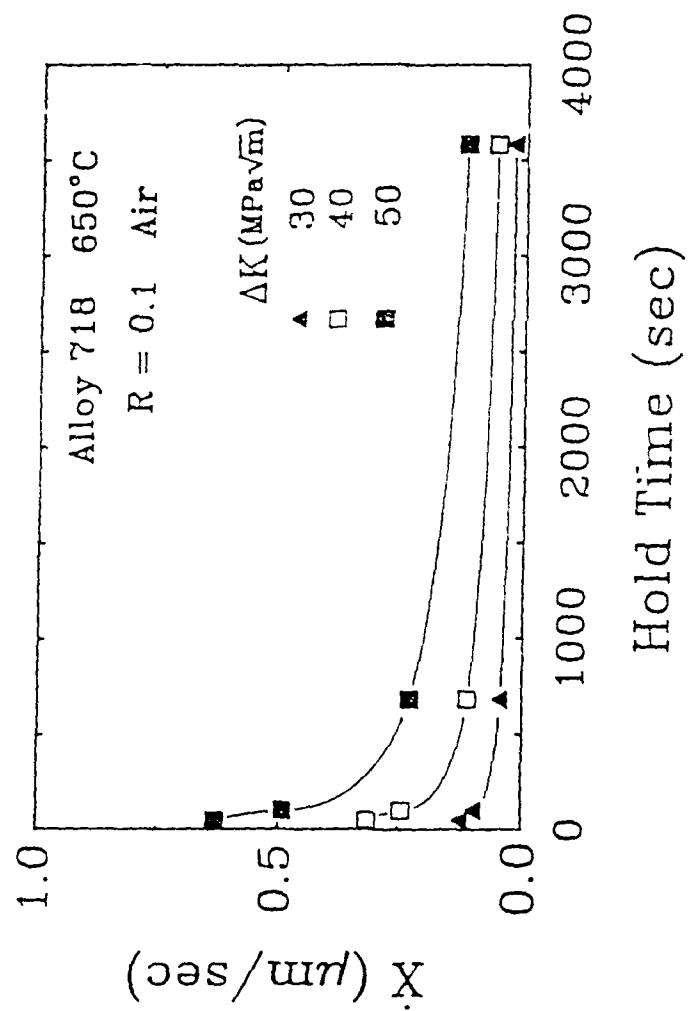


Fig (A)

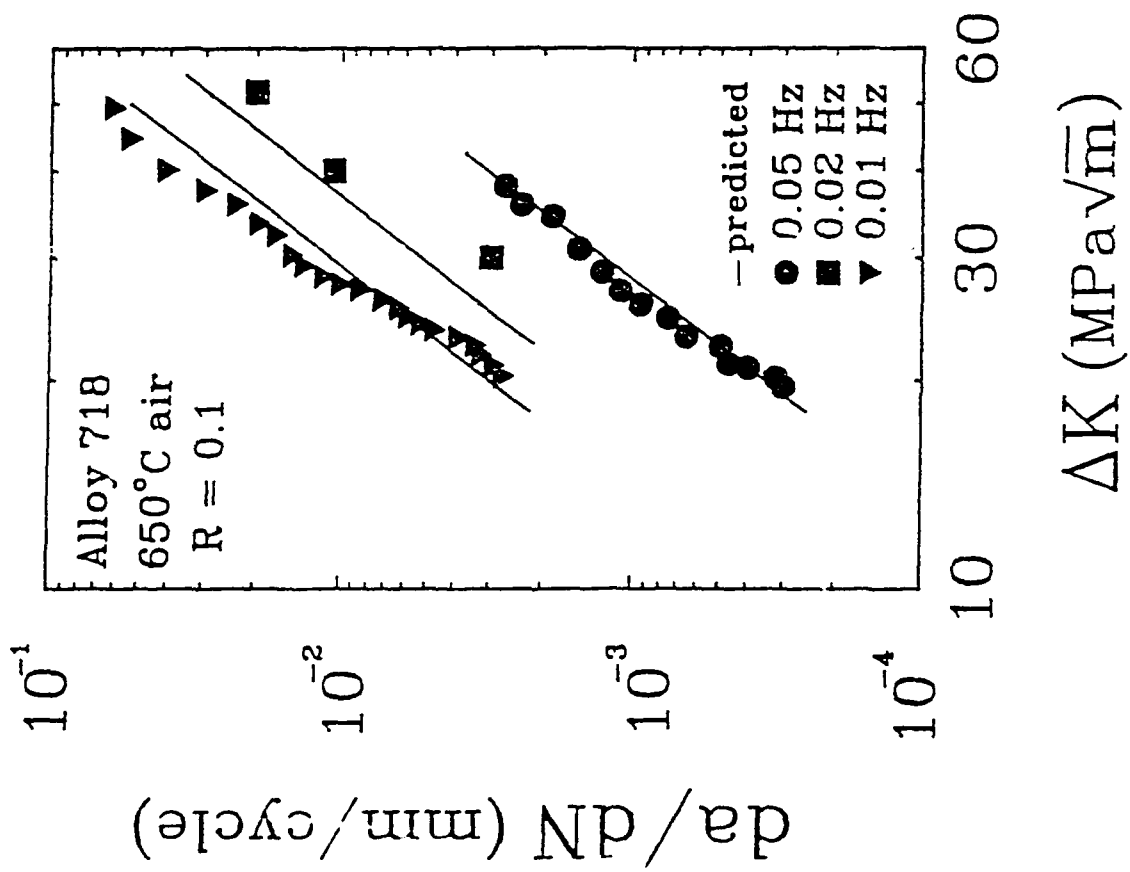
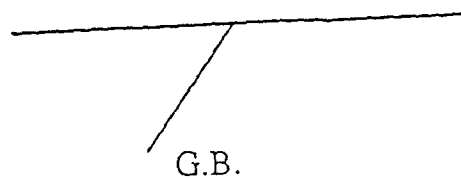
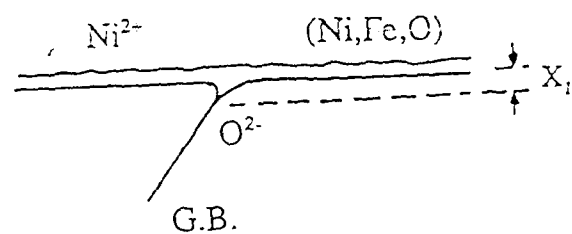


Fig (5)

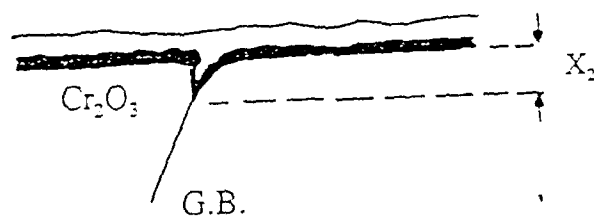
initial conditions



$t < t_p$



$t = t_p$



$t > t_p$

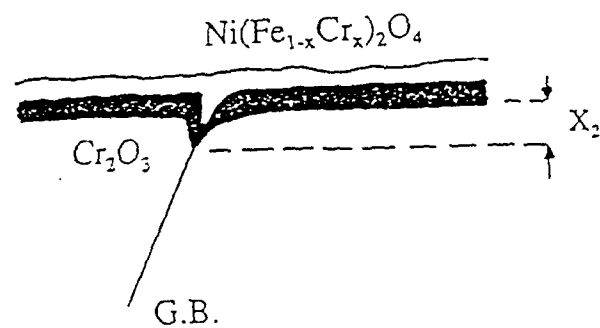


Fig. (6) Suggested mechanisms of grain boundary oxidation.

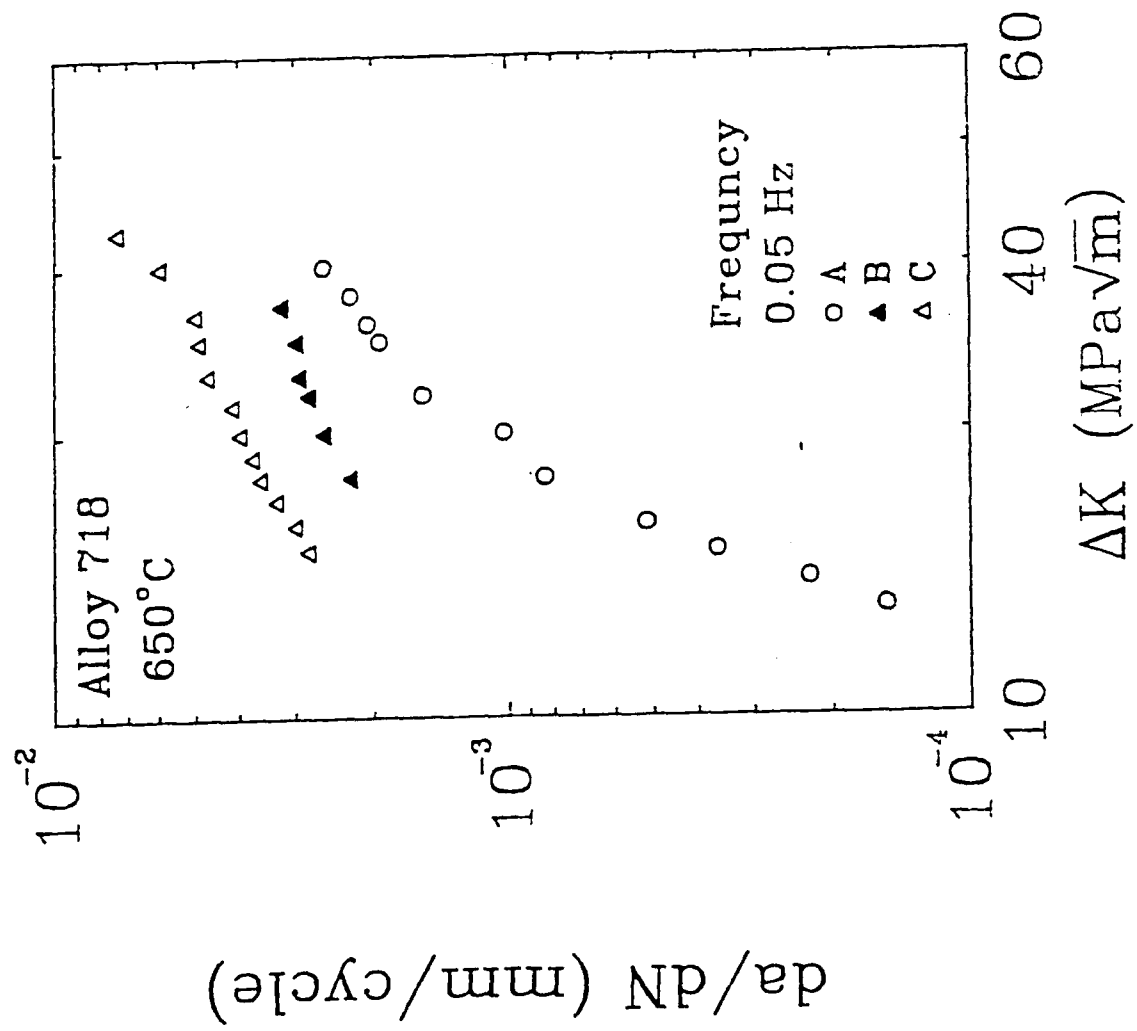
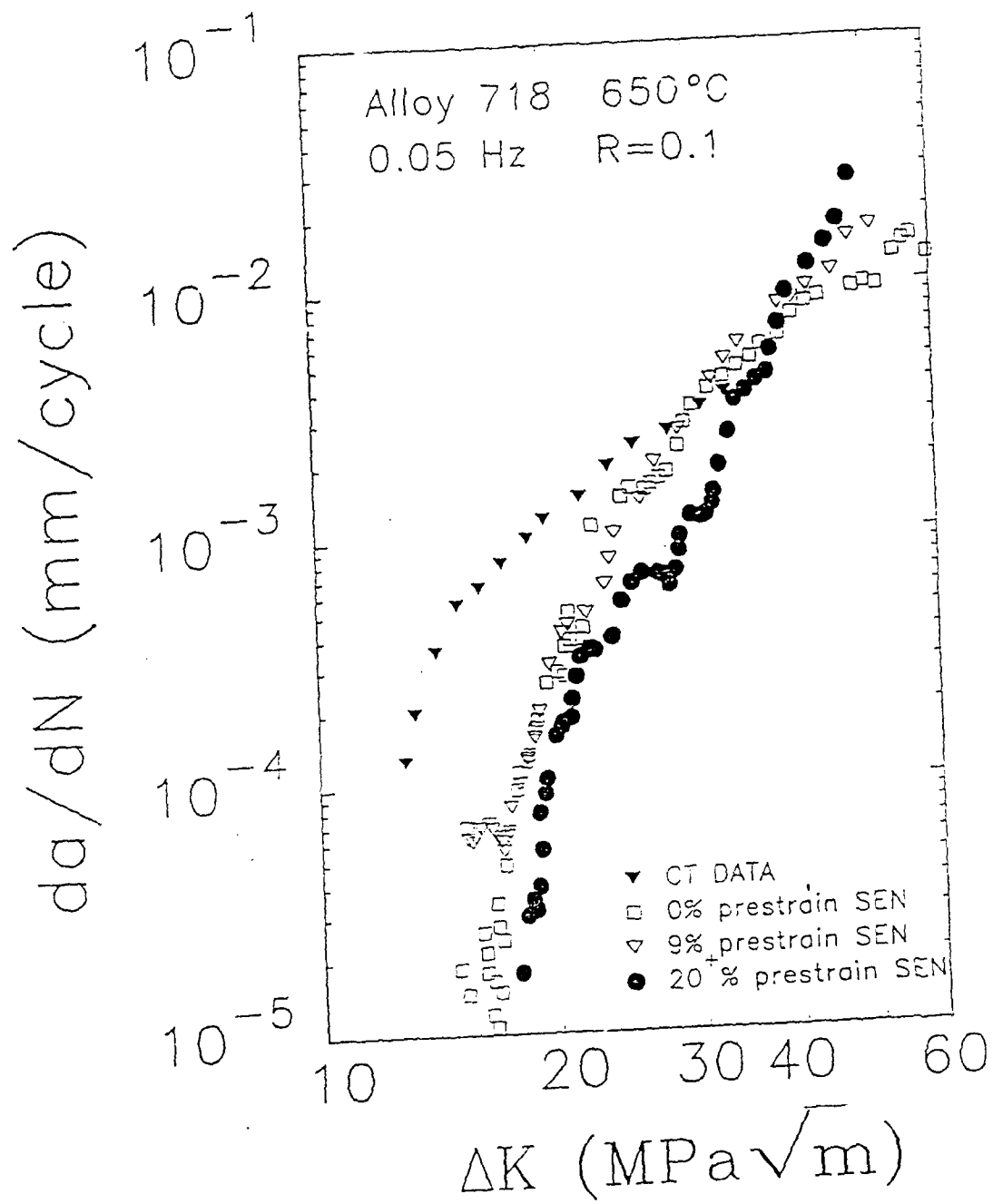
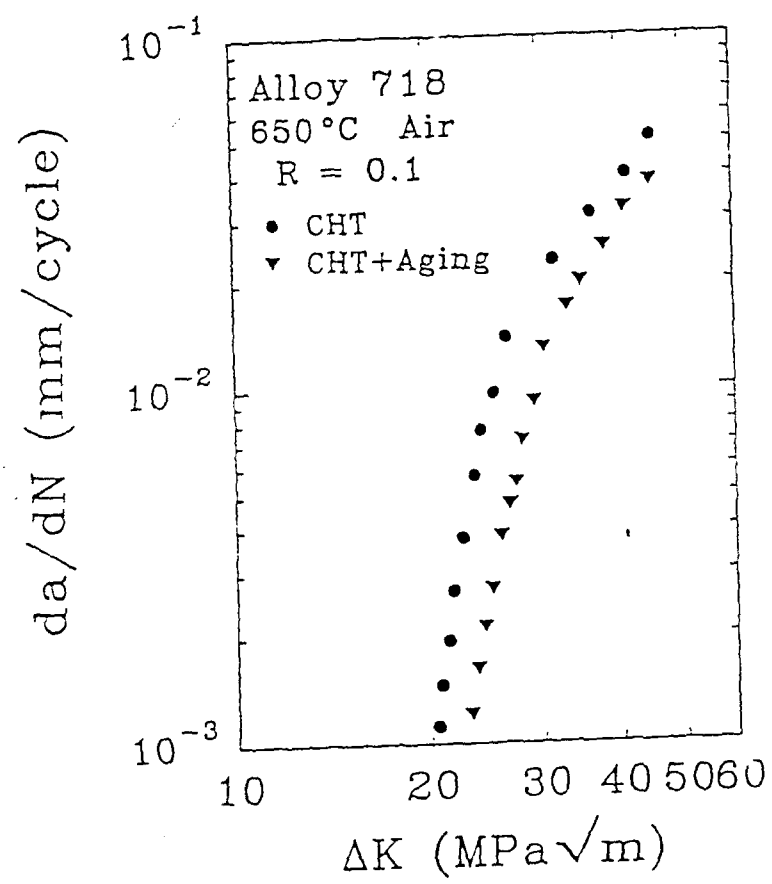


Fig. 7



Fig(8)



Fig(9)

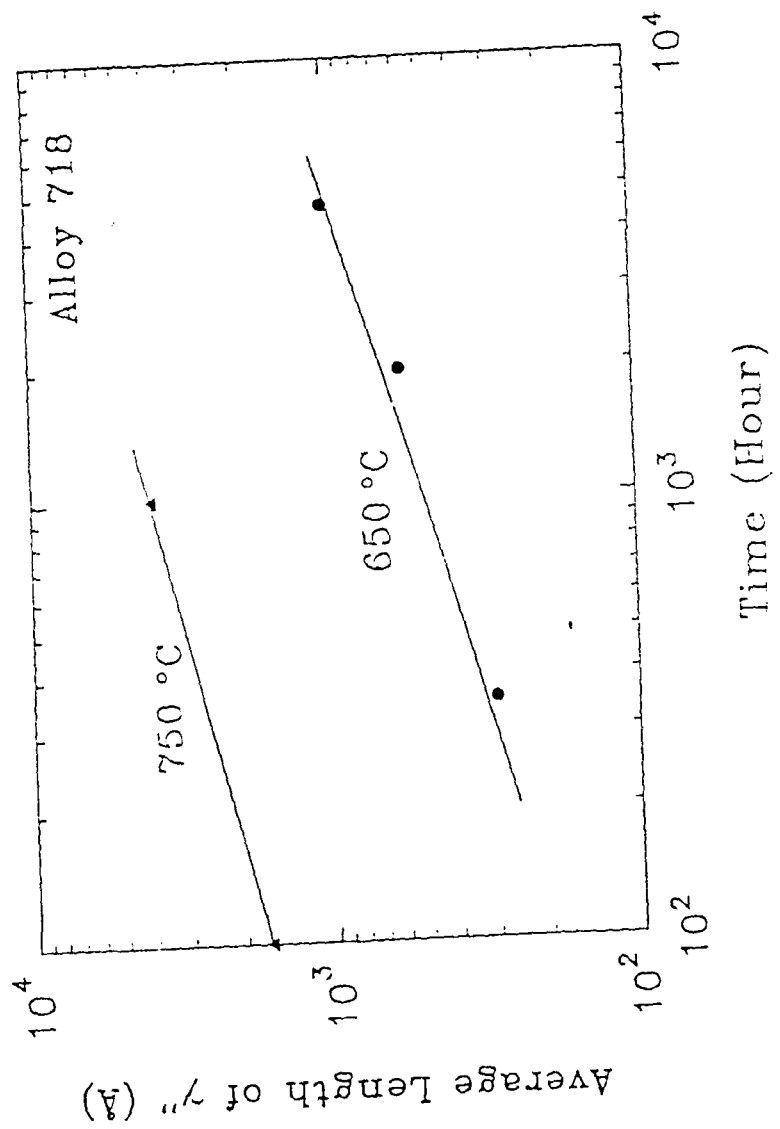


Fig 10